ESCOLA POLITÉCNICA
PROGRAMA DE PÓS-GRADUAÇÃO EM ENGENHARIA E TECNOLOGIA DE MATERIAIS
DOUTORADO EM ENGENHARIA E TECNOLOGIA DE MATERIAIS

VINÍCIUS GONÇALVES MACIEL

AVALIAÇÃO DO CICLO DE VIDA DE POLI(LÍQUIDOS IÔNICOS) IMIDAZÓLICOS SINTETIZADOS POR FOTOPOLIMERIZAÇÃO EM MANUFATURA ADITIVA

Porto Alegre
2018

Pontifícia Universidade Católica do Rio Grande do Sul
ESCOLA POLITÉCNICA
PROGRAMA DE PÓS-GRADUAÇÃO EM ENGENHARIA E TECNOLOGIA DE MATERIAIS

AVALIAÇÃO DO CICLO DE VIDA DE POLI(LÍQUIDOS IÔNICOS) IMIDAZÓLICOS SINTETIZADOS POR FOTOPOLIMERIZAÇÃO EM MANUFATURA ADITIVA

VINÍCIUS GONÇALVES MACIEL
QUÍMICO INDUSTRIAL
MESTRE EM ENGENHARIA E TECNOLOGIA DE MATERIAIS

TESE PARA A OBTENÇÃO DO TÍTULO DE DOUTOR EM ENGENHARIA E TECNOLOGIA DE MATERIAIS

Porto Alegre

Dezembro, 2018

Pontifícia Universidade Católica do Rio Grande do Sul
ESCOLA POLITÉCNICA
PROGRAMA DE PÓS-GRADUAÇÃO EM ENGENHARIA E TECNOLOGIA DE MATERIAIS

AVALIAÇÃO DO CICLO DE VIDA DE POLI(LÍQUIDOS IÔNICOS) IMIDAZÓLICOS SINTETIZADOS POR FOTOPOLIMERIZAÇÃO EM MANUFATURA ADITIVA

VINÍCIUS GONÇALVES MACIEL
QUÍMICO INDUSTRIAL
MESTRE EM ENGENHARIA E TECNOLOGIA DE MATERIAIS

ORIENTADOR: PROF. DR. MARCUS SEFERIN

Tese realizada no Programa de Pós-Graduação em Engenharia e Tecnologia de Materiais (PGETEMA) da Pontifícia Universidade Católica do Rio Grande do Sul, como parte dos requisitos para a obtenção do título de Doutor em Engenharia e Tecnologia de Materiais.

Porto Alegre
Dezembro, 2018

Ficha Catalográfica

M152a Maciel, Vinícius Gonçalves

Avaliação do ciclo de vida de poli(líquidos iônicos) imidazólicos sintetizados por fotopolimerização em manufatura aditiva / Vinícius Gonçalves Maciel . – 2018.

173.

Tese (Doutorado) – Programa de Pós-Graduação em Engenharia e Tecnologia de Materiais, PUCRS.

Orientador: Prof. Dr. Marcus Seferin.

1. Poli(liquídos iônicos). 2. Impressora 3D. 3. Avaliação do Ciclo de vida. 4. polímero. 5. estereolitografia. I. Seferin, Marcus. II. Título.

Elaborada pelo Sistema de Geração Automática de Ficha Catalográfica da PUCRS
com os dados fornecidos pelo(a) autor(a).
Bibliotecária responsável: Salete Maria Sartori CRB-10/1363

Pontifícia Universidade Católica do Rio Grande do Sul
ESCOLA POLITÉCNICA
PROGRAMA DE PÓS-GRADUAÇÃO EM ENGENHARIA E TECNOLOGIA DE MATERIAIS

AVALIAÇÃO DO CICLO DE VIDA DE POLI(LÍQUIDOS IÔNICOS) IMIDAZÓLICOS SINTETIZADOS POR FOTOPOLIMERIZAÇÃO EM MANUFATURA ADITIVA

CANDIDATO: VINICIUS GONÇALVES MACIEL

Esta Tese de Doutorado foi julgada para obtenção do título de DOUTOR EM ENGENHARIA E TECNOLOGIA DE MATERIAIS e aprovada em sua forma final pelo Programa de Pós-Graduação em Engenharia e Tecnologia de Materiais da Pontifícia Universidade Católica do Rio Grande do Sul.

DR. MARCUS SEFERIN - ORIENTADOR

BANCA EXAMINADORA

DRA. ANA CAROLINA BADALOTTI PASSUELO - PROGRAMA DE PÓS-GRADUAÇÃO EM ENGENHARIA CIVIL - UFRGS

DR. JACKSON DAMIANI SCHOLTEN - DO INSTITUTO DE QUÍMICA - UFRGS

DR. RICARDO CUNHA MICHEL - INSTITUTO DE QUÍMICA - UFRJ

DRA. ROSANE ANGÉLICA LIGABUE - DO PGETEMA - PUCRS

PUCRS
Campus Central
Av. Ipiranga, 6681 - Prédio 32 - Sala 505 - CEP: 90619-900
Telefone: (51) 3353.4059 - Fax: (51) 3320.3625
E-mail: engenharia.pg.materiais@pucrs.br
www.pucrs.br/politecnica

“Work gives you meaning and purpose and life is empty without it”

(Stephen Hawking)

DEDICATÓRIA

Dedico este trabalho aos meus pais Paulo Maciel e Rosiara Maciel que me ensinaram, com seus exemplos, o que verdadeiro significado das palavras: honestidade, disciplina e dedicação. Também dedico este trabalho a minha irmã Vanessa Maciel e a minha esposa Cristiane Kramer. Especialmente dedido este trabalho ao meu avô Jairo Gonçalves e minha vó Maria de Loudes Gonçalves (*in memoriam*).

AGRADECIMENTOS

À minha família, que sempre me incentivou em especial a minha esposa Cristiane Kramer pela paciência e apoio para seguir em frente e buscar sempre o meu máximo;

Ao orientador Marcus Seferin, pela oportunidade de desenvolver este trabalho, pela confiança, amizade e principalmente aos ensinamentos.

Aos colegas do GSK Carbon Neutral Laboratory for Sustainable Chemistry da Universidade de Nottingham, em especial ao Dr. Dominic Wales e ao Dr. Jesum Fernandes;

Ao professor Victor Sans, meu orientador na Universidade de Nottingham no Reino Unido, pela oportunidade e disponibilidade de sua atenção e tempo;

Ao professor Dr. Jairton Dupont pela confiança e apoio para concretizar a possibilidade de estudar na Universidade de Nottingham;

Ao meu amigo mexicano Alberto Robles Linares que foi um grande irmão durante o meu período fora do Brasil;

A professora Cássia Ugaya da Universidade Federal Tecnológica do Paraná, pela amizade, orientação e principalmente por não ter medido esforços para me ajudar;

Aos colegas do Laboratório de Química Industrial, em especial a Cristiane Izahias e ao Igor Grillo pela amizade e proveitosa convivência;

Ao Prof. Dr. Rafael Zortea, meu amigo e colega, pela colaboração indireta no desenvolvimento deste estudo e de tantos outros durante esta jornada;

Ao grupo de pesquisa da professora Cássia Ugaya, em ACV social da Universidade Federal Tecnológica do Paraná (UFTPR);

Ao grupo de pesquisa em ACV da professora Ana Passuello da Universidade Federal do Rio Grande do Sul pela confiança depositada;

Aos meus amigos de longa data Zuleica Furh e José Tormes pela amizade;

A ACV Brasil, em especial ao Felipe Lion Motta, pela disponibilidade da licença *Faculty* do Software Simapro®;

A ecoinvent pela disponibilidade gratuita de suas bases de dados de ciclo de vida;

A Capes e ao Governo Brasileiro que financiaram meus estudos na Inglaterra.

SUMÁRIO

LISTA DE FIGURAS

LISTA DE TABELAS

LISTA DE SÍMBOLOS E SIGLAS

[Bmim][Ac] .....1-butyl-3-methylimidazolium acetate

$[P_{66614}]$[124Triz]..... trihexyltetradecylphosphonium 1,2,4-triazolide

$[Bmim][BF_4]$ ..... 1-butyl-3-methyl-imidazolium tetrafluoroborate

$[Bmim][BF_4]$..... 1-butyl 3- methylimidazolium tetrafluoroborate

$[Bmim][BF_6]$..... 1- butyl-3-methylimidazolium hexafluorophosphate

[Bmim][Br]..... 1- butyl-3-methylimidazolium bromide

[Bmim][Cl] ..... 1-butyl 3-methylimidazolium chloride

$[Bmim][NTf_2]$ .....1-butyl-3-methylimidazolium bis(trifluoromethane)sulfonimide

[BPy][Cl] ..... 1-butylpyridinium chloride

$[C_{18}MIM]Br$..... 1-Octadecyl-3-methylimidazolium bromide

$[C_4mim][Cl]$..... 1-alkyl-3-methylimidazolium chloride

$[C_6MIM][Cl]$ ..... 1-hexyl-3-methylimidazolium chloride

$[C_6Py][Cl]$ .....n-hexylpyridinium chloride

$[hmim][TNf_2]$.....1-hexyl-3-methylimidazolium bis(trifluoromethylsulfonyl)imide

$[N(CN)_2]^-$ ..... ânion dicianamida

$[NTf_2]^-$ .....ânion bis(trifluorometanosulfonil)imidato

$[P_{66614}]$[3triazolide] .....trihexyl(tetradecyl)phosphonium 1,2,3-triazolide

CML .....Centre of Environmental Science

CO .....Monóxido de Carbono

CO_2 ..... Dióxido de Carbono

CV .....Ciclo de Vida

E ..... Exponencial (Notação matemática) 10=1,00e+01=$1,00x10^1$

EC .....European Commission

EDIP ..... Environmental Design of Industrial Products

Eq. .....equivalente

FU .....sigla em Inglês para unidade funcional

g ..... grama (unidade de massa)

GEE ..... Gás de Efeito Estufa

HPA ..... Hidrocarboneto Policíclico Aromático

ISO .....International Standards Organization

kg .....quilogramas (unidade de massa)

TRABALHOS PUBLICADOS RELACIONADOS AO TEMA DA TESE

1. **MACIEL, VINÍCIUS GONÇALVES**; ZORTEA, RAFAEL BATISTA; MENEZES DA SILVA, WAGNER ; CYBIS, LUIZ FERNANDO DE ABREU ; EINLOFT, SANDRA ; SEFERIN, MARCUS . Life Cycle Inventory for the agricultural stages of soybean production in the state of Rio Grande do Sul, Brazil. *Journal of Cleaner Production*, v. 93, p. 65-74, 2015. (CAPES A1, Engenharia II)

2. **MACIEL, VINÍCIUS GONÇALVES**; ZORTEA, RAFAEL BATISTA; GRILLO, IGOR BARDEN; LIE UGAYA, CÁSSIA MARIA; EINLOFT, SANDRA ; SEFERIN, MARCUS .Greenhouse gases assessment of soybean cultivation steps in southern Brazil. *Journal of Cleaner Production*, v. 131, p. 747-753, 2016. (CAPES A1, Engenharia II)

3. DE ALMEIDA, CÁSSIO FLORISBAL; **MACIEL, VINÍCIUS GONÇALVES**; TSAMBE, MALAQUIAS; DE ABREU CYBIS, LUIZ FERNANDO. Environmental assessment of a bi-fuel thermal power plant in an isolated power system in the Brazilian Amazon region. *Journal of Cleaner Production*, v. 154, p. 41-50, 2017. (CAPES A1, Engenharia II)

4. NUNES, FLÁVIA APARECIDA ; SEFERIN, MARCUS; **MACIEL, VINÍCIUS GONÇALVES**; AYUB, MARCO ANTÔNIO ZÁCHIA. Life Cycle Assessment comparison between brow parboiled rice produced under organic and minimal tillage cultivation systems. *Journal of Cleaner Production*, v. 161, p. 95-104, 2017. (CAPES A1, Engenharia II)

5. **MACIEL, VINÍCIUS GONÇALVES**; BOCKORNY, GEOVANA; DOMINGUES, NEI ; SCHERER, MOARA BRITZ; ZORTEA, RAFAEL BATISTA; SEFERIN, MARCUS. Comparative Life Cycle Assessment among Three Polyurethane Adhesive Technologies for the Footwear Industry. *ACS Sustainable Chemistry & Engineering*, v. 5, p. 8464-8472, 2017. (CAPES A1, Engenharia II)

6. DE ALMEIDA, CÁSSIO FLORISBAL; **MACIEL, VINÍCIUS GONÇALVES**; CYBIS, LUIZ FERNANDO DE ABREU. Global warming potential assessment for operation of thermoelectric power plant in Manaus. *LALCA- Revista Latino Americana em Avaliação do Ciclo de Vida*, v. 1, p. 45, 2017.

7. NUNES, FLÁVIA APARECIDA; SEFERIN, MARCUS; **MACIEL, VINÍCIUS GONÇALVES**; FLÔRES, SIMONE HICKMANN ; AYUB, MARCO ANTÔNIO ZÁCHIA. Life cycle greenhouse gas emissions from rice production systems in Brazil: A comparison between minimal tillage and organic farming. *Journal of Cleaner Production*, v. 139, p. 799-809, 2016. (CAPES A1, Engenharia II)

8. ZORTEA, RAFAEL BATISTA; **MACIEL, VINÍCIUS GONÇALVES**; PASSUELLO, ANA. Sustainability assessment of soybean production in Southern Brazil: A life cycle approach. *Sustainable Production and Consumption*, v. 13, p. 102-112, 2018.

RESUMO

MACIEL, GONÇALVES. VINÍCIUS. **Avaliação do Ciclo de vida de poli(líquidos iônicos) imidazólicos sintetizados por fotopolimerização em manufatura aditiva**. Porto Alegre. 2018. Tese. Programa de Pós-Graduação em Engenharia e Tecnologia de Materiais, PONTIFÍCIA UNIVERSIDADE CATÓLICA DO RIO GRANDE DO SUL.

Palavras-Chaves: Impressora 3D, polímero, líquidos iônicos polimerizáveis, estereolitografia.

Este trabalho apresenta uma Avaliação do Ciclo de Vida (ACV) do “berço-ao-portão” de líquidos iônicos polimerizáveis (PILs) em impressão 3D usando aparelho de estereolitografia. Primeiramente, a fim de fornecer uma visão geral atualizada sobre o estado da arte envolvendo os estudos da ACV em líquidos iônicos (LIs), uma revisão sobre o tema foi conduzida. Esta revisão recomenda uma lista de questões que requerem de maior atenção para a aplicação da ACV para avaliar os processos de LIs, tais como: i) acesso a um inventário completo e adequado do ciclo de vida e ii) desenvolvimento e inclusão de fatores de caracterização de impactos de LIs. Além disso, algumas boas práticas em ACV de LI foram identificadas e são recomendadas. Posteriormente, este trabalho teve como foco o emprego do cátion 3-butil-1-vinilimidazólio ($[BVim]^+$), com o ânion não-coordenado e hidrofóbico bis(trifluorometanosulfonil)imidato ($[NTf_2]^-$) como contra-íon. Os resultados indicam que o processo de impressão não exacerba significativamente os impactos ambientais. O monômero polimerizável de LI tem impacto comparável ao análogo, não-polimerizável, 3-butil-1-metilimidazólio $[NTf_2]^-$, portanto, permitindo potencialmente o uso mais eficiente das propriedades dos LI por imobilização em fases sólidas. Também, é demonstrado que a troca do ânion $[NTf_2]^-$ pelo ânion dicianamida $[N(CN_2)]^-$, para produção de PILs, diminui significativamente os impactos em todas as categorias avaliadas. Este trabalho representa a primeira fase em direção à geração quantitativa de dados de ACV, para o processo de impressão 3D de PILs, que será um grande suporte para a tomada de decisões durante o projeto de desenvolvimento de processos de impressão 3D de PILs em escala de laboratório.

ABSTRACT

MACIEL, GONÇALVES. VINÍCIUS. **Life cycle assessment of imidazolium Poly(ionic liquids) synthesized by Photopolymerization-based additive manufaturing.** Porto Alegre. 2018. Tese. Programa de Pós-Graduação em Engenharia e Tecnologia de Materiais, PONTIFÍCIA UNIVERSIDADE CATÓLICA DO RIO GRANDE DO SUL.

Palavras-Chave: 3D printer, polymer, polymerizable ionic liquid, stereolithography apparathus.

This work presents a “cradle-to-gate” Life Cycle Assessment (LCA) of 3D-printing polymerisable ionic liquids (PILs) using stereolithography apparathus. Firstly, in order to provide an up-to-date overview on the currently state-of-the-art involving the life cycle assessment (LCA) studies on ionic liquids (ILs) a review on the subject was employed. This review recommends a list of issues that need further precision for application of LCA to evaluate ILs processes, such as: i) access to comprehensive and adequate life cycle inventory and ii) development and inclusion of characterization factors for IL impacts. Also, some good practices in LCA of IL were identified and are recommended. Later, this work focused on the employment of the 3-butyl-1-vinylimidazolium [BVim] cation, with the non-coordinating and hydrophobic bis(trifluoromethane)sulfonimide $[NTf_2]^-$ anion as the counter anion. The results indicate that the printing process does not significantly exacerbate the environmental impacts. The polymerisable monomer IL has similar impact compared to the analogous non-polymerisable 3-butyl-1-methylimidazolium $[NTf_2]^-$ IL, thus potentially allowing for the more efficient use of the IL properties by immobilization in solid phases. Furthermore, it is demonstrated that switching the anion from $[NTf_2]^-$ to dicyanamide $[N(CN_2)]^-$ significantly decreases the impacts in all categories evaluated for PIL production. This work represents the first phase toward quantitative LCA data generation for the process of 3D-printing IL, which will be great support for decision making during design of PIL 3D-printing processes at a laboratory scale.

1. INTRODUÇÃO

Atualmente o consenso acerca da necessidade de um ambiente ecologicamente equilibrado atrelado ao esgotamento progressivo dos recursos naturais, motivam as reflexões em torno da pesquisa e desenvolvimento de materiais e seus possíveis impactos ambientais.

Nos últimos anos, uma classe de materiais que tem recebido destaque são os líquidos iônicos (LEI *et al.*, 2017). Inicialmente, estas substâncias foram promovidas como “solventes verdes” e associadas à produção limpa (DISASA IRGE, 2016; GHANDI, 2014; PLECHKOVA; SEDDON, 2008; ZHU *et al*., 2009). Além disso, líquidos iônicos podem ser sintetizados a partir da combinação entre diferentes cátions e ânions possibilitando a obtenção de uma notável variedade destas substâncias (ZHU *et al*., 2009), favorecendo a sua versatilidade e considerável potencial de aplicação (QIAN; TEXTER; YAN, 2017).

No entanto, apesar dos líquidos iônicos serem considerados uma nova classe de materiais sustentáveis, vários autores afirmam que estas substâncias apresentam certa toxicidade sobre animais aquáticos e a saúde humana (HECKENBACH *et al*., 2016; MEHRKESH; KARUNANITHI, 2016a, 2016b; PHAM; CHO; YUN, 2010; ZHAO *et al.*, 2014). Igualmente, estudos considerando seu ciclo de vida corroboram que processos envolvendo líquidos iônicos têm alta probabilidade de apresentar maiores impactos ambientais quando comparado aos métodos convencionais (CUÉLLAR-FRANCA *et al.*, 2016; ZHANG; BAKSHI; DEMESSIE, 2008). Vários autores, utilizando esta abordagem, também demostraram que a recuperação do líquido iônico é um dos parâmetros fundamentais para minimizar os impactos ambientais dos processos que empregam estas substâncias (ALVIZ; ALVAREZ, 2017; RIGHI *et al*., 2011; ZHANG; BAKSHI; DEMESSIE, 2008).

Estas são questões importantes no que tange os líquidos iônicos (LIs) e a busca pela sustentabilidade ao longo do seu ciclo de vida, uma vez que é conhecido que a transferência eficaz de propriedades dos líquidos iônicos para materiais suportados com unidades análogas ajuda a ultrapassar as limitações tipicamente associadas ao emprego destas substâncias (SANS *et al*., 2011), como o elevado consumo energético necessário para etapa de regeneração (DISASA IRGE, 2016). Abordagens como esta poderiam reduzir a quantidade de líquidos iônicos utilizadas a partir da separação e reciclagem do material (SANS *et al*., 2011). Em outras palavras, sugere-se que a transferência das propriedades notáveis dos LIs para fases sólidas pode ajudar a minimizar os impactos ambientais relacionados ao ciclo de vida destas substâncias.

Dentre as maneiras de se promover esta transferência destaca-se o processo de polimerização de LIs (SHAPLOV; PONKRATOV; VYGODSKII, 2016), sintetizando líquidos iônicos polimerizáveis (MECERREYES, 2011) ou poli(líquidos iônicos) (YUAN; MECERREYES; ANTONIETTI, 2013) (PILs). Estes novos materiais poliméricos são um tipo de polieletrólitos com estrutura semelhante a líquidos iônicos homogêneos (WELTON, 1999) com uma transferência efetiva de propriedades para as fases suportadas (SANS et al., 2011). Estas substâncias são uma nova classe de materiais poliméricos formados a partir de monômeros de líquidos iônicos que combinam as propriedades dos líquidos iônicos com as propriedades mecânicas dos polímeros (MECERREYES, 2011).

Recentemente, novas descobertas científicas demostraram que PILs podem ser sintetizados a partir da manufatura aditiva (impressão 3D) que além de promover a imobilização do LI (KARJALAINEN *et al.*, 2018; SCHULTZ *et al*., 2014a; WALES *et al.*, 2018) também é uma tecnologia associada às perspectivas do desenvolvimento sustentável (YUAN; MECERREYES; ANTONIETTI, 2013). Por exemplo, estudos publicados pelo grupo de pesquisa do *GKS Neutral Carbon Laboratory for sustainable of chemistry* da Universidade de Nottingham no Reino Unido demonstraram a possibilidade da impressão de PILs com sistema de impressora a jato de tinta (KARJALAINEN et al., 2018) e também impressão 3D de PILs com materiais moleculares fotocrômicos orgânicos-inorgânicos híbridos avançados baseados em polioxometalatos (WALES et al., 2018).

Embora tenha ocorrido um avanço considerável na pesquisa e desenvolvimento dos PILs e sua produção a partir da tecnologia de impressão 3D, pouco pode ser encontrado na literatura sobre o seu desempenho ambiental no contexto do ciclo de vida. Deste modo, a compreensão do impacto ambiental da síntese de PILs é fundamental para permitir processos de tomada de decisão baseados na sustentabilidade (CERDAS *et al.*, 2017). Neste cenário, a Avaliação do Ciclo de Vida (ACV) apresenta-se como uma metodologia robusta e de sólido reconhecimento cientifico para avaliação do desempenho ambiental de processos e produtos como os PILs (JACQUEMIN; PONTALIER; SABLAYROLLES, 2012).

Entretanto, dificuldades para construir inventários do ciclo de vida (ICV), quando há LIs envolvidos no sistema de produto avaliado, vem sendo relatadas na literatura (ALVIZ; ALVAREZ, 2017; KRALISCH *et al*., 2005; PETERSON, 2013; ZHANG; BAKSHI; DEMESSIE, 2008). A característica emergente destas substâncias e a falta de dados de produção em escala industrial são apontadas como motivos para isso ocorrer (FARAHIPOUR; KARUNANITHI, 2014). Por outro lado, deve-se destacar que é um fato conhecido, pelos praticantes da ACV, a importância de dados de ICVs adequados para o material investigado, a fim de levar em consideração o material de maneira mais adequada para o apoio da tomada de decisão (HISCHIER; WALSER, 2012).

Portanto, neste trabalho, uma revisão da literatura sobre o uso da ACV para avaliar LIs é conduzida, com objetivo de fornecer uma visão geral atualizada sobre o tema, identificar as limitações que dificultam uma aplicação abrangente da estrutura de ACV e fornecer dados suficientes para nortear a condução de futuros estudos sobre o tema. Além disso, este trabalho apresenta um estudo de ACV considerando a abordagem *cradle-to-gate*, da síntese de líquidos iônicos polimerizáveis a base de imidazólio sintetizados pela tecnologia de impressão 3D, especificamente no sistema de estereolitografia. Adicionalmente, baseando-se nos pressupostos, este estudo também visou entender como esses impactos se comparam a um líquido iônico homogêneo e análogo a precursores de PIL e como a troca do contra-íon bis(trifluorometanosulfonil)imidato [NTf_2^-] pelo o ânion dicianamida [$N(CN)_2^-$] pode afetar o desempenho ambiental do PIL.

2. OBJETIVOS

O presente trabalho propôs-se a avaliar o desempenho ambiental de Poli(Líquidos Iônicos) imidazólicos, sintetizados em impressora 3D baseada em estereolitografia, a partir da metodologia de Avaliação do Ciclo de Vida.

2.1. Objetivos Específicos

Os objetivos específicos deste estudo são:

- Realizar uma revisão do estado da arte sobre o uso da metodologia da Avaliação do Ciclo de Vida aplicada à investigação do desempenho ambiental de líquidos iônicos;
- Construir Inventários do Ciclo de Vida dos Poli(líquidos Iônicos) avaliados, sendo eles: poli(BDA-co-BVimNTf_2) e poli(BDA-co-BVim$N(CN)_2$);
- Realizar uma Avaliação do Ciclo de Vida do berço-ao-portão (*cradle-to-gate*) do laboratório dos Poli(Líquidos Iônicos) imidazólicos sintetizados pela tecnologia de impressão 3D baseada no sistema de estereolitografia;
- Avaliar a contribuição da manufatura aditiva para os impactos do ciclo de vida do PIL;
- Conduzir a análise de contribuição de processos e identificar os principais processos e substâncias que contribuem sobre os diferentes impactos avaliados;
- Avaliar os efeitos da troca do ânion bis(trifluorometanosulfonil)imidato ([NTf_2]) pelo dicianamida [$N(CN_2)]^-$ nos impactos do ciclo de vida do PIL;
- Conduzir uma comparação entre monômeros de líquidos iônicos ([BVim][NTf_2]) e um líquido iônico convencional ([Bmim][NTf_2]).

3. REVISÃO BIBLIOGRÁFICA

3.1. Sustentabilidade dos líquidos iônicos e da manufatura aditiva

Nos últimos anos, os liquídos iônicos e a manufatura aditiva (impressão 3D) vêm sendo relacionados como alternativas tecnológicas sustentáveis e definitivamente são uma tendência crescente, demonstrando grande potencial e um futuro promissor com uma vasta possibilidade de aplicações (GHANDI, 2014; HECKENBACH *et al.,* 2016).

Contudo, preocupações de segurança com líquidos iônicos (LIs) para proteção ambiental ou saúde humana têm sido destacadas por vários relatórios e trabalhos recentes (MEHRKESH; KARUNANITHI, 2016c, 2016a, 2016b; PHAM; CHO; YUN, 2010; ZHU et al., 2009). Por exemplo, estudos relataram que muitos LIs possuem um nível relativamente alto de toxicidade para organismos de água doce (MEHRKESH; KARUNANITHI, 2016a, 2016b; RADOŠEVIĆ *et al.*, 2013) e uma extensa revisão da toxicidade de LIs à organismos aquáticos pode ser encontrada em Pham *et al.* (2010).

Além disso, estas substâncias teriam toxicidade equivalente aos solventes orgânicos tradicionais. De acordo com WELLS; COOMBE, (2006), que conduziu uma ampla investigação sobre a toxicidade de LIs em invertebrados *D. magna* e algas verdes *P. Subcapitata*, os LIs imidazólicos seguidos pelos fosfônios, ambos de cadeia mais longa, são os mais tóxicos entre os avaliados. Estes LIs teriam uma toxicidade mais aguda do que os solventes orgânicos comuns, como diclorometano, metanol, éter terc-butilometílico e acetonitrila. Além disso, o estudo demostrou que os LIs menos tóxicos (piridinas, amônio e imidazólios, mais especificamente LIs de

cadeia alquíla curta) possuem toxicidade comparáveis aos solventes xileno e tolueno.

Apensar do mecanismo de toxicidade envolvendo os LIs ainda não ter sido bem compreendido (CVJETKO BUBALO *et al.,* 2014), há um consenso que a toxicidade dos LIs à animais áquaticos tem relação com o aumento da cadeia lateral alquila de seu cátion (MEHRKESH; KARUNANITHI, 2016a, 2016b; ZHU *et al*., 2009). Além disso, o transporte de cátion imidazólicos e piridínios no ambiente pode estar relacionado a sua hidrofobicidade, assim, LIs hidrofóbicos poderiam se tornar contaminantes persistentes acumulando-se, por exemplo, no solo ou em sedimentos marinhos, enquanto que LIs hidrofílicos estariam nos ecossistemas aquáticos (CVJETKO BUBALO *et al.*, 2014).

Por estes motívos, de acordo com LEI *et al.,* (2017) alguns líquidos iônicos estão longe da imagem “verde” frequentemente atribuída na literatura. Por outro lado, a sustentabilidade de um LI não deve ser atribuída exclusivamente à molécula, mas, também deve-se considerar os impactos decorrentes da sua produção e dos seus intermediários, ou seja, os impactos relacionados ao ciclo de vida (CV) da molécula (ZHU *et al.,* 2009). Alguns autores afirmam que processos que usam LIs são altamente prováveis de apresentar um impacto ambiental maior ao considerar o seu ciclo de vida do que métodos convencionais (ALVIZ; ALVAREZ, 2017; KRALISCH *et al*., 2005; ZHANG; BAKSHI; DEMESSIE, 2008). Isto ocorre devido a que, para a maioria dos casos, a síntese de LIs inclui sempre uma série de reações e etapas onde há demanda de energia, insumos e por muitas vezes são empregados solventes orgânicos. De acordo com KRALISCH *et al*. (2005) a redução da emissão gasosa, devido a pressão de vapor negligenciável, não pode ser relacionada diretamente a um processo ambientalmente sustentável.

Logo, é justificável que o desempenho ambiental de produtos e processos que tenham LIs envolvidos em seu CV deve ser avaliado usando métodos de sólido reconhecimento científico como a ACV. De acordo com ZHU *et al.*, (2009) esta avaliação deve ser realizada considerando todo o processo: desde a síntese do liquido iônico e seus precursores, passando pelo processo de aplicação (fase de uso) até a sua recuperação para reutilização e disposição final.

Por outro lado, embora tenha ocorrido um avanço considerável na pesquisa e desenvolvimento de líquidos iônicos, pouco pode ser encontrado na literatura sobre o seu desempenho ambiental no contexto de ciclo de vida. Isto ocorre principalmente devido à indisponibilidade de dados das sínteses de LIs em escala industrial (MEHRKESH; KARUNANITHI, 2016a). Assim, uma série de suposições e métodos vem sendo empregados para qualificar e quantificar os fluxos materiais e energéticos imprescindíveis para condução de estudos de ACV sobre o tema (RIGHI et al., 2011; ZHANG; BAKSHI; DEMESSIE, 2008).

Em situação semelhante encontra-se a tecnologia de impressão 3D. Em contraste ao sistema tradicional de manufatura, que é responsável por considerável contribuição de impactos ambientais, devido ao consumo de energia e materiais, geração de resíduos e emissões gasosas (DUFLOU *et al.*, 2012), a manufatura aditiva tem sido relatada como uma tecnologia capaz de reduzir os impactos ambientais (GEBLER; SCHOOT UITERKAMP; VISSER, 2014; HUANG *et al*., 2017), sociais (HUANG *et al*., 2013) e os custos ao longo do seu ciclo de vida (HUANG *et al*., 2017; MAMI *et al*., 2017).

As vantagens associadas à manufatura aditiva, quando comparada a manufatura convencional de impressão, são principalmente atribuídas ao fato desta tecnologia ser baseada em um sistema de manufatura distribuída, ou seja, que pode ocorrer em qualquer lugar, por exemplo, em residências, contra um sistema tradicional de manufatura onde a produção é centralizada (FORD; DESPEISSE, 2016). Assim, vários autores relatam que a manufatura aditiva é capaz de promover mudanças significativas na cadeia de suprimentos atual, isto ocorre, por exemplo, devido à produção localizada, redução de matérias prima, possibilidade de reparo e remanufatura (BAUMERS *et al*., 2017; GEBLER; SCHOOT UITERKAMP; VISSER, 2014; HUANG *et al*., 2017; SREENIVASAN; GOEL; BOURELL, 2010; *CERDAS et al*., 2017; NGO *et a*l., 2018). Estima-se que a implementação da impressão 3D possa permitir a redução das intensidades de emissão de energia e dióxido de carbono em cerca de 5% até 2025 (GEBLER; SCHOOT UITERKAMP; VISSER, 2014).

Além disso, a manufatura aditiva democratiza o papel do consumidor colocando-o na posição de fabricante e permitindo-o otimizar o processo e personalizar ou diferenciar unidades, assim, proporcionando ganhos de eficiência ambiental (BAUMERS *et al.*, 2017). No entanto, alguns autores relataram que processos de manufatura 3D possuem um nível relativamente alto de consumo de energia (BARROS; ZWOLINSKI; MANSUR, 2017; KREIGER; PEARCE, 2013; YANG et al., 2017) e que o estágio de fabricação aditiva tem a maior influência no desempenho ambiental (Ma *et al.* 2018). Por estes motivos, há um consenso que considerações pertinentes à sustentabilidade imprescindivelmente devem ser aplicadas aos processos de impressão 3D e necessariamente devem incluír a metodologia da ACV (BAUMERS *et al.*, 2017; FORD; DESPEISSE, 2016; KREIGER; PEARCE, 2013; MAMI *et al*., 2017; SREENIVASAN; GOEL; BOURELL, 2010).

Embora a disponibilidade de estudos de ACV sobre este tema ainda seja limitado, iniciativas recentes relaram o uso da metodologia cobrindo os diferentes pilares da sustentabilidade. WITTBRODT *et al.,* (2013) utilizou a abordagem do ciclo de vida para avaliar impressoras 3D sobre a perspectiva econômica. Um estudo abrangente das dimensões ambientais atuais da manufatura aditiva, cobrindo todo o ciclo de vida dos produtos manufaturados, foi reportado por KELLENS *et al*., (2017b). A esfera ambiental também foi explorada por Cerdas *et al.* (2017) que reportou um estudo comparativo entre um sistema tradicional de manufatura e um sistema baseado na impressão 3D para produção de armações de óculos.

No âmbito da dimensão social, vários autores relatam que a manufatura aditiva poderia apresentar impactos consideráveis nesta esfera (FORD; DESPEISSE, 2016; KREIGER; PEARCE, 2013; MAMI *et al.*, 2017). Além disso, a manufatura aditiva seria capaz de apresenta melhores indicadores para a saúde do trabalhador quando comparada ao sistema de manufatura tradicional (HUANG *et al*., 2013). No entanto, segundo HUANG *et al*., (2013) a indisponibilidade de inventários de ciclo de vida consistentes são limitações que dificultam a abordagem da metodologia.

Portanto, no que diz respeito ao desempenho ambiental dos LIs e a da manufatura aditiva, é possível afirmar que ambos podem apresentar certas

vantagens ambientais quando comparadas aos sistemas tradicionais. No entanto, a pouca disponibilidade de estudos e as lacunas de informações são questões que permeiam este tema e devem ser superadas em futuros estudos.

3.2. Líquidos Iônicos

LIs são sais orgânicos compostos principalmente de cátions orgânicos e ânions inorgânicos (LEI *et al.*, 2017). Estas substâncias são eletrólitos líquidos em temperaturas inferiores a 100 ℃ compostos inteiramente por íons e exibem na maioria dos casos viscosidades relativamente baixas (DISASA IRGE, 2016; DUPONT, 2011).

Frequentemente os líquidos iônicos têm sido amplamente associados a processos de produção limpa ou sustentáveis o que ajudou na exponencial atenção atualmente dada a estas substâncias (DISASA IRGE, 2016; GHANDI, 2014; PLECHKOVA; SEDDON, 2008).

Além disso, o interesse nestas moléculas cresceu significativamente principalmente devido a suas propriedades como a sua negligenciável pressão de vapor, alta condutividade iônica e estabilidade química e térmica (DISASA IRGE, 2016). Estas características despertaram muita atenção para aplicações em vários campos da química e da indústria, sendo propostos, por exemplo, para separar o gás carbônico em correntes de gás exausto provenientes da queima de combustíveis (TORRALBA-CALLEJA; SKINNER; GUTIÉRREZ-TAUSTE, 2013), em reações químicas, principalmente em catálise e biocatálise (BURGUETE *et al*., 2010; PLECHKOVA; SEDDON, 2008), como fluido térmico em sistemas de refrigeração (PETERSON, 2013), como líquidos eletricamente condutores na eletroquímica (HAGIWARA; LEE, 2007), na síntese de nanomateriais (DUPONT *et al.,* 2002), em materiais poliméricos (LU; YAN; TEXTER, 2009), entre outros. A Figura 1 apresenta as principais aplicações dos líquidos iônicos.

Figura 1.Principais aplicações dos líquidos iônicos

Fonte: traduzido de CVJETKO BUBALO *et al.*, (2014)

Convencionalmente, os LIs contêm cátions orgânicos volumosos, tais como imidazólio, piridínio, pirrolidínio, amônio quaternário ou tetraalquilfosfônio (DISASA IRGE, 2016; WELTON, 1999). Entre os cátions que podem formar um LI, o mais utilizado é do tipo imidazólio (ZHENG *et al.*, 2014). Para os ânions, os mais comuns são os fluorados como bis(trifluorometanosulfonil)imidato ([NTf_2]), tetrafluorborato ([BF_4]) e hexafluorofosfato ([PF_6]) (DISASA IRGE, 2016; GHANDI, 2014). Uma seleção de típicos cátions e ânions de LIs é apresentada na Figura 2.

Cátions	Ânions
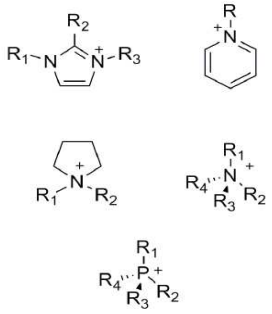	Cl^- / $AlCl_3^-$ Cl^-, Br^-, I^-, $(CN)_2N^-$ NO_3^-, SO_4^{2-}, $EtSO_4^-$ CF_3COO^-, CH_3COO^-, $CF_3SO_3^-$ BF_4^-, PF_6^- $(CF_3SO_2)_2N^-$

Figura 2.Representação dos principais cátions e ânions empregados em líquidos iônicos.

A síntese dos LIs pode ser genericamente simplificada a duas etapas: a formação do cátion desejado e a troca do ânion necessário para formação do produto final, como apresentado na Figura 3.

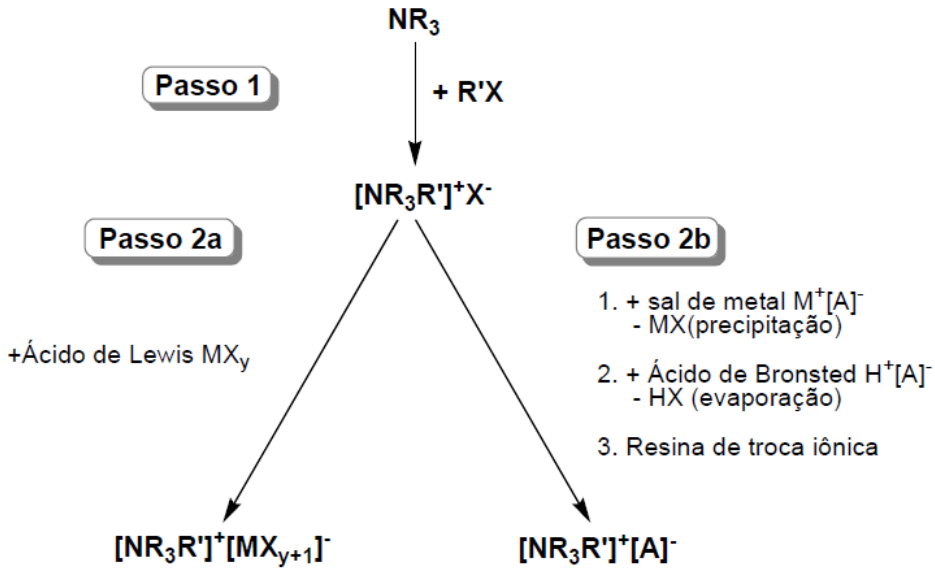

Figura 3. Típicas etapas da reação de síntese de LIs
(WASSERSCHEID; WELTON, 2008)

A formação do cátion ocorre pela reação de protonação ou quaternização empregando um haloalcano. Este processo tem vantagens como: os haloalcanos apresentam custos menores e as reações de substituição geralmente ocorrem em temperaturas entre 70 ℃ e 90 ℃ e, além disso, est es sais podem ser facilmente convertidos com outros ânions (WASSERSCHEID; WELTON, 2008).

O segundo passo ocorre quando não há formação do ânion desejado na reação de quaternização, ou quando este se torna instável. Este processo ocorre através da reação do haleto do cátion orgânico com um ácido de Lewis, ou através da troca (metátese) de um ânion por outro. Os ácidos de Lewis geralmente utilizados são cloreto de alumínio ($AlCl_3$), tricloreto de boro (BCl_3), cloreto de cobre ($CuCl_2$), cloreto de ferro (II) ($FeCl_2$) ou cloreto de estanho ($SnCl_2$) (WASSERSCHEID; WELTON, 2008).

A capacidade de ser “criado” a partir da combinação de diferentes cátions e ânions, que consequentemente afetam suas características físico-químicas, fazem destas substâncias únicas e com uma gama de possibilidades (GHANDI, 2014).

Assim, à medida que novos LIs foram criados também divisões para classificá-los foram propostas e atualmente existem vários tipos de LIs, por exemplo, LI a temperatura ambiente (RTILs - sigla em Inglês para *room-temperature ionic liquids*), LIs específicos para tarefas (TSILs- sigla em Inglês para *task-specific ionic liquids*; membranas de LI suportadas (SILMs - sigla em Inglês para *supported IL membranes*) que incluem compostos de LI suportados em estruturas metal-orgânicas (MOFs - sigla em Inglês para LIs *supported on metal−organic*) e LIs polimerizáveis (PILs - sigla em Inglês para *poly(ionic liquids*)) (LEI et al., 2017)

No âmbito da engenharia de materiais, mais especificamente aos materiais poliméricos, o uso de LIs em reações de polimerização, não é recente, sendo empregado como solvente oferecem uma série de vantagens, como o efeito positivo sobre a cinética da reação, separação do polímero do catalisador residual ou a redução da extensão das reações secundárias (DISASA IRGE, 2016). No entanto, mais recentemente, maiores possibilidades são oferecidas por LIs polimerizáveis, isto é, LIs contendo funções capazes de polimerizar formando materiais poliméricos, sólidos com as características físico-químicas dos LIs (MECERREYES, 2011).

3.3. Poli (líquidos iônicos)

Os poli(líquidos iônicos) são uma nova classe de materiais poliméricos formados a partir de monômeros de LIs que combinam as propriedades dos LIs com as propriedades mecânicas e o controle dimensional dos polímeros (MECERREYES, 2011). Os PILs com unidades análogas a líquidos iônicos (SHAPLOV; PONKRATOV; VYGODSKII, 2016) constituem uma categoria de materiais muito interessante devido à modularidade inerente de suas propriedades a partir da escolha de cátions e ânions, que em sinergia com as propriedades físicas do polímero têm um efeito considerável sobre as propriedades macroscópicas (MECERREYES, 2011; QIAN; TEXTER; YAN, 2017; YUAN; MECERREYES; ANTONIETTI, 2013).

PILs podem ser sintetizados a partir de líquidos iónicos que têm ligação dupla (SHAPLOV; PONKRATOV; VYGODSKII, 2016). Eles incluem um mínimo de um centro iônico semelhante a LIs. Em muitos casos, os PILs também compreendem cátions, como, por exemplo: imidazólio. Estes cátions podem ser ligados ao polímero principal ou ocorrer como íons opostos livres. Além disso, uma mistura de cátions e ânions permitem aos PILs diferentes aplicações (SHAPLOV; PONKRATOV; VYGODSKII, 2016). A Figura 4 apresenta uma comparação entre dois líquidos iônicos com estruturas semelhantes, o líquido iônico bis(trifluorometanosulfonil)imidato de 1-butil-3-metilimidazólio [Bmim][NTf_2], que possuí o grupo metilo, onde não há ligação dupla e na estrutura do LI bis(trifluorometanosulfonil)imidato de 3-butil-1-vinilimidazólio ([BVim][NTf_2]), que possui o grupo vinil.

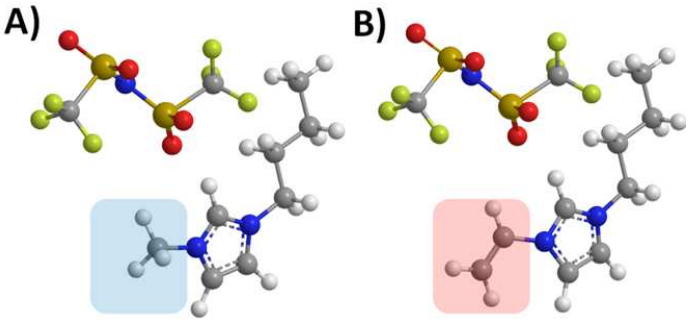

Figura 4. Estruturas de [Bmim][NTf_2] (a) onde o grupo metilo é sombreado azul claro e [BVim][NTf_2] (b), onde o grupo vinil é destacado em rosa.

Nos PILs, assim como ocorre com os LIs, a possibilidade de diferentes combinações entre ânions e cátions possibilita o desenvolvimento de inúmeros materiais iônicos com aplicações potenciais em uma ampla gama de campos, incluindo como polieleletrólitos para células solares sensibilizadas com corantes (ZHAO *et al.*, 2011), membranas para células de combustível (YAN *et al*., 2009), supercondensadores (AYALNEH TIRUYE et al., 2015), suporte para catalisadores (BURGUETE et al., 2010), antimicrobianos (RIDUAN; ZHANG, 2013) e na captura de CO_2 (SADEGHPOUR; YUSOFF; AROUA, 2017). Além disso, suas forças intermoleculares altamente ajustáveis tornam-os materiais ideais para estabilizar nanopartículas (MONTOLIO *et al*., 2016) e outros materiais avançados, como

nanotubos de carbono (MAO *et al.*, 2015), grafeno (KIM *et al*., 2010) e óxido de grafeno (TOKUDA *et al*., 2016).

Os PILs têm sido sintetizados na maioria dos casos, por polimerização radicalar direta dos monômeros de LI (SHAPLOV; PONKRATOV; VYGODSKII, 2016), a qual pode ser realizada através de dois caminhos diferentes: um pelo qual a metátese do ânion é feita antes da polimerização e o outro realizando a metátese após a polimerização, como pode ser visto na Figura 5.

Da mesma forma que os LIs os PILs sintetizados via polimerização radicalar direta são do tipo catiônicos, ou seja, a estrutura da cadeia principal apresenta porções catiônicas enquanto que a parte móvel (contra-íon) é a aniônica (MECERREYES, 2011).

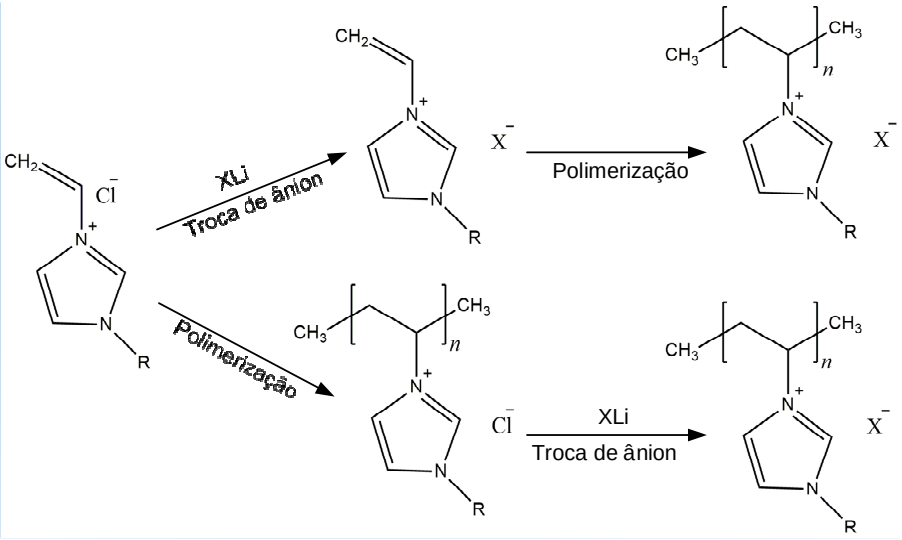

Figura 5.Ilustração genérica das rotas de sínteses dos Poli(líquidos iônicos)
(Fonte: MECERREYES, 2011)

Por sua vez, a síntese de monômeros polimerizáveis pode ser realizada a partir de diferentes rotas, como segue: (a) substituição do cátion ou ânion em monômeros iônicos através da reação de metátese; (b) formação de monômeros quaternizados via reações de aminas, fosfinas ou heterocíclicos com compostos contendo ânions polimerizáveis; c) Quaternização ou protonação de monómeros contendo grupo amina, grupo fosfina ou heterocíclicos; e (d) reações de substituição ou adição entre um LI funcionalizado e compostos contendo grupos reativos (vinil,

metacrilato, entre outros) (SHAPLOV; PONKRATOV; VYGODSKII, 2016). A Figura 6 apresenta uma representação ilustrativa destas rotas de síntese.

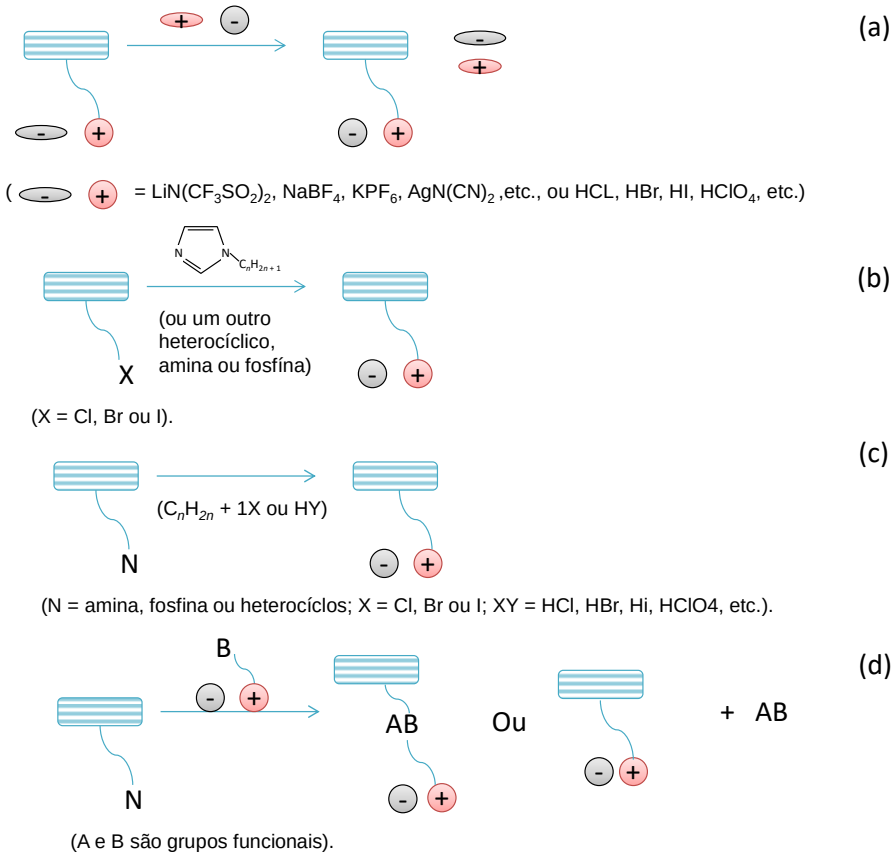

Figura 6. Ilustração da síntese de monómeros polimerizáveis

Cabe salientar que, os LIs têm sido utilizados na ciência de polímeros, em vários tipos de processos de polimerização, tais como polimerização via radical livre, polimerização via radical livre controlada (polimerização radical de transferência de átomos e transferência de fragmentação reversível), bem como em polimerizações iônicas e de coordenação (LU; YAN; TEXTER, 2009).

A polimerização por radicais livres é um método de polimerização pelo qual um polímero se forma pela adição sucessiva de blocos de construção de radicais livres, podendo ser formados por vários mecanismos diferentes, geralmente envolvendo moléculas iniciadoras separadas. Após a sua geração, o radical livre iniciador adiciona unidades monoméricas (não radicais), aumentando assim a cadeia polimérica (ODIAN, 2004).

A iniciação é o primeiro passo do processo de polimerização. Durante a iniciação, um centro ativo é criado a partir do qual uma cadeia de polímero é gerada. Nem todos os monômeros são suscetíveis a todos os tipos de iniciadores. A iniciação radicalar funciona melhor na ligação dupla carbono-carbono dos monômeros de vinil e na ligação dupla carbono-oxigênio nos aldeídos e cetonas. A iniciação tem dois passos. No primeiro passo, um ou dois radicais são criados a partir das moléculas iniciadoras. No segundo passo, os radicais são transferidos das moléculas iniciadoras para as unidades monoméricas presentes (ODIAN, 2004).

Várias opções estão disponíveis para esses iniciadores, entre eles, iniciadores fotossensíveis à luz ultravioleta (ODIAN, 2004). Os sistemas de polímeros curáveis por ultravioleta (UV) são de particular interesse no desenvolvimento de novos materiais. A fotopolimerização é iniciada por fotoiniciadores que podem ser sistemas de fotoiniciadores monocomponentes ou multicomponentes. Eles formam espécies iniciadoras (radicais livres ou íons) na absorção da luz UV. Os fotoiniciadores de radical livre, por sua vez, podem ser classificados em dois grupos principais: clivagem (Tipo I) e abstração de hidrogênio (Tipo II). A formação de radicais iniciadores ocorre (i) em uma reação monomolecular por meio de uma clivagem da ligação homolítica dos fotoiniciadores (reacão 3.1) e (ii) em uma reação bimolecular entre o fotoiniciador e o doador de hidrogênio DH (co-iniciador) em sistemas do Tipo II (reação 3.2) (ANDRZEJEWSKA, 2017)

$$PI + h\nu \rightarrow R1^{\cdot} + R2^{\cdot} \qquad (3.1)$$

Onde PI é o fotoiniciador, *hv* representa a luz ultravioleta e $R1^{\cdot}$ e $R2^{\cdot}$ são radicais livres formados. Radicais são tipicamente gerados por fotoindução de transferência eletrônica na qual o co-iniciador (DH) participa do processo de transferência de elétrons (reação 3.2a) ou por transferência direta de hidrogênio (reação 3.2b) (ANDRZEJEWSKA, 2017):

$$PI + DH + h\nu \rightarrow PI^{-\bullet} + DH^{+\bullet} \rightarrow PIH \cdot + D \cdot \qquad (3.2a)$$
$$PI + DH + h\nu \rightarrow PIH \cdot + D \cdot \qquad (3.2b)$$

A maioria dos fotoiniciadores Tipo I são compostos carbonílicos aromáticos substituídos. Os sistemas do tipo II são baseados em cetonas aromáticas, como benzofenona, tioxantonas, benzil, quinonas (que não sofrem fotoclivagem), em combinação com co-iniciador (doador de hidrogênio) (ANDRZEJEWSKA, 2017).

Iniciação fotoquímica de polimerização oferece várias vantagens em comparação com a iniciação térmica como alta velocidade da reação. O uso da luz permite o controle temporal e espacial do processo de cura, possibilitanto que a polimerização ocorra apenas durante o período de irradiação (começa com o início da exposição e cessa após sua conclusão) e somente nas áreas irradiadas. Como a fotopolimerização usa a reação fotoquímica exclusivamente na etapa de iniciação, a reação iniciada em suas etapas adicionais procede da mesma maneira que induzida por outros métodos (ANDRZEJEWSKA, 2017).

Devido a estas características, recentemente, as tecnologias de manufatura aditiva, mais especificamente o processos de estereolitografia, vem destacando-se no desenvolvimento de materiais poliméricos (SCHULTZ et al., 2014a). Estas tecnologias usam material de impressão líquida e baseia-se no princípio da fotopolimerização para produzir modelos 3D usando fotoiniciadores e luz visível, ou ultravioleta (WANG et al., 2017).

3.4. Manufatura aditiva

A manufatura aditiva, também conhecida por impressão em 3D, é uma tecnologia que produz objetos tridimensionais camada-a-camada com base em modelos CAD (Desenho assistido por computador, do inglês: *Computer Aided Design*). Nas últimas décadas várias técnicas de impressão vêm sendo exploradas para fabricar compósitos de polímero. Segundo Wang *et al.* (WANG et al., 2017) algumas destas técnicas estão bem estabelecidas, como modelagem de deposição fundida, sinterização seletiva de laser, impressão a jato de tinta 3D e a estereolitografia. Cada técnica tem suas próprias vantagens e limitações na produção de produtos compostos. A seleção da técnica de fabricação depende dos materiais de partida, dos requisitos de velocidade de processamento e resolução, custos e requisitos de desempenho dos produtos finais (WANG *et al.*, 2017). As

técnicas estabelecidas de prototipagem rápida estão resumidas na Figura 7. Entre estas tecnologias, destaca-se a impressão 3D baseada em sistema de estereolitografia.

A estereolitografia é considerada o processo por trás da impressão em 3D, com o primeiro equipamento a ser patenteado em 1986 por Charles Hull (WANG et al., 2017). O processo de estereolitografia, também conhecido como SLA (sigla em Inglês para *Stereolithography Apparatus*), usa material de impressão líquida e baseia-se no princípio da foto-polimerização para produzir modelos 3D usando substância química sensível a ultravioleta (UV) (SINGH; RAMAKRISHNA; SINGH, 2017). Assim, os reagentes são solidificados pela passagem de um feixe de laser (YANG et al., 2017). A estereolitografia é uma tecnologia de fabricação que permite o design e a criação de objetos geometricamente complexos com características <100 μm, com topologia adaptada e, portanto, possibilitando atribuir funcionalidade ao objeto (SCHULTZ et al., 2014b).

Tal como acontece com qualquer técnica convencional de impressão em 3D, na impressão por SLA é necessário um arquivo digital 3D. Isso pode ser obtido através de software de CAD (SolidWorks, Sculpt ou SelfCAD, por exemplo). Esses arquivos (geralmente arquivos de extensão tipo STL) são utilizados por um *slicer*, que é um software que converte modelos digitais 3D em camadas finas e após envia as instruções de impressão para que a impressora 3D construa um objeto (SINGH; RAMAKRISHNA; SINGH, 2017). Uma vez que o contorno da camada foi produzido, o interior é preenchido (parcialmente) e, portanto, solidificado (BIKAS; STAVROPOULOS; CHRYSSOLOURIS, 2016). Após a conclusão da camada, a plataforma de construção é reduzida por uma distância igual à espessura da camada (normalmente entre 0,003-0,002 in ou seja 0,0762-0,0508 mm), e uma camada posterior é formada em cima das camadas previamente concluídas. Este processo continua a repetir o procedimento acima mencionado até a última camada do modelo/protótipo é traçada pelo laser (SINGH; RAMAKRISHNA; SINGH, 2017).

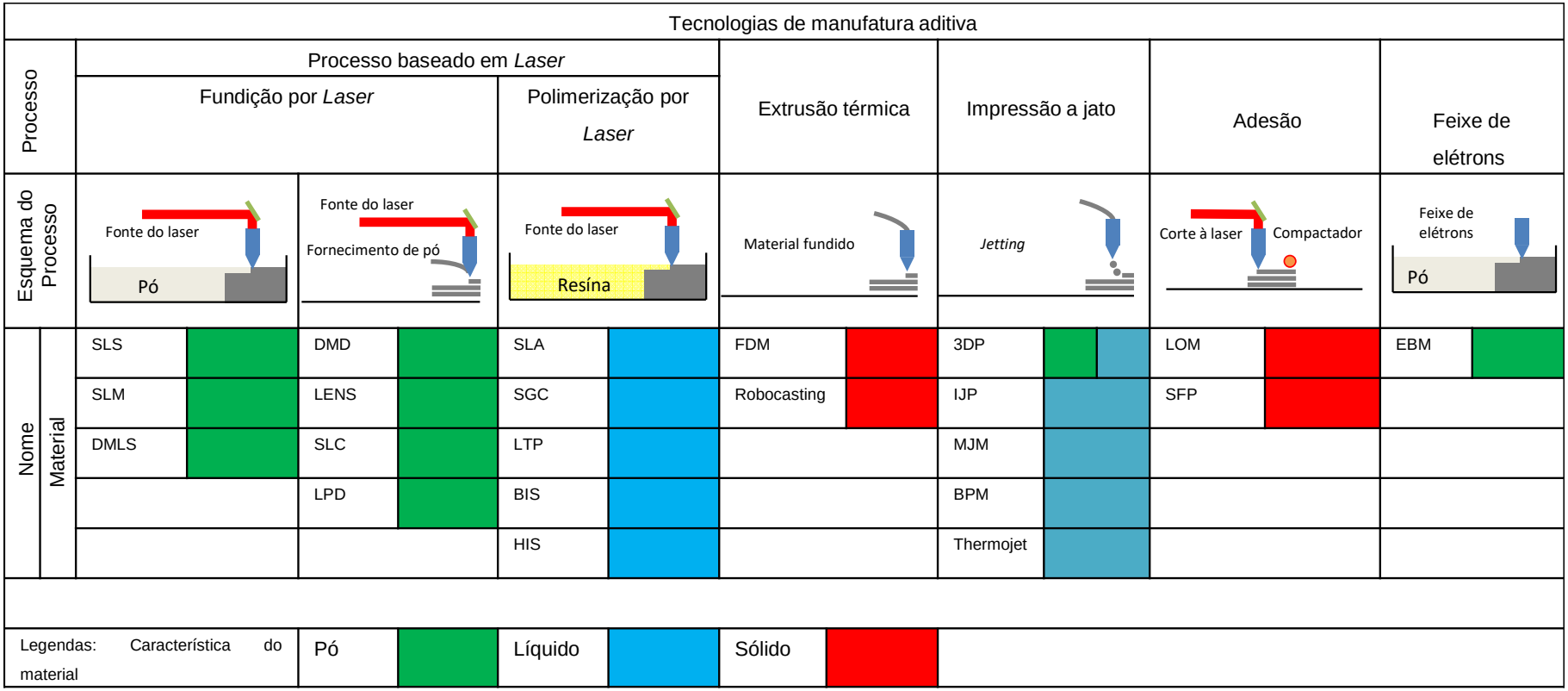

Figura 7. Categorização do processo das tecnologias de manufatura aditiva. (*Selective laser sintering (SLS), Direct metal laser sintering (DMLS), selective laser melting (SLM), Direct metal deposition (DMD), Laser engineered net shaping (LENS), Selective laser cladding (SLC), Selective laser cladding (SLC), Laser powder deposition (LPD), Stereolithography Apparatus (SLA), Solid ground curing (SGC), Liquid thermal polymerization (LTP), Beam interference solidification (BIS), Holographic interference solidification (HIS), Fused deposition modelling (FDM), Three-dimensional printing (3DP), Inkjet printing (IJP), Multijet modelling (MJM), Ballistic particle manufacturing (BPM), Laminated object manufacturing (LOM), Solid foil polymerization (SFP), Electron beam manufacturing (EBM)*)

Fonte: traduzido de BIKAS; STAVROPOULOS; CHRYSSOLOURIS, (2016)

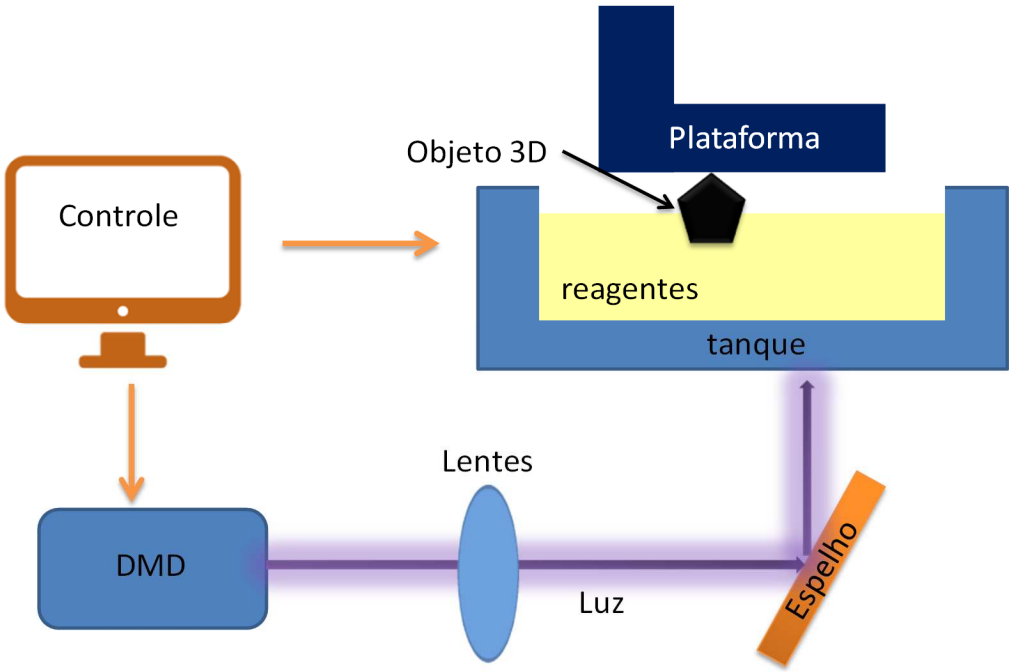

Figura 8. Diagrama de processo de fabricação aditiva baseada em estereolitografia. DMD = Dispositivo de microespelhos digital; UV = ultravioleta.
(Adaptado de YANG et al., 2017)

Uma impressora SLA consiste principalmente em uma plataforma móvel, que é imersa em um banho de reagentes e uma fonte laser, incluindo o hardware apropriado e software para controle (Figura 8). Como pode ser observado na Figura 8 as impressoras de estereolitografia contêm um tanque, uma plataforma móvel (eixo Z), um sistema de separação (peça/plataforma) (eixo X), um laser, uma óptica de focagem e um espelho galvanométrico (eixos X e Y).

3.5. Avaliação do Ciclo de Vida (ACV)

A Avaliação do Ciclo de Vida é um processo voltado a avaliar as implicações ambientais de um produto, processo ou atividade, através da identificação e da quantificação dos usos de energia e matéria e das emissões ambientais. A partir da ACV é possível identificar e avaliar oportunidades de realizar melhorias ambientais (UNEP/SETAC, 2011).

A ACV é uma ferramenta robusta, sendo parte integrante da tomada de decisões na indústria e em organizações governamentais e não governamentais, bem como tem sido explorada pela comunidade científica. As razões para essa ampla aplicação podem ser encontradas, por exemplo, devido que a ACV é uma metodologia reconhecida internacionalmente e possui uma sólida base científica, sendo padronizada pelas normas NBR 14040:2009 e NBR 14044:2009 (ABNT, 2009a, 2009b).

O termo “ciclo de vida” refere-se à as atividades no curso da vida do produto desde sua fabricação, utilização, manutenção e diposição final; incluindo aquisição de matéria-prima necessária para a fabricação do produto (DE BRUIJN; DUIN; HUIJBREGTS, 2002). Um estudo de ACV é composto por quatro etapas: (1) Definição de objetivo e escopo; (2) Análise do inventário; (3) Avaliação dos impactos; e (4) Interpretação. Essas etapas serão detalhadas a seguir.

3.5.1. Definição dos Objetivos e do Escopo

A definição do objetivo e do escopo é a primeira fase de uma ACV. Nela deve ser claramente justificada a motivação, o objetivo, os limites do sistema, a unidade funcional (UF) e considerações particulares ao estudo (ABNT, 2009a, 2009b). A seguir as principais terminologias relacionadas a esta etapa são apresentadas:

Função do produto: Característica de desempenho do produto, a função é a finalidade do produto selecionada para ser o objeto do estudo de ACV (ABNT, 2009a);

Unidade funcional: Desempenho quantificado de um sistema de produto para utilização como uma unidade de referência (ABNT, 2009b);

Fluxo de referência: Quantidade do produto necessária para que ele exerça a função na quantidade estabelecida pela unidade funcional (ABNT, 2009b);

Sistema de produto: Conjunto de processos elementares conectados material e energeticamente pelos fluxos elementares, intermediários e de produto, que modela o ciclo de vida de um produto(ABNT, 2009a);.

Fronteira do Sistema: Interface entre um sistema de produto e o meio ambiente ou outros sistemas de produto. Conjunto de critérios que especificam quais processos elementares fazem parte de um sistema de produto (ABNT, 2009a);

3.5.2. Análise do Inventário

Nesta etapa são apresentados todos os fluxos materiais e energéticos e suas devidas emissões para os diferentes compartilhamentos (ar, água e solo) (DE BRUIJN; DUIN; HUIJBREGTS, 2002), assim, constituindo-se um Inventário de Ciclo de Vida (ICV). Em outras palavras, nesta fase, as entradas (*inputs*) e as saídas (*outputs*) devem ser qualificadas e quantificadas levando-se em consideração a unidade funcional definida. Os procedimentos necessários para a construção do ICV são ilustrados na Figura 9.

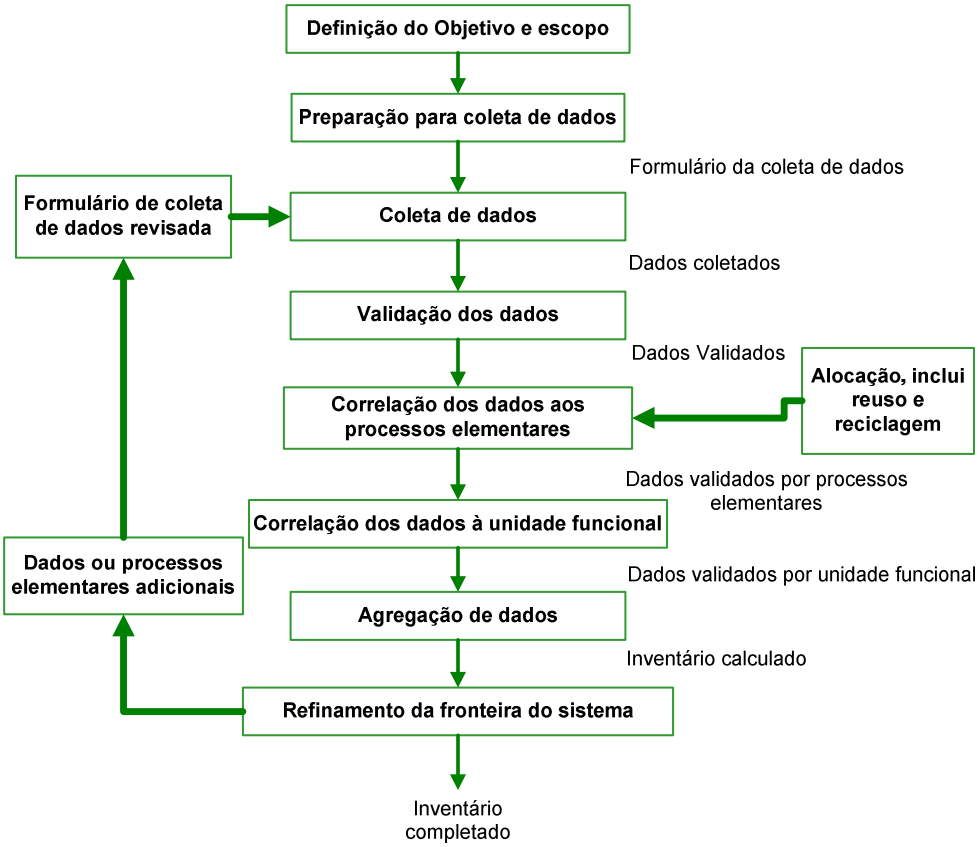

Figura 9. Procedimentos simplificados para análise de inventário.

Fonte: (adaptado de ABNT, 2009b).

Por fim, a coleta dos dados para construção do inventário é uma das etapas mais importantes na análise de inventário. De acordo com DE BRUIJN; DUIN; HUIJBREGTS, (2002) os dados podem ser divididos em dois grupos: (a) dados primários: construídos a partir de questionários, mensurados ou calculados; e (b) dados secundários: dados de literatura, tabelados ou de base de dados.

3.5.3. Avaliação do Impacto Ambiental

Nesta etapa os dados de inventário são convertidos em categorias de impacto ambiental a partir de métodos de caracterização. Existem muitos métodos de caracterização, eles diferem numericamente em suas equivalências e ou nas substâncias abordadas em uma determinada categoria de impacto (DE BRUIJN; DUIN; HUIJBREGTS, 2002).

3.5.4. Interpretação de Resultados

Os resultados são analisados de acordo com as definições do objetivo e escopo do estudo. Consequentemente, esta fase permite tomar medidas remediadoras e decisões estratégicas (DE BRUIJN; DUIN; HUIJBREGTS, 2002), reduzindo o risco sobre o impacto ambiental do projeto.

4. METODOLOGIA

Nesta seção, é introduzida a estrutura metodológica pertinente aos artigos elaborados a partir deste trabalho. Cabe salientar que este estudo foi conduzido conforme os preceitos e diretrizes preconizados pela metodologia da ACV. Adicionalmente, os resultados obtidos na etapa 1 (revisão) foram empregados para nortear a condução deste estudo. De forma geral, é possível segregar a metodologia em 6 etapas, como apresentado na Figura 10.

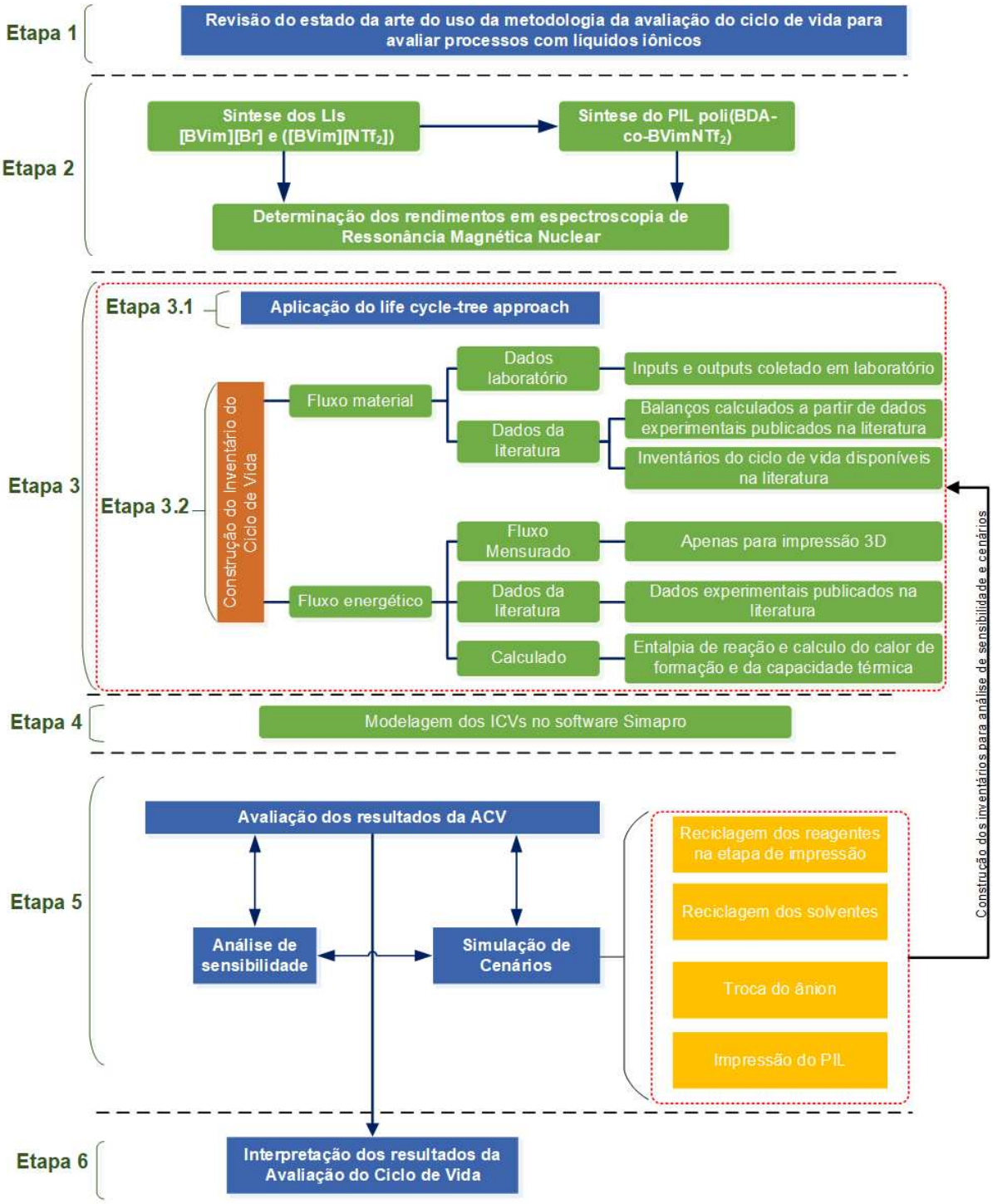

Figura 10. Representação das etapas metodológicas empregadas neste estudo.

4.1. Etapa 1 – Revisão da aplicação da ACV para avaliar LI

Inicialmente, uma revisão da literatura sobre o tema foi realizada com objetivo de conhecer o atual estado da arte e nortear a condução de futuros estudos de ACV envolvendo processos que utilizam LI. A busca de literatura científica foi realizada

até o mês de fevereiro do ano e 2018 e utilizando as seguintes fontes de pesquisa: banco de dados on-line da *Web of Science*, *Science Direct* e *Google Scholar*. A busca foi limitada as palavras “líquido iônico” e “ciclo de vida”, sendo considerados apenas trabalhos publicadas na língua Inglesa.

4.2. Etapa 2 – Procedimentos experimentais

Os procedimentos experimentais relacionados à síntese dos LIs (brometo de 3-butil-1-vinilimidazólio e bis(trifluorometanosulfonil)imidato de 3-butil-1-vinilimidazólio) e do processo de impressão 3D foram conduzido no *GSK Carbon Neutral Laboratory* for *sustainable chemistry* da Universidade de Nottingham no Reino Unido. Nesta etapa, os fluxos foram qualificados e quantificados para posterior construção dos inventários do ciclo de vida.

A determinação do rendimento reacional foi realizada em um espectrómetro de Ressonância Magnética Nuclear (RMN) Bruker AVX400 disponível na Universidade de Nottigham. A seguir os procedimentos experimentais são brevemente descritos.

4.2.1. Síntese do brometo de 3-butil-1-vinilimidazólio ([BVim][Br])

Carregou-se um frasco com 1-vinil-imidazole (37,64 g, 400 mmol) e 1-bromobutano (42,95 mL, 400 mmol) e depois selou-se com uma tampa untada com lubrificante. A reação foi aquecida a 40 ℃ com agi tação durante 16 horas. Depois, o produto bruto foi obtido por adição de éter dietílico (200 mL) e trituração com um bastão de vidro. O sólido resultante foi recolhido por filtração e lavado com éter dietílico (200 mL) três vezes. Depois o produto bruto foi redissolvido em diclorometano (100 mL), antes de ser adicionado éter dietílico (500 mL), gota-a-gota, sobre rapida agitação para formar um precipitado branco cristalino. Este produto foi seco sob pressão reduzida a 40 ℃ durante 6 horas p ara proporcionar brometo de 3-butil-1-vinilimidazólio.

4.2.2. Síntese do bis(trifluorometanosulfonil)imidato de 3-butil-1-vinilimidazólio ([BVim][NTf_2])

Inicialmente o bis(trifluorometanosulfonil)imidato de lítio ($LiNTf_2$) (113,75 g, 396,21 mmol) em água (100 mL) e a esta solução foi adicionada uma solução aquosa (100 mL) de brometo de 3-butil-1-vinilimidazólio (60,77 g, 264 mmol), o que causou a formação de duas fases líquidas. Esta mistura foi agitada rapidamente durante 6 horas à temperatura ambiente. As fases foram separadas e a fase aquosa foi extraída três vezes com diclorometano (200 mL). As fases orgânicas combinadas foram lavadas três vezes com água (100 mL) e depois secas com $MgSO_4$. Em seguida, a fase orgânica foi então passada através de uma coluna básica de Al_2O_3 e depois reduzida em vácuo para formar um líquido oleoso incolor. Em seguida, o produto foi ainda seco em linha *Schlenk* a 40 ℃ durante 5 horas para obter bis(trifluorometanosulfonil)imidato de 3-butil-1-vinilimidazólio como um líquido oleoso viscoso límpido e incolor.

4.2.3. Síntese do Poli(líquido iônico)

Nesta etapa, projeções de PIL com dimensões de 24 mm x 16 mm x 0,5 mm constituídas de poli(BDA-co-BVimNTf_2) com 80% molar do líquido iônico [BVim][NTf_2] foram sintetizadas. Nesta etapa o software Creation Workshop RC36 foi usado para gerar as fatias de uma espessura desejada (50 μm/camada), controlar o tempo de projeção das imagens e o movimento tridimensional. Uma impressora 3D LittleRP FlexVat foi preenchida com uma mistura de reagentes que continha 80% molar [BVim][NTf_2] (8 mmol, 3,44 g), 20 mol% diacrilato de 1,4-butanodiol (2 mmol, 0,39 g) e óxido de (2,4,6-trimetil benzoil)difenil fosfina (1 mmol, 0,035 g). A Figura 11 apresenta a síntese do PIL. Em seguida, a plataforma foi mergulhada no reagente em direção ao filme de Teflon transparente do FlexVat. A luz UV passou da lâmpada do projetor e do espelho para o filme de Teflon transparente do FlexVat atingindo a plataforma. Cada camada (50 μm) foi curada por 8s. O processo foi repetido até que o objeto fosse completamente fabricado. A Figura 12 apresenta um esquema geral das etapas que envolvem a síntese dos PILs a partir do sistema de estereolitografia. Depois que o objeto foi fabricado, o objeto foi isolado e lavado com isopropanol para remover qualquer reagente não curado. Em seguida, o objeto foi seco no escuro à

temperatura ambiente durante a noite. A Figura 12c apresenta a imagem do PIL síntesizado a partir do sistema de estereolitografia neste estudo.

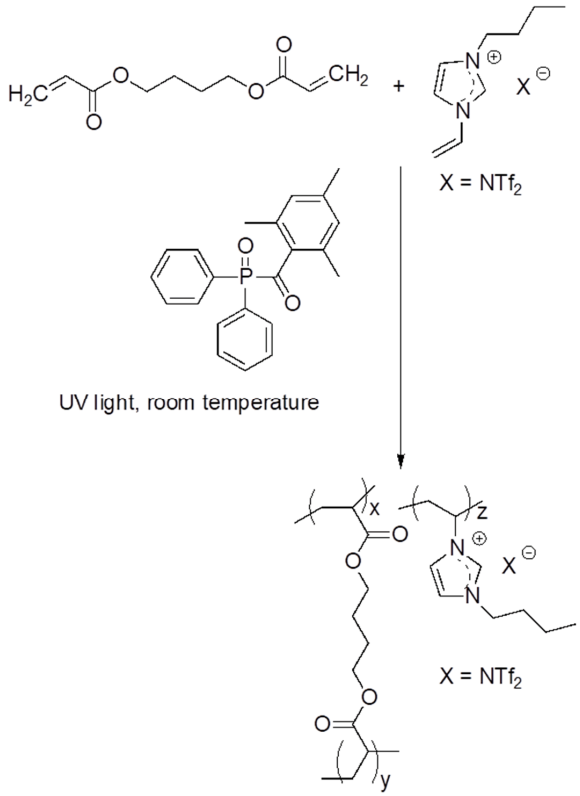

Figura 11. Síntese do PIL imidazólio por impressão 3D a partir do sistema de estereolitografia

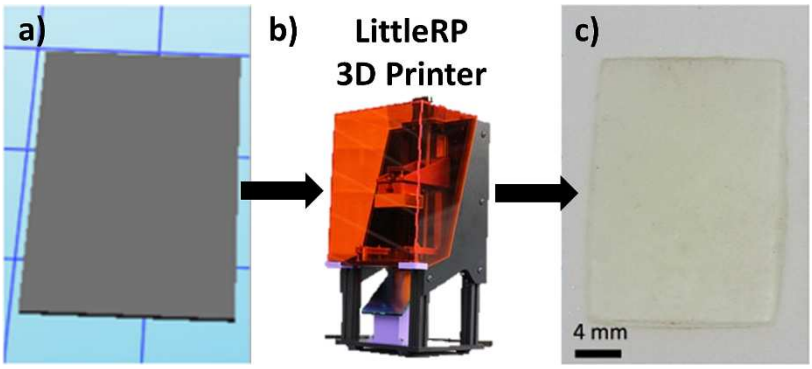

Figura 12. Esquema geral das etapas que envolvem a síntese de PILs a partir do sistema de estereolitografia. Desenho do objeto em software CAD (a); modelo comunicado à Impressora 3D Little RP, utilizada neste estudo (b); objeto 3D desejado (PIL) (c).

4.3. Etapa 3 – Inventário do Ciclo de Vida.

No que diz respeito, especificamente, à condução da ACV os fluxos materiais e energéticos do ciclo de vida relacionados à produção dos PILs, LIs e seus precursores foram derivados de uma combinação de dados primários obtidos em laboratório, literatura, cálculos teóricos e fontes de dados secundários, como bancos de dados. Nesta oportunidade, também foram construídos os inventários relacionados às análises de sensibilidade e para os diferentes cenários avaliados. Esta etapa pode ser dividida em duas subetapas, como segue:

4.3.1. Etapa 3.1 – Aplicação da abordagem “*life cycle tree*”.

Neste trabalho, uma avaliação completa do ciclo de vida foi realizada usando a abordagem “*life cycle tree*”. A partir desta abordagem é possível traçar todas as rotas químicas e processos envolvidos, o que irá permitir uma visão sistêmica do produto avaliado e identificar quais substâncias não estão disponíveis nas bases de dados e que deverão ter seus ICVs construídos. Esta abordagem foi identificada na revisão da literatura (etapa 1) como uma metodologia recomendada para construção de ICVs, quando a disponibilidade de dados é limitada ou inexistente, portanto, sendo recomendado para substâncias emergentes como os LIs. Nesta abordagem, uma árvore do ciclo de vida da substância em estudo é construída, considerando a rota de síntese, remontando aos precursores básicos para os quais dados do ciclo de vida estão disponíveis (por exemplo, hidrogênio, amoníaco, benzeno, metanol etc.). A principal característica desse método é que ele começa a partir da "porta" ou "túmulo", e passa por todos os processos principais até o "berço" (Cuéllar-Franca *et al*., 2016; Mehrkesh e Karunanithi, 2013; Peterson, 2013; Zhang *et al.* , 2008).

4.3.2. Etapa 3.2 – Balanços materiais e energéticos

4.3.2.1. *Fluxos materiais*

As entradas e saídas de material na fase de impressão 3D dos PILs baseados em imidazólio foram obtidas de dados experimentais. As entradas de [BVim][Br] e [BVim][NTf_2] foram coletadas de dados primários gerados no laboratório. Os resultados dessas substâncias foram calculados a partir do balanço de massa. Os balanços mássicos para os precursores PIL, que não estavam disponíveis no banco de dados ecoinvent v3.2, foram calculados, levando-se em consideração o consumo de reagentes e o rendimento da reação obtidos a partir da literatura, conforme preconizado em Felder e Rousseau, (2005).

4.3.2.2. *Fluxos energéticos*

O fluxo de energia do processo de impressão 3D foi determinado medindo o consumo de energia do processo de impressão através do uso de equipamento específico que mede o consumo de eletricidade (modelo Brennenstuhl® PM 231E).

Para todas as demais substâncias, não disponíveis no banco de dados ecoinvent v3.2 ou cujos dados energéticos não estavam disponíveis na literatura, a energia relacionada à sua fabricação foi calculada a partir de um cálculo do consumo energético teórico. Este cálculo foi baseado na multiplicação das entalpias de reação por fatores de correção, seguindo métodos da literatura (Cuéllar-Franca *et al*., 2016; Mehrkesh e Karunanithi, 2013). De acordo com Mehrkesh e Karunanithi, (2013) a estimativa do consumo de energia em escala industrial pode ser realizada multiplicando-se a entalpia de reação por um fator de correção de 4,2, quando a reação for endotérmica e 3,2 para reações exotérmicas. Propriedades termodinâmicas para condução dos cálculos foram obtidas nas bases de dados do *National Institute of Standards and Technology* (Instituto Nacional de Padrões e Tecnologia) (NIST, 2017) e da *Society for Chemical Engineering and Biotechnology* (Sociedade para Engenharia Química e Biotecnologia) (DETHERM, 2017).

Valores de entalpia de formação de líquidos iônicos que não estavam disponíveis na literatura foram calculados usando um método de regressão linear multivariado baseado em algoritmos genéticos proposto por Vatani et al. (2007). Similarmente, a capacidade térmica de líquidos iônicos, que não estavam disponíveis na literatura, foi calculada de acordo com o método de contribuição do grupo de Joback (Stouffer *et al.,* 2008). Cabe salientar que estas ponderações foram consideradas como limitações do estudo e uma análise de sensibilidade foi conduzida para estimar o efeito dos parâmetros termodinâmicos assumidos.

4.4. Etapa 4 – Modelagem no Software de ACV

Nesta etapa o ICV da produção de PILs imidazólico sintetizados por impressão 3D e os dados da análise de sensibilidade e dos cenários propostos foram modelados no Software SimaPro® versão *faculty* 8.4.0.0, utilizando a base de dados da ecoinvent v.3.2. No Apêndice A são apresentadas as bases de dados utilizadas para modelagem da ACV.

4.5. Etapa 5 – Avaliação do Ciclo de Vida

Nesta etapa, a etapa de Avaliação do Ciclo de Vida foi conduzida. Além disso, algumas análises de sensibilidade e cenários foram realizadas, como segue:

a) Análise de sensibilidade: Foi investigada a influência das variáveis termodinâmicas calculadas sobre os resultados da ACV. As variáveis termodinâmicas (entalpia de formação e capacidade térmica), quando não disponíveis na literatura, foram calculadas, portanto, sendo atribuídas como limitações ao estudo da ACV.

b) Análise de sensibilidade à reciclagem dos reagentes: Foi investigada a influência da reciclagem dos reagentes durante a síntese do PIL na etapa de impressão 3D. Para tanto, os ICVs relacionados a estes cenários foram calculados.

c) Análise de sensibilidade aos solventes: Foi investigada a influência da recuperação dos solventes orgânicos empregados na síntese de algumas substâncias e decorrente da lavagem das peças 3D após impressão. Para tanto, os

ICVs relacionados a estes cenários foram calculados considerando cenários de reciclagem e o gasto energético decorrente deste processo.

d) Cenário da troca de ânion: Nesta oportunidade foram avaliados os efeitos da troca do ânion bis(trifluorometanosulfonil)imidato ($[NTf_2]^-$) pelo dicianamida $[N(CN_2)]^-$ nos impactos do ciclo de vida do PIL. Cabe salientar que para esta comparação foi necessário a construção de ICVs relacionados à substância dicianamida $[N(CN_2)]^-$ e da etapa de impressão.

e) Cenário comparativo entre monômeros e LI convencional: Nesta oportunidade foi comparado o monômero de LI, polimerizável, $[BVim][NTf_2]$ e LI convencional, não polimerizável, $[Bmim][NTf_2]$. Cabe salientar que, para esta comparação foi necessário a construção de ICVs, do berço-ao-portão, da produção do LI $[Bmim][NTf_2]$.

4.6. Etapa 6 – Interpretação dos resultados

Nesta etapa foi realizada uma análise de contribuição de processos com objetivos de identificar os principais processos e substâncias que contribuem sobre os diferentes impactos avaliados. Além disso, os resultados de todos os cenários e das análises de sensibilidade foram avaliados com objetivo de fundamentar as conclusões.

5. RESULTADOS

Nesta secção, em forma de artigos, serão apresentados os métodos, resultados e discussões pertinentes a esta tese, divididos da seguinte forma: ACV de líquidos Iônicos: estado da arte e recomendações (Capítulo I) e Avaliação da performance ambiental de Líquidos Iônicos polimerizáveis via impressão 3D (Capítulo II).

5.1. Capítulo I: ACV de líquidos iônicos: estado da arte e recomendações

O artigo de revisão intitulado "*State-of-the-art and limitations in the life cycle assessment of ionic liquids*" foi submetido e encontra-se sobre revisão em um periódico qualificado pela Capes com o Qualis A1 (Química e Engenharias II), Cite Score de 5,79 e fator de impacto de 5,65. Este estudo apresenta uma revisão que fornecer uma visão geral atualizada dos estudos de ACV ambiental estabelecidos até o momento sobre líquidos iônicos e propõem recomendações para uma aplicação abrangente da estrutura de ACV. O estudo retrata que há toda uma lista de questões que precisam de maior precisão para uma aplicação de ACV para avaliar o LI. Onze trabalhos foram avaliados e uma série de suposições e abordagens foram identificadas para estimar os fluxos materiais e energéticos. Este artigo de revisão apresenta novos avanços para diminuir as lacunas que envolvem a falta de inventário de ciclo de vida de LI, tais como: utilizar uma abordagem que não negligencie as fases do ciclo de vida, considerar sua reutilização e reciclagem e estimar balanços materiais considerando o rendimento das reações envolvendo os LIs e substâncias intermediárias. Além disso, os resultados deste trabalho servem como um norteador para condução de futuros estudos sobre o tema ou na avaliação de sustâncias químicas emergentes.

State-of-the-art and limitations in the life cycle assessment of ionic liquids

Vinícius Gonçalves Maciel,[1,2] Dominic J. Wales,[3,4,†] Marcus Seferin,[1,2] Cássia Maria Lie Ugaya,[5] Victor Sans* [3,4]

[1]School of Chemistry, Pontifical Catholic University of Rio Grande do Sul, Porto Alegre, Brazil
[2] Polytechnic School, Post-Graduation Program in Materials Engineering and Technology, Pontifical Catholic University of Rio Grande do Sul, Porto Alegre, Brazil
[3]Faculty of Engineering, University of Nottingham, Nottingham, NG7 2RD, U.K.
[4]GSK Carbon Neutral Laboratory, University of Nottingham, Nottingham, NG7 2GA, U.K.
[5]Gyro Center of Life Cycle Sustainability Assessment, Federal University of Technology- Paraná, UTFPR, Brazil, CNPq fellow
* victor.sanssangorrin@nottingham.ac.uk

Abstract: Even though the development and use of ionic liquids (ILs) has rapidly grown in recent years, in the literature, information addressing the environmental performance of these substances in a life cycle context is comparatively scarce. This review critiques the state-of-the-art environmental life cycle assessment (LCA) studies on ILs in the literature, identifies the existing shortcomings, which could be delaying complete employment of the LCA framework to the field of ILs, and also identifies strategies for overcoming these shortcomings. This review indicates that there are several limitations associated with the implementation of the LCA in all steps and discusses them. Since data about manufacturing at industrial scale are generally inaccessible, a set of methods and assumptions have been used in previous studies to determine the life cycle inventories (LCIs), such as simplified LCA, "tree life-cycle approach", use of energy monitor devices, thermodynamic methods, chemical simulation process and other secondary data. However, the analysis of the data quality has not always been performed. Also, currently, the shortage of the characterisation factors of ILs for human toxicity and ecotoxicity impact categories, which prevent its inclusion within the life cycle impact assessment (LCIA) step. Therefore, sufficient and complete life cycle inventory data for ionic liquids and precursor chemicals are essential for inventory analysis; and the LCIA needs to be clearly defined about the level of detail on the IL emissions. Current LCA studies on ILs have not covered all these

† Present Affiliation: The Hamlyn Centre, Faculty of Engineering, South Kensington Campus, Imperial College London, London, SW7 2AZ, U.K.

aspects. To improve the present situation, it is proposed herein that for future LCA of processes involving ILs each of the LCA steps must be completed as far as scientific advances allow.

Key words: life cycle inventory, chemical inventory, ionic liquids, life cycle assessment

1 INTRODUCTION

Ionic liquids (ILs) are ionic compounds that feature intermolecular interactions between a cationic organic moiety and an inorganic or organic anion. Since 2000, the number of published papers concerning ionic liquids has rapidly grown (**Figure 1**). Indeed, the potential and benefits of ILs in various industrial applications have been recognized and highlighted extensively (Disasa Irge, 2016). An advantage of ILs is the capacity for adjusting the properties through appropriate choice of the cations and anions (D'Alessandro *et al*., 2010). Therefore, many different ILs have been reported because of the huge amount of possible combinations of anions and cations (Ghandi, 2014). Furthermore, these substances show advanced properties such as non-flammability, thermal stability, negligible vapour pressure and wide electrochemical windows (Ghandi, 2014; Wasserscheid and Welton, 2008). These unique and promising characteristics, in addition to the near-infinite combinations of anions and anions, mean that ILs are good candidates for a vast array of uses including, use as solvents (Ghandi, 2014; Kowsari, 2011; Zhang *et al.*, 2012), in chemical synthesis (Plechkova and Seddon, 2008), in electrochemistry (Hagiwara and Lee, 2007), for carbon capture (Bernard *et al.*, 2016; Torralba-Calleja *et al.*, 2013), polymeric derived materials and devices (Karjalainen *et al.*, 2018; Sans *et al.*, 2011; Wales *et al.*, 2018; Yuan *et al.*, 2013) and many more.

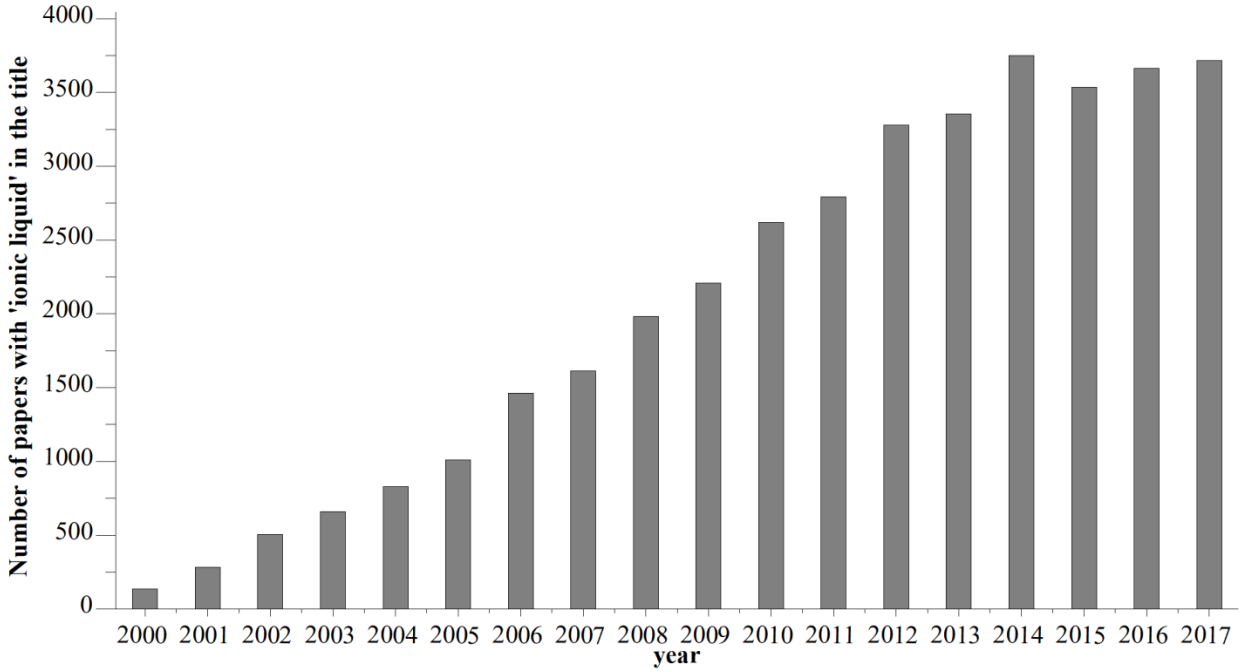

Figure 1. The number of published papers with the term 'ionic liquid' within the title has grown steadily since 2000. Data obtained by searching for number of publications each year with 'ionic liquid' within the title in the period of 2000 – 2017 inclusive in the Web of Science™ database by Clarivate Analytics.

Over the past decade, it has been claimed that ILs are "green solvent" replacements for organic solvents due to negligible volatility (Disasa Irge, 2016; Zhu *et al.*, 2009). However, a reduction in vapour emissions does not automatically make a greener process (Kralisch *et al.*, 2005). Furthermore, in most cases, synthesis of ILs includes a series of reactions and purification steps using volatile organic solvents (Zhu *et al.*, 2009). Compared to processes that use conventional organic solvents, it is highly likely that processes that use ILs as a solvent will have a larger life-cycle environmental impact (Zhang *et al.,* 2008).

Concerns regarding to the impact of ILs on the environment and human health have been reported (Disasa Irge, 2016; Heckenbach *et al.*, 2016). Many ILs present a comparatively high level of toxicity toward freshwater organisms, (Mehrkesh and Karunanithi, 2016a) and indeed, Pham *et al.* (2010) wrote an extensive review on IL toxicity to aquatic organisms. Furthermore, the limited number of ionic liquid toxicological studies published thus far indicate that the ionic liquids may have deleterious effects on human health (Mehrkesh and Karunanithi, 2016b; Zhu *et al.,* 2009).

Zhu *et al.*(2009) recommended that the environmental performance of the application of ILs ought to be assessed with the life cycle assessment (LCA) method, which considers the full process; raw material extraction, through the ionic liquids synthesis, to process applications, and to the recovery of ILs for reuse. Life cycle assessment (LCA) is an exhaustive framework that quantifies the environmental sustainability of a system, product or process over the complete life cycle (de Bruijn *et al.*, 2002). Nowadays, LCA has become an essential part of decision-making in industrial, governmental and non-governmental organizations, (Kralisch *et al.*, 2015) as well as being explored by the scientific community (Cerdas *et al.*, 2017; Cuéllar-Franca *et al.*, 2016; Jacquemin *et al.*, 2012). The wide application of LCA is due to the credibility, scientific recognition and clear application guidance of the ISO 14040 standard (ISO 14040, 2006), and the ISO 14044 standard (ISO 14044, 2006).

However, there are very few LCA studies on processes that involve ILs, despite the huge growth in ionic liquid science and applications (see **Figure 1**) This is attributed to these compounds being recently emerging materials (Cuéllar-Franca *et al.*, 2016) and because there are few inventory database available on the ILs and their precursors (Mehrkesh and Karunanithi, 2016a). Besides that, particular guidance for conducting a life cycle assessment for the case of ILs is absent. Thus, the core question which must be asked before utilization of the LCA framework to processes involving ionic liquids is whether there are sufficient and comprehensive Life Cycle Assessments (LCAs) for the ILs reported in the published literature.

The purpose of this perspective review is to give a critique of environmental life cycle assessment studies established on ionic liquids, to distinguish the existing shortcomings, which are delaying a complete utilization of the life cycle assessment framework to processes involving ILs, and designation of strategies to overcome the disadvantages. This review consists of six distinct parts. Firstly, section 3 covers a detailed review and analysis of existing LCA studies. Afterwards, the goal and scope of studies are investigated in section 4. Then the methods and strategies used to build life cycle inventory of ionic liquids are discussed in section 5, followed by an overview on the impact categories and methods applied (section 6). The interpretation step

is addressed in section 7 and finally, a summary of the shortcomings that were identified, and the proposed strategies to overcome the shortcomings, is presented in section 8.

2 METHODOLOGY

A scientific literature search up until February 2018 was conducted using the following literature databases: Web of Science online database, Science Direct, and Google Scholar. The search was strategy followed a sequential search limited to “ionic liquid” and “life cycle” published in English, excluding commentaries, news articles, reviews and letters or opinion pieces.

In this review, for a better understanding of the current situation involving the use of LCA methodology for evaluation of ILs and IL processes, four criteria were applied for each LCA step. The description of criteria and an associated ‘criteria weight’ attributed to them are presented in **Table 1**.

Table 1 Criteria for the analysis of studies applied in this review for each life cycle assessment steps.

Steps of LCA	**Description of criteria**		**Criteria weight**	
		High	Medium	Low
Goal and Scope	Life Cycle Stages covered	Cradle-to-grave, product systems and system boundaries clearly defined	Cradle-to-gate or product systems and system boundaries partially defined	Gate-to-gate or product systems or system boundaries are not defined
Life Cycle Inventory analysis	Clear information about the data used	Comprehensive data, inclusive of information on masses, energies and by-products	Incomplete data with the gaps in the data filled with qualified assumptions	Incomplete data with the data gaps not filled
Life cycle Impact Assessment	Impact categories covered	Covered multiple impact categories, also impact categories and characterization methods are clearly defined and justified	Only one impact category evaluated and/or its choice and characterization methods partially defined and/or justified	Impact categories and/or characterization methods not defined and justified
Interpretation	Data quality	Performed an analysis of the data quality	Analysis of the data quality partially performed	Did not perform an analysis of the data quality.

Goal and Scope: the stages of the life cycle covered (cradle-to-grave, gate-to-gate and cradle-to-gate) and product systems were chosen as parameters to evaluate the studies. The ISO 14044 standard states that the whole life cycle should be accounted for (cradle-to-grave) and only similar processes can be left out in LCA studies of comparison. Furthermore, product systems and system boundaries need to be clearly defined (de Bruijn *et al*., 2002). Besides that, the guideline of the World Business Council for Sustainable Development's Chemical Sector (WBCSD, 2014) recommended that system boundaries should be cradle-to-grave for chemical product footprint, and when the goal of the assessment is to provide environmental information at a business-to-business level (*e.g.* chemical industry products are intermediates and can be used in multiple applications), cradle-to-gate studies are acceptable. Thus, it was assumed that cradle-to-grave or cradle-to-gate is a better approach than gate-to-gate.

Life Cycle Inventory analysis: This step of the life cycle assessment in each published study was analyzed considering the completeness of data quality based on the indicator recommended by Kralisch *et al.* (2015). It is important to highlight that the purpose of this evaluation is to investigate if LCA studies were built from a comprehensive life cycle inventory studies. Hence, life cycle inventories that presented clear information about the data used, inclusive of data on masses, energies, by-products, and recycling were assumed as "high completeness".

Life cycle impact assessment step: LCA studies were awarded a 'high criteria weight' if more than one impact category was reported and if categories and characterization methods were justified. The selection of category indicators, impact categories and characterization models should be consistent and justified with respect to the goal and scope of the LCA, in agreement with the UNEP/SETAC Life Cycle Initiative (Margni *et al.*, 2008).. Also, the WBCSD, (2014) recommended in their guidelines concerning assessment and reporting of product environmental footprints, , that a decision tree for choosing impact categories should be included, if using the life cycle assessment approach. For instance, by applying this decision tree it implies that global warming potential and human toxicity potential must be included in chemical sector LCA studies.

Finally, in the interpretation step, LCA studies were analysed by considering if data quality analysis was performed within the study. ISO 14040 (ISO 14040, 2006) and ISO 14044 (ISO 14044, 2006) state that the data quality analysis is a compulsory part of the LCIA.

3 LIFE CYCLE ASSESSMENT STUDIES OF IONIC LIQUIDS

In this literature search, eleven LCA studies on ionic liquids were found. **Table 2** shows these eleven studies, the ionic liquids evaluated and a short introduction to each study. Generally speaking, the studies published to date have covered mainly butylmethylimidazolium ($[Bmim]^+$) as the IL cation, as well as applications (*e.g.* as a solvent in reactions) of several of these $[Bmim]^+$ cation-based ILs.

Table 1.Life Cycle Assessment studies of Ionic liquids

Entry	Reference	Description	ILs studied
1	Huebschmann *et al.* (2011)	Two case studies were shown: (i) a continuously running phase transfer catalysis of phenyl benzoate without catalyst and with ionic liquids as a catalyst; (ii) synthesis of the ionic liquid [Bmim][Cl].	[Bmim][Cl], $[C_{18}mim][Br]$, $[MIM][BuSO_3]$.
2	Zhang *et al*., (2008)	$[Bmim][BF_4]$ was the solvent and compared to conventional solvents for the synthesis of cyclohexane and for the Diels–Alder reaction	$[Bmim][BF_4]$
3	Kralisch *et al.*, (2005)	LCA study of the synthesis of ionic liquid $[Bmim][BF_4]$ and subsequent use of $[Bmim][BF_4]$ as a solvent in the metathesis of 1-octene	$[Bmim][BF_4]$
4	Kralisch *et al*., (2007)	Cost and environmental LCA of the $[C_6MIM][Cl]$ synthesis and comparison to $[C_6Py][Cl]$.	$[C_6MIM][Cl]$ and $[C_6Py][Cl]$
5	Farahipour and Karunanithi, (2014)	LCA study of carbon capture storage (CCS) using [Bmim][Ac] as a solvent to CO_2 absorption and LCA comparison to the organic solvent.	[Bmim][Ac]
6	Cuéllar-Franca et al., (2016)	This study presents a discussion on the estimation of the life cycle environmental impacts of ILs, and an application employing trihexyltetradecylphosphonium 1,2,4-triazolide ($[P_{66614}][124Triz]$)	$[P_{66614}][124Triz]$
7	Mehrkesh and Karunanithi, (2013)	Comparative LCA focusing on the synthesis of an energetic ionic liquid (1,2,3-triazolium nitrate) and 2,4,6-trinitrotoluene (TNT), a traditional energetic material.	1,2,3-triazolium nitrate
8	Mehrkesh and Karunanithi, (2016a)	The study compared the aquatic ecotoxicity impacts resulting from the production and application phase of five ionic liquids.	$[Bmim][BF_4]$, [Bmim][Br], [Bmim][Cl], $[Bmim][PF_6]$ and [BPy][Cl]
9	Righi *et al*., (2011)	The authors performed a "cradle to gate" LCA to analyse the environmental impacts of the dissolution of cellulose in the ionic liquid 1-butyl-3-methylimidazolium chloride ([Bmim][Cl])	[Bmim][Cl]
10	Peterson, (2013)	LCA of ionic liquids applied as a co-fluid of CO_2 in a refrigeration system	$[Hmim][NTf_2]$, $[P_{66614}]$[3triazolide]
11	Amado Alviz and Alvarez, (2017)	The environmental impact of [Bmim][Br] ionic liquid was compared to that of toluene when used in the synthesis of acetylsalicylic acid.	[Bmim][Br], [Bmim][Cl]

One of the first studies that used LCA to evaluate ILs was by Kralisch *et al.* (2005). They studied the employment of ILs as solvent for the metathesis of 1-octene compared to conventional solvents. Furthermore, they analyzed the energy requirement, environmental impact and substrate costs for the synthesis of 1-butyl-3-methylimidazolium tetrafluoroborate ([Bmim][BF_4]). Their results demonstrated that in certain circumstances, a reaction which is solvent-free may not necessarily be advantageous ecologically. In addition, the study questioned the assumption that a biphasic reaction is superior to a homogeneous phase reaction due to facilitated recycling. This was done by comparison of the energy requirement for the synthesis of a solvent which enables biphasic operation (*e.g.* ionic liquid) to the energy required to separate an homogeneous reaction mixture by distillation. The results showed a small difference between both processes.

Over the last ten years, several studies have assessed the use of ILs as a solvent to improve chemical processes. For example, an LCA study that compared the use of different solvents, such as organic solvents (acetone, benzene, ethyl ether), water and the ionic liquid [Bmim][BF_4], for the synthesis of cyclohexane and also for a Diels-Alder reaction (Zhang *et al.,* (2008)). The results indicated that for processes that use ILs it is highly likely that there will be a bigger life cycle environmental impact than for processes that use the other solvents analyzed. One recent study used LCA analysis to evaluate, during the synthesis of a pharmaceutical product, the employment of an IL as solvent. compared to the use of toluene. The results of comparing the environmental profile of the ionic liquid [Bmim][Br] to that of toluene in the synthesis of aspirin (acetylsalicylic acid) indicated that the IL had larger environmental impacts than the organic solvent, particularly in the ecotoxicity impact categories (Alviz and Alvarez, (2017)). Also, the effect of solvent recovery using separation technologies, and the effect of replacement of the anion (Br^- to Cl^-) of the ionic liquid were studied. Here, the environmental profile of [Bmim][Cl] and [Bmim][Br] were similar , although the toxicity of the former is comparatively higher.

There has been much interest paid to the use of ILs as potential candidates for carbon capture (Zhang *et al.*, 2012). Cuéllar-Franca *et al.,* (2016) recommended the use of LCA for evaluation of the environmental performance of ILs used for CO_2 capture. The example of [P_{66614}][124Triz]

was employed to demonstrate the use of the life cycle methodology through estimation of the life cycle environmental impacts of the ionic liquid in comparison to monoethanolamine (MEA).

An LCA comparison between 1-butyl-3-methylimidazolium acetate ([Bmim][Ac]) and MEA for carbon capture and sequestration (CCS) processes was made by Farahipour and Karunanithi (2014). The study did not consider the synthesis of the IL, but it was considered a full LCA. Energy and mass flows were estimated from pilot plant results and chemical simulation processes. The results indicated that a CCS process, using the ionic liquid [Bmim][Ac], with 90% CO_2 capture efficiency reduced life cycle greenhouse gas (GHG) emissions by only 50%. Peterson, (2013) conducted a full LCA, meaning a cradle-to-grave analysis of the synthesis of the ionic liquids 1-hexyl-3-methylimidazolium bis(trifluoromethylsulfonyl)imide and trihexyl(tetradecyl)phosphonium 1,2,3-triazolide and their use as a co-fluid involving CO_2 in refrigerant systems. This author reported that ionic liquid synthesis did not cause a significant contribution to the environmental impacts assessed.

The use of the ionic liquid [Bmim][Cl] to dissolve cellulose was compared to the environmental performance of the dissolution process currently used at an industrial scale with LCA analyses (Righi *et al.,* (2011)). Their results suggest that the process with IL could be significant from an in terms of impact on the environment, since the impacts of the process are similar to the impacts of the method developed by McCorsley, (1981) which uses a mixture of water and N-methylmorpholine N-oxide (NMMO/H_2O). However, it was shown that the process that used [Bmim][Cl] generated a higher environmental load in terms of abiotic resource depletion, ecotoxicity and volatile organic compound emissions than the mixed NMMO/H_2O solvent system.

An advantage of ionic liquids is the ability to diversify the properties through appropriate choice of the anion and cation and (D'Alessandro *et al.,* 2010). Kralisch *et al.,* (2007) compared the effect of the exchange of the N-base cation (where –base is either methylimidazole or pyridine). In this study, the configuration of optimized parameters for the synthesis of 1-hexyl-3-methylimidazolium chloride ([C_6mim][Cl]) was chosen as the starting configuration for the synthesis of n-hexylpyridinium chloride ([C_6Py]Cl).

Huebschmann *et al.*, (2011) have presented their research of a simplified life cycle assessment (SLCA), which is complemented with a superficial cost analysis that is exemplified with a pair of case studies: continuous running phase transfer catalysis of phenol and benzoyl chloride producing phenyl benzoate, and the solventless synthesis of [Bmim][Cl]. Ionic liquids ([Bmim][Cl], [mim][$BuSO_3$] and [C_{18}mim][Br]) were used in catalytic amounts, as opposed to being used as solvents. Nevertheless, from an ecological viewpoint, [mim][$BuSO_3$] was found to be more beneficial than [C_{18}mim][Br], due to the exothermic synthesis, whereas the latter is synthesized in an endothermic reaction, which requires 48 h of heating to 90 $^{\circ}$C. However, for the batch synthesis, the use of [Bmim][Cl] had the lowest overall environmental impacts. Also, the results are contrary to the cumulative energy demand (CED) of the batch syntheses, which indicates, that under similar conditions (*i.e.* with an identical energy demand for controlling and pumping) the continuously running synthesis would have a threefold ecological benefit.

Mehrkesh and Karunanithi, (2013) reported a cradle-to-gate life cycle environmental impacts for the synthesis of the ionic liquid 1,2,3-triazolium nitrate and compared it to the synthesis of 2,4,6-trinitrotoluene (TNT). It was found that synthesis of the IL has a significant larger environmental impact than the production process for TNT.

4 GOAL AND SCOPE OF LCA STUDIES

The step which involves defining the goal and scope of the LCA is the phase in which the first decisions concerning the working plan of the entire LCA are formed. The goal should be formulated with respect to the exact question, intended application and target audience (de Bruijn *et al.*, 2002). The scope of the study should be performed related to technological, geographical and temporal coverage, and the degree of sophistication relative to the goal (ISO 14040 (ISO 14040, 2006)). Also, the product or process assessed must be defined relative to the function and functional unit (de Bruijn *et al.*, 2002), and that all the inputs and outputs are assigned to the functional unit (Kralisch et al., 2015). ILs feature many specific functions and material properties (Ghandi, 2014; Wasserscheid and Welton, 2008). Therefore, the functional unit (FU) defines the main function or functions fulfilled by a product system and also specifies the extent of the function that will be examined in the resultant LCA study (de Bruijn *et al.*, 2002). For instance, for a synthesis, the functional unit could be defined in terms of the product synthesized.

In general, the goal and scope of the studies assessed in this work focused on the use of ionic liquids as a substitute for traditional organic solvents in chemical reactions. **Table 3** shows the scope of the LCA studies of ILs in the literature, the functional unit assumed and the IL applications described.

Table 2. The scope of LCA studies, functional unit and applications of IL.

Entry	Reference	Applications	System boundaries	Functional Unit
1	Huebschmann *et al.* (2011)	Catalyst	Cradle-to-Gate	1 kg of phenyl benzoate
2	Zhang *et al*., (2008)	Solvent	Cradle-to-Gate	1 kg of the solvent
3	Kralisch *et al.*, (2005)	Solvent	Cradle-to-Gate	n/a
4	Kralisch *et al*., (2007)	n/a	n/a	n/a
5	Farahipour and Karunanithi, (2014)	Solvent	Cradle-to-Gate	1 MWh
6	Cuéllar-Franca *et al.*, (2016)	n/a	Cradle-to-Gate	1 kg of $[P_{66614}][124Triz]$
7	Mehrkesh and Karunanithi, (2013)	Energetic ionic salt	Cradle-to-Gate	1 MJ energy content
8	Mehrkesh and Karunanithi, (2016a)	n/a	Cradle-to-Gate	1 kg of IL
9	Righi *et al*., (2011)	Cellulose dissolution	Cradle-to-Gate	1 kg of the dissolved cellulose
10	Peterson, (2013)	As a co-fluid of CO_2 in a refrigeration system	Cradle-to-Grave	n/a
11	Amado Alviz and Alvarez, (2017)	Solvent	Cradle-to-Gate	1 kg of acetylsalicylic acid

n/a: not available

Defining the system boundaries is a very crucial part of the scope definition in the life cycle assessment. Both the system boundaries and the product systems need to be clearly defined in each step of the life cycle, inclusive of inputs, processing routes, temporal and spatial considerations (de Bruijn et al., 2002). Furthermore, it is recommended that the system boundaries are justified towards the goal of the study (de Bruijn et al., 2002). However, some studies reviewed here did not show clearly defined system boundaries (see **Table 3**). The product system describes which of the processes that constitute the whole life cycle are to be within the assessment. In the most complete and inclusive LCA, the system boundaries should include the acquisition of raw materials, the production, use, treatment at end-of-life, recycling and final disposal (*i.e.* cradle-to-grave). However, simplifications may be made as long as they are systematic, justified and intentional, as opposed to inherently unconscious and implicit(de Bruijn *et al*., 2002). For instance, Cuéllar-Franca *et al.*(2016) reported a study considering the environmental impacts from extraction of raw materials until the 'laboratory gate'. Hence, the application (use phase) and the final disposal of the ILs were neglected. This scope, in LCA terms, is termed a cradle-to-gate boundary (**Figure 2**). For studies of comparison, the most facile simplification is omission of life cycle stages that are the same for all products of comparison (de Bruijn *et al*., (2002); ISO 14044 (ISO 14044, 2006)). However, due to the unique characteristics of ILs the processes downstream (gate-to-grave), are often included within the system boundaries for comparative assessment of the use of ILs (Amado Alviz and Alvarez, 2017; Righi et al., 2011).

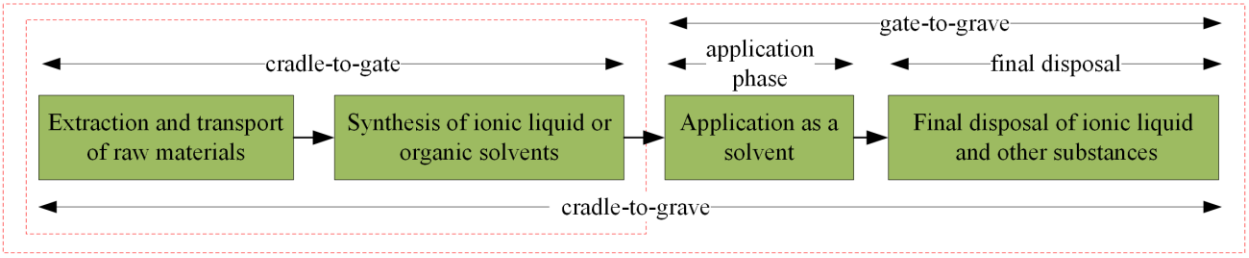

Figure 2. Scheme with a comparison of system boundaries between a conventional solvent and a IL used as a solvent in synthesis processes.

Table 3. Results of criteria applied in this study for goal and scope step

Entry	Study	Result	Justification
1	Huebschmann *et al.* (2011)	Medium	Product systems and system boundaries were partially defined
2	Zhang *et al*., (2008)	Medium	Cradle-to-gate approach
3	Kralisch *et al.*, (2005)	Medium	Product systems and system boundaries were partially defined
4	Kralisch *et al*., (2007)	Low	Product systems and system boundaries were not defined
5	Farahipour and Karunanithi, (2014)	Medium	Cradle-to-gate approach
6	Cuéllar-Franca et al., (2016)	Medium	Cradle-to-gate approach
7	Mehrkesh and Karunanithi, (2013)	Medium	Cradle-to-gate approach
8	Mehrkesh and Karunanithi, (2016a)	Medium	Cradle-to-gate approach
9	Righi *et al*., (2011)	Medium	Cradle-to-gate approach
10	Peterson, (2013)	High	Cradle-to-grave approach
11	Amado Alviz and Alvarez, (2017)	Medium	Cradle-to-gate approach

Notes: Criteria weight scale: Low = gate-to-gate or product systems or system boundaries are not defined. Medium = cradle-to-gate or system boundaries and product systems are partially defined. High = cradle-to-grave and system boundaries and product systems are clearly defined.

5 LIFE CYCLE INVENTORY ANALYSIS

For the Life Cycle Inventory (LCI) large amount of data are required, to enable identification and quantification of the inputs and outputs of the studied system. Recently, various databases that provide transparent, relevant, accessible and reliable data for the creation of inventories have been developed (de Bruijn *et al*., 2002).

The importance of adequate and available LCI data is well known (Hischier and Walser, 2012). ILs are a relatively newly researched class of compounds and therefore there is not much primary data from industrial scale production available (Mehrkesh and Karunanithi, 2013). Furthermore, these substances can be synthesized from many precursors (Disasa Irge, 2016) that are not always available in inventory database. Thus, different methods have been utilized to 'plug' the data gaps, including known stoichiometric data, primary data from laboratory scale, thermodynamic methods, empirical scale-up and other relevant relationships. **Table 4** shows a description of the main strategies applied to build the LCIs in the previously highlighted IL LCA studies in the literature.

Table 4. Main strategies applied for building the life cycle inventories

		Material balance			Energy balance			
Entry	Study	Data from laboratory scale	Data from literature	Chemical simulation software	Calculated from thermo-dynamic models	Measurements	Energy data from literature	Chemical simulation software
1	Huebschmann *et al.* (2011)	X			X			
2	Zhang *et al*., (2008)	X					X	X
3	Kralisch *et al.*, (2005)	X				X		
4	Kralisch *et al*., (2007)	X				X		
5	Farahipour and Karunanithi, (2014)		X	X			X	X
6	Cuéllar-Franca et al., (2016)	X			X			
7	Mehrkesh and Karunanithi, (2013)		X		X			
8	Mehrkesh and Karunanithi, (2016a)		X	X				X
9	Righi *et al*., (2011)		X	X				X
10	Peterson, (2013)		X	X				X
11	Amado Alviz and Alvarez, (2017)		X				X	

A life cycle assessment can be conducted with varying levels of sophistication; the ISO standard guidelines differentiate between the baseline detailed level, a simplified level, and any feasible expansions of the detailed level (ISO 14040, 2006; ISO 14044, 2006). However, it is necessary to rationalize and state the appropriate and required level of sophistication relative to the study goal and the specific decision situation (de Bruijn *et al.*, 2002).

5.1 Material balance

The approaches employed by other researchers to build the material balance of processes involving ILs can be divided into three different methods; simplified life cycle approach

(SLCA), life cycle tree approach and chemical simulation processes. **Figure 3** highlights these three approaches and the works in which they have been utilized.

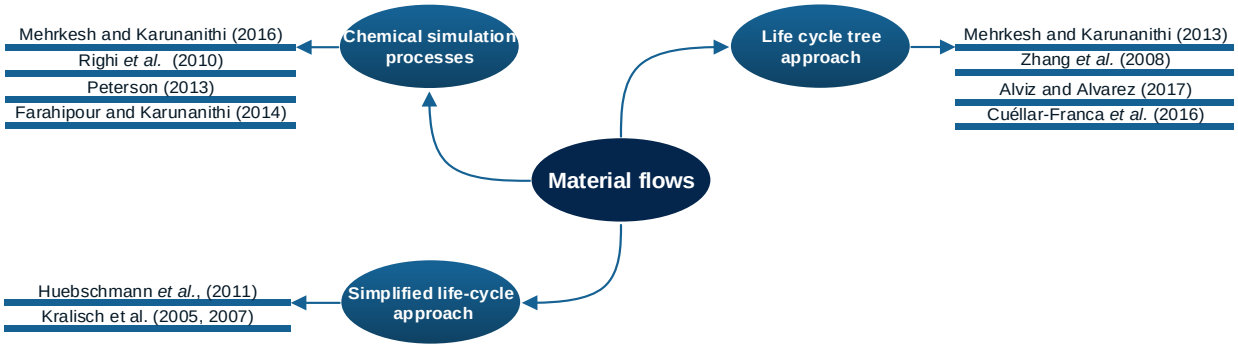

Figure 3. Main approaches used for determining material flows

Kralisch *et al.* (2005) were one of the first groups that reported an SLCA where upstream process and some inputs were neglected. Later, other studies also employed SLCA *(*Huebschmann *et al.*, 2011; Kralisch *et al.*, 2007, 2005). Overall, in this approach the main data employed were laboratory scale data and some life cycle phases were neglected, mainly the upstream phases (de Bruijn *et al.*, 2002). The authors justified the SLCA approach due to the complexity, time spent and effort needed for conducting a full LCA study, mainly because of a scarcity of information concerning the background processes. In these processes the decision-maker may apply none or indirect influence for which a life cycle assessment is carried out (Frischknecht, 1998). However, other LCA studies on ILs reported the biggest contribution impacts from background processes (Amado Alviz and Alvarez, 2017; Cuéllar-Franca et al., 2016; Righi et al., 2011). For example, in Alviz and Alvarez, (2017) the highest contributor to the impact categories evaluated in the [Bmim][Br] life cycle were the background processes, namely the production of hydrogen bromide (HBr), *n*-butanol, methylamine and glyoxal. Thus, the synthesis of precursor substances present in the synthetic route of ionic liquids should not be neglected.

Recently, studies have employed the method known as the "life cycle tree approach" (Cuéllar-Franca *et al.*, 2016; Mehrkesh and Karunanithi, 2013). In this approach, a life cycle tree of the ionic liquid to be studied is built, going back to the basic precursor substances for which available life cycle data can be accessed and used (*e.g.* hydrogen (H_2), ammonia (NH_3), benzene

(C_6H_6), methanol (CH_3OH), *etc.*). The main characteristic of that method is that it starts from the 'gate' or 'grave', and goes through all the main processes until the 'cradle'. Different to the SLCA, the life cycle tree approach can be considered a full life-cycle. However, this all-encompassing approach is exceptionally time-consuming and an exhaustive step-by-step evaluation is necessary. This method is suitable for newly emergent chemical substances, like ILs, which have complex structures and involve various precursors where life cycle data are either scarce or unavailable (Cuéllar-Franca *et al.*, 2016). In **Figure 4,** an example of a life cycle tree for [Bmim][NTf_2], based on routes of syntheses reported by Dunn *et al.*, (2012) for [Bmim][NTf_2], Righi *et al.*, (2011) for [Bmim][Cl], Perterson, (2013) for lithium bis(trifluoromethane)sulfonamide ($LiNTf_2$), and available life cycle databases in *Ecoinvent v 3.0* database software is highlighted. For this example, the LCIs of [Bmim][Cl], N-methylimidazole, 1-chlorobutane and [Bmim][Cl] are not available in the ecoinvent database, and thus needed to be built. In the case of the life cycle tree for $LiNTf_2$, the LCIs of methanesulfonyl chloride, methanesulfonyl fluoride, trifluoromethanesulfonyl fluoride, lithium nitride and $LiNTf_2$ are not available in the *ecoinvent* database. In general, in this approach, the required raw materials for each precursor are estimated using the chemical reaction stoichiometric relationships (Cuéllar-Franca *et al.*, 2016). However, limitations of this approach are the choice of synthetic route and the source of data used for building the life cycle inventory for each substance.

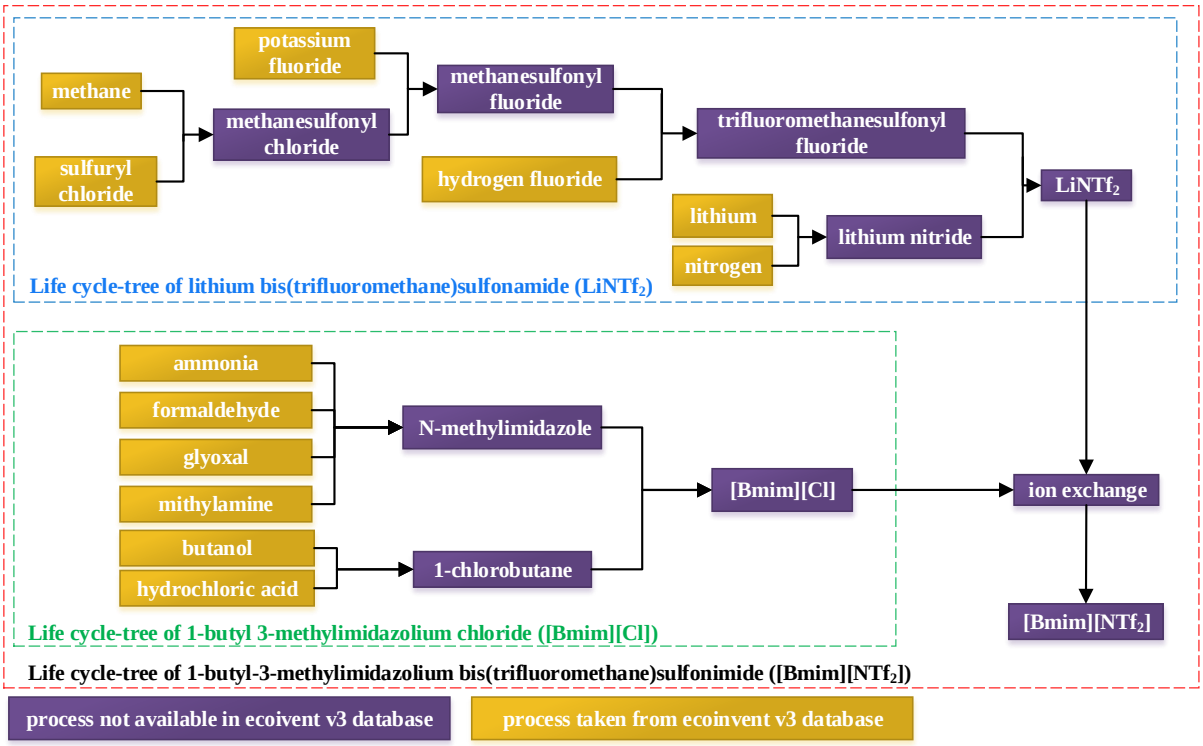

Figure 4. Example of life cycle tree for 1-butyl-3-methylimidazolium bis(trifluoromethane)sulfonimide [Bmim][NTf_2]. Considering routes of syntheses reported by Dunn *et al.*, (2012) for [Bmim][NTf_2], Righi *et al.*, (2011) for [Bmim][Cl], Perterson, (2013) for $LiNTf_2$ and available life cycle databases in *ecoinvent v 3.0* database software.

Very recently, Alviz and Alvarez (2017) published an LCA study on the production of acetyl salicylic acid from the 'cradle' to 'gate' in the pharmaceutical, which included the synthesis of acetic anhydride, salicylic acid, and the solvents ([Bmim][Br] or toluene), and the entirety of the production chain precursors. However, even though in this work by Alviz and Alvarez did not explicitly report the use of life-cycle tree approach, all the precursors were considered from cradle-to-gate. Therefore, it can be considered that a life cycle tree approach was made.

The other approach to estimate the material balance is the use of chemical simulation processes. This approach is advantageous as it is feasible to simulate and predict both material and energy flows. However, in the case of ILs, the use of process design and simulation software for modelling production processes of the ionic liquids is sometimes not possible because of a scarcity of complete thermodynamic and physical property models for those substances and associated precursors (Mehrkesh and Karunanithi, 2013).

5.2 Energy balance

The energy consumption has also been reported as an important source of impacts during the life cycle of ILs. For instance, it has been determined that 17% of ecotoxicity impacts were from consumption of energy in the IL life cycle (Mehrkesh and Karunanithi, 2016a). With regard to energy flows, different approaches have been used to calculate the energy demands of both the synthesis and usage of ionic liquids. The methods used in the literature to estimate the energy balance are divided into four approaches (**Figure 5**): use of an energy monitoring socket, energy balance (heat of reaction), chemical simulation processes and secondary data.

Kralisch *et al.*, (2007, 2005) determined the energy demand for heating, stirring and other steps (use of a vacuum pump, water bath heating and condensation) by using an energy monitoring socket. Additionally, the cumulative of energy demand (CED) was considered from secondary data; the CEDs for chemicals not listed in inventories were determined experimentally by measuring the energy needed for certain processes or synthesis steps. When this was not achievable, the CEDs for compounds with a high degree of structural similarity, which were present in the database, were used.

The use of some assumptions and methods has been performed to estimate the energy consumption, since industrial scale manufacturing data were not available, and it was expected to be more intensive in terms of energy requirements than the theoretical energy requirements. In the work of Huebschmann *et al.*, (2011) the mass flows of reactions were determined at the laboratory scale, and the amount of energy consumed as a result of the reactions (syntheses) was estimated based on energy balance (heat of reaction). Also, a heat transfer efficiency of 40% (in laboratory-based experiments) was assumed. On the other hand, the energy consumed by auxiliary equipment for the case of the continuously-flow syntheses, *e.g.* control systems and pumps, was obtained from measurements.

Mehrkesh and Karunanithi (2013) suggested that the estimation of energy flows could be achieved by using theoretical energy values and, later, used empirical factors for scale-up of chemical processes **(Equation 1-3)**. For exothermic reactions, the authors suggested that

electricity usage is 3.2 times higher than the theoretical consumption of electricity. In the case of endothermic reactions, heated through combustion of natural gas, it was assumed that the energy usage is 4.2 times higher than theoretically required. Furthermore, it was assumed that natural gas was used for heating of endothermic reactions and electricity was used for the cooling of exothermic reactions. Later, Cuéllar-Franca *et al*., (2016) reported using this method to calculate the theoretical energy usage during the synthesis of the ionic liquid $[P_{66614}][124Triz]$ and precursors, and they recommended it as an approach to calculate the energetic scale-up gaps for ILs. The method used by Cuéllar-Franca *et al*. consisted of calculating the heat of reaction based on the work of Felder and Rousseau, (2005) **(Equation 2 and 3),** and then these values were multiplied by the factors stated above (Mehrkesh and Karunanithi, 2013). However, one of the difficulties in applying this method is that in order to determine the heat of reaction (ΔH) it is necessary to know the heat capacities and heats of formation of the ionic liquid and intermediate substances/precursors (Felder and Rousseau, 2005). Cuéllar-Franca *et al*., (2016) reported the use of thermodynamic databases and use of data from substances with similar structure. However, there is also a method put forward by Valderrama *et al.*, (2009) that allows for prediction of the heat capacities (Cp) of ionic liquids. This method uses the group contribution approach to find values for the heat capacity of ionic liquids. Other methods for estimation of the heats of formation ($\Delta\widehat{H}f°$) have been reported in the literature, such as experimental methods (Dong *et al*., 2013; Zhu *et al*., 2012) and estimation through the use of genetic algorithm-based multivariate linear regression methods (Peterson, 2013; Vatani *et al*., 2007). Furthermore, in the literature, authors have reported the use of thermodynamics databases (ATcT (Active Thermochemical Tables), n.d.; DETHERM, 2017; NIST, 2017) to obtain heats of formation, or with the assumption that the required heat of formation is equivalent to that of a similar structure that can be determined (Cuéllar-Franca *et al.*, 2016).

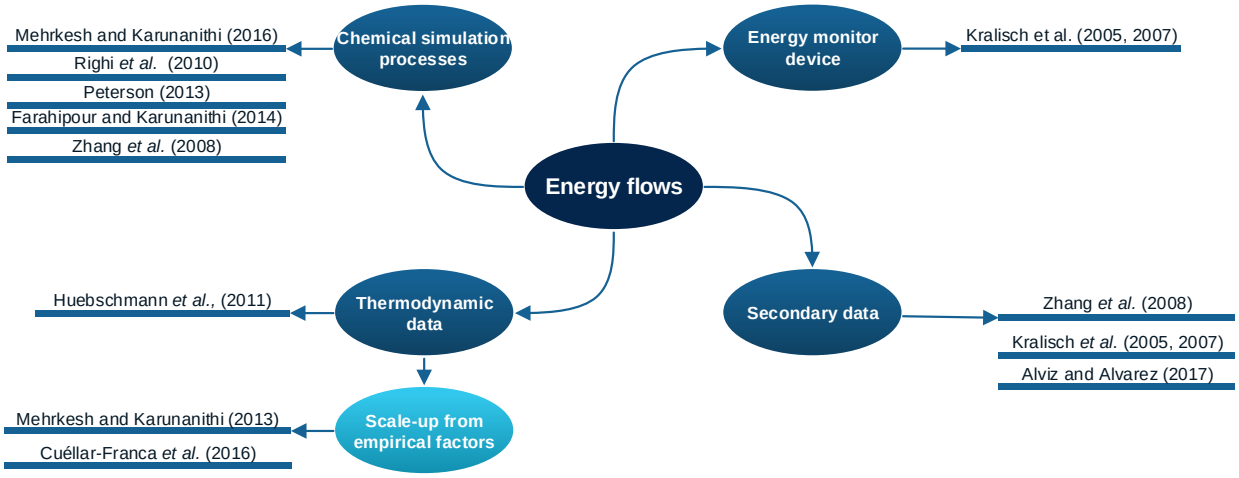

Figure 5. Main approaches employed to determine energy flows

$$E_i = \Delta H \times Fc \qquad \textbf{Eq. 1}$$

$$\Delta H = \sum(n.\hat{H})outputs - \sum(n.\hat{H})inputs \qquad \textbf{Eq. 2}$$

$$\hat{H} = \Delta\hat{H}f° + \int_{T1}^{T2} Cp.\Delta T \qquad \textbf{Eq. 3}$$

where:

E_i: theoretical energy consumption

ΔH: heat of reaction

n = molecular weight of reactants

$\hat{H}$= specific enthalpy of reactants

$\Delta\hat{H}f°$ = heat of formation of reactants

Cp = calorific value of reactants

T1 = reference temperature

T2 = temperature of the reactants

Fc= a factor of 4.2 for endothermic reactions with the assumption of natural gas-powered heating and a factor of 3.2 for exothermic reactions with the assumption that cooling uses electricity (Mehrkesh and Karunanithi, 2013).

In some cases the life cycle material and energy consumption data were estimated from chemical process simulation (Righi *et al.* (2011); Zhang *et al.* (2008); Mehrkesh and Karunanithi,

(2016a)). In general, for use of chemical process simulation, it is necessary to have a large amount of available data derived from the combination of energy balances, mass balances, theoretical calculations and secondary data from the literature. In addition, specific data on ILs and intermediate substances could be necessary for conducting a chemical process simulation, for instance, in Huang *et al.,* (2014) some physical-chemistry data necessary for conducting their simulation were shown, *i.e.* heat capacity, density, viscosity, surface tension, thermal conductivity and scalar property parameters (*e.g.* molecular mass, acentric factor, normal boiling point, critical pressure and temperature, critical volume and critical compressibility factor) amongst other thermodynamic parameters.

5.3 Overview of the Life Cycle Inventories

The results of the criteria applied in this study for the life cycle inventory analysis are highlighted in **Table 5.** In this review, four aspects are identified as key issues that strongly affect the completeness of the LCA studies: (i) yield of reaction, (ii) reuse, (iii) recycling and (iv) final disposal (see **Figure 6**). The principle of completeness is to account for all inputs and outputs for the functional unit and within the chosen inventory boundary (Kralisch et al., 2015). Only six of the analysed studies reported definite numbers for input flow and/or output flow, including quantitative LCI information reported in publications: in tables, flow diagrams and/or supporting materials (Zhang *et al.* (2008), Cuéllar-Franca *et al.*, (2016), Mehrkesh and Karunanithi, (2013), Righi *et al.*, (2011), Alviz and Alvarez, (2017)). In terms of the input, all studies covered in detail the energy inputs and, also in many of the studies, the material inputs; whilst for many of the studies assessed, the output side was less well described. Only two studies partially covered all aspects of the processes; the IL-based carbon capture study by Cuéllar-Franca *et al*., (2016) and the study focussed on aquatic ecotoxicity impacts of ILs by Mehrkesh and Karunanithi, (2016a).

Table 5. Summary of criteria applied in this study for life cycle inventory analysis (completeness of studies)

		Input		Emissions to water		Emission to soil		Emissions to air	
Entry	Study	Material input	Energy input	General	Ionic liquids	General	Ionic liquids	General	Overall evaluation
1	Huebschmann *et al.* (2011)								Low Completeness
2	Zhang *et al*., (2008)	X	X						Medium Completeness
3	Kralisch *et al.*, (2005)								Low Completeness
4	Kralisch *et al*., (2007)								Low Completeness
5	Farahipour and Karunanithi, (2014)								Medium Completeness
6	Cuéllar-Franca et al., (2016)	X	X	X	X	X	X	X	High Completeness
7	Mehrkesh and Karunanithi, (2013)	X	X						Medium Completeness
8	Mehrkesh and Karunanithi, (2016a)	X	X	X	X	X	X	X	High Completeness
9	Righi *et al*., (2011)	X	X						Medium Completeness
10	Peterson, (2013)								Medium Completeness
11	Amado Alviz and Alvarez, (2017)	X	X						Medium Completeness

Dark blue: High completeness data coverage; Light Blue: Medium completeness data coverage; grey: low completeness/no data coverage or no information given; marked with "x": quantitative LCI information was reported in study (inclusive of supporting materials). General: Emission from other chemical substances that are not ionic liquids. Notes: Criteria weight scale: Low to Medium and then High. Low = Incomplete data or no filling of data gaps. Medium = Incomplete data, gaps filled with qualified assumptions. High = Comprehensive data including information about energies, masses and by-products.

In order to obtain high completeness during LCI, every energy and mass and flow that is within the study scope should be documented (Kralisch *et al.*, 2015). The yield of a chemical reaction is an important process parameter, as it determines the amount of substrate required (Piccinno *et al.*, 2016; Tufvesson *et al.*, 2013). According to Tufvesson *et al*., (2013), the entire environmental performance of a product can be greatly improved by a high yielding reaction, because up to 90 % of the entire environmental impact is due to raw material production.

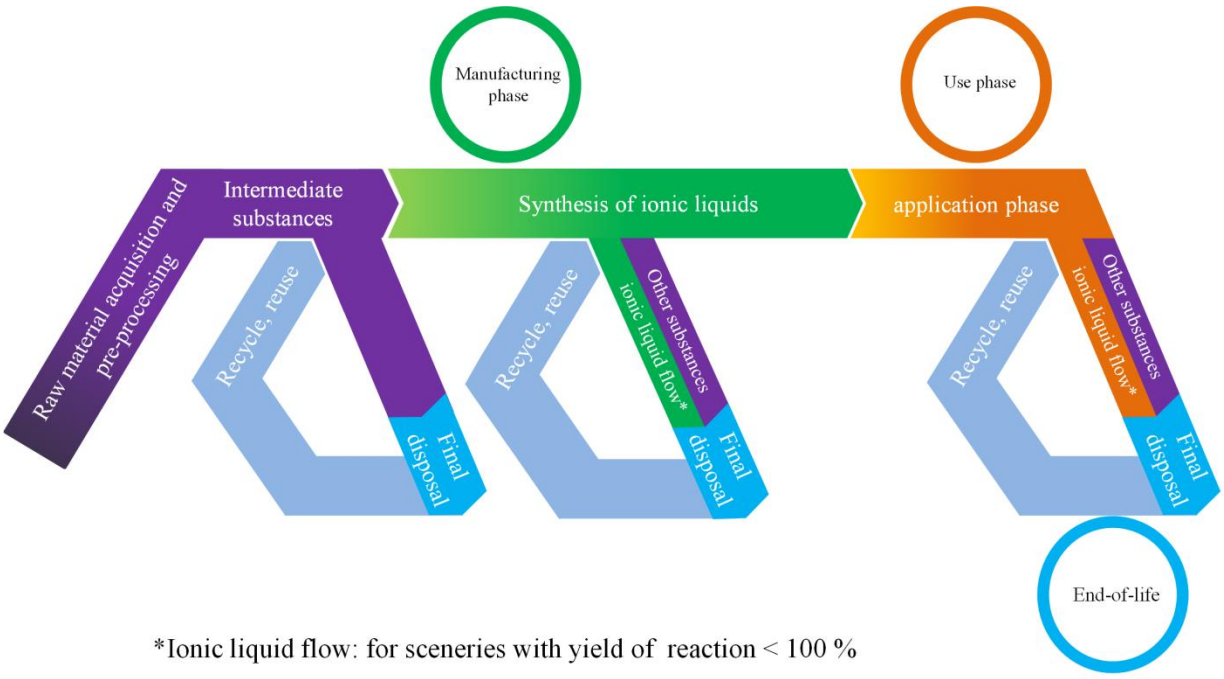

Figure 6.Schematic representation of life cycle perspective of Ionic liquids

The reuse, recycling or final disposal of ionic liquids are important parameters associated with the completeness of studies. Overall, the final disposal of ionic liquids has not been thoroughly reported in the literature thus far. One study treated the disposal of the ionic liquid as 'disposal of organic waste' (Huebschmann *et al*., 2011), and in another work, only the transport to final disposal was assumed (Peterson, 2013). However, many methods for the recycling and reuse of ionic liquids have been researched. The most explored options include extraction, adsorption, use of supercritical CO_2, and also membrane separation processes (Mai *et al.*, 2014). Furthermore, a distillation method using a membrane to separate water from the ILs that were used for biomass pre-treatment was reported by Lynam *et al.*, (2016).

Previous studies have shown the importance of IL reuse, especially when employed as a solvent (Amado Alviz and Alvarez, 2017; Farahipour and Karunanithi, 2014; Huebschmann et al., 2011; Zhang et al., 2008). It has been found that recovery of the solvent is an important parameter that may make the utilization of ILs an alternative comparable to the use of toluene for production of acetylsalicylic acid (Alviz and Alvarez, (2017)). The influence of solvent recovery was evaluated using sensitivity analysis assuming recovery rates in the range of 89 to 98%. Sensitivity analysis was also used by Zhang *et al.*, (2008) to evaluate the impact of the number of times an IL was

reused, by considering recycling from 5 to 20 times. Furthermore, Zhang *et al.*, (2008) showed that even with a recycling of the ionic liquid 20 times, conventional processes for the production of cyclohexane still had a smaller life cycle impact than the process that utilized an ionic liquid for the production of cyclohexane. In contrast, Farahipour and Karunanithi, (2014) and Peterson, (2013) assumed no loss or degradation with complete reuse of ILs. In this case, the authors assumed that the impacts of the extraction, synthesis, and transport of the raw substrates, synthesis of ionic liquids and end-of-life are neglected, due to reuse of the ionic liquid.

6 LIFE CYCLE IMPACT ASSESSMENT STEP

This section presents the impact categories and characterization methods employed in the studies reviewed in this paper (**Table 7**). The results of the criteria applied in this study for the life cycle impact assessment steps are highlighted in **Table 9**. The life cycle impact assessment methods define the environmental impact categories based on characterization factors. In turn, these factors are further expanded by considering the inherent properties of chemicals (*e.g.*, toxicity), in addition to information on the transport and potential mode of exposure (Mehrkesh and Karunanithi, 2013). Twenty different impact categories were considered in the studies assessed in this review. From those, only five impacts categories are common to at least 70% of the studies; eutrophication, acidification, ozone depletion, global warming and human toxicity. Furthermore, there were few studies that reported complete LCA results, and it must be noted that these results are very important for future comparison. **Table 7** shows the there is a lack of information of the methods of characterization of impacts applied for each study evaluated in this work. CML 2001 was determined to be the most preferable LCIA method assumed. The employment of this method or a superior one (*e.g.* CML 2002) in future studies has been highly recommended (Jolliet *et al.*, 2003). In some studies, the method employed is not clear or is not mentioned, therefore, in these cases, it was assumed as not available for that work.

Table 6. Categories impacts used for studies.

	Reference number (see table notes)										
Impact categories	**1**	**2**	**3**	**4**	**5**	**6**	**7**	**8**	**9**	**10**	**11**
Abiotic resource	yes	yes	no	yes	no	yes	no	no	yes	no	yes
Acidification	yes	yes	no	yes	yes	yes	yes	no	yes	yes	yes
Ecotoxicity	no	no	no	no	yes	no	yes	no	yes	yes	no
Eutrophication	yes	yes	no	yes	yes	yes	yes	no	yes	no	yes
Fresh water aquatic ecotoxicity potential	yes	yes	no	yes	no	yes	no	yes	yes	no	yes
Fresh water sedimental ecotoxicity potential	yes	no	yes	no	no	no	no	no	no	no	no
Global warming	yes	yes	no	yes	yes	yes	yes	no	yes	yes	yes
High-NOx POCP	yes	no	no	no	no	no	no	no	no	no	no
Human health cancer	no	no	no	no	yes	no	yes	no	no	no	no
Human health criteria	no	no	no	no	yes	no	yes	no	no	no	no
Human health non-cancer	no	no	no	no	yes	no	yes	no	no	no	no
Human toxicity	yes	yes	yes	yes	no	yes	no	no	yes	no	yes
Land use	yes	no	no	no	no	no	no	no	no	no	no
Low - NOx POCP	yes	no	no	no	no	no	no	no	no	no	no
Marine sedimental ecotoxicity	yes	yes	yes	yes	no	yes	no	no	no	no	no
Ozone depletion	yes	yes	no	yes	no	yes	no	no	yes	no	Yes
Photochemical oxidation	no	yes	no	yes	no	yes	no	no	yes	no	No
Smog	no	no	no	no	yes	no	yes	no	no	yes	No
Terrestrial ecotoxicity potential*	yes	yes	no	no	no	yes	no	no	yes	no	Yes
VOC emissions	no	yes	no	no	no	no	no	no	yes	no	No
Energy demand	yes	no	yes	yes	no	no	no	no	no	no	No
Dichlorobenzene	no	no	no	no	no	yes	no	no	no	no	No
Cost	yes	no	yes	no	no	no	no	no	no	no	No

Notes: Studies: 1: Huebschmann *et al.,* (2011); 2: Zhang *et al,.* (2008); 3: Kralisch *et al.,* (2005); 4: Kralisch *et al.,* (2007); 5: Farahipour and Karunanithi, (2014); 6: Cuéllar-Franca *et al.,* (2016) ; 7: Mehrkesh and Karunanithi, (2013) ;8: Mehrkesh and Karunanithi, (2016a); 9: Righi *et al.* (2011); 10: Peterson, (Peterson, 2013);11: Alviz and Alvarez, (2017)
VOC: volatile organic solvent; POCP: Photochemical Ozone Creation Potential;

Table 7. Life cycle assessment methods of characterization used in the previous studies.

Entry	Study	LCA method of characterization
1	Huebschmann *et al.* (2011)	CML 2001 and CED
2	Zhang *et al*., (2008)	N/A
3	Kralisch *et al.*, (2005)	CED
4	Kralisch *et al*., (2007)	CED and another
5	Farahipour and Karunanithi, (2014)	TRACI
6	Cuéllar-Franca et al., (2016)	CML 2001
7	Mehrkesh and Karunanithi, (2013)	TRACI
8	Mehrkesh and Karunanithi, (2016a)	USEtox-Based
9	Righi *et al*., (2011)	CML 2001
10	Peterson, (2013)	N/A
11	Amado Alviz and Alvarez, (2017)	CML 2001

N/A: Not available; CED: Cumulative Energy Demand V1.09 method (PRé Consultants, 2014); TRACI: TRACI Method (the "Tool for Reduction and Assessment of Chemical and other Environmental Impacts") by the U.S. EPA (Bare, 2008); CML 2001: CML 2001 method by Institute of Environmental Sciences (PRé Consultants, 2014); USEtox-Based effect factors for the ionic liquids [Bmim][Br], [Bmim][Cl], [Bmim][BF_4], [Bmim][PF6], and [BPy][Cl] were made and used (Kadziński *et al*., 2016).

In general, a common limitation in the entirety of the studies listed above is that consideration of any possible impacts associated with final disposal of ionic liquids, as well as toxicity was not given (Mehrkesh and Karunanithi, 2016a). Indeed, some studies have reported that ionic liquids present some toxicity to aquatic organisms (Heckenbach et al., 2016; Thuy Pham et al., 2010). On the contrary, ionic liquid toxicity information has not been included in LCA studies to date, due to the scarcity of toxicity-based characterization factors for ionic liquids. Recently, Mehrkesh and Karunanithi, (2016a) have proposed freshwater ecotoxicity characterization factors for a set of five ionic liquids (**Table 8**). In that study, the USEtox model, an up-to-date modeling framework built on scientific consensus for characterization of human and ecotoxicological impacts of chemicals (Rosenbaum *et al.*, 2008), was utilized to develop characterization factors. All the evidence indicates that ionic liquids emissions in freshwater may cause damage to the ecosystem, and thus of inclusion of those impacts into boundary system could lead to modification of LCA results.

Table 8.Characterization factors for freshwater ecotoxicity of some common ionic liquids

Ionic Liquid	Characterization factors (CTUe / kg)
[Bmim][Br]	624
[Bmim][Cl]	748
[Bmim][BF_4]	823
[Bmim][PF_6]	927
[BPy][Cl]	1768

Source: Mehrkesh and Karunanithi, (2016a); CTUe: Comparative Toxic Unit

In this review, it is not fully possible to afford a full comparison of the environmental impact results of the studies highlighted, as the goals and scopes, inventory completeness, methods of characterization applied and impact categories of these studies greatly differ. However, there are some previous studies that compared the environmental performance of some ionic liquids, such as butylmethylimidazoluim chloride [Bmim][Cl], (Amado Alviz and Alvarez, 2017; Righi et al., 2011) and trihexyltetradecylphosphonium 1,2,4-triazolide ([P_{66614}][124Triz]) (Cuéllar-Franca *et al.*, 2016). These studies reported Global Warming Potential (GWP) impacts estimated at 6.30 kg CO_2 eq. per kg of [P_{66614}][124Triz] and 6.40 kg CO_2 per kg of [Bmim][Cl]. Also, Huebschmann *et al.* (2011) reported large differences between the environmental performances of ionic liquids using life cycle methodology. In their study, [Bmim][Cl] showed GWP impacts five times smaller than 1-octadecyl-3-methylimidazolium bromide ([C_{18}MIM][Br]) (Huebschmann *et al.*, 2011).

Table 9. Results of criteria applied in this study for life cycle assessment

Entry	Reference	Assessment Result	Justification
1	Huebschmann *et al.* (2011)	Medium	Impact categories were partially justified
2	Zhang *et al*., (2008)	Low	Characterization methods not clearly defined and justified
3	Kralisch *et al.*, (2005)	Medium	Characterization method partially defined and justified
4	Kralisch *et al*., (2007)	Medium	Characterization method partially defined and justified
5	Farahipour and Karunanithi, (2014)	High	CCovered more than one impact category, also impact categories and characterization methods clearly defined and justified
6	Cuéllar-Franca et al., (2016)	High	CCovered multiple impact categories, also impact categories and characterization methods clearly defined and justified
7	Mehrkesh and Karunanithi, (2013)	High	CCovered multiple impact categories, also impact categories and characterization methods clearly defined and justified
8	Mehrkesh and Karunanithi, (2016a)	Medium	One impact category evaluated
9	Righi *et al*., (2011)	High	CCovered more than one impact category, also impact categories and characterization methods clearly defined and justified
10	Peterson, (2013)	Low	Characterization methods not defined and justified
11	Amado Alviz and Alvarez, (2017)	High	CCovered more than one impact category, also impact categories and characterization methods clearly defined and justified

Notes: Criteria weight scale: Low to Medium and then High. Low = generally where characterization methods were not clearly defined and justified. Medium = generally where characterization methods were partially defined and justified. High = generally where more than one impact category was considered and the characterization methods were clearly defined and justified.

7 LCA INTERPRETATION

According to ISO 14044, the interpretation step consists of three approaches; (i) identification of a significant issue, analysis of the results, comparisons and hot-spots, (ii) evaluation and (iii) conclusions. The first step is mostly performed by building the results of the LCI and LCIA (de Bruijn *et al.,* 2002). The evaluation step deals with how complete a database may be, the indication of data quality and the sensitivity analysis of the results due to data changes. Kralisch *et al.,* (2015) have checked these criteria, conclusions (step iii) can be made concerning the resultant recommendations based on analysis of the results and comparison, identify opportunities for improvements and also identify the limitations of the LCA study (de Bruijn *et al*., 2002; Kralisch *et al.,* 2015)

As highlighted above, the inventory database involving ILs are scarce and often different methods and sources of data are needed for building them. Therefore, the data quality depends on the sources that were available for the particular study (Kralisch *et al.,* 2015). A common procedure in the literature to indicate the quality of the data in an LCA is known as the 'Pedigree Matrix', which was developed for this purpose of indicating data quality by Weidema and Wesnaes, (1996). The indicators of data quality utilized by Weidema and Wesnaes, (1996) is scored (1 to 5, where 1 is best and 5 is worst) on the following independent data quality characteristics; (i) Completeness (statistical representativeness of the data and the periods of time for data collection); (ii) temporal correlation, (iii) geographic correlation, (iv) further technological and (v) reliability (sampling methods and verification procedures).

None of the studies highlighted in this review performed the data quality analysis on the data of the LCI data, thus are being considered as 'Low'. The necessity for large amount of information on the LCI data, and time expenditure for conducting this analysis are some of the reason why it was not applied. In this context, Kralisch *et al.,* (2015) proposed a 'modified Pedigree Matrix' applicable to indication of data quality in the context of design of chemical processes and syntheses, where the following quality indicators are used; completeness, representativeness, and reliability. One significant difference between the well-established Weidema valuation system and the system proposed by Kralisch *et al.* is the aggregation of the time, space and technological correspondence

indicators into one indicator named ‘representativeness’. For the interested reader, more discussion about analysis of data quality and recommendations on analysis of data quality can be found in the works of Weidema and Wesnaes, (1996) and Kralisch *et al.*,(2015).

Therefore, the indicators of data quality derived from the use of the “Pedigree Matrix” is a tool for data quality management (Muller *et al*., 2016) and is recommended for analysis of data quality in life cycle studies (de Bruijn *et al*., 2002). Hence, considering the state-of-art of the LCI of ILs it is recommended that it is essential to incorporate data quality indicators.

8 RECOMMENDATIONS TO OVERCOME EXISTING GAPS

Several limitations associated with implementation of the LCA in all its steps to ILs have been identified in this review. However, the major limitations occur due to the absence of LCIs and characterisation factors, thus these should be the focus of future LCA studies on ILs to improve the knowledge on the environmental performance of the life cycle of ILs. The LCI step is the critical phase of LCA that corresponds to the accumulation and quantification of system inputs and output data. Hence, different methods for building LCIs may afford differing results in terms of environmental impact for the same process or product (Islam et al., 2016). Thus, the current lack of complete data complicates the task. It is a fact that, in terms of impact assessment, it is important to have sufficient LCI data in order to be able to take account of the material in a more appropriate manner to support the decision making of the LCA practitioner (Hischier and Walser, 2012). In other words, it was identified that:

i) inventory database of ILs synthesis, application phase and final disposal with a high degree of representativeness and completeness are needed;
ii) better information on separation efficiencies, recovery and amounts of reuse is needed;
iii) potential environmental impacts associated with direct environmental release of ionic liquids were not considered in the studies;
iv) efficiency of reaction (yield of reaction) of ionic liquid synthesis should be considered;
v) use of data quality indicators for the analysis of data into LCI.

To enable a choice of a particular approach to build LCIs, the calculation technique and relative limitations and advantages for the purpose should be known. Hence, the choice of the approaches used for building LCIs firstly should consider the goal and scope of the specific study. Also, it is recommended to consider the data requirements, availability of data and the associated time expenditure. In **Figure 7** the relationship between the need for data and the ease of applying it for each approach is illustrated.

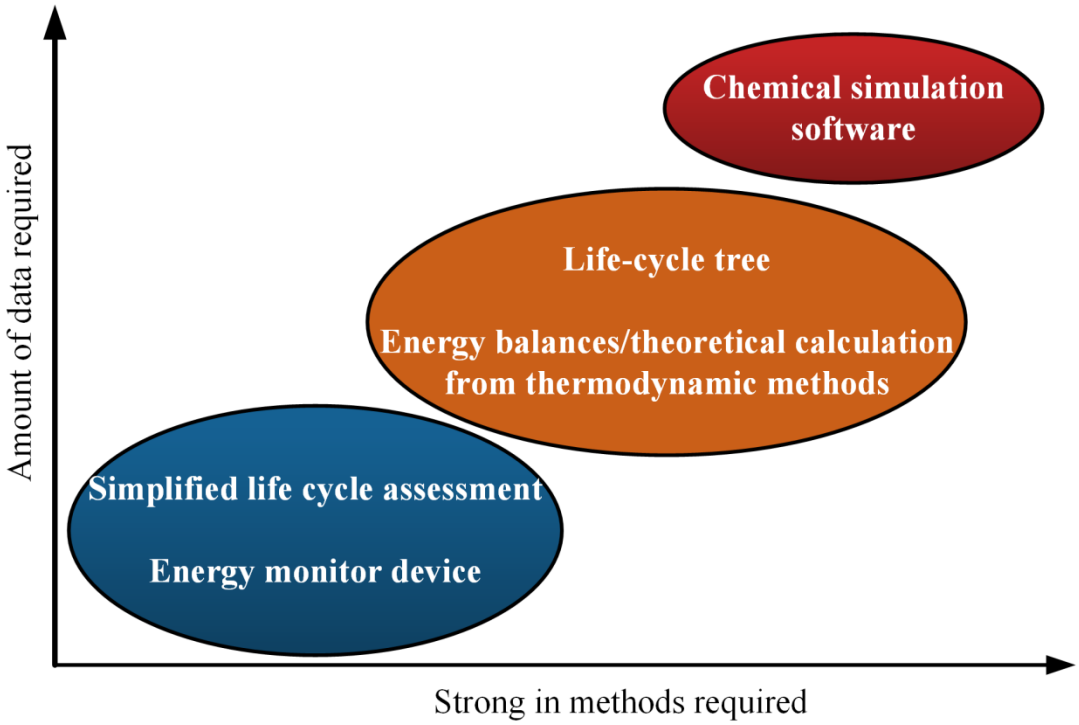

Figure 7. Illustration of the relationship between the need for data and the ease of applying it for each approach

In this review, the life-cycle tree approach is recommended for the LCA of emergent chemical substances, such as ILs, which normally have complex structures involving many precursors for which inventory databases are scarce or unavailable. This approach can be applied in a first screening of the life cycle of ILs, and it can also be useful for supporting of chemical simulations.

The lack of industrial data involving the manufacture of IL has been identified as a current limitation for applying LCA studies on ILs, mainly data associated with energy demanded for manufacturing of ILs and their precursors. However, the impact of this limitation can be minimized by using the following methods: chemical simulation software, empirical factors as proposed in Mehrkesh and Karunanithi, (2013) or other methods reported in literature. For example, the scale up of chemical synthesis process for life cycle assessment studies using only laboratory scale experimental data can be achieved through of the framework reported by Piccinno *et al.*, (2016).

To improve the completeness of LCA studies an important factor that needs to be determined when building the LCI of a chemical substance is the efficiency of reaction (yield of reaction). Indeed, several studies have reported the influence of yield on LCA results (Huebschmann *et al.*, 2011; Kralisch *et al.*, 2015, 2007; Sell *et al.*, 2014; Zhang *et al.*, 2008). The amounts of by-products and unreacted materials are calculated from the known reaction conversion rate and product yield of the reaction. Therefore, for small conversion rates more supplies are demanded and more waste is generated, consequently the environmental impact increases. Often the functional unit (as defined above) assumed has a relationship with the number of ionic liquids synthesised or with the reaction assessed, hence it is expected that the efficiency of reaction has influence on the LCA results. Primary source data of yield rates are recommended, *e.g.* data from industrial plants, pilot scales, laboratory scales or data from literature based on experimental results. The yield can be theoretically assumed to 100 % when data is not available, but it is recommended to assume lesser amount. For instance in Hischier *et al.* (2005) the yield assumed was 95 %. For these assumptions, the use of sensitivity analysis for assessment of the effect of each variable on LCA result, is recommended.

Regarding the interpretation step, the analysis of data quality has not been applied in the studies reviewed herein. The employment of methods for analysing data quality is useful, mainly due to the characteristics of emerging substances, such as ILs, which have inventory database built using different methods and sources. Thus, the method proposed by Weidema and Wesnaes, (1996), and more recently the simplified method by Kralisch *et al.*, (2015) for applying data quality indicators, should be considered in future LCA studies with ILs. Several studies have tested the robustness of the results obtained through use of a combination of methods for material and energy balances by applying sensitivity and uncertainty analyses (Cuéllar-Franca *et al.*, 2016; Huebschmann *et al.*, 2011; Kralisch *et al.*, 2015; Zhang *et al.*, 2008). Sensitivity analysis is a practical tool for evaluating how robust results are and for determining the sensitivity of the results to particular factors in the LCA (Kralisch *et al.*, 2015). Thus, these practices are highly recommended and should be applied when the data are estimated and/or there is a lack of information.

Finally, for the characterisation factors related to ILs, the initial question that needs to be answered is “Which environmental organisms and compartments are affected, to what extent, and by which particular characteristics of the ionic liquids?” According to Mehrkesh and Karunanithi, (2016b) the intermediate transference and spread of chemical compounds between differing environmental compartments are modelled as an array of mass balance equations, assuming equilibrium conditions. However, knowledge about these methods and application of these methods to ILs currently is scarce and must be the focus of future studies.

9 CONCLUSIONS

This review has provided a summary of current environmental life cycle assessment case studies on ionic liquids (ILs), and also has identified the existing shortcomings that are delaying the analysis of ionic liquid based processes with the life cycle assessment framework. Previous studies have reported large environmental impacts when ionic liquid life cycles were considered. Thus, the utilization of life cycle assessment to ionic liquids has been instrumental to the recognition of the real environmental impacts of these emergent substances. However, its use has not kept up with the fast development of these new substances and the ionic liquids field.

Overall, the number of available LCAs of ionic liquids in the literature is limited when compared with the number of ILs which can be made or have been used (*cf.* **Figure 1**). Furthermore, the largest type of ILs analysed are based on the butylmethylimidazolium cation ($[Bmim]^+$). In the eleven LCA studies on ionic liquids reviewed in this work, various life-cycle approaches (from gate-to-gate, cradle-to-gate, and cradle-to-crave) and impact assessment approaches have been used, depending on the definite questions to be answered with the analysis. However, cradle-to-gate was the approach mainly used, and CML 2001 was determined to be the preferred LCIA method. Eutrophication, acidification, ozone depletion, global warming and human toxicity were common impact categories reported among the studies.

The necessary features of the life cycle assessment methodology were reviewed and several particular limitations in the application of LCA have been established and reviewed. These include the lack of information involving the background processes, mainly for building inventory of IL precursors, how system boundaries and product systems are defined, the quality of data, and there are few characterisation factors for IL.

A set of issues that need to be more precise for application of LCA to evaluate IL processes has been proposed. These issues are; access to complete and sufficient life cycle inventory data during the phase of inventory analysis, and the growth and subsequent inclusion of characterization factors for the impacts of ILs during the impact assessment phase. Also, a

limitation in every study evaluated is that potential impacts arising from the environmental release of ionic liquids were not considered.

Thus, some practices are recommended in LCA of ILs, such as: to use approach that considers life cycle phases (using life cycle-tree for building LCIs is recommended), to consider reuse and recycle of the ILs and to consider the yield of reaction involving ILs and intermediate substances. Different studies adopt different methods of LCI, also a series of assumptions and approaches were used to estimate them. For this reason, the employment of data quality analysis is essential and should be included for building LCI of ILs. Furthermore, the robustness of the results needs to be examined by use of uncertainty and sensitivity analyses.

Besides that, the scarcity of the characterisation factors of IL for human toxicity and ecotoxicity impact categories halts inclusion in the LCIA. Therefore, a comprehensive LCIA for a chemical process that involves ILs will only be achievable when the characterisation factors of the IL are fully available.

Therefore, to improve the present situation, it is important to improve each of the steps of the LCA to the extent allowed by scientific advances. This review demonstrates new advances to decrease the gaps in LCIs and the characterised factors that will be the focus of future studies on application of LCA to IL processes. Indeed, it should be noted that the authors very recently published a LCA study on the environmental performance of 3D-printing ionic liquids, which incorporates the recommended practices highlighted in this review (Maciel et al., 2018).

10 ABBREVIATIONS

1-butyl-3-methyl-imidazolium tetrafluoroborate ([Bmim][BF_4])

1-alkyl-3-methylimidazolium chloride [C_4mim]Cl

n-hexylpyridinium chloride [C_6Py][Cl]

1-hexyl-3-methylimidazolium chloride [C_6MIM][Cl]

1-butyl-3-methylimidazolium acetate ([Bmim][Ac])

trihexyltetradecylphosphonium 1,2,4-triazolide ([P_{66614}] [124Triz])

1- butyl-3-methylimidazolium bromide ([Bmim][Br]),

1-butyl 3-methylimidazolium chloride ([Bmim][Cl])

1-butyl 3- methylimidazolium tetrafluoroborate [Bmim][BF_4]

1- butyl-3-methylimidazolium hexafluorophosphate [Bmim][PF_6]

1-butylpyridinium chloride [BPy][Cl]

1-hexyl-3-methylimidazolium bis(trifluoromethylsulfonyl)imide

trihexyl(tetradecyl)phosphonium 1,2,3-triazolide

1-hexyl-3-methylimidazolium bis(trifluoromethylsulfonyl)imide [hmim][TNF_2]

trihexyl(tetradecyl)phosphonium 1,2,3-triazolide [P_{66614}][3triazolide]

1-octadecyl-3-methylimidazolium bromide [C18MIM]Br

1-butyl-3-methylimidazolium bis(trifluoromethane)sulfonimide [Bmim][NTf_2]

11 ACKNOWLEDGMENTS

V.G-M. and M.S. wish to thank the Brazilian Government by National Council for the Improvement of Higher Education (*CAPES*) support and the University of Nottingham is gratefully acknowledged for the Research Priority Areas for funding. This study was financed in part by the Coordenação de Aperfeiçoamento de Pessoal de Nível Superior – Brasil (CAPES) – Finance Code 001. C.M.L-U. wishes to thank the Brazilian Government by National Council of Technological and Scientific Development (*CNPq*).

12 CONFLICTS OF INTEREST

The authors declare no conflicts of interest.

13 REFERENCES

Amado Alviz, P.L., Alvarez, A.J., 2017. Comparative life cycle assessment of the use of an ionic liquid ([Bmim]Br) versus a volatile organic solvent in the production of acetylsalicylic acid. J. Clean. Prod. 168, 1614–1624. https://doi.org/10.1016/j.jclepro.2017.02.107

ATcT (Active Thermochemical Tables), n.d. Thermochemical Tables [WWW Document]. URL https://atct.anl.gov/

Bare, J.C., 2008. TRACI:The Tool for the Reduction and Assessment of Chemical and Other Environmental Impacts. J. Ind. Ecol. 6, 49–78. https://doi.org/10.1162/108819802766269539

Bernard, F.L., Rodrigues, D.M., Polesso, B.B., Donato, A.J., Seferin, M., Chaban, V. V., Vecchia, F.D., Einloft, S., 2016. New cellulose based ionic compounds as low-cost sorbents for CO2 capture. Fuel Process. Technol. 149, 131–138. https://doi.org/10.1016/J.FUPROC.2016.04.014

Cerdas, F., Juraschek, M., Thiede, S., Herrmann, C., 2017. Life Cycle Assessment of 3D Printed Products in a Distributed Manufacturing System. J. Ind. Ecol. 21, S80–S93. https://doi.org/10.1111/jiec.12618

Cuéllar-Franca, R.M., García-Gutiérrez, P., Taylor, S.F.R., Hardacre, C., Azapagic, A., 2016. A novel methodology for assessing the environmental sustainability of ionic liquids used for CO2 capture. Faraday Discuss. 192, 283–301. https://doi.org/10.1039/C6FD00054A

D'Alessandro, D.M., Smit, B., Long, J.R., 2010. Carbon dioxide capture: Prospects for new materials. Angew. Chemie - Int. Ed. 49, 6058–6082. https://doi.org/10.1002/anie.201000431

de Bruijn, H., Duin, R. van, Huijbregts, M.A.J., 2002. Handbook on Life Cycle Assessment, Operational Guide to the ISO Standards. Kluwer Academic Publishers, USA. https://doi.org/10.1007/0-306-48055-7

DETHERM, 2017. thermophysical property data [WWW Document]. DETHERM - Soc. Chem. Eng. Biotechnol.

Disasa Irge, D., 2016. Ionic Liquids: A Review on Greener Chemistry Applications, Quality Ionic Liquid Synthesis and Economical Viability in a Chemical Processes. Am. J. Phys. Chem. 5, 74. https://doi.org/10.11648/j.ajpc.20160503.14

Dong, L.L., He, L., Tao, G.H., Huang, M., Hu, C., 2013. Theoretical enthalpies of formation of [AA]X and [AAE]X type amino acid ionic liquids. J. Chem. Eng. Data 58, 1176–1185. https://doi.org/10.1021/je301285c

Dunn, M.H., Cole, M.L., Harper, J.B., 2012. Effects of an ionic liquid solvent on the synthesis of γ-butyrolactones by conjugate addition using NHC organocatalysts. RSC Adv. 2, 10160. https://doi.org/10.1039/c2ra21889e

Farahipour, R., Karunanithi, A., 2014. Life Cycle Environmental Implications of CO2 Capture and Sequestration with Ionic Liquid 1-butyl-3-methylimidazolium acetate. ACS Sustain. Chem. Eng. 2, 2495–2500. https://doi.org/10.1021/sc400274b

Felder, R.M., Rousseau, R.W., 2005. Elementary Principes of Chemical Processes, 3rd ed. John Wiley & Sons, Inc., USA.

Frischknecht, R., 1998. Life cycle Inventory Analysis for decision-making. Swiss Federal Institute of Technology Zurich.

Ghandi, K., 2014. A Review of Ionic Liquids , Their Limits and Applications. Green Sustain. Chem. 4, 44–53. https://doi.org/10.4236/gsc.2014.41008

Hagiwara, R., Lee, J.S., 2007. Ionic Liquids for Electrochemical Devices. Electrochemistry 75, 23–34. https://doi.org/10.5796/electrochemistry.75.23

Heckenbach, M.E., Romero, F.N., Green, M.D., Halden, R.U., 2016. Meta-analysis of ionic liquid literature and toxicology. Chemosphere 150, 266–274. https://doi.org/10.1016/j.chemosphere.2016.02.029

Hischier, R., Hellweg, S., Capello, C., Primas, A., 2005. Establishing life cycle inventories of chemicals based on differing data availability. Int. J. Life Cycle Assess. 10, 59–67. https://doi.org/10.1065/lca2004.10.181.7

Hischier, R., Walser, T., 2012. Life cycle assessment of engineered nanomaterials: State of the art and strategies to overcome existing gaps. Sci. Total Environ. 425, 271–282. https://doi.org/10.1016/j.scitotenv.2012.03.001

Huang, Y., Zhang, X., Zhang, X., Dong, H., Zhang, S., 2014. Thermodynamic Modeling and Assessment of Ionic Liquid-Based CO_2 Capture Processes. Ind. Eng. Chem. Res. 53, 11805–11817. https://doi.org/10.1021/ie501538e

Huebschmann, S., Kralisch, D., Loewe, H., Breuch, D., Petersen, J.H., Dietrich, T., Scholz, R., 2011. Decision support towards agile eco-design of microreaction processes by

accompanying (simplified) life cycle assessment. Green Chem. 13, 1694. https://doi.org/10.1039/c1gc15054e

Islam, S., Ponnambalam, S.G., Lam, H.L., 2016. Review on life cycle inventory: methods, examples and applications. J. Clean. Prod. 136. https://doi.org/http://dx.doi.org/10.1016/j.jclepro.2016.05.144

ISO 14040, 2006. Environmental management - Life Cycle Assessment - Principles and Framework, International Organization for Standardization. https://doi.org/10.1016/j.ecolind.2011.01.007

ISO 14044, 2006. Environmental management - Life cycle assessment - Requirements and guidelines, International Organization for Standardization.

Jacquemin, L., Pontalier, P.-Y., Sablayrolles, C., 2012. Life cycle assessment (LCA) applied to the process industry: a review. Int. J. Life Cycle Assess. 17, 1028–1041. https://doi.org/10.1007/s11367-012-0432-9

Jolliet, O., Margni, M., Charles, R., Humbert, S., Payet, J., Rebitzer, G., 2003. Presenting a New Method IMPACT 2002 +: A New Life Cycle Impact Assessment Methodology. Int. J. Life Cycle Assesment 8, 324–330. https://doi.org/10.1007/BF02978505

Kadziński, M., Cinelli, M., Ciomek, K., Coles, S.R., Nadagouda, M.N., Varma, R.S., Kirwan, K., 2016. Co-constructive development of a green chemistry-based model for the assessment of nanoparticles synthesis. Eur. J. Oper. Res. 0, 1–19. https://doi.org/10.1016/j.ejor.2016.10.019

Karjalainen, E., Wales, D.J., Gunasekera, D.H.A.T., Dupont, J., Licence, P., Wildman, R.D., Sans, V., 2018. Tunable Ionic Control of Polymeric Films for Inkjet Based 3D Printing. ACS Sustain. Chem. Eng. 6, 3984–3991. https://doi.org/10.1021/acssuschemeng.7b04279

Kowsari, E., 2011. Advanced Applications of Ionic Liquids in Polymer Science. Ion. Liq. Appl. Perspect. 3–28. https://doi.org/10.5772/15224

Kralisch, D., Ott, D., Gericke, D., 2015. Rules and benefits of Life Cycle Assessment in green chemical process and synthesis design: a tutorial review. Green Chem. 17, 123–145. https://doi.org/10.1039/C4GC01153H

Kralisch, D., Reinhardt, D., Kreisel, G., 2007. Implementing objectives of sustainability into ionic liquids research and development. Green Chem. 9, 1308. https://doi.org/10.1039/b708721g

Kralisch, D., Stark, A., Koersten, S., Kreisel, G., Ondruschka, B., 2005. Energetic, environmental and economic balances: Spice up your ionic liquid research efficiency. Green Chem. 7, 301–309. https://doi.org/10.1039/b417167e

Lynam, J.G., Chow, G.I., Coronella, C.J., Hiibel, S.R., 2016. Ionic liquid and water separation by membrane distillation. Chem. Eng. J. 288, 557–561. https://doi.org/10.1016/J.CEJ.2015.12.028

Maciel, V.G., Wales, D.J., Seferin, M., Sans, V., 2018. Environmental performance of 3D-Printing polymerisable ionic liquids. J. Clean. Prod. 214, 29–40. https://doi.org/10.1016/J.JCLEPRO.2018.12.241

Mai, N.L., Ahn, K., Koo, Y.-M., 2014. Methods for recovery of ionic liquids—A review. Process Biochem. 49, 872–881. https://doi.org/10.1016/J.PROCBIO.2014.01.016

Margni, M., Gloria, T., Bare, J., Seppälä, J., Steen, B., Struijs, J., Toffoletto, L., Jolliet, O., 2008. Life Cycle Impact Assessment Programme Guidance on how to move from current practice to recommended practice in Life Cycle Impact Assessment, UNEP/SETAC Life Cycle Initiative.

McCorsley, C., 1981. Process For Shaped Cellulose Article Prepared From A Solution Containing Cellulose Dissolved In A Tertary Amene N-Oxde Solvent. US Patent 4,246,221.

Mehrkesh, A., Karunanithi, A.T., 2016a. Life-Cycle Perspectives on Aquatic Ecotoxicity of Common Ionic Liquids. Environ. Sci. Technol. 50, 6814–6821. https://doi.org/10.1021/acs.est.5b04721

Mehrkesh, A., Karunanithi, A.T., 2016b. Life Cycle Perspectives on Human Health Impacts of Ionic Liquids. bioRxiv 091454–091466. https://doi.org/10.1101/091454

Mehrkesh, A., Karunanithi, A.T., 2013. Energetic ionic materials: How green are they? A comparative life cycle assessment study. ACS Sustain. Chem. Eng. 1, 448–455. https://doi.org/10.1021/sc3001383

Muller, S., Lesage, P., Ciroth, A., Mutel, C., Weidema, B.P., Samson, R., 2016. The application of the pedigree approach to the distributions foreseen in ecoinvent v3. Int. J. Life Cycle Assess. 21, 1327–1337. https://doi.org/10.1007/s11367-014-0759-5

NIST, 2017. NIST Chemistry WebBook [WWW Document]. Natl. Inst. Stand. Technol.

Peterson, J.E., 2013. Ionic Liquid/CO2 Co-Fluid Refrigeration: CO2 Solubility Modeling and Life Cycle Analysis. PhD Thesis, University of Notre Dame.

Piccinno, F., Hischier, R., Seeger, S., Som, C., 2016. From laboratory to industrial scale: a scale-up framework for chemical processes in life cycle assessment studies. J. Clean. Prod. 135, 1085–1097. https://doi.org/10.1016/j.jclepro.2016.06.164

Plechkova, N. V, Seddon, K.R., 2008. Applications of ionic liquids in the chemical industry. Chem. Soc. Rev. 37, 123–150. https://doi.org/10.1039/b006677j

PRé Consultants, 2014. SimaPro Database Manual - Methods Library. San Francisco.

Righi, S., Morfino, A., Galletti, P., Samorì, C., Tugnoli, A., Stramigioli, C., 2011. Comparative cradle-to-gate life cycle assessments of cellulose dissolution with 1-butyl-3-methylimidazolium chloride and N-methyl-morpholine-N-oxide. Green Chem. 13, 367. https://doi.org/10.1039/c0gc00647e

Rosenbaum, R.K., Bachmann, T.M., Jolliet, O., Juraske, R., Koehler, A., Hauschild, M.Z., 2008. USEtox — the UNEP-SETAC toxicity model : recommended characterisation factors for human toxicity and freshwater ecotoxicity in life cycle impact assessment. Int J Life Cycle Assess 13, 532–546. https://doi.org/10.1007/s11367-008-0038-4

Sans, V., Karbass, N., Burguete, M.I., Compañ, V., García-Verdugo, E., Luis, S. V., Pawlak, M., 2011. Polymer-Supported Ionic-Liquid-Like Phases (SILLPs): Transferring Ionic Liquid Properties to Polymeric Matrices. Chem. - A Eur. J. 17, 1894–1906. https://doi.org/10.1002/chem.201001873

Sell, I., Ott, D., Kralisch, D., 2014. Life Cycle Cost Analysis as Decision Support Tool in Chemical Process Development. ChemBioEng Rev. 1, 50–56. https://doi.org/10.1002/cben.201300007

Thuy Pham, T.P., Cho, C.W., Yun, Y.S., 2010. Environmental fate and toxicity of ionic liquids: A review. Water Res. 44, 352–372. https://doi.org/10.1016/j.watres.2009.09.030

Torralba-Calleja, E., Skinner, J., Gutiérrez-Tauste, D., 2013. CO 2 Capture in Ionic Liquids: A Review of Solubilities and Experimental Methods. J. Chem. 473584. https://doi.org/10.1155/2013/473584

Tufvesson, L.M., Tufvesson, P., Woodley, J.M., Börjesson, P., 2013. Life cycle assessment in green chemistry: overview of key parameters and methodological concerns. Int. J. Life Cycle Assess. 18, 431–444. https://doi.org/10.1007/s11367-012-0500-1

Valderrama, J.O., Rojas, R.E., 2009. Critical Properties of Ionic Liquids. Revisited. Ind. Eng. Chem. Res. 48, 6890–6900. https://doi.org/10.1021/ie900250g

Vatani, A., Mehrpooya, M., Gharagheizi, F., 2007. Prediction of standard enthalpy of formation by a QSPR model. Int. J. Mol. Sci. 8, 407–432. https://doi.org/10.3390/i8050407

Wales, D.J., Cao, Q., Kastner, K., Karjalainen, E., Newton, G.N., Sans, V., 2018. 3D-Printable Photochromic Molecular Materials for Reversible Information Storage. Adv. Mater. 30, 1800159. https://doi.org/10.1002/adma.201800159

Wasserscheid, P., Welton, T. (Eds.), 2008. Ionic liquids in Synthesis. Wiley-VCH Verlag GmbH & Co. KGaA. https://doi.org/10.1055/s-2003-40869

WBCSD, 2014. Life Cycle Metrics for Chemical Products 120.

Weidema, B., Wesnaes, M., 1996. Data quality management for life cycle inventories-an example of using data quality indicators, Journal of Cleaner Production. https://doi.org/10.1016/S0959-6526(96)00043-1

Yuan, J., Mecerreyes, D., Antonietti, M., 2013. Poly(ionic liquid)s: An update. Prog. Polym. Sci. 38, 1009–1036. https://doi.org/10.1016/j.progpolymsci.2013.04.002

Zhang, X., Zhang, X., Dong, H., Zhao, Z., Zhang, S., Huang, Y., 2012. Carbon capture with ionic liquids: overview and progress. Energy Environ. Sci. 5, 6668. https://doi.org/10.1039/c2ee21152a

Zhang, Y., Bakshi, B.R., Demessie, E.S., 2008. Life cycle assessment of an ionic liquid versus molecular solvents and their applications. Environ. Sci. Technol. 42, 1724–1730. https://doi.org/10.1021/es0713983

Zhu, J.-F., He, L., Zhang, L., Huang, M., Tao, G.-H., 2012. Experimental and theoretical enthalpies of formation of glycine-based sulfate/bisulfate amino acid ionic liquids. J. Phys. Chem. B 116, 113–9. https://doi.org/10.1021/jp209649h

Zhu, S., Chen, R., Wu, Y., Chen, Q., Zhang, X., Yu, Z., 2009. A Mini-Review on Greenness of Ionic Liquids. Chem. Biochem. Eng. Q. 23, 207–211.

5.2. Capítulo II: Avaliação do desempenho ambiental de Líquidos Iônicos polimerizáveis via impressão 3D.

O artigo intitulado "*Environmental Performance of 3D-Printing Polymerisable Ionic Liquids*" foi publicado em um periódico qualificado pela Capes com o Qualis A1 (Química e Engenharias II), Cite Score de 5,79 e fator de impacto de 5,65. Este estudo apresenta um estudo de Avaliação do Ciclo de Vida do berço–ao-portão da síntese do poli(liquido iônico) sintetizado a partir do sistema de estereolitografia. O estudo foi conduzido a partir de dados primários da síntese dos LIs e do processo de impressão 3D realizados no *GSK Carbon Neutral Laboratory* for *sustainable chemistry* da Universidade de Nottingham no Reino Unido. Este trabalho apresenta o primeiro estudo de ACV de líquidos iônicos à base de imidazólio, com o cátion $[BVim]^+$ à base de vinilimidazólio e $[NTf_2]^-$ como contra-íon e polimerizáveis a partir de impressão 3D. Este estudo demonstra que a natureza do monómero de PIL tem um impacto comparável ao LI convencional não polimerizável. Este resultado sugere que os monômeros PIL são viáveis em termos de impactos ambientais com a vantagem adicional de versatilidade devido à estrutura de dupla ligação. Além disso, o processo de fabricação aditiva mostrou-se tecnicamente viável e não exacerba os impactos ambientais a partir de líquidos iônicos monômeros constituintes. No entanto, excelentes oportunidades para mitigar os impactos do CV dos PILs estão associadas a esta etapa. A recuperação total dos reagentes na etapa de impressão é crucial, tanto quanto a escolha do ânion para o desempenho ambiental da impressão 3D do PIL. A mudança do ânion $N(CN)_2^-$ pelo NTf_2^-, do precursor do PIL, apresentou redução significativa dos impactos em todas as categorias de impacto avaliadas.

Journal of Cleaner Production 214 (2019) 29–40

Contents lists available at ScienceDirect

Journal of Cleaner Production

journal homepage: www.elsevier.com/locate/jclepro

Environmental performance of 3D-Printing polymerisable ionic liquids

Vinícius Gonçalves Maciel [a, b], Dominic J. Wales [c, d, 1], Marcus Seferin [a, b], Victor Sans [c, d, *]

[a] School of Chemistry, Pontifical Catholic University of Rio Grande do Sul – PUCRS, Brazil
[b] Post-Graduation Program in Materials Engineering and Technology, Pontifical Catholic University of Rio Grande do Sul – PUCRS, Brazil
[c] Faculty of Engineering, University of Nottingham, Nottingham, NG7 2RD, UK
[d] GSK Carbon Neutral Laboratory, University of Nottingham, Nottingham, NG7 2GA, UK

ARTICLE INFO

Article history:
Received 28 June 2018
Received in revised form
22 November 2018
Accepted 23 December 2018
Available online 28 December 2018

Keywords:
Life cycle assessment
3D-printing
Additive manufacturing
Ionic liquids
Stereolithography
Polymers

ABSTRACT

This work presents a "cradle-to-gate" Life Cycle Assessment (LCA) of 3D-printing polymerisable ionic liquids (PILs) using digital light projection (DLP). It is based on primary data from environmental emissions, wastewater, chemical components, and manufacturing of PIL based devices. The results indicate that the printing process does not significantly exacerbate the environmental impacts. However, it is shown that excellent opportunities for further mitigation of the life cycle impacts of PILs can be realised are by practising reagent recovery, which reduces the amount of reagents emitted as waste, and by reduction/recycling of solvents used for cleaning the 3D part. The major impact contributor in the 3D-printing of PILs is the synthesis of the IL monomers. The effective reduction of solvent consumption and recovery significantly improves the impact of the synthetic process. This work focuses on the employment of the 3-butyl-1-vinylimidazolium [BVim] cation, with the non-coordinating and hydrophobic bis(trifluoromethane)sulfonimide $[NTf_2]^-$ anion as the counter anion. The polymerisable monomer IL has comparable impact compared to the analogous non-polymerisable 3-butyl-1-methylimidazolium $[NTf_2]^-$ ionic liquid, thus potentially allowing for the more efficient use of the ionic liquid properties by immobilization in solid phases. Furthermore, it is demonstrated that switching the anion from $[NTf_2]^-$ to dicyanamide $[N(CN_2)]^-$ significantly decreases the impacts in all categories evaluated for PIL production. This work represents the first phase toward quantitative LCA data generation for the process of 3D-printing ionic liquids, which will be great support for decision making during design of PIL 3D-printing processes at a laboratory scale.

1. Introduction

Polymerisable ionic liquids or poly(ionic liquid)s (PILs) (Mecerreyes, 2011) (Yuan et al., 2013) are a type of polyelectrolytes with similar structure to homogeneous ionic liquids (ILs), (Welton, 1999) with an effective transfer of IL properties to the supported phases, (Sans et al., 2011) and are increasingly gaining popularity in a broad range of fields, including energy, catalysis and semiconductors (Yu et al., 2015) (Qian et al., 2017). Despite having been long considered green solvents due to their negligible vapour pressure at STP conditions, life cycle assessment (LCA) of ILs have been performed, (Cuéllar-Franca et al., 2016) and it has been found that employing ILs as solvent is highly likely to have a larger life cycle environmental impact than conventional solvents (Zhang et al., 2008). Hence, the reduction in gaseous emissions related to the negligible vapour pressure, do not necessarily translate into more sustainable processes (Kralisch et al., 2005). Employing ILs as proxy, it has been found that recovery of the IL and solvents employed are key parameters to optimise the environmental impacts of the modelled processes (Amado Alviz and Alvarez, 2017; Righi et al., 2011; Zhang et al., 2008). Hence, immobilization of the IL should help to mitigate the environmental impacts of processes that employ ILs. Indeed, the effective transfer of properties from the bulk ionic liquids to supported materials with analogous units helps to overcome the limitations typically associated with the employment of ionic liquids, by minimizing the amount of IL units

* Corresponding author. Faculty of Engineering, University of Nottingham, Nottingham, NG7 2RD, UK.
E-mail address: victor.sanssangorrin@nottingham.ac.uk (V. Sans).
[1] Current address: The Hamlyn Centre, Faculty of Engineering, South Kensington Campus, Imperial College London, London, SW7 2AZ, U.K.

https://doi.org/10.1016/j.jclepro.2018.12.241
0959-6526/

used and facilitating the separation and recycling of the material (Sans et al., 2011).

Additive manufacturing, commonly known as three-dimensional printing (3DP) is a relatively novel manufacturing technology that allow for the generation of complex geometries in a layer by layer fashion (Gunasekera et al., 2016). The additive nature of these techniques minimizes the amount of material employed, potentially lowering energy use, resource demands and related carbon dioxide (CO_2) emissions over the entire product life cycle. It is estimated that the implementation of 3D-printing might allow reduction of energy and carbon dioxide emission intensities by about 5% by 2025 (Gebler et al., 2014). Furthermore, it may induce changes in manufacturing logistic supply chains, generating shifts towards digital distributed supply chains (Gebler et al., 2014) (OECD, 2017).

However, concerns with 3D-printing have been highlighted by various recent studies in terms of environmental protection and sustainability (Bekker and Verlinden, 2018; Li et al., 2017; Ma et al., 2018a). According to Ma et al. (2018a, b) additive manufacture stage has the highest influence on environmental performance. Several studies have reported that many 3D-printing processes have relatively high levels of energy consuption (Barros et al., 2017; Kreiger and Pearce, 2013; Yang et al., 2017). An extensive review of 3D-printing and its societal impact can be found in Huang et al. (2013).

Despite the efforts to develop novel materials for 3D-printing, the molecular functionalization of printable 'inks' remains challenging, thus hindering the range of applications accessible with these techniques. Long and collaborators recently demonstrated the possibility of 3D-printing PILs (Schultz et al., 2014). Very recently, we demonstrated the possibility of inkjet printing PILs (Karjalainen et al., 2018) and also 3D-printing of advanced photochromic materials based on PILs containing molecular hybrid organic-inorganic polyoxometalates (Wales et al., 2018). Furthermore, the possibility of 3D-printing layers with high resolution (5 μm) employing inkjet allows further minimization of the material employed (Karjalainen et al., 2018).

Despite the potential of these new materials to develop novel applications, there are no specific studies of the environmental impact associated with their manufacture. Understanding the environmental impact of manufacturing PILs is key to enable sustainability based decision-making processes for the development of novel materials, devices and applications using additive manufacture (Cerdas et al., 2017). Life cycle assessment (LCA) is a powerful tool to evaluate the environmental impacts of the product and process involving additive manufacture of PILs (Jacquemin et al., 2012). Here, we present the first cradle-to-gate LCA analysis of the manufacturing of imidazolium-based polymerisable ionic liquids with 3D-printing, with a modular analysis that allows for the identification of the magnitude of the contribution from the different process steps. Primary laboratory scale data was used to model the synthesis of the PIL precursors and the subsequent printing step. Sensitivity analyses were also performed to elucidate how optimisation of the additive manufacture of advanced devices based on PILs can lead to significant reductions in the environmental impacts.

2. Methodology

2.1. Goal and scope

The goal of this study is to provide a cradle-to-gate LCA analysis of the manufacturing of imidazolium-based PILs with 3D-printing, with a modular analysis that allows for the identification of the magnitude of the contribution from the different process steps. Also, this study aims to understand how these impacts compare to an analogous non-polymerisable homogeneous ionic liquid, and from PIL precursors with a different anion. The synthesis of the ionic liquids and the 3D-printing of the PILs was conducted at laboratory scale. Therefore, these data are considered as primary data. Use of secondary data was necessary to provide intermediate substances and for making comparative scenarios.

The Functional Unit (FU) for this study is a 1.2 g printed part of PIL; all the inputs and outputs are related to the FU. In the "cradle-to-gate" model used in this study, all of the process steps from raw material extraction (the cradle), up to the printed material step (the gate of the laboratory), are considered. The synthesis of poly(ionic liquids) was based on the reported synthesis procedure for 3-butyl-1-vinylimidazolium bis(trifluoromethane)sulfonimide ([BVim][NTf_2]) (Wales et al., 2018). The production of [BVim][NTf_2]) is achieved via a metathesis reaction between lithium bis(trifluoromethane)sulfonimide ($LiNTf_2$) and 3-butyl-1-vinylimidazolium bromide ([BVim][Br]). The system boundaries assessed in this work are defined in Fig. 1. The LCA study has been performed based on Standards ISO 14040 (ISO, 2006a) and ISO 14044 (ISO, 2006b). Data necessary to model the upstream processes was obtained from the Ecoinvent v3.2 database and Simapro Software v 8.003 version faculty was used for process modelling and impact characterisation.

2.2. Life cycle inventory data collection

The life cycle material and energy consumption data related to production of the PILs, ILs and their precursors were derived from a combination of mass and energy balance primary data from the laboratory, literature, theoretical calculations, and secondary data sources, such as databases. Full life cycle assessments involving ILs are difficult, (Cuéllar-Franca et al., 2016; Mehrkesh and Karunanithi, 2016, 2013) due to the lack of LCI data for most novel ILs in the literature, because of complex synthetic routes involving numerous precursors. In this work a full life cycle assessment was conducted using the "life cycle tree" approach reported previously to assess the LCA of ILs (Cuéllar-Franca et al., 2016; Mehrkesh and Karunanithi, 2013; Peterson, 2013; Zhang et al., 2008).

2.2.1. Mass balances

The material inputs and outputs of 3D-printing the imidazolium based PILs were obtained from experimental data (see Table S8 in the ESI). A schematic overview of the 3D printing process is given in Scheme 1 and Scheme 2 in the ESI. The inputs of the [BVim][Br] and [BVim][NTf_2] were collected from primary data generated in the laboratory. The outputs of these substances were calculated from the mass balance (Table S1 – S8 in the ESI). The mass balances for PIL precursors that were not available in the Ecoinvent v3.2 database were calculated following literature methods (Felder and Rousseau, 2005). Table 1 summarises the synthetic routes considered in this study for all substances not available in LCI databases.

2.2.2. Energy balances

The energy flow of the 3D-printing process was determined by measuring the energy consumption of the printing process through use of an electricity monitor socket (Brennenstuhl® PM 231E model). This approach has been previously used in lifecycle assessment studies of fabrication at the laboratory scale (Kralisch et al., 2007). Reaction enthalpies were calculated for the different transformations summarised in Table 1, except for $LiNTf_2$ which has been previously determined (Peterson, 2013). The theoretical energy consumption for the production of substances was calculated through the use of Eqs (1)–(3). The calculation of the theoretical energy consumption was based on multiplying the reaction enthalpies by a series of correction factors, following literature

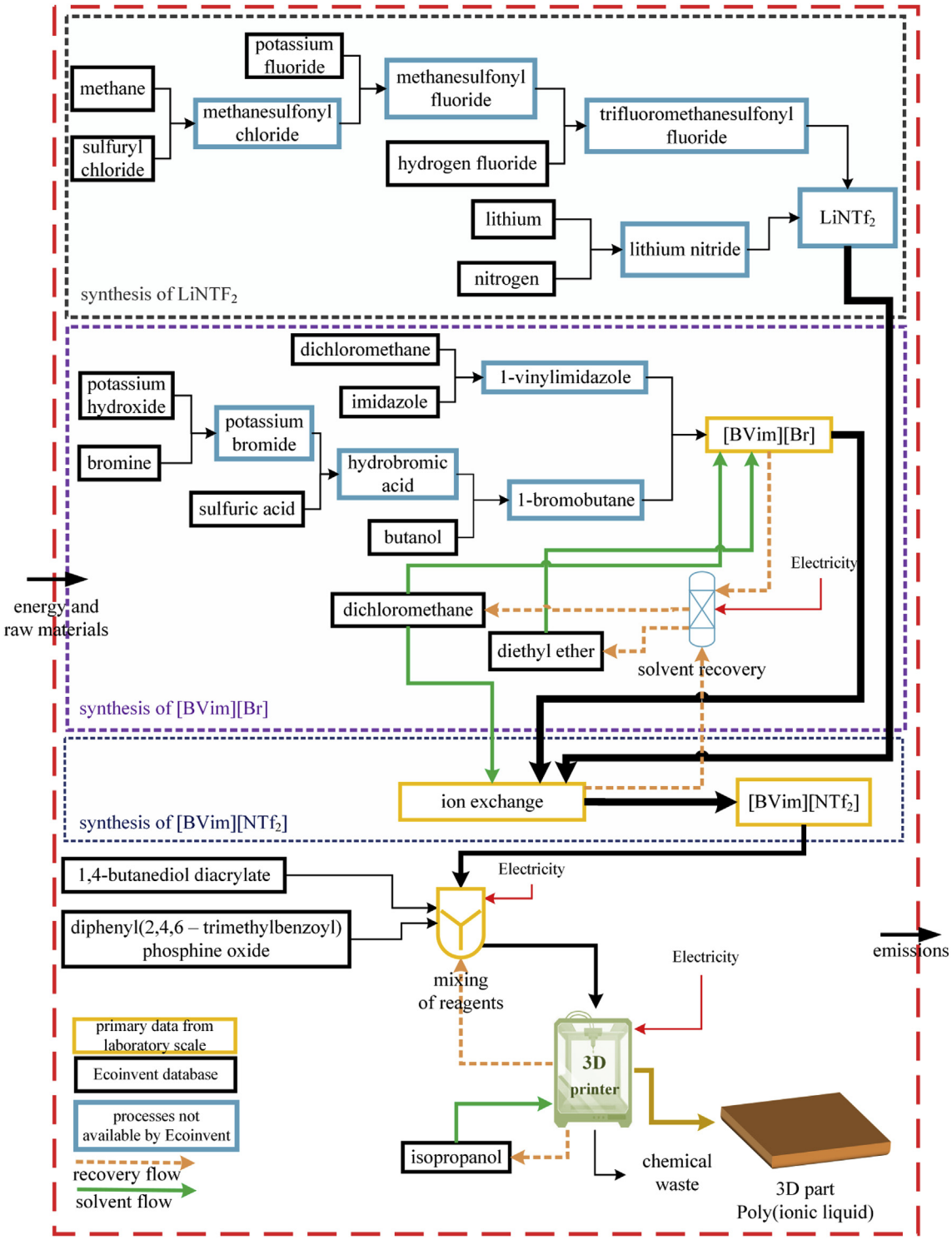

Fig. 1. Diagram highlighting the system boundaries of the life cycle assessment presented in this work. [BVim][Br]: 3-butyl-1-vinylimidazolium bromide; [BVim][NTf_2]: 3-butyl-1-vinylimidazolium bis(trifluoromethane)sulfonimide; $LiNTf_2$: lithium bis(trifluoromethane)sulfonimide; IUPAC name for "isopropanol": propan-2-ol.

methods (Cuéllar-Franca et al., 2016; Mehrkesh and Karunanithi, 2013). According to Mehrkesh and Karunanithi (2013) the estimated theoretical value can be converted to the actual heat consumption (with heating assumed to be supplied by combustion of natural gas) using a correction factor of 4.2 for endothermic and 3.2 for exothermic reactions. It is important to highlight that, in the method by Mehrkesh and Karunanithi, and in this work, an assumption was made that no work is performed and that the kinetic and potential energy are zero. Thermophysical property data have been extracted from National Institute of Standards and Technology (NIST, 2018) and Society for Chemical Engineering and Biotechnology (DETHERM, 2018) databases. Values for the heat of formation of ionic liquids that were not available in the literature, were calculated (Table S1) using a genetic algorithm-based

Table 1
Synthesis routes considered to chemical substances not available in LCI databases.

Entry	Substance	Abbreviation	Chemical routes assumed	Reference
1	3-butyl-1-vinylimidazolium bromide ($C_9H_{15}BrN_2$)	[BVim][Br]	$C_5H_6N_2 + C_4H_9Br \rightarrow C_9H_{15}BrN_2$	This work
2	1-vinylimidazole ($C_5H_6N_2$)	–	$C_3H_4N_2 + C_2H_4Cl_2 \rightarrow C_5H_6N_2 + 2HCl$	Ding and Shen (2012)
3	1-bromobutane (C_4H_9Br)	–	$C_4H_{10}O + HBr \rightarrow C_4H_9Br + H_2O$	Kamm and Marvel (1921)
4	hydrobromic acid (HBr)	–	$H_2SO_4 + KBr \rightarrow KHSO_4 + HBr$	Booth (1939)
5	potassium bromide (KBr)	–	$6KOH + 3Br_2 \rightarrow KBrO_3 + 5KBr + 3H_2O$	Blanchard et al. (1936)
6	3-butyl-1-vinylimidazolium bis(trifluoromethane)sulfonimide ($C_{11}H_{15}F_6N_3O_4S_2$)	[BVim][NTf_2]	$C_9H_{15}BrN_2 + C_2F_6LiO_4S_2N \rightarrow C_{11}H_{15}F_6N_3O_4S_2 + LiBr$	This work
7	lithium bis(trifluoromethane)sulfonimide ($C_2F_6LiO_4S_2N$)	$LiNTf_2$	$2CF_3SO_2F + Li_3N \rightarrow C_2F_6LiO_4S_2N + 2LiF$	Peterson (2013)
8	lithium nitride (Li_3N)	–	$6Li + N_2 \rightarrow 2Li_3N$	Peterson (2013)
9	trifluoromethanesulfonyl fluoride (CF_3SO_2F)	–	$CH_3SO_2F + 3HF \rightarrow CF_3SO_2F + 3H_2$	Peterson (2013)
10	methanesulfonyl fluoride (CH_3SO_2F)	–	$CH_3SO_2Cl + KF \rightarrow CH_3SO_2F + KCl$	Peterson (2013)
11	methanesufonyl chloride (CH_3SO_2Cl)	–	$CH_4 + SO_2Cl_2 \rightarrow CH_3SO_2Cl + HCl$	Peterson (2013)
12	sulfuryl chloride (SO_2Cl_2)	–	$SO_2 + Cl_2 \rightarrow SO_2Cl_2$	Peterson (2013)

multivariate linear regression method (Vatani et al., 2007). Heat capacities of ionic liquids that were not available in the literature were calculated according to the Joback group contribution method (Stouffer et al., 2008). Sensitivity analysis was performed to estimate the effect of the assumed thermodynamic parameters.

$$E_i = \Delta H \; x \; Fc \quad (1)$$

$$\Delta H = \sum\left(RMM.\widehat{H}\right)outputs \; - \; \sum\left(RMM.\widehat{H}\right)inputs \quad (2)$$

$$\widehat{H} = \Delta\widehat{H}f^{\circ} + \int_{T1}^{T2} C_R.\Delta T \quad (3)$$

where:

E_i : theoretical energy consumption
ΔH: heat of reaction
RMM = molecular weight of reactants
$\widehat{H}$ = specific enthalpy of reactants
$\Delta\widehat{Hf^{\circ}}$ = heat of formation of reactants
C_R = calorific value of reactants
T1 = reference temperature (25 °C)
T2 = temperature of the reactants
Fc = a factor of 4.2 for endothermic reactions with the assumption of natural gas powered heating and a factor of 3.2 for exothermic reactions with the assumption that cooling uses electricity (Mehrkesh and Karunanithi, 2013).

2.3. Life cycle impact assessment and interpretation

The choice of environmental impact categories is a very important part of an LCA study and impacts categories that permit an overall assessment of impacts must be considered (de Bruijn et al., 2002). Thus, the methods for calculating environmental impacts chosen for this study were CML baseline (PRé Consultants, 2014) and Cumulative Energy Demanded (CED v1.09), which are the most widely employed for life cycle studies on ILs or 3D-printing (Cuéllar-Franca et al., 2016; Huebschmann et al., 2011; Kreiger and Pearce, 2013; Ma et al., 2018b; Righi et al., 2011). The following impact category groups were analysed: global warming potential (GWP), abiotic depletion potentials (ABP), acidification potential (AP), eutrophication potential (EP), human toxicity potential (HTP), ozone layer depletion potential (ODP), fresh aquatic ecotoxicity potentials (FAEP), marine aquatic ecotoxicity potentials (MAEP) and cumulative energy demand (CED). These impact categories were chosen as they have been previously employed in LCA studies of ILs (Amado Alviz and Alvarez, 2017; Cuéllar-Franca et al., 2016; Farahipour and Karunanithi, 2014; Huebschmann et al., 2011; Kralisch et al., 2007, 2005; Mehrkesh and Karunanithi, 2013; Righi et al., 2011; Zhang et al., 2008). Moreover, CED has been reported as an important indicator of sustainability in additive manufacturing (Kellens et al., 2017; Kreiger and Pearce, 2013; Quinlan et al., 2017).

2.4. Assumptions and limitations

For the evaluation of the system, the following assumptions have been made:

Theoretical energy: only the energy requirements of reactors (heating and cooling) have been considered as it is not known what other unit operations may be needed in a future commercial production process and what their configuration and capacity might be. Therefore, energy consumption for separation, pumping and other operations is excluded from the estimation.

Power grid UK: For database consistency, all the laboratorial scale processes analysed in this work were located in United Kingdom (UK). Thus the UK power generation mix (Energy UK, 2017) was considered in this work for the production of [BVim][NTf_2], [BVim][Br] and the 3D-printing step.

Upstream process: For database consistency with the Ecoinvent database 3.2, (Frischknecht et al., 2005) all the industrial processes analysed in this paper were located in Europe. Ecoinvent database establishes transport distances and infrastructure for each process. For potassium fluoride the "Sodium fluoride {GLO}| market for | Alloc Def, U" database within the Ecoinvent v3.2 database was used.

Transport: For those processes not included in the Ecoinvent v3.2 database, the transport of substances was considered as 100 km by lorry and 600 km by train transport within Europe (Hischier et al., 2005).

Emissions of ionic liquids and $LiNTf_2$*:* [BVim][NTf_2], [BVim][Br] and $LiNTf_2$ outputs were considered as unspecified organic compounds in the Simapro software. In this case emissions are defined as all releases of chemicals during the synthesis of the ionic liquids and the utilisation of the ionic liquids.

Solvent recycling: In this study the recycling and refeeding of 99% of all solvents used for syntheses of [BVim][NTf_2], [BVim][Br] and work-up were assumed (Cuéllar-Franca et al., 2016; Kralisch et al., 2007, 2005). Thus, the impact of recycling the organic solvents isopropanol, diethyl ether and dichloromethane was estimated by assuming the solvent distillation and the energy consumption from thermodynamic data. The energy demand for solvent recycling were calculated using Eq. (4) according to the work of Felder and Rousseau (2005), with an additional correction factor of either 4.2 or 3.2 (Mehrkesh and Karunanithi, 2013). The results are shown in

Table 2.

$$Q_{cal} = \left(n \times \int_{T1}^{T_{evap}} Cp \times dT + \Delta H_{vap} \right) \times Fc \quad (4)$$

Where,

Q_{cal}: Heat transported
n: number of mols
T1 = reference temperature (25 °C)
T_{evap} = evaporation temperature of the substance
Cp: heat capacity
dT: temperature differential
ΔH_{vap}: Heat of vaporisation.

F_C: The estimated theoretical value could be converted to the actual heat consumption (assumed to be supplied by natural gas) using a correction factor of 4.2 and the theoretical energy by exothermic reactions to the actual cooling electricity requirements using a correction factor of 3.2 (Mehrkesh and Karunanithi, 2013).

Overall limitations: In this study, the potential limitations are as follows: (i) all calculations were based on the life-cycle tree and it is possible that alternative methods (reactions) exist for producing one or more of the precursors; (ii) the reaction yields of ionic liquid syntheses were based on the literature when available, and a yield of 100% was assumed when the data was not available; (iii) the calculations in this study are based on small-scale batch processes in laboratory scale experiments for producing the PIL and the ionic liquids ([BVim][NTf_2] and [BVim][Br]).

3. Results and discussion

3.1. Life cycle inventory results

The LCI results from this work are presented in Tables S8–S10 of the Electronic Supplementary Material. The input and output flows for each substance consider the amounts required to produce one part of PIL (the FU) with a mass of 1.2 g. Table S8 shows the LCI results from primary data collected at laboratory scale. Table S9 shows the LCIs of chemical substances that were employed in the synthesis of [BVim][Br] and were not available in the Ecoinvent v3.2 database. Table S10 shows the LCIs of $LiNTf_2$ and its intermediate chemical substances.

3.2. Life cycle assessment results

Once all input and output flows and their amounts had been determined, the next step was to determine the impacts attributed to manufacturing one of the FU. Thus, the environmental impacts for each environmental impact category caused by the production of the FU are shown in Table 3.

Due to a lack of life cycle studies on 3D-printing of polymerisable ionic liquids, studies about 3D-printing manufacture of non-ionic liquid polymers were employed for comparison (*Cerdas* et al., 2017). Regarding the global warming potential, the impact magnitude was 9.19×10^{-2} kg CO_2 eq./1.2 g of PIL printed. In comparison, Cerdas et al. (2017) reported a LCA study of 3D-printing products from polylactic acid employing Fused Deposition Modelling (FDM) and stated that the production of one frame for eyeglasses (~30 g) gave rise to a GWP impact of between 0.006 and 0.021 kg CO_2 eq./g of part. This means that even though both processes are not directly comparable, the PILs have higher GWP (0.0785 kg CO_2 eq./g of PIL printed).

In order to determine the contribution of inputs in the 3D-printing step (reagents, solvents, heat and electricity consumed) on the life cycle of the PIL, a contribution analysis of this step was made (see Fig. 2). The results indicate that the ionic liquid [BVim][NTf_2] was the major source of impacts for all environmental categories evaluated. In contrast, the additive manufacturing step (3D-printing process) did not show a significant contribution to the final results. Also, the electricity energy consumed for 3D-printing had an impact contribution between 0.86% and 6.9%. Energy consumption of 3D manufacturing processes is an important environmental performance consideration for additive manufacturing (Gebler et al., 2014; Gutowski et al., 2017; Peng, 2016). In this study the energy consumed during printing was 8.91 kWh/kg of PIL printed by stereolithography (SLA). This result is in agreement with previous reports, which found that the energy consumption of various additive manufacture technologies ranges between 1.11 kWh/kg to 2140 kWh/kg (Gutowski et al., 2017). Another previous study reported the energy consumed during a stereolithography manufacture process using epoxy resin was 32.5 kWh/kg (Luo et al., 1999). Yang et al. (2017) developed a mathematical model for the energy consumption of SLA-based processes where according to their results the layer and total printing time are major factors significant to the overall energy consumed. In addition, Yang et al. calculated using their mathematical model that the energy consumed to print LS600M material (a commercial photopolymer) is 175.95 kWh/kg of material printed (Yang et al., 2017).

The energy consumed at laboratory scale for mixing and preparation of reagents plus the electrical energy consumed during 3D-printing had a contribution of 1.60% and 13.3% for ozone layer depletion and global warming, respectively. The mixing and preparation of reagents steps can be considered independent of the use of the 3D printer, since these steps are necessary in traditional synthesis (Shaplov et al., 2016).

The [BVim][NTf_2] synthesis process presents a long supply chain from natural resources to the end product, therefore it requires large quantities of materials, energy and solvents, and it involves organic compound emissions to air and water. The total score of each environmental impact category resulting from classification and characterization of the compounds used in the synthesis of [BVim][NTf_2] production are shown in Table 7. Previous studies reported the environmental performance of other ionic liquids such as butylmethylimidazoluim chloride [Bmim][Cl], (Amado Alviz and Alvarez, 2017; Righi et al., 2011) and trihexyltetradecylphosphonium 1,2,4-triazolide ([P_{66614}][124Triz]) (Cuéllar-Franca et al., 2016). These studies reported GWP impacts estimated at 6.30 kg CO_2 eq. per kg of [P_{66614}][124Triz] and 6.40 kg CO_2 per kg [Bmim][Cl]. In this work, the [BVim][Br] showed similar

Table 2
Solvent recycling and theoretical energy calculated by heat transport referenced to the FU.

Entry	Solvent	Process	Amount/mol	ΔH_{vap}/kJ mol^{-1}	C_p(l)/kJ mol^{-1} K^{-1}	Q_{cal}/kJ
1	isopropanol	Washing 3D part	0.11	39.95	0.16	22.40
2	dichloromethane	[BVim][NTf_2]	3.09	28.06	0.10	137.23
3	diethyl ether	[BVim][Br]	0.67	27.10	0.17	118.65
4	dichloromethane	[BVim][Br]	0.16	28.06	0.10	118.52

Table 3
Characterised LCA results of one 3D printed part (1x FU).

Entry	Impact Categories	Unit	PIL printed	Method
1	Abiotic depletion	kg Sb eq.	7.87×10^{-4}	CML 2001
2	Acidification	kg SO_2 eq.	3.14×10^{-3}	CML 2001
3	Cumulative Energy Demand	MJ	1.74	CED
4	Eutrophication	kg PO_4^{3-} eq.	5.33×10^{-5}	CML 2001
5	Freshwater aquatic ecotoxicity	kg 1,4-DB eq.	1.21×10^{-3}	CML 2001
6	Global warming	kg CO_2 eq.	9.19×10^{-2}	CML 2001
7	Human toxicity	kg 1,4-DB eq.	6.46×10^{-2}	CML 2001
8	Marine aquatic ecotoxicity	kg 1,4-DB eq.	7.50×10^{-3}	CML 2001
9	Ozone layer depletion	kg CFC-11 eq.	1.85×10^{-8}	CML 2001

CML 2001: CML method 2001 (PRé Consultants, 2014). CED: Cumulative Energy Demand V1.09 method (PRé Consultants, 2014). FU: functional unit used in this work = 1.2 g of PIL printed. Sb = antimony, SO_2 = sulfur dioxide, PO_4^{3-} = phosphate, CO_2 = carbon dioxide, CFC-11 = trichlorofluoromethane, 1,4-DB = 1,4-dichlorobenzene, MJ = mega joules.

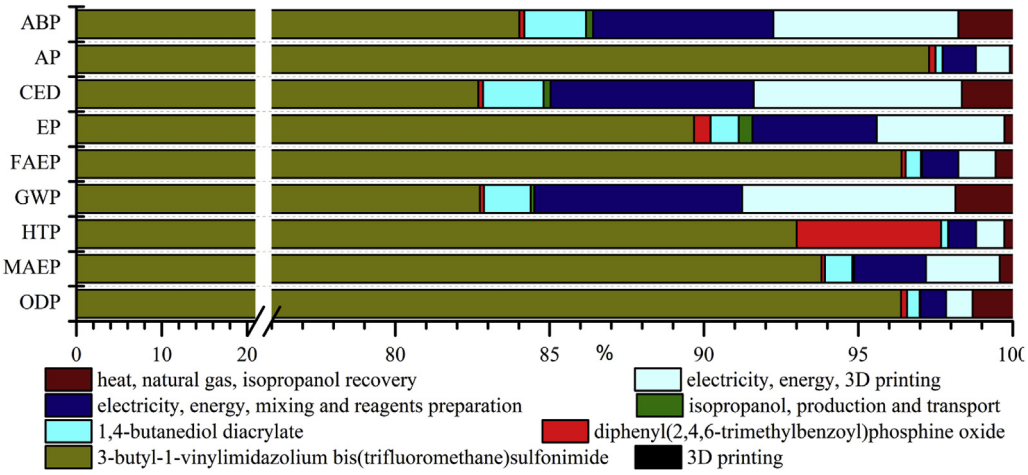

Fig. 2. Contribution relative of inputs to life cycle of PIL printed.

environmental performance (8.9 kg CO_2/kg of [BVim][Br]), however the $LiNTf_2$ and [BVim][NTf_2] showed higher emissions. Huebschmann et al. (2011) reported large differences between environmental performances of ionic liquids using life cycle methodology. In that study, the [Bmim][Cl] showed GWP impacts five times smaller than 1-octadecyl-3-methylimidazolium bromide ([C_{18}MIM][Br]) (Huebschmann et al., 2011).

Fig. 3 shows the relative impact contribution of the three steps of the [BVim][NTf_2] synthesis: (Step 1) synthesis of $LiNTf_2$; (Step 2) synthesis of 3-butyl-1-vinylimidazolium bromide and (Step 3) the synthesis of [BVimi][NTf_2]. The results suggest that $LiNTf_2$ is the biggest contributor to the environmental impacts in the [BVim][NTf_2] life cycle. On the other hand, Step 3 shows the lowest contribution. The $LiNTf_2$ represents 65.2% of total mass of the reagents consumed in the synthesis of [BVim][NTf_2], and 39.4% is considered to be chemical waste output. Hence, good practices

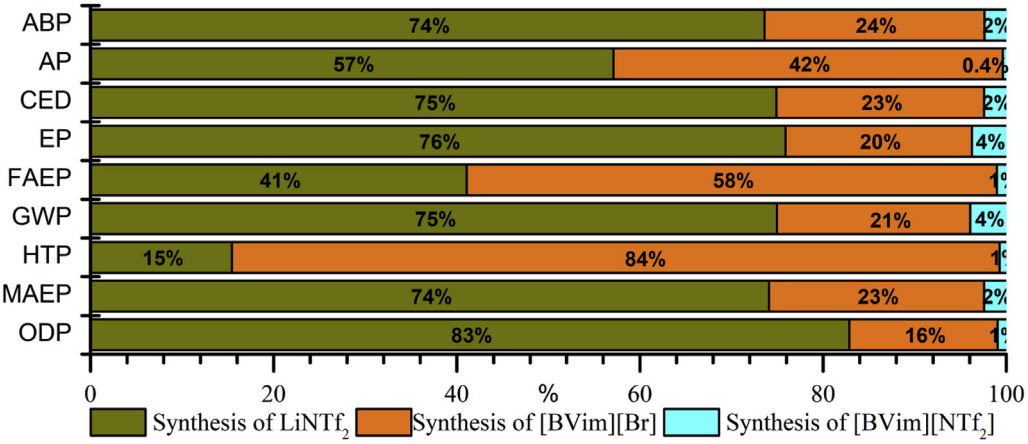

Fig. 3. Life cycle Assessment results of [BVim][NTf_2] step syntheses for impact categories. GWP: global warming potential; ABP: abiotic depletion potentials; AP: acidification potential; EP: eutrophication potential; HTP: human toxicity potential: ODP: ozone layer depletion potential; FAEP: fresh aquatic ecotoxicity potentials; MAEP: marine aquatic ecotoxicity potentials and CED: cumulative energy demanded.

related to this reaction are necessary to obtain a good environmental performance of the [BVim][NTf_2] product. An environmental improvement for [BVim][NTf_2], and consequently the imidazolium-based PIL, could be achieved by development of new synthesis routes or synthesis routes that require less $LiNTf_2$ input. Table 4 shows the values calculated for each impact category.

3.2.1. Contribution of processes

Fig. 4 shows the percentage contributions of each impact categories for the main impact processes for printing PILs. Processes that showed a contribution ≥5% were considered a significant contribution. Contributions of <5% were added together and named "other processes".

Based on the contribution analysis (see Fig. 4), it can be observed that the methanesulfonyl fluoride (CH_3SO_2F) showed a significant contribution in seven of the nine impact categories assessed, and it was the major source of impact in four categories. Methanesulfonyl fluoride (CH_3SO_2F) is a precursor in the synthesis of trifluoromethanesulfonyl fluoride, which in turn is an intermediate in the synthesis of $LiNTF_2$. Thus, these results are consistent with the IL being the largest contributor to the environmental impact in this system. In contrast, the methanesulfonyl fluoride did not show significant contribution to either human toxicity potential or abiotic depletion potential. However, both those impact categories showed a significant contribution of trifluoromethanesulfonyl fluoride which is a substance synthesized from methanesulfonyl fluoride.

In the Abiotic Depletion Potential (ABP) category, the trifluoromethanesulfonyl fluoride life cycle contributed the most (46.0%). This is mostly due to the energy consumed for upstream processes. In terms of the substance, combustion of natural gas was the largest contributor with *ca.* 40% and combustion of hard coal contributed *ca.* 29% - both of these substances are used for generation of the thermal energy and electricity energy consumed during the trifluoromethanesulfonyl fluoride life cycle. The Acidification Potential (AP) category has methanesulfonyl fluoride and 1-vinyimidazole as the biggest contributors with 49.0% and 25.0%, respectively. In terms of substances in the synthesis of methanesulfonyl fluoride, sulfuric acid emissions to air and water were the biggest contributor in ACP with 29.0% participation. Besides that, the sulfur dioxide emitted to air showed contribution about 27.7% for this category. In the eutrophication potential 45.0% of impacts was coming from trifluoromethanesulfonyl fluoride and 19.0% from lithium nitride. In terms of substance, nitrogen oxide showed participation of 47.4% and phosphate emitted to water has participation of 28.6% in the life cycle of the PIL. It is important to highlight that these processes are intermediate substances used in the synthesis of $LiNTf_2$.

The FAEP and MAEP impact categories have the similar processes and substances as the biggest contributors. Methanesulfonyl fluoride showed contribution of the 27.0% and 45.0% for FAEP and MAEP, respectively. Also, 1-vinyimidazole showed contribution of the 49% and 12% for FAEP and MAEP, respectively. Besides that, lithium nitride had the next greatest contribution with about 6% for FAEP and 10% for MAEP. Note that methanesulfonyl fluoride and lithium nitride are direct precursors in the synthesis of $LiNTf_2$. Moreover, the substance that contributes most for FAEP was formaldehyde with participation of 42.3%. In MAEP vanadium was the substance that had the major contribution with 34.9%. The human toxicity impact category showed great contribution from glyoxal production (75.0%). Glyoxal is used as an intermediate in the synthesis of imidazole, which in turn is an intermediate substance in the synthesis of 3-butyl-1-vinylimidazolium bromide. Also, the impact is dominated by ethylene oxide emissions (48.8% for water and 25.4% for air). This substance has been previously reported in LCA studies as contributing greatly to the environmental performance of substances that have imidazole as a precursor (Amado Alviz and Alvarez, 2017; Righi et al., 2011).

Ozone layer depletion also showed methanesulfonyl fluoride as the biggest source of its impacts with participation of 64%. The intermediate substances to methanesulfonyl fluoride that contribute the most is tetrachloromethane (CFC-10) with participation of 65.9%. In the accumulative energy demand methane sulfonyl fluoride and isopropanol were the biggest contributors to this impact category, with participation of 26.0% and 16.0%, respectively. In terms of substances, natural gas is the largest contributor with 32.9%, followed by crude oil, which contributed 25.2%. Both of these substances are used for generation of the thermal energy and electricity energy consumed during the methanesulfonyl fluoride process. Natural gas represents *ca.* 41% of source energy in the United Kingdom power generation mix (Energy UK, 2017).

Finally, global warming potential (GWP) has methanesulfonyl fluoride and lithium nitride as the biggest contributors to this impact category, with participation of 32.0% and 17.0%, respectively. In terms of substances the GWP was dominated by fossil fuel CO_2 emissions. Fossil fuel CO_2 emissions account for 89.7% of total GWP, with methane accounting for 7.40%. However, it was not possible to identify the greatest source of these emissions in the $LiNTf_2$ life cycle (including the methanesulfonyl fluoride and lithium nitride processes). This can be explained by the large number of processes that each contribute a small proportion to the emissions. Therefore, these results suggest that for a reduction of GWP, reduction of emissions must be focused on the chemical formulation or upstream processes of the IL life cycle. Summarizing, the results of contribution analysis indicate that the intermediate substances of $LiNTf_2$ had the largest contribution of environmental impacts on

Table 4
Cradle-to-gate life cycle assessment results for production of 1 kg of the ionic liquids and $LiNTf_2$ used in this study.

Entry	Impact categories	Unit	[BVim][Br]	$LiNTf_2$	[BVim][NTf_2]	Method
1	Abiotic depletion	kg Sb eq.	8.89×10^{-2}	1.46×10^{-1}	2.17×10^{-1}	CML 2001
2	Acidification	kg SO_2 eq.	7.26×10^{-1}	5.22×10^{-1}	1.00	CML 2001
3	Cumulative Energy Demand	MJ	183	323	475	CED
4	Eutrophication	kg PO_4^{3-} eq.	5.45×10^{-2}	1.08×10^{-2}	1.57×10^{-2}	CML 2001
5	Freshwater aquatic ecotoxicity	kg 1,4-DB eq.	3.78×10^{-1}	1.43	3.83×10^{-1}	CML 2001
6	Global warming	kg CO_2 eq.	8.98	17.1	25.0	CML 2001
7	Human toxicity	kg 1,4-DB eq.	28.2	2.77	19.8	CML 2001
8	Marine aquatic ecotoxicity	kg 1,4-DB eq.	9.25×10^{-1}	15.6	2.31	CML 2001
9	Ozone layer depletion	kg CFC-11 eq.	1.62×10^{-6}	4.42×10^{-6}	5.87×10^{-6}	CML 2001

[BVim][Br]: 3-butyl-1-vinylimidazolium bromide; $LiNTf_2$: Lithium bis(trifluoromethane)sulfonimide; [BVim][NTf_2]: 3-butyl-1-vinylimidazolium bis(trifluoromethane)sulfonimide; CED: Cumulative Energy Demand V1.09. Sb = antimony, SO_2 = sulfur dioxide, PO_4^{3-} = phosphate, CO_2 = carbon dioxide, CFC-11 = trichlorofluoromethane, 1,4-DB = 1,4-dichlorobenzene, MJ = mega joules.

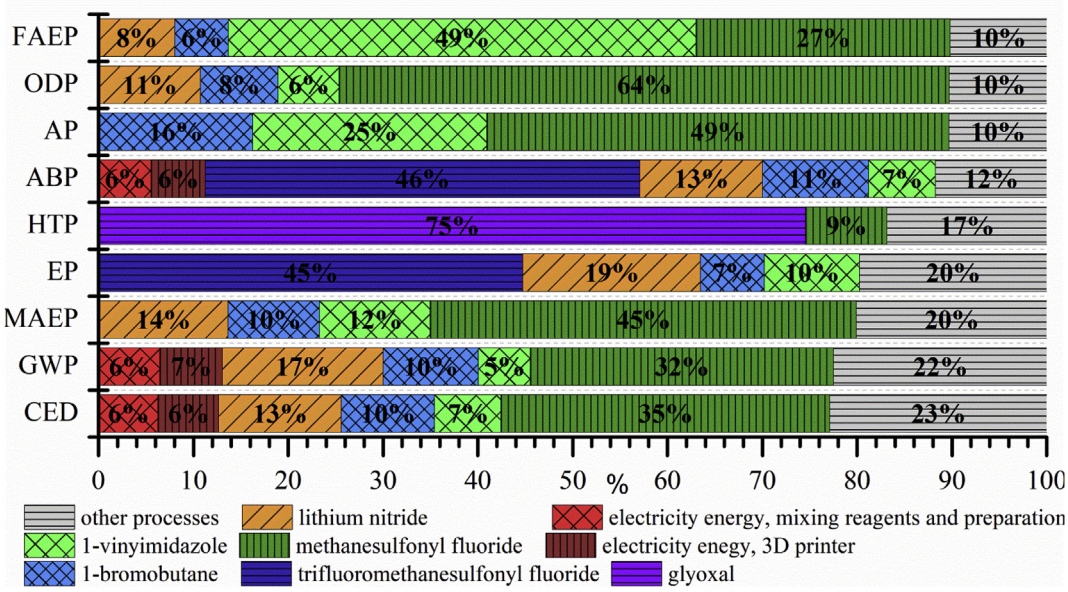

Fig. 4. Life cycle processes contribution analysis. GWP: global warming potential; ABP: abiotic depletion potentials; AP: acidification potential; EP: eutrophication potential; HTP: human toxicity potential: ODP: ozone layer depletion potential; FAEP: fresh aquatic ecotoxicity potentials; MAEP: marine aquatic ecotoxicity potentials and CED: cumulative energy demanded.

the life cycle of PIL printed in seven of nine the categories studied. Also, the 3D-printing step did not make a significant contribution to the overall total electrical energy consumed.

3.2.2. Sensitivity analysis

A sensitivity analysis was performed to assess the robustness of the results and to understand the potential effects of changing the experimental methodology, leading to development of best practises(Amado Alviz and Alvarez, 2017). In this study the sensitivity analysis was applied to: (i) thermodynamic parameters used for extrapolating theoretical energy calculations; (ii) reagent recovery in the 3D manufacturing step; and (iii) recovery of solvent that was used for syntheses of [BVim][NTf_2], [BVim][Br] and for cleaning the 3D printed part.

3.2.2.1. Effect of thermodynamic parameters calculated. The influence of the heat of formation and heat capacity parameters calculated for substances for which this data was not readily available was studied through a sensitivity analysis. The effect of using these data has been considered by varying the impacts of these parameters (arbitrarily) by ± 50%. As it is possible to observe in Table S22, the results indicate that the LCA results demonstrated low sensitivity to the degree of variation in the thermodynamic parameters that were evaluated in this work.

3.2.2.2. Effect of reagent recovery in the 3D manufacturing step. The influence of the recovery of the reagent mixture after the 3D-printing step on the environmental profile of the life cycle was modelled by comparing four different degrees of recovery. It was determined that the degree of reagent formulation recovery, which was performed in the primary data experimental work for this study, was 73.8%. The *ca.* 25% loss of reagent formulation in this step occurs due to a small amount of print reagent formulation remaining in the processing area of the 3D printer. However, optimization of the process could significantly improve this figure. Thus, the influence of the degree of reagent recovery was studied. Four degrees of reagent formulation recovery were investigated; 73.8%, 80.0%, 90.0% and 100%. Table 5 shows the effect of each degree of reagent recovery on each environmental impact categories. As expected, the environmental impact scores are reduced as the reagent recovery rate increases. For example, for the global warming impact category the reduction was calculated to be 59.0% for full recovery (100% reagent recovery). Also, Fig. 5 shows a relative comparison of the life cycle impacts of PIL production using those recovery rates. These results show that reagent recovery is critical as it can significantly reduce the environmental impacts of the PIL printed. Note that for this analysis the inputs and outputs of 3D-printing step (reagents, waste of reagents and reagent recovery) had been changed for each rate of recovery investigated. Also, the energy consumed for mixing and preparation of reagents was re-calculated considering the input of recovered reagent formulation. The flows assumed for this analysis are in Tables S11 and S12 in the electronic supplementary material.

3.2.2.3. Effect of solvent recovery. Several studies suggest that the solvent recovery is a key parameter in the environmental assessment and an important task for chemical engineers to minimize burden upon the environment (Righi et al., 2011). Thus, in this study, two scenarios for the recovery of organic solvents used in this work were calculated. The first scenario (S1) is the standard scenario of this study where it was considered that there was a recycling and refeeding of 99% of all solvents used for the syntheses of [BVim][NTf_2], [BVim][Br] and used to clean the 3D part. In the second scenario (S2) all organic solvent consumed in these processes were assumed as not recovered. The solvents not recovered were considered as 100% emitted to air. The results of this analysis are show in Table 6 and Fig. 6 shows a LCA results comparison between S1 and S2 for use of the organic solvent. Note that the flows of energy consumed for recycling the solvent for S2 were changed as well as the amount of waste solvent. These estimations are given in Table S13 of the electronic supplementary material.

The results indicate that solvent recovery had significant impact for all impact categories that were evaluated. The impact categories abiotic depletion, eutrophication, global warming and cumulative energy demand exhibited the biggest differences between the scenarios S1 and S2, demonstrating that these impact categories

Table 5
Effect of solvent recovery rate on environmental impact categories producing 1.2 g of PIL printed.

Entry	Impact categories	Unit	Reagent recovery rate			
			73.8 %[a]	80%	90%	100%
1	Abiotic depletion	kg Sb eq.	7.87×10^{-4}	6.76×10^{-4}	4.96×10^{-4}	3.17×10^{-4}
2	Acidification	kg SO_2 eq.	3.14×10^{-3}	2.66×10^{-3}	1.89×10^{-3}	1.13×10^{-3}
3	Cumulative Energy Demand	MJ	1.74	1.50	1.10	7.10×10^{-1}
4	Eutrophication	kg PO_4^{3-} eq.	5.33×10^{-5}	4.55×10^{-5}	3.29×10^{-5}	2.04×10^{-5}
5	Freshwater aquatic ecotoxicity	kg 1,4-DB eq.	1.21×10^{-3}	1.03×10^{-3}	7.33×10^{-4}	4.38×10^{-4}
6	Global warming	kg CO_2 eq.	9.19×10^{-2}	7.09×10^{-2}	5.83×10^{-2}	3.76×10^{-2}
7	Human toxicity	kg 1,4-DB eq.	6.46×10^{-2}	5.48×10^{-2}	3.89×10^{-2}	2.32×10^{-2}
8	Marine aquatic ecotoxicity	kg 1,4-DB eq.	7.50×10^{-3}	6.38×10^{-3}	4.58×10^{-3}	2.77×10^{-3}
9	Ozone layer depletion	kg CFC-11 eq.	1.85×10^{-8}	1.57×10^{-8}	1.13×10^{-8}	6.76×10^{-9}

[a] Reagent recovery rate data from laboratory scale. Sb = antimony, SO_2 = sulfur dioxide, PO_4^{3-} = phosphate, CO_2 = carbon dioxide, CFC-11 = trichlorofluoromethane, 1,4-DB = 1,4-dichlorobenzene, MJ = mega joules.

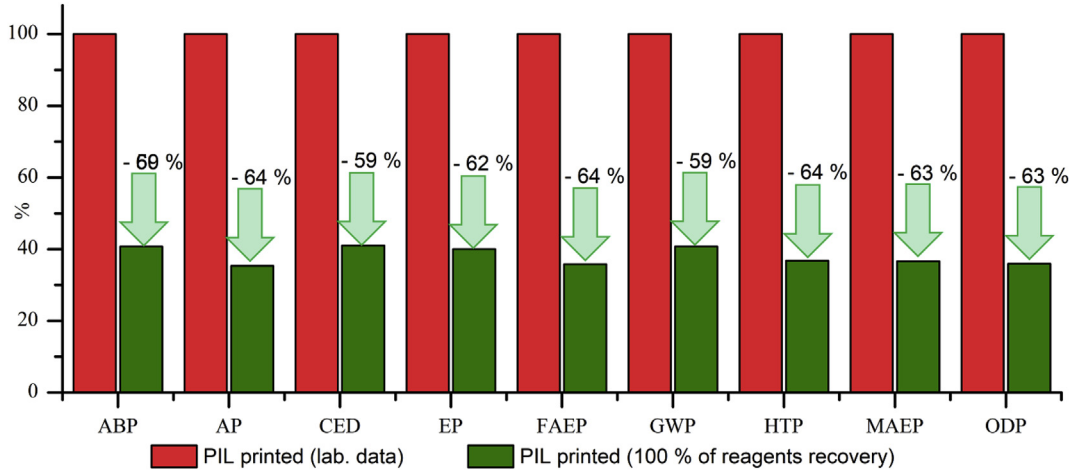

Fig. 5. Comparison of the life cycle impacts of PIL with reagent recovery of ~74% (Lab data) and 100% in the 3D-printing step.

Table 6
Influence of solvent recovery on life cycle impacts of PIL printed (1.2 g of PIL printed).

Impact Categories	Unit	S1 (with solvent recovery)	S2 (without solvent recovery)	Difference
Abiotic depletion	kg Sb eq.	7.87×10^{-4}	1.16×10^{-3}	+48%
Acidification	kg SO_2 eq.	3.14×10^{-3}	3.41×10^{-3}	+9%
Cumulative Energy Demand	MJ	1.74	2.62	+50%
Eutrophication	kg PO_4^{3-} eq.	5.33×10^{-5}	9.86×10^{-5}	+85%
Freshwater aquatic ecotoxicity	kg 1,4-DB eq.	1.21×10^{-3}	1.32×10^{-3}	+9%
Global warming	kg CO_2 eq.	9.19×10^{-2}	2.26×10^{-1}	+146%
Human toxicity	kg 1,4-DB eq.	6.46×10^{-2}	8.40×10^{-2}	+30%
Marine aquatic ecotoxicity	kg 1,4-DB eq.	7.50×10^{-3}	8.58×10^{-3}	+14%
Ozone layer depletion	kg CFC-11 eq.	1.85×10^{-8}	2.10×10^{-8}	+14%

Sb = antimony, SO_2 = sulfur dioxide, PO_4^{3-} = phosphate, CO_2 = carbon dioxide, CFC-11 = trichlorofluoromethane, 1,4-DB = 1,4-dichlorobenzene, MJ = mega joules.

were the more sensitive to solvent recycling. Moreover, the recovery of solvent promoted reduction of life cycle impacts of [BVim][NTf_2] in all categories evaluated (S1) (see Fig. S1 in the ESI). Also, the solvents employed for synthesis of ionic liquids were the major contributors to increasing the impacts in S2 (see Fig. S1 and Table S14 in the ESI). Furthermore, the impact of energy consumed for recovery of the isopropanol, employed for cleaning the 3D part, did not show significant contribution (<1.8%). These results suggest that emissions of solvent at lab-scale had a big environmental impact and thus good practices for reduction of solvent consumption and increased recovery must be applied. Moreover, solvent recovery is a critical process as it can reduce significantly the environmental impacts of the printed PIL life cycle.

3.3. Comparison between monomer IL and conventional IL

The major impact contributor in the printing of PILs is the synthesis of the IL monomers. For this reason, it is important to understand how these impacts compare to an analogous homogeneous ionic liquid (*e.g.* Fig. 6). It is expected that by printing the PIL, the impact of the material during its utilisation phase (cradle-to-grave) will be reduced compared to the homogeneous IL due to simplified protocols for handling and reutilisation of the polymers. Therefore, the conventional IL 3-butyl-1-methylimidazolium bis(trifluoromethane)sulfonimide [Bmim][NTf_2] was chosen as it has a similar structure to 3-butyl-1-vinylimidazolium bis(trifluoromethane)sulfonamide [BVim][NTf_2]. However, [BVim][NTf_2] has additional advantages such as the possibility of being

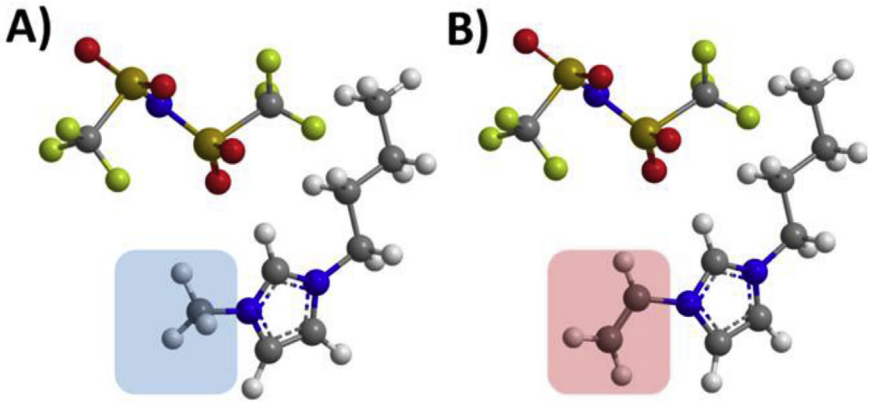

Fig. 6. Structures of [Bmim][NTf_2] (A) where the methyl group is shaded light blue and [BVim][NTf_2] (B), where the vinyl group is highlighted in pink. (For interpretation of the references to colour in this figure legend, the reader is referred to the Web version of this article.)

polymerisable (Shaplov et al., 2016); functionalization versatility is afforded by the double bond functional group moiety Therefore, a comparison for production of 1 kg of each ionic liquid was made. The data used for this assessment can be found in Section 9 of the **ESI**.

The results indicate that the nature of the vinylimidazolium cation of the monomer had comparable impact compared to the non-polymerisable conventional IL. Fig. S4 in the ESI shows a comparison of contribution of the different processes to the life cycle impact categories for [BVim][NTf_2] and [Bmim][NTf_2]. The [BVim][NTf_2] presents less impact for human toxicity than [Bmim][NTf_2] (Table 7). In this study, for production of 1 kg of the [BVim][NTf_2] 0.239 kg of glyoxal are consumed, compared to 0.669 kg in the synthesis of [Bmim][NTf_2]. Glyoxal is used in the synthesis of imidazole, (Ebel et al., 2002) which in turn is an intermediate substance used in the synthesis of [BVim][Cl] and [Bmim][Cl]. Based on the contribution analysis (see Fig. S4) it is possible to claim that in general the methanesulfonyl chloride (CH_3ClO_2S) and sodium fluoride showed the most significant contribution in seven of nine impact categories assessed for both IL. Methanesulfonyl chloride and sodium fluoride are used in the synthesis of trifluoromethanesulfonyl fluoride which is an intermediate chemical during synthesis of $LiNTF_2$. Summarizing, the most significant life cycle impacts of monomer and conventional IL that have NTf_2^- in their structure arise due to the anion synthetic process.

3.4. Comparison between the effect of PIL anion on LCA

This study has focussed on the employment of a vinylimidazolium-based cation the $[BVim]^+$ cation with the non-coordinating and hydrophobic $[NTf_2]^-$ as the counter anion, (Karjalainen et al., 2014) leading to stable ILs with low viscosity that are relatively easy to handle and process. Nevertheless, as demonstrated in this work, the largest LCA impact is associated with the synthesis of the anion. Hence, it is interesting to compare the overall LCA of the use of PIL precursors with a different anion. The large environmental impact associated with the anion synthesis is not surprising due to the large number of synthetic steps required. The $[NTf_2]^-$ was compared to another anion that led to a printable PIL; the dicyanamide anion $[N(CN)_2]^-$. The data used for this assessment can be found in Section 8 of the ESI. 1.2 g of each compound, and two scenarios of reagent recovery were assumed. Scenario 1 (S1) considered the production of 1.2 g of compound without reagent recovery and the Scenario 2 (S2) considered with full reagent recovery. As is evident in Table 8, the change of anion significantly decreased the impacts in all categories evaluated. However, the magnitude of the difference is smaller with full reagent recovery, which is attributed to the difference in mass of the $[N(CN)_2^-]$ and $[NTf_2^-]$ anions.

4. Conclusions

LCA study for the process of DLP-based 3D-printing of imidazolium-based PILs has been presented. The results indicate that the additive manufacturing process is technically viable and does not exacerbate the environmental impacts from synthesising the constituent monomeric ionic liquids. However, this study also highlights that there are excellent opportunities for mitigating the life cycle impacts of PIL associated with the synthetic steps, mainly through the reduction of reagents emitted as waste by practising reagent recovery and reduction/recycling of solvents used for cleaning the 3D part. This work has focused on the employment of 3D-printing, using digital light projection, of a polymerisable ionic liquid, with the vinylimidazolium-based $[BVim]^+$ cation, and the

Table 7
LCA results of production of monomer IL and conventional IL (results for 1 kg of IL).

Entry	Impact categories	Unit	[BVim][NTf_2]	[Bmim][NTf_2]	Difference
1	Abiotic depletion	kg Sb eq.	0.22	0.19	- 12%
2	Acidification	kg SO_2 eq.	1.01	0.54	- 46%
3	Cumulative Energy Demand	MJ	475	428	- 10%
4	Eutrophication	kg PO_4^{3-} eq.	1.57×10^{-2}	1.26×10^{-2}	- 20%
5	Freshwater aquatic ecotoxicity	kg 1,4-DB eq.	0.38	0.23	- 40%
6	Global warming	kg CO_2 eq.	25.00	20.98	- 16%
7	Human toxicity	kg 1,4-DB eq.	19.8	47.7	+141%
8	Marine aquatic ecotoxicity	kg 1,4-DB eq.	2.31	2.03	- 12%
9	Ozone layer depletion	kg CFC-11 eq.	5.87×10^{-6}	4.77×10^{-6}	- 19%

Sb = antimony, SO_2 = sulfur dioxide, PO_4^{3-} = phosphate, CO_2 = carbon dioxide, CFC-11 = trichlorofluoromethane, 1,4-DB = 1,4-dichlorobenzene, MJ = mega joules.

Table 8
Comparison of the effect of changing the anion for priting 1.2 g of PILs for scenario of reagent recovery.

Impact categories	Unit	Scenario	Anion		
			$[NTf_2^-]$	$[N(CN)_2^-]$	Difference
Abiotic depletion	kg Sb eq.	S1	7.87×10^{-4}	4.32×10^{-4}	−45%
		S2	3.17×10^{-4}	2.55 × 10-4	−20%
Acidification	kg SO_2 eq.	S1	3.14×10^{-3}	1.57×10^{-3}	−50%
		S2	1.13×10^{-3}	7.64×10^{-4}	−26%
Eutrophication	kg PO_4^{3-} eq.	S1	5.33×10^{-5}	2.44×10^{-5}	−54%
		S2	2.04×10^{-5}	1.39×10^{-5}	−32%
Global warming	kg CO_2 eq.	S1	9.19×10^{-2}	5.14×10^{-2}	−44%
		S2	3.76×10^{-2}	3.07×10^{-2}	−18%
Ozone layer depletion	kg CFC-11 eq.	S1	1.85×10^{-8}	7.36×10^{-9}	−60%
		S2	6.76×10^{-9}	4.03×10^{-9}	−40%
Human toxicity	kg 1,4-DB eq.	S1	6.46×10^{-2}	6.33×10^{-2}	−2%
		S2	2.32×10^{-2}	3.35×10^{-2}	+44%
Freshwater aquatic ecotoxicity	kg 1,4-DB eq.	S1	1.21×10^{-3}	8.53×10^{-4}	−29%
		S2	4.38×10^{-4}	4.53×10^{-4}	+4%
Marine aquatic ecotoxicity	kg 1,4-DB eq.	S1	7.50×10^{-3}	3.21×10^{-3}	−57%
		S2	2.77×10^{-3}	1.77×10^{-3}	−36%
Cumulative Energy demand	MJ	S1	1.74	9.47×10^{-1}	−46%
		S2	7.10×10^{-1}	5.65×10^{-1}	−20%

S1: No reagent recovery; S2: full reagent recovery. Sb = antimony, SO_2 = sulfur dioxide, PO_4^{3-} = phosphate, CO_2 = carbon dioxide, CFC-11 = trichlorofluoromethane, 1,4-DB = 1,4-dichlorobenzene, GJ = giga joules.

non-coordinating and hydrophobic $[NTf_2]^-$ as the counter anion. The contribution analysis results suggest that the anion had the largest contribution to the environmental impacts on the life cycle of the PIL studied manly due of intermediate substances (methanesulfonyl fluoride and lithium nitride) used for synthesis of $LiNTf_2$. Overall good practice relating to the synthesis of the [BVim][NTf_2] ionic liquid is necessary to minimise the environmental performance.

A comparison between polymerizable and the analogous homogeneous ionic liquid has been made. The results indicate that the nature of the PIL monomer had comparable impact compared to the structurally similar conventional non-polymerisable IL. This result suggests that PIL monomers are viable in terms of environmental impacts with the additional advantage of versatility due to the double-bond structure.

Comparative analysis of the use of PIL precursors with a different anion indicated that the change of anion has influence on the environmental performance of PILs. The change of anion bis(trifluoromethane)sulfonimide anion $[NTf_2^-]$ to dicyanamide anion $[N(CN)_2^-]$ significantly decreased the impacts in all categories evaluated for PIL production. However, the magnitude of the difference is smaller with full reagent recovery. This suggests that full reagent recovery is just as crucial as the choice of anion in terms of environmental performance of 3D-printing of PIL.

This works represents the first LCA study, which will be of great support for decision making for PIL 3D-printing processes at a laboratory scale. The results of this study help to identify the main aspects and environmental impacts involving the production of the monomer ILs, PILs and the additive manufacturing.

Conflicts of interest

The authors declare no conflicts of interest.

Acknowledgments

V.G-M. and M.S. wish to thank the Brazilian Government and the National Council for the Improvement of Higher Education (*CAPES*) for their support. The University of Nottingham is gratefully acknowledged for funding.

Appendix A. Supplementary data

Supplementary data to this article can be found online at https://doi.org/10.1016/j.jclepro.2018.12.241.

List of symbols

Cp:	heat capacity
C_R	calorific value of reactants
dT	temperature differential
E_i :	theoretical energy consumption
Fc	A factor of 4.2 for endothermic reactions with the assumption of natural gas powered heating and a factor of 3.2 for exothermic reactions with the assumption that cooling uses electricity
ΔH	heat of reaction
$\widehat{H}$	specific enthalpy of reactants
$\Delta\widehat{Hf^{\circ}}$	heat of formation of reactants
ΔH_{vap}:	Heat of vaporisation
n	number of mols
Q_{cal}	Heat transported
RMM	molecular weight of reactants
T1	reference temperature (25 °C)
T2	temperature of the reactants
T_{evap}	evaporation temperature of the substance

References

Amado Alviz, P.L., Alvarez, A.J., 2017. Comparative life cycle assessment of the use of an ionic liquid ([Bmim]Br) versus a volatile organic solvent in the production of acetylsalicylic acid. J. Clean. Prod. 168, 1614–1624. https://doi.org/10.1016/j.jclepro.2017.02.107.

Barros, S., Zwolinski, P., Mansur, A.I., 2017. Where do the environmental impacts of Additive Manufacturing come from? Case study of the use of 3d-printing to print orthotic insoles. In: 12ème Congrès International de Génie Industriel (CIGI 2017). Compiegne, p. 9.

Bekker, A.C.M., Verlinden, J.C., 2018. Life cycle assessment of wire + arc additive manufacturing compared to green sand casting and CNC milling in stainless steel. J. Clean. Prod. 177, 438–447. https://doi.org/10.1016/j.jclepro.2017.12.148.

Blanchard, A.A., Phelan, J.W., Davis, A.R., 1936. Synthetic Inorganic Chemistry, fifth ed. John Wiley & Sons, Inc., London.

Booth, H.S., 1939. Inorganic syntheses, volume I. In: Booth, H.S. (Ed.), Inorganic Syntheses, Volume I. McGraw-Hill Book Company, Inc., New York, pp. 151–157. https://doi.org/10.1002/9780470132326.

Cerdas, F., Juraschek, M., Thiede, S., Herrmann, C., 2017. Life cycle assessment of 3D

printed products in a distributed manufacturing system. J. Ind. Ecol. 21, S80–S93. https://doi.org/10.1111/jiec.12618.
Cuéllar-Franca, R.M., García-Gutiérrez, P., Taylor, S.F.R., Hardacre, C., Azapagic, A., 2016. A novel methodology for assessing the environmental sustainability of ionic liquids used for CO2 capture. Faraday Discuss 192, 283–301. https://doi.org/10.1039/C6FD00054A.
de Bruijn, H., Duin, R. van, Huijbregts, M.A.J., 2002. Handbook on Life Cycle Assessment, Operational Guide to the ISO Standards. Kluwer Academic Publishers, USA. https://doi.org/10.1007/0-306-48055-7.
DETHERM (Society for Chemical Engineering and Biotechnology), 2018. Thermophysical Property Data [WWW Document]. URL. http://detherm.cds.rsc.org/detherm/index.php. (Accessed 5 November 2018).
Ding, J., Shen, J., 2012. Method for Preparation of N-vinylimidazole. Chinese Patent CN102382059 (A).
Ebel, K., Koehler, H., Gamer, A.O., Jäckh, R., 2002. Imidazole and derivatives. In: Ullmann's Encyclopedia of Industrial Chemistry. Wiley-VCH Verlag GmbH & Co. KGaA, Weinheim. https://doi.org/10.1002/14356007.
Energy UK, 2017. Energy in the UK. London.
Farahipour, R., Karunanithi, A., 2014. Life cycle environmental implications of CO2 capture and sequestration with ionic liquid 1-butyl-3-methylimidazolium acetate. ACS Sustain. Chem. Eng. 2, 2495–2500. https://doi.org/10.1021/sc400274b.
Felder, R.M., Rousseau, R.W., 2005. Elementary Principes of Chemical Processes, third ed. John Wiley & Sons, Inc., USA.
Frischknecht, R., Jungbluth, N., Althaus, H.-J., Doka, G., Dones, R., Heck, T., Hellweg, S., Hischier, R., Nemecek, T., Rebitzer, G., Spielmann, M., 2005. The ecoinvent database: overview and methodological framework (7 pp). Int. J. Life Cycle Assess. 10, 3–9. https://doi.org/10.1065/lca2004.10.181.1.
Gebler, M., Schoot Uiterkamp, A.J.M., Visser, C., 2014. A global sustainability perspective on 3D printing technologies. Energy Pol. 74, 158–167. https://doi.org/10.1016/J.ENPOL.2014.08.033.
Gunasekera, D.H.A.T., Kuek, S., Hasanaj, D., He, Y., Tuck, C., Croft, A.K., Wildman, R.D., 2016. Three dimensional ink-jet printing of biomaterials using ionic liquids and co-solvents. Faraday Discuss 190, 509–523. https://doi.org/10.1039/C5FD00219B.
Gutowski, T., Jiang, S., Cooper, D., Corman, G., Hausman, M., Manson, J.-A., Schudeleit, T., Wegener, K., Sabelle, M., Ramos-Grez, J., Sekulic, D.P., 2017. Note on the rate and energy efficiency limits for additive manufacturing. J. Ind. Ecol. 21, S69. https://doi.org/10.1111/jiec.12664.
Hischier, R., Hellweg, S., Capello, C., Primas, A., 2005. Establishing life cycle inventories of chemicals based on differing data availability. Int. J. Life Cycle Assess. 10, 59–67. https://doi.org/10.1065/lca2004.10.181.7.
Huang, S.H., Liu, P., Mokasdar, A., Hou, L., 2013. Additive manufacturing and its societal impact: a literature review. Int. J. Adv. Manuf. Technol. 67, 1191–1203. https://doi.org/10.1007/s00170-012-4558-5.
Huebschmann, S., Kralisch, D., Loewe, H., Breuch, D., Petersen, J.H., Dietrich, T., Scholz, R., 2011. Decision support towards agile eco-design of microreaction processes by accompanying (simplified) life cycle assessment. Green Chem. 13, 1694. https://doi.org/10.1039/c1gc15054e.
ISO (The International Standards Organisation), 2006a. ISO 14040:2006 - environmental management - life cycle assessment - principles and framework. Int. Organ. Stand. 20.
ISO (The International Standards Organisation), 2006b. ISO 14044:2006 - environmental management - life cycle assessment - requirements and guidelines. Int. Organ. Stand. 46.
Jacquemin, L., Pontalier, P.-Y., Sablayrolles, C., 2012. Life cycle assessment (LCA) applied to the process industry: a review. Int. J. Life Cycle Assess. 17, 1028–1041. https://doi.org/10.1007/s11367-012-0432-9.
Kamm, O., Marvel, C.S., 1921. Alkyl and alkylene bromides. Org. Synth. 1, 3. https://doi.org/10.15227/orgsyn.001.0003.
Karjalainen, E., Aseyev, V., Tenhu, H., 2014. Influence of hydrophobic anion on solution properties of PDMAEMA. Macromolecules 47, 2103–2111. https://doi.org/10.1021/ma5000706.
Karjalainen, E., Wales, D.J., Gunasekera, D.H.A.T., Dupont, J., Licence, P., Wildman, R.D., Sans, V., 2018. Tunable ionic control of polymeric films for inkjet based 3D printing. ACS Sustain. Chem. Eng. 6, 3984–3991. https://doi.org/10.1021/acssuschemeng.7b04279.
Kellens, K., Baumers, M., Gutowski, T.G., Flanagan, W., Lifset, R., Duflou, J.R., 2017. Environmental dimensions of additive manufacturing: mapping application domains and their environmental implications. J. Ind. Ecol. 21, S49–S68. https://doi.org/10.1111/jiec.12629.
Kralisch, D., Stark, A., Koersten, S., Kreisel, G., Ondruschka, B., 2005. Energetic, environmental and economic balances: spice up your ionic liquid research efficiency. Green Chem. 7, 301–309. https://doi.org/10.1039/b417167e.
Kralisch, D., Reinhardt, D., Kreisel, G., 2007. Implementing objectives of sustainability into ionic liquids research and development. Green Chem. 9, 1308. https://doi.org/10.1039/b708721g.
Kreiger, M., Pearce, J.M., 2013. Environmental life cycle analysis of distributed three-dimensional printing and conventional manufacturing of polymer products. ACS Sustain. Chem. Eng. 1, 1511–1519. https://doi.org/10.1021/sc400093k.
Li, Y., Linke, B.S., Voet, H., Falk, B., Schmitt, R., Lam, M., 2017. Cost, sustainability and surface roughness quality – a comprehensive analysis of products made with personal 3D printers. CIRP J. Manuf. Sci. Technol. 16, 1–11. https://doi.org/10.1016/j.cirpj.2016.10.001.
Luo, Yanchun, Ji, Zhiming, Leu, M.C., Caudill, R., 1999. Environmental performance analysis of solid freedom fabrication processes. In: Proceedings of the 1999 IEEE International Symposium on Electronics and the Environment (Cat. No.99CH36357), Danvers, MA, USA, pp. 1–6. https://doi.org/10.1109/ISEE.1999.765837.
Ma, J., Harstvedt, J.D., Dunaway, D., Bian, L., Jaradat, R., 2018a. An exploratory investigation of additively manufactured product life cycle sustainability assessment. J. Clean. Prod. 192, 55–70. https://doi.org/10.1016/j.jclepro.2018.04.249.
Ma, J., Harstvedt, J.D., Dunaway, D., Bian, L., Jaradat, R., 2018b. An exploratory investigation of additively manufactured product life cycle sustainability assessment. J. Clean. Prod. 192, 55–70. https://doi.org/10.1016/j.jclepro.2018.04.249.
Mecerreyes, D., 2011. Polymeric ionic liquids: broadening the properties and applications of polyelectrolytes. Prog. Polym. Sci. 36, 1629–1648. https://doi.org/10.1016/j.progpolymsci.2011.05.007.
Mehrkesh, A., Karunanithi, A.T., 2013. Energetic ionic materials: how green are they? A comparative life cycle assessment study. ACS Sustain. Chem. Eng. 1, 448–455. https://doi.org/10.1021/sc3001383.
Mehrkesh, A., Karunanithi, A.T., 2016. Life-cycle perspectives on aquatic ecotoxicity of common ionic liquids. Environ. Sci. Technol. 50, 6814–6821. https://doi.org/10.1021/acs.est.5b04721.
NIST (National Institute of Standards and Technology), 2018. NIST Chemistry WebBook [WWW Document]. NIST Chem. Webb. URL. https://webbook.nist.gov/chemistry/. (Accessed 5 November 2018).
OECD, 2017. 3D printing and its environmental applications. In: The Next Production Revolution: Implications for Governments and Business. OECD, Paris, pp. 171–213. https://doi.org/10.1787/9789264271036-en.
Peng, T., 2016. Analysis of energy utilization in 3D printing processes. Procedia CIRP 40, 62–67. In: https://doi.org/10.1016/j.procir.2016.01.055.
Peterson, J.E., 2013. Ionic Liquid/CO2 Co-fluid Refrigeration: CO2 Solubility Modeling and Life Cycle Analysis. PhD Thesis. University of Notre Dame.
PRé Consultants, 2014. SimaPro Database Manual - Methods Library. San Francisco.
Qian, W., Texter, J., Yan, F., 2017. Frontiers in poly(ionic liquid)s: syntheses and applications. Chem. Soc. Rev. 46, 1124–1159. https://doi.org/10.1039/C6CS00620E.
Quinlan, H.E., Hasan, T., Jaddou, J., Hart, A.J., 2017. Industrial and consumer uses of additive manufacturing: a discussion of capabilities, trajectories, and challenges. J. Ind. Ecol. 21, S15–S20. https://doi.org/10.1111/jiec.12609.
Righi, S., Morfino, A., Galletti, P., Samorì, C., Tugnoli, A., Stramigioli, C., 2011. Comparative cradle-to-gate life cycle assessments of cellulose dissolution with 1-butyl-3-methylimidazolium chloride and N-methyl-morpholine-N-oxide. Green Chem. 13, 367. https://doi.org/10.1039/c0gc00647e.
Sans, V., Karbass, N., Burguete, M.I., Compañ, V., García-Verdugo, E., Luis, S.V., Pawlak, M., 2011. Polymer-supported ionic-liquid-like phases (SILLPs): transferring ionic liquid properties to polymeric matrices. Chem. Eur J. 17, 1894–1906. https://doi.org/10.1002/chem.201001873.
Schultz, A.R., Lambert, P.M., Chartrain, N.A., Ruohoniemi, D.M., Zhang, Z., Jangu, C., Zhang, M., Williams, C.B., Long, T.E., 2014. 3D printing phosphonium ionic liquid networks with mask projection microstereolithography. ACS Macro Lett. 3, 1205–1209. https://doi.org/10.1021/mz5006316.
Shaplov, A.S., Ponkratov, D.O., Vygodskii, Y.S., 2016. Poly(ionic liquid)s: synthesis, properties, and application. Polym. Sci. B 58, 73–142. https://doi.org/10.1134/S156009041602007X.
Stouffer, S., Guttman, L., Suchman, E., Lazarsfeld, P.F., Star, S., Clausen, J., 2008. Heat capacities of ionic liquids as a function of temperature at 0.1 MPa. Measurement and prediction. J. Chem. Eng. Data 53, 2148–2153. https://doi.org/10.1021/je800335v.
Vatani, A., Mehrpooya, M., Gharagheizi, F., 2007. Prediction of standard enthalpy of formation by a QSPR model. Int. J. Mol. Sci. 8, 407–432. https://doi.org/10.3390/i8050407.
Wales, D.J., Cao, Q., Kastner, K., Karjalainen, E., Newton, G.N., Sans, V., 2018. 3D-Printable photochromic molecular materials for reversible information storage. Adv. Mater. 30, 1800159. https://doi.org/10.1002/adma.201800159.
Welton, T., 1999. Room-temperature ionic liquids. Solvents for synthesis and catalysis. Chem. Rev. 99, 2071–2083. https://doi.org/10.1021/cr1003248.
Yang, Y., Li, L., Pan, Y., Sun, Z., 2017. Energy consumption modeling of stereolithography-based additive manufacturing toward environmental sustainability. J. Ind. Ecol. 21, S168–S178. https://doi.org/10.1111/jiec.12589.
Yu, H., Zhang, C., Anderson, J.L., 2015. Ionic liquids and polymeric ionic liquids in analytical environmental applications. In: Mecerreyes, D. (Ed.), Applications of Ionic Liquids in Polymer Science and Technology. Springer Berlin Heidelberg, Berlin, pp. 153–198. https://doi.org/10.1007/978-3-662-44903-5_7.
Yuan, J., Mecerreyes, D., Antonietti, M., 2013. Poly(ionic liquid)s: an update. Prog. Polym. Sci. 38, 1009–1036. https://doi.org/10.1016/j.progpolymsci.2013.04.002.
Zhang, Y., Bakshi, B.R., Demessie, E.S., 2008. Life cycle assessment of an ionic liquid versus molecular solvents and their applications. Environ. Sci. Technol. 42, 1724–1730. https://doi.org/10.1021/es0713983.

Environmental Performance of 3D printing Polymerisable Ionic Liquids

Vinícius Gonçalves Maciel[1,2], Dominic J. Wales[3,4,†], Marcus Seferin[1,2] ,Victor Sans*[3,4]

[1]School of Chemistry, Pontifical Catholic University of Rio Grande do Sul – PUCRS, Brazil
[2]Post-Graduation Program in Materials Engineering and Technology, Pontifical Catholic University of Rio Grande do Sul – PUCRS, Brazil
[3]Faculty of Engineering, University of Nottingham, Nottingham, NG7 2RD, U.K.
[4]GSK Carbon Neutral Laboratory, University of Nottingham, Nottingham, NG7 2GA, U.K.
* victor.sanssangorrin@nottingham.ac.uk

Electronic Supplementary Information (ESI)

Contents

† Current address: The Hamlyn Centre, Faculty of Engineering, South Kensington Campus, Imperial College London, London, SW7 2AZ, U.K.

1 Experimental methodology

The synthesis of the ionic liquids and the 3D-printing of the poly(ionic liquids) was conducted at laboratory scale. 1-vinyl imidazole was purchased from Alfa Aesar. 1-bromobutane was purchased from Acros Organics. Diethyl ether was purchased from Fisher Scientific. Dichloromethane (DCM) was purchased from Fisher Scientific. Isopropanol (IUPAC name = 2-propanol) was purchased from Fisher Scientific. Deuterated chloroform ($CDCl_3$) for NMR was purchased from Sigma Aldrich. Lithium bis(trifluoromethane)sulfonimide ($LiNTf_2$) was purchased from IOLITEC. Anhydrous magnesium sulfate ($MgSO_4$) was purchased from Fisher Scientific. Basic alumina (Al_2SO_3) was purchased from Sigma Aldrich. 1,4-butanediol diacrylate was purchased from Sigma Aldrich. Diphenyl(2,4,6-trimethylbenzoyl)phosphine oxide was purchased from Sigma Aldrich. The solvents and reagents were used directly as received, except for 1-vinylimidazole and 1,4-butanediol diacrylate, which were both passed through basic alumina (Al_2O_3) before use. ^{1}H NMR spectra were recorded on a Bruker AVX400 (400 MHz) spectrometer at ambient temperature. ^{13}C NMR spectra were recorded on a Bruker AVX400 (101 MHz) spectrometer at ambient temperature. ^{19}F NMR spectra were recorded on a Bruker AVX400 (376 MHz) spectrometer at ambient temperature.

1.1 Synthesis of Ionic Liquids

1.1.1 3-butyl-1-vinylimidazolium bromide ([BVim][Br])

A flask was charged with 1-vinyl imidazole (37.64 g, 400 mmol) and 1-bromobutane (42.95 mL, 400 mmol), and then sealed with a greased cap. The reaction was heated at 40 °C with stirring for 16 hours. Afterwards, the crude product was obtained by addition of diethyl ether (200 mL) and scratching of the internal surface of the round bottom flask with a glass rod. The resulting solid was collected by filtration and washed with diethyl ether (200 mL) three times. Then the crude product was re-dissolved in dichloromethane (100 mL), before being added dropwise to rapidly stirred diethyl ether (500 mL) to form a white crystalline precipitate. This solid product was dried under reduced pressure at 40 °C for 6 hours to afford 3-butyl-1-vinylimidazolium bromide. The yield was 60.77 g (66 %). ^{1}H NMR (400 MHz, $CDCl_3$): δ / ppm = 10.82 (t, *J* = 1.7 Hz, 1H), 7.95 (t, *J* = 1.9 Hz, 1H), 7.66 (t, *J* = 1.9 Hz, 1H), 7.45 (dd, *J* = 15.7, 8.7 Hz, 1H), 6.00 (dd, *J* = 15.7, 3.0 Hz, 1H), 5.34 (dd, *J* = 8.7, 3.0 Hz, 1H), 4.38 (t, *J* = 7.4 Hz, 2H), 10.82 (t, *J* = 1.7 Hz, 1H), 1.97-1.81 (m, 1H), 1.48-1.25 (m, 2H),

0.92 (t, *J* = 7.4 Hz, 3H); ^{13}C NMR (100 MHz, $CDCl_3$): δ / ppm = 135.8, 128.3, 122.9, 119.6, 109.8, 50.2, 32.1, 19.5, 13.5. NMR data is consistent with literature values (Wojnarowska et al., 2015). Elemental Analysis: Calculated: C, 46.77; H, 6.54; N, 12.12; Found: C, 46.42; H, 6.99; N, 12.13.

1.1.2 3-butyl-1-vinylimidazolium bis(trifluoromethane)sulfonimide ([BVim][NTf_2])

Lithium bis(trifluoromethane)sulfonimide ($LiNTf_2$) (113.75 g, 396.21 mmol) was dissolved in water (100 mL) and to this solution an aqueous solution (100 mL) of 3-butyl-1-vinylimidazolium bromide (60.77 g, 264 mmol) was added, which caused formation of two liquid phases. This mixture was stirred rapidly for 6 hours at R.T. The phases were separated and the aqueous phase was extracted three times with dichloromethane (200 mL). The combined organic phases were washed three times with water (100 mL) and then dried over $MgSO_4$. Then organic phase was then passed through a basic Al_2O_3 column and then reduced *in vacuo* to form a colourless oily liquid. Then the product was further dried in Schlenk line at 40 °C for 5 hours to obtain 3-butyl-1-vinylimidazolium bis(trifluoromethane)sulfonimide as a clear and colourless viscous oily liquid. The yield was 103.41 g (90.8%). ^{1}H NMR (400 MHz, $CDCl_3$): δ / ppm = 8.95 (t, *J* = 1.7 Hz, 1H), 7.64 (t, *J* = 1.9 Hz, 1H), 7.45 (t, *J* = 1.9 Hz, 1H), 7.10 (dd, *J* = 15.6, 8.7 Hz, 1H), 5.77 (dd, *J* = 15.6, 3.1 Hz, 1H), 5.40 (dd, *J* = 8.7, 3.1 Hz, 1H), 4.21 (t, *J* = 7.5 Hz, 2H), 1.91-1.80 (m, 2H), 1.42-1.29 (m, 2H), 0.94 (t, *J* = 7.4 Hz, 3H); ^{13}C NMR (100 MHz, $CDCl_3$): δ / ppm = 134.3. 128.0, 123.3, 119.9 (q, CF_3), 119.5, 110.3, 50.4, 31.9, 19.4, 13.2. ^{19}F NMR (376 MHz, $CDCl_3$): δ / ppm = -79.0 (CF_3). NMR data is consistent with literature values (Cui et al., 2015). Elemental Analysis: Calculated: C, 30.63; H, 3.50; N, 9.74; Found: C, 31.83; H, 2.33; N, 9.55.

1.1.3 Synthesis of PILs by 3D printing

The 3D printed polymeric imidazolium ionic liquid pieces were fabricated using the following procedure. The pieces were sized 24 mm x 16 mm x 0.5 mm and consisted of poly(BDA-co-BVimNTf_2) with 80 mol% [BVim][NTf_2] ionic liquid. **Scheme 1** below shows the synthesis of PIL. Stereolithography fabrication began first by slicing a 3D computer aided design (CAD) model into individual images for projecting onto the photo curable ink. An additive manufacturing software, Creation Workshop RC36, was used to create slices of a desired thickness (50 μm/layer), control the projection time of the images by the projector

and the movement of the build plate (**Scheme 2a**). A LittleRP 3D Printer FlexVat (**Scheme 2b**) was filled with premixed PIL ink which contained 80 mol % [BVim][NTf_2] (8 mmol, 3.44 g), 20 mol % 1,4-butanediol diacrylate (2 mmol, 0.39 g) and 1 mol % diphenyl(2,4,6-trimethylbenzoyl)phosphine oxide (1 mmol, 0.035 g). Then the build plate was lowered into the ink against the transparent Teflon film of the FlexVat.

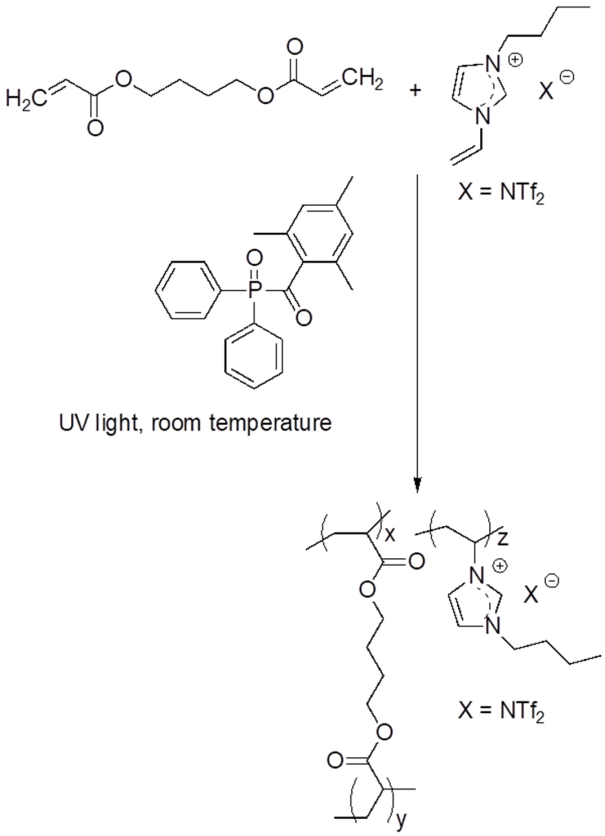

Scheme 1. Synthesis of imidazolium PIL by 3D printing

The Creation Workshop RC36 software then controlled the projector to show a black background with white images of each of the layers which were to be photo cured. The UV light passed from the projector lamp and mirror to the transparent Teflon film of the FlexVat. Each layer (50 μm) was cured for 8 s. After 8 s, the projector showed black background; so negligible light was projected into the photocurable ink while the build plate was lifting up for 50 μm. Then the Creation Workshop RC36 software loaded the image of the next layer and turned "on" the projector by showing the next white colour image. The process was repeated until the object was completely fabricated. After the object was fabricated, the object was isolated and washed with isopropanol to remove any uncured ink. Then the object was dried in the dark at room temperature overnight, to yield the final printed part (**Scheme 2c**).

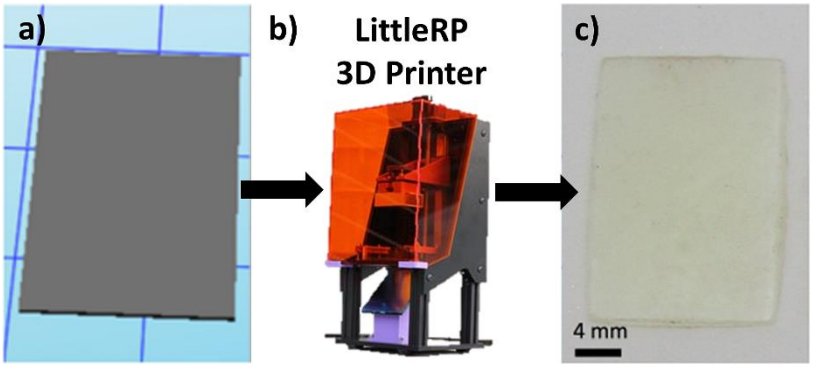

Scheme 2: Overall scheme of design of the desired 3D printed part within the software as a CAD model (**a**), then this model was communicated to the Little RP 3D Printer that was used in this work (**b**) to print the desired final 3D printed PIL part (**c**).

2 Material and energy balances for chemical substances that were not available in life cycle databases

This section details the estimation of the energy and material balances for the chemical substances that were not available in either Ecoinvent v 3.2 database, or in previous life cycle studies. Note the inputs for the fabrication of the PIL part (the 3D printing process) were collected from primary data at the laboratory scale and the outputs were calculated from material balance. The LCI results of 3D printing process are show in **Table S8**.

2.1 Material balances

The **Eq. S1–S2** by Felder and Rousseau (Felder and Rousseau, 2005) were used to calculate the mass flows of chemical reactions. The data used in these calculations are listed in **Table S1**.

$$n_i = n_{oi} + \xi_{ri} \pm \nu_i \qquad \textbf{Eq. S1}$$

$$f_r = \frac{\text{mols reacted}}{\text{mols fed}} \qquad \textbf{Eq. S2}$$

Where,

n_i = amount (in mol) of material remaining at the end of a chemical reaction;

n_{oi} = amount (in mol) of material at the start of chemical reaction;

ξ_i = extent of reaction "i";

ν_i = stoichiometric coefficient of a specific species (it is positive if the species is being generated and negative if the species is being consumed);

f_r = factor of reaction, it is the yield reaction divided per 100;

Mols reacted: Amount of reagent consumed;

Mols fed: amount of reagent fed;

According to Felder and Rousseau (2005), the reactant that would run out if a reaction proceeded to completion is called the 'limiting reactant', and the other reactants are termed 'excess reactants'. A reactant is limiting if it is present in less than its stoichiometric proportion relative to every other reactant. If all reactants are present in stoichiometric proportion, then no reactant is limiting. The extent of reaction in **Eq. S1** must be calculated for all reagents and the smallest magnitude value must be used for estimating the reaction balances.

Table S1.Physicochemical properties assumed in this work

Substance	Formula	CAS number	RMM / g mol^{-1}	ΔHf / kJ mol^{-1}	Cp (298 k) / kJ mol^{-1} K^{-1}
dichloroethane	$C_2H_4Cl_2$	75-09-2	98.96	-167.2[a]	0.1294[a]
water	H_2O	7732-18-5	18.01	-292.74[c]	0.0752[c]
3-butyl-1-vinylimidazolium bis(trifluoromethane)sulfonimide	[BVim][NTf_2]	758716-72-2	431.39	-953.40[d]	0.5418[h]
1-butanol	C_4H_9OH	71-36-3	74.12	-327.01[a]	0.1742[a]
3-butyl-1-vinylimidazolium bromide	[BVim][Br]	85100-77-2	231.13	-205.52[d]	0.2694[h]
lithium bromide	LiBr	7550-35-8	86.85	-350.91[a]	0.0566[a]
1-vinylimidazole	$C_5H_6N_2$	1072-63-5	94.11	22.98[d]	0.0824[f]
1-bromobutane	C_4H_9Br	109-65-9	137.02	-143.80[a]	0.1622[a]
potassium chloride	KCl	7447-40-7	74.55	-421.79[a]	0.0735[a]
1-imidazole	$C_3H_4N_2$	288-32-4	68.08	49.80[a]	0.0824[a]
hydrobromic acid	HBr	10035-10-6	80.91	-36.44[a]	0.0295[g]
potassium bromide	KBr	7758-02-3	119.00	-180.08[a]	0.0369[a]
sulfuric acid	H_2SO_4	7664-93-9	98.07	-811.30[a]	0.1099 [a]
potassium bisulfate	$KHSO_4$	7646-93-7	136.16	-811.30[e]	0.0886[b]
bromine	Br_2	7726-95-6	159.81	30.91[a]	0.0359[a]
potassium bromate	$KBrO_3$	7758-01-2	166.99	-361.00[a]	0.1038[a]
potassium hydroxide	KOH	1310-58-3	56.11	-412.71[a]	0.0831[a]
hydrogen chloride	HCl	7698-05-7	36.46	-92.31[a]	0.0281[a]
lithium chloride	LiCl	7447-41-8	42.39	-408.27[a]	0.0480[a]
1-butyl-3-methylimidazolium bis(trifluoromethane)sulfonimide	[Bmim][NTf_2]	174899-83-3	419.36	-980.17[d]	0.5363[i]
1-butyl-3-methylimidazolium chloride	[Bmim][Cl]	79917-90-1	174.67	-111.28[d]	0.3227[i]
lithium bis(trifluoromethane)sulfonimide	$LiNTf_2$	90076-65-6	287.08	-1147.39[d]	0.3062[j]
calcium carbonate	$CaCO_3$	471-34-1	100.09	-1206.9 [a]	0.0371 [a]
hydrogen cyanide	HCN	74-90-8	27.03	130.5 [a]	0.0288 [a]
calcium cyanamide	$CaCN_2$	156-62-7	80.10	58.79 [a]	0.0291 [a]
carbon dioxide	CO_2	124-38-9	44.01	-393.51 [a]	0.0937 [a]
hydrogen	H_2	1333-74-0	2.02	0 [a]	0.0937 [a]
carbon monoxide	CO	630-08-0	28.01	-110.53 [a]	0.0368 [a]
cyanamide	NH_2CN	420-04-2	42.04	58.79 [l]	0.0597 [l]
sodium dicyanamide	$NaN(CN)_2$	1934-75-4	89.03	58.79 [a]	0.0440 [a]
sodium chloride	NaCl	7647-14-5	58.44	-411.12 [a]	0.0364 [a]
sodium hydroxide	NaOH	1310-73-2	40.00	-427 [a]	0.0514 [a]
cyanogen chloride	CNCl	506-77-4	61.47	137.95 [a]	0.0371 [a]
3-butyl-1-vinylimidazolium dicyanamide	[BVim][$N(CN)_2$]	n/a	217.27	206 [m]	0.0288 [m]
sodium bromide	NaBr	7647-15-6	102.89	-143.93 [a]	0.0291 [a]

[a] Taken from NIST (National institute of standard and technology) (NIST, 2017). [b] Taken from DETHERM database (DETHERM, 2017). [c] Taken from ATcT (Active Thermochemical Tables) database (ATcT, 2017). [d] Value estimated using a genetic algorithm based multivariate linear regression method reported by Lee *et al*. (2017) (see **Section 3**); [e] Heat of formation was considered the same as for sulfuric acid. [f] This Cp value was considered the same as Cp value for 1-imidazole; [g] Taken from the work of Green and Perry (1999); [h] Calculated according to Joback group contribution method reported by Stouffer *et al*.(2008); [i] Taken from Yang (2011); [j] Calculated using Joback group method (Stouffer *et al.*, 2008) assuming the anion structure (NTf_2^-).[l] Taken from

William (2010), [m] Heat of formation and heat capacity values were considered the same as for 1-butyl-3-methylimidazolium dicyanamide from Emel'yanenko *et al.* (2007). n/a: not available.

2.1.1 3-butyl-1-vinylimidazolium bromide

The mass balances for the synthesis of 60.77 g (0.263 mol) of 3-butyl-1-vinylimidazolium bromide are as follows:

Stoichiometry of reaction: $C_5H_6N_2 + C_4H_9Br \rightarrow C_9H_{15}BrN_2$

Yield: 65.73 g (primary data)

$n_{0\ (C_5H_6N_2)} = 0.4\ \text{mol} \rightarrow 37.64\ \text{g}$ (primary data)

$n_{0\ (C_4H_9Br)} = 0.4\ \text{mol} \rightarrow 54.81\text{g}$ (primary data)

Limiting reactant/s: both reagents.

Note: inputs were collected at laboratory scale.

Estimating the extent of reaction:

$$\xi_r = \frac{0.4\ \text{mol} - (0.4\ \text{mol} - 0.263\ \text{mol})}{1} = 0.263\ \text{mol}$$

Calculate reaction balance by Eq. 1 and extent of reaction calculated above:

$n_{(C_5H_6N_2)} = 0.4\ \text{mol} + (0.263\ \text{mol} \times -1) = 0.14\ \text{mol} \rightarrow 12.90\ \text{g}$

$n_{(C_4H_9Br)} = 0.4\ \text{mol} + (0.263\ \text{mol} \times -1) = 0.14\ \text{mol} \rightarrow 18.78\ \text{g}$

$n_{(C_9H_{15}BrN_2)} = 0\ \text{mol} + (0.263\ \text{mol} \times 1) = 0.26\ \text{mol} \rightarrow 60.77\ \text{g}$ (primary data)

2.1.2 1-vinylimidazole

1-vinylimidazole is prepared by reaction of imidazole with an alkali metal hydroxide to obtain an imidazole alkali metal salt, followed by alkylation with dichloroethane to give chloroethylimidazole, which then undergoes further reaction with alkali metal hydroxide to generate 1-vinylimidazole (Ding and Shen, 2012). The alkali metal hydroxide is either NaOH or KOH. The yield is 99 % (Ding and Shen, 2012).

The calculations for the production of 1 kg of 1-vinylimidazole (94.11 $gmol^{-1}$, 10.63 mol) are shown below:

Stoichiometry of reaction (Ding and Shen, 2012): $C_3H_4N_2 + C_2H_4Cl_2 \rightarrow C_5H_6N_2 + 2HCl$

Limiting reactant/s considered: both reagents.

$$0.99 = \frac{10.63 \text{ mol}}{\text{moles fed}}$$

Rearranged for $'\text{moles fed}' = 10.63 \text{ mol} / 0.99 = 10.73 \text{ mol}$

Estimating the extent of reaction:

$$\xi_r = 10.73 \text{ mol} - \frac{(10.73 \text{ mol} - 10.63 \text{ mol})}{1} = 10.63 \text{ mol}$$

Calculating the reaction balance through use of **Eq. 1** and extent of reaction as calculated above:

$n_{0\,(C_3H_4N_2)} = 10.73 \text{ mol} \rightarrow 730.72 \text{ g}$

$n_{0\,(C_2H_4Cl_2)} = 10.73 \text{ mol} \rightarrow 1.06 \text{ kg}$

$n_{(C_3H_4N_2)} = 10.73 \text{ mol} + (10.63 \text{ mol x } -1) = 0.11 \text{ mol} \rightarrow 7.31 \text{ g}$

$n_{(C_2H_4Cl_2)} = 10.73 \text{ mol} + (10.63 \text{ mol x } -1) = 0.11 \text{ mol} \rightarrow 10.62 \text{ g}$

$n_{(C_5H_6N_2)} = 0 \text{ mol} + (10.63 \text{ mol x } 1) = 10.63 \text{ mol} \rightarrow 1 \text{ kg}$

$n_{(HCl)} = 0 \text{ mol} + (21.25 \text{ mol x } 1) = 21.25 \text{ mol} \rightarrow 774.80 \text{ g}$

2.1.3 1-bromobutane

1-bromobutane is a primary alkyl halide (primary alkyl) and it is produced by a bimolecular nucleophilic substitution reaction (Sn2). The preparation is based on conversion of a primary alcohol into an alkyl halide using an acid catalysed halogenation reaction and the yield is 90% (Kamm and Marvel, 1921).

The calculations for the production of 1 kg of 1-bromobutane (137.02 $gmol^{-1}$, 7.3 mol) are shown below:

Global stoichiometry of reaction (Kamm and Marvel, 1921): $C_4H_9OH + HBr \rightarrow C_4H_9Br + H_2O$

Limiting reactant/s considered: both reagents.

$$0.90 = \frac{7.30\ \text{mol}}{\text{moles fed}}$$

Rearranged for 'moles fed' = 7.30 mol / 0.9 = 8.11 mol

Estimating the extent of reaction:

$$\xi_r = 8.11\ \text{mol} - \frac{(8.11\ \text{mol} - 7.30\ \text{mol})}{1} = 7.30\ \text{mol}$$

Calculation of reaction balance through use of **Eq. 1** and the extent of reaction as calculated above:

$n_{0\ (C_4H_{10}O)} = 8.11\ \text{mol} \rightarrow 601.07\ \text{g}$

$n_{0\ (HBr)} = 8.11\ \text{mol} \rightarrow 656.11\ \text{g}$

$n_{(C_4H_9Br)} = 0\ \text{mol} + (7.30\ \text{mol} \times 1) = 7.30\ \text{mol} \rightarrow 1\ \text{kg}$

$n_{(C_4H_{10}O)} = 8.11\ \text{mol} + (7.30\ \text{mol} \times -1) = 0.81\ \text{mol} \rightarrow 60.11\ \text{g}$

$n_{(HBr)} = 8.11\ \text{mol} + (7.30\ \text{mol} \times -1) = 0.81\ \text{mol} \rightarrow 65.61\ \text{g}$

$n_{(H_2O)} = 0\ \text{mol} + (7.30\ \text{mol} \times 1) = 7.30\ \text{mol} \rightarrow 131.37\ \text{g}$

2.1.4 Hydrobromic acid

The synthesis of the hydrobromic acid was reported by Booth (1939). According to Booth, for the production of 1 mol of hydrobromic acid, 1 mol of potassium bromide and 1.7 mols of sulfuric acid were needed and the overall yield is 85 %.

The calculations for the production of 1 kg of hydrobromic acid (80.91 $gmol^{-1}$, 12.36 mol) are shown below:

Global stoichiometry of reaction (Booth, 1939): $H_2SO_4 + KBr \rightarrow KHSO_4 + HBr$
First the limiting reagent was determined, as follows:

14.54 mol of potassium bromide and 21.01 mol of sulfuric acid are necessary.

$$\text{potassium bromide: } 0.85 = \frac{\text{mols reacted}}{14.540 \text{ mol}}$$

$$\text{rearranged for 'mols reacted'} = 14.54 \text{ mol x } 0.85 = 12.36 \text{ mol}$$

$$\text{sulfuric acid: } 0.85 = \frac{\text{mols reacted}}{21.011 \text{ mol}}$$

$$\text{rearranged for 'mols reacted'} = 21.01 \text{ mol x } 0.85 = 17.86 \text{ mol}$$

Thus, the limiting reagent is potassium bromide as it is in the smaller molar proportion(Felder and Rousseau, 2005). Next the extent of reaction was calculated, as follows:

$$\xi_r = 14.540 \text{ mol} - \frac{(14.54 \text{ mol} - 12.36 \text{ mol})}{1} = 12.35 \text{ mol}$$

Calculated the reaction balance through use of **Eq.1** and the extent of reaction was calculated as above:

Calculate reaction balance from reaction extension

$n_{0\,(H_2SO_4)} = 21.01 \text{ mol} \rightarrow 2.06 \text{ kg}$

$n_{0\,(KBr)} = 14.54 \text{ mol} \rightarrow 1.73 \text{ kg}$

$n_{(H_2SO_4)} = 21.01 \text{ mol} - (12.36 \text{ mol x } 1) = 8.65 \text{ mol} \rightarrow 848.46 \text{ g}$

$n_{(KBr)} = 14.54 \text{ mol} - (12.36 \text{ mol x } 1) = 2.18 \text{ mol} \rightarrow 259.55 \text{ g}$

$n_{(KHSO_4)} = 0 \text{ mol} - (12.36 \text{ mol x } -1) = 12.36 \text{ mol} \rightarrow 1.68 \text{ kg}$

$n_{(HBr)} = 0 \text{ mol} - (12.36 \text{ mol x } -1) = 12.36 \text{ mol} \rightarrow 1 \text{ kg}$

2.1.5 Potassium bromide

The material balance to production of 1 kg of potassium bromide (119.00 g mol^{-1}, 8.40 mol) of potassium bromide was based on reaction stoichiometry reported by Blanchard (1936). In this case as the yield is 100 % there was no need to calculate the extent of reaction. Thus, the material balance was calculated from the global stoichiometry of reaction, as follows:

Global stoichiometry of reaction (Blanchard et al., 1936): $6KOH + 3Br_2 \rightarrow KBrO_3 + 5KBr + 3H_2O$

$$KOH = \frac{6 \text{ mols KOH}}{5 \text{ mols KBr}} \text{ x } 8.40 \text{ mol KBr} = 10.08 \text{ mol x } 119.00 \text{ g mol}^{-1} = 565.80 \text{ g}$$

$$Br_2 = \frac{3 \text{ mols } Br_2}{5 \text{ mols KBr}} \text{ x } 8.40 \text{ mol KBr} = 5.04 \text{ mol x } 159.80 \text{ g mol}^{-1} = 805.73 \text{ g}$$

$$KBrO_3 = \frac{1 \text{ mol}}{5 \text{ mols KBr}} \text{ x } 8.40 \text{ mol KBr} = 1.68 \text{ mol x } 167.00 \text{ g mol}^{-1} = 280.66 \text{ g}$$

$$H_2O = \frac{3 \text{ mols } H_2O}{5 \text{ mols KBr}} \text{ x } 8.40 \text{ mol KBr} = 5.04 \text{ mol x } 18.00 \text{ g mol}^{-1} = 90.75 \text{ g}$$

2.1.6 3-butyl-1-vinylimidazolium bis(trifluoromethane)sulfonimide

The mass balance for the production of 103.41 g (0.240 mol) of 3-butyl-1-vinylimidazolium bis(trifluoromethane)sulfonimide was calculated, as follows:

Global stoichiometry of reaction: $C_9H_{15}BrN_2 + C_2F_6LiO_4S_2N \rightarrow C_{11}H_{15}F_6N_3O_4S_2 + LiBr$

Yield: 90.8 % (primary data)

$n_{0\ (C_9H_{15}BrN_2)} = 0.26$ mol → 60.77 g (primary data)

$n_{0\ (C_2F_6LiO_4S_2N)} = 0.396$ mol → 113.76 g (primary data)

$n_{\ (C_{11}H_{15}F_6N_3O_4S_2)} = 0.24$ mol → 103.41 g (primary data)

Note: inputs were collected at laboratory scale.

First the limiting reagent was determined, as follows:

$$C_9H_{15}BrN_2\text{: } 0.908 = \frac{\text{mols reacted}}{0.264 \text{ mol}}$$

so rearranged for $'\text{mols reacted}' = 0.908 \text{ x } 0.264 = 0.24 \text{ mol}$

$$C_2F_6LiO_4S_2N:\ 0.908 = \frac{\text{mols reacted}}{0.396 \text{ mol}}$$

rearranged for $'\text{mols reacted}' = 0.908 \text{ x } 0.396 \text{ mol} = 0.36 \text{ mol}$

Thus, the limiting reagent is $C_9H_{15}BrN_2$, as it is in the smaller molar proportion (Felder and Rousseau, 2005) The extent of reaction was calculated, as follows:

$$\xi_r = 0.264 \text{ mol} - \frac{(0.264 \text{ mol} - 0.239 \text{ mol})}{1} = 0.24 \text{ mol}$$

Calculate reaction balance by **Eq. 1** and extent of reaction calculated above:

$n_{(C_9H_{15}BrN_2)} = 0.26 \text{ mol} + (0.24 \text{ mol x } -1) = 0.02 \text{ mol} \rightarrow 5.61 \text{ g}$

$n_{(C_2F_6LiO_4S_2N)} = 0.396 \text{ mol} + (0.240 \text{ mol x } -1) = 0.16 \text{ mol} \rightarrow 44.93 \text{ g}$

$n_{(C_9H_{15}BrN_2)} = 0 \text{ mol} + (0.240 \text{ mol x } 1) = 0.24 \text{ mol} = 103.41 \text{ g} \rightarrow 103.41 \text{ g}$

$n_{(LiBr)} = 0 \text{ mol} + (0.24 \text{ mol x } 1) = 0.24 \text{ mol} \rightarrow 20.82 \text{ g}$

2.2 Energy balances

The energy consumed for the synthesis of the IL and their precursors was calculated from the method proposed by Mehrkesh and Karunanithi (2013) and reported by Cuéllar-Franca *et al*.(2016) (**Equations S3-5**). In this method, the theoretical energy consumption for synthesis of a chemical compound is estimated from the heat of reaction. Then the heat of reaction is scaled-up to industrial scale using empirical factors that take into account energy losses. In this work, it was assumed that no work is performed and that kinetic and potential energy are zero (Mehrkesh and Karunanithi, 2013). The heats of reaction for the syntheses of ILs and the precursors were calculated using the reaction heats based on the methods used by Felder and Rousseau (2005). For heat of formation values that were not available, estimates were made using the method of Vatani *et al.* (2007). Ionic liquid heat capacity values that were not available in the literature were calculated according to Joback group contribution method (Stouffer et al., 2008). The physical-chemical properties of the chemicals involved in the synthesis of ionic liquids and its precursors are summarised in **Table S1**.

$E_i = \Delta H \times Fc$ **Eq. S3**

$\Delta H = \sum(n \times \hat{H})outputs - \sum(n \times \hat{H})inputs$ **Eq. S4**

$\hat{H} = \Delta\hat{H}f^{\circ} + \int_{T1}^{T2} Cp \times \Delta T$ **Eq. S5**

where:

ΔH: heat of reaction

n = molecular weight of reactants

H= specific enthalpy of reactants

$\Delta\hat{H}f^{\circ}$= heat of formation of reactants

Cp = calorific value of reactants

T1 = reference temperature (25 ºC)

T2 = temperature of the reactants

Fc= empirical factors, 4.2 for endothermic reactions and assumed to be supplied by natural gas and 3.2 for exothermic reactions and assumed the cooling is supplied by electricity (Mehrkesh and Karunanithi, 2013).

2.2.1 3-butyl-1-vinylimidazolium bromide

The theoretical energy consumption for the production of 60 g of 3-butyl-1-vinylimidazolium bromide was estimated such as shown in **Table S2**.

Table S2. Input and output streams for the production of 3-butyl-1-vinylimidazolium bromide

Substances	**Empirical formula**	**Inputs**		**Outputs**	
		mol	$\hat{H}$	**mol**	$\hat{H}$
1-vinylimidazole	$C_5H_6N_2$	0.40	$\hat{H}_1$	0.13	$\hat{H}_3$
1-bromobutane	C_4H_9Br	0.40	$\hat{H}_2$	0.13	$\hat{H}_4$
3-butyl-1-vinylimidazolium bromide	$C_9H_{15}BrN_2$	-	-	0.26	$\hat{H}_5$

The specific enthalpies $\hat{H}$ for each chemical substance were calculated by **Equation S3** as follows:

$$\hat{H}_1 = \Delta Hf^{o}{}_{(C_5H_6N_2)} + \int_{25}^{25} Cp \times dT = 22.98\ kJ\ mol^{-1} + 0 = 22.98\ kJ\ mol^{-1}$$

$$\hat{H}_2 = \Delta Hf^{o}{}_{(C_4H_9Br)} + \int_{25}^{25} CpdT = -143.80\ kJ\ mol^{-1} + 0 = -143.80\ kJ\ mol^{-1}$$

$$\hat{H}_3 = \Delta Hf^{o}_{(C_5H_6N_2)} + \int_{25}^{40} CpdT = 22.98\ \text{kJ mol}^{-1} + (0.08\ \text{kJ mol}^{-1}\ \text{K}^{-1}\ \text{x}\ 15\ \text{K})$$

$$= 24.22\text{kJ mol}^{-1}$$

$$\hat{H}_4 = \Delta Hf^{o}_{(C_4H_9Br)} + \int_{25}^{40} CpdT = -143.80\ \text{kJ mol}^{-1} + (0.16\ \text{kJ mol}^{-1}\ \text{x}\ 15\text{K})$$

$$= -141.36\ \text{kJ mol}^{-1}$$

$$\hat{H}_5 = \Delta Hf^{o}_{(C_9H_{15}BrN_2)} + \int_{25}^{40} CpdT = -205.52 + \left(0.27\ \text{kJ mol}^{-1}\ \text{K}^{-1}\ \text{x}\ 15\ \text{K}\right)$$

$$= -201.48\ \text{kJ mol}^{-1}$$

The enthalpy of reaction was calculated by **Eq. S4**, as follows.

$$\Delta H_r = (0.14\ \text{mol x}\ 24.21\ \text{kJ mol}^{-1} + 0.14\ \text{mol x} - 141.36\ \text{kJ mol}^{-1} + 0.26\ \text{mol} - 201.48\ \text{kJ mol}^{-1}) - (0.4\ \text{mol x}\ 22.98\ \text{kJ mol}^{-1} + 0.4\ \text{mol x} - 143.80\ \text{kJ mol}^{-1}) = -20.70\ \text{kJ}$$

Thus, the electricity energy demand for cooling is estimated at 66.24 kJ = (3.2 x $|-20.70\ \text{kJ}|$).

2.2.2 1-vinylimidazole

The theoretical energy consumption for the production of 1 kg of 1-vinylimidazole was estimated such as shown in **Table S3**.

Table S3. Input and output streams for the production of 1-vinylimidazole

Substances	**Empirical formula**	**Inputs**		**Outputs**	
		mol	$\hat{H}$	**mol**	$\hat{H}$
1-vinylimidazole	$C_5H_6N_2$	-	-	10.62	$\hat{H}_3$
imidazole	$C_3H_4N_2$	10.73	$\hat{H}_1$	0.11	$\hat{H}_4$
diclhoroethane	$C_2H_4Cl_2$	10.73	$\hat{H}_2$-	0.11	$\hat{H}_5$
hydrogen chloride	HCl	-	-	21.25	$\hat{H}_6$

The specific enthalpies $\hat{H}$ for each chemical substance were calculated by **Eq. S3** as follows:

$$\hat{H}_1 = \Delta Hf^{o}_{(C_3H_4N_2)} + \int_{25}^{25} CpdT = 58.50\ \text{kJ mol}^{-1} + 0 = 49.80\ \text{kJ mol}^{-1}$$

$$\widehat{H}_2 = \Delta Hf^{o}_{(C_2H_4Cl_2)} + \int_{25}^{25} CpdT = -167.20\ \text{kJ mol}^{-1} + 0 = -167.20\ \text{kJ mol}^{-1}$$

$$\widehat{H}_3 = \Delta Hf^{o}_{(C_5H_6N_2)} + \int_{25}^{85} CpdT = 22.98\ \text{kJ mol}^{-1} + \left(0.08\ \text{kJ mol}^{-1}\ \text{K}^{-1}\ \text{x}\ 60\ \text{K}\right)$$

$$= 27.93\ \text{kJ mol}^{-1}$$

$$\widehat{H}_4 = \Delta Hf^{o}_{(C_3H_4N_2)} + \int_{25}^{85} CpdT = \ 49.80\ \text{kJ mol}^{-1} + (0.08\ \ \text{kJ mol}^{-1}\ \text{K}^{-1}\ \text{x}\ 60\ \text{K}$$

$$= 54.74\ \text{kJ mol}^{-1}$$

$$\widehat{H}_5 = \Delta Hf^{o}_{(C_2H_4Cl_2)} + \int_{25}^{85} CpdT = -167.20\ \text{kJ mol}^{-1}\ + \left(0.13\ \text{kJ mol}^{-1}\ \text{K}^{-1}\ \text{x}\ 60\ \text{K}\right)$$

$$= -159.44\ \text{kJ mol}^{-1}$$

$$\widehat{H}_6 = \ \Delta Hf^{o}_{(HCl)} + \int_{25}^{85} CpdT = -92.31\ \text{kJ mol}^{-1}\ + \left(00.03\ \text{kJ mol}^{-1}\ \text{K}^{-1}\ \text{x}\ 60\ \text{K}\right)$$

$$= -90.62\ \text{kJ mol}^{-1}$$

The enthalpy of reaction was calculated by **Eq. S4**, as follows.

$$\Delta H_r = (10.62\ \text{mol x}\ 27.93\ \text{kJ mol}^{-1} + 0.11\ \text{mol x}\ 54.74\ \text{kJ mol}^{-1} + 0.11\ \text{mol x} - 159.43\ \text{kJ mol}^{-1}\ + 21.25\ \text{mol x} - 90.62\ \text{kJ mol}^{-1}) - (10.73\ \text{mol x}\ 49.8\ \text{kJ mol}^{-1} + 10.73\ \text{mol x} - 167.20\ \text{kJ mol}^{-1}) = -380.27\ \text{kJ}$$

Thus, the electricity energy demand for cooling is estimated at 1216.87 kJ = (3.2 x $|-380.27\ \text{kJ}|$).

2.2.3 1-bromobutane

The theoretical energy consumption for the production of 1 kg of 1-bromobutane was estimated such as shown in **Table S4**.

Table S4. Input and output streams for the synthesis of 1-bromobutane

Substances	**Empirical formula**	**Inputs**		**Outputs**	
		mol	$\widehat{H}$	mol	$\widehat{H}$
butanol	$C_4H_{10}O$	8.11	$\widehat{H}_1$	0.81	$\widehat{H}_3$
hydrobromic acid	HBr	8.11	$\widehat{H}_2$	0.81	$\widehat{H}_4$
1-bromobutane	C_4H_9Br	-	-	7.29	$\widehat{H}_5$
water	H_2O	-	-	7.29	$\widehat{H}_6$

The specific enthalpies $\widehat{H}$ for each chemical substance were calculated by **Eq. S3** as follows:

$$\widehat{H}_1 = \Delta Hf^{o}_{(C_4H_{10}O)} + \int_{25}^{25} CpdT = -327.01\ \text{kJ mol}^{-1} + 0 = -327.01\ \text{kJ mol}^{-1}$$

$$\widehat{H}_2 = \Delta Hf^{o}_{(HBr)} + \int_{25}^{25} CpdT = -36.44\ \text{kJ mol}^{-1} + 0 = -36.44\ \text{kJ mol}^{-1}$$

$$\widehat{H}_3 = \Delta Hf^{o}_{(C_4H_{10}O)} + \int_{25}^{210} CpdT = -327.01\ \text{kJ mol}^{-1} + \left(0.17\ \text{kJ mol}^{-1}\ \text{K}^{-1}\ \text{x}\ 185\ \text{K}\right)$$

$$= -294.772\ \text{kJ mol}^{-1}$$

$$\widehat{H}_4 = \Delta Hf^{o}_{(HBr)} + \int_{25}^{210} CpdT = -36.44\ \text{kJ mol}^{-1} + (0.03\ \text{kJ mol}^{-1}\ \text{x}\ 185\ \text{K})$$

$$= -30.98\ \text{kJ mol}^{-1}$$

$$\widehat{H}_5 = \Delta Hf^{o}_{(C_4H_9Br)} + \int_{25}^{210} CpdT = -143.80\ \text{kJ mol}^{-1} + \left(0.16\ \text{kJ mol}^{-1}\ \text{K}^{-1}\ \text{x}\ 185\ \text{K}\right)$$

$$= -133.79\ \text{kJ mol}^{-1}$$

$$\widehat{H}_6 = \Delta Hf^{o}_{(H_2O)} + \int_{25}^{210} CpdT = -292.74\ \text{kJ mol}^{-1} + (0.08\ \text{kJ mol}^{-1}\ \text{K}^{-1}\ \text{x}\ 185\ \text{K})$$

$$= -278.81\ \text{kJ mol}^{-1}$$

The enthalpy of reaction was calculated by **Eq. S4**, as follows.

$$\Delta H_r = \left(0.81\ \text{mol x} - 294.77\ \text{kJ mol}^{-1} + 0.811\ \text{mol x} - 30.98\ \text{kJ mol}^{-1} + 7.29\ \text{mol x} - 113.79\ \text{kJ mol}^{-1}\right) - \left(8.11\ \text{mol x} - 327.01\ \text{kJ mol}^{-1} + 8.11\ \text{mol x} - 36.44\ \text{kJ mol}^{-1}\right) = -182.19\ \text{kJ}$$

Thus, the electricity energy demand for cooling is estimated at 583.01 kJ = (3.2 x $|-182.19\ \text{kJ}|$).

2.2.4 Hydrobromic acid

The theoretical energy consumption for the synthesis of 1 kg of hydrobromic acid was estimated such as shown in

Table S5.

Table S5. Input and output streams for the synthesis of hydrobromic acid

Substances	Empirical formula	Inputs		Outputs	
		mol	$\hat{H}$	mol	$\hat{H}$
sulfuric acid	H_2SO_4	21.01	$\hat{H}_1$	8.65	$\hat{H}_3$
potassium bromide	KBr	14.54	$\hat{H}_2$	2.18	$\hat{H}_4$
potassium bisulfate	$KHSO_4$	-	-	12.36	$\hat{H}_5$
hydrobromic acid	HBr	-	-	12.36	$\hat{H}_6$

The specific enthalpies $\hat{H}$ for each chemical substance were calculated by equation S3 as follows:

$$\hat{H}_1 = \Delta Hf^{o}_{(H_2SO_4)} + \int_{25}^{25} CpdT = -811.30 \text{ kJ mol}^{-1} + 0 = -811.30 \text{ kJ mol}^{-1}$$

$$\hat{H}_2 = \Delta Hf^{o}_{(KBr)} + \int_{25}^{25} CpdT = -180.08 \text{ kJ mol}^{-1} + 0 = -180.08 \text{ kJ mol}^{-1}$$

$$\hat{H}_3 = \Delta Hf^{o}_{(H_2SO_4)} + \int_{25}^{75} CpdT = -811.30 \text{ kJ mol}^{-1} + \left(0.10 \text{ kJ mol}^{-1}K^{-1} \text{ x } 50 \text{ K}\right)$$

$$= -805.8 \text{ kJ mol}^{-1}$$

$$\hat{H}_4 = \Delta Hf^{o}_{(KBr)} + \int_{25}^{75} CpdT = -180.08 \text{ kJ mol}^{-1} + (0.03 \text{ kJ mol}^{-1}K^{-1} \text{ x } 50 \text{ K})$$

$$= -178.23 \text{ kJ mol}^{-1}$$

$$\hat{H}_5 = \Delta Hf^{o}_{(KHSO_4)} + \int_{25}^{25} CpdT = -811 \text{ kJ mol}^{-1} + \left(0.09 \text{ kJ mol}^{-1}K^{-1} \text{ x } 50 \text{ K}\right)$$

$$= -761.21 \text{ kJ mol}^{-1}$$

$$\hat{H}_6 = \Delta Hf^{o}_{(HBr)} + \int_{25}^{25} CpdT = -36.44 + \left(0.03 \text{ kJ mol}^{-1}K^{-1} \text{ x } 50 \text{ K}\right) = -34.96 \text{ kJ mol}^{-1}$$

The enthalpy of reaction was calculated by **Eq. S4**, as follows.

$$\Delta H_r = (8.65 \text{ mol x} - 805.00 \text{ kJ mol}^{-1} + 2.18 \text{ mol x} - 178.23 \text{ kJ mol}^{-1} + 12.36 \text{ mol x} - 761.21 \text{ kJ mol}^{-1} + 12.36 \text{ mols x} - 34.96 \text{ kJ mol}^{-1}) - (21.01 \text{ mol x} - 811.30 \text{ kJ mol}^{-1} + 14.54 \text{ mol x} - 180.08 \text{ kJ mol}^{-1}) = 2464.22 \text{ kJ}$$

So, the total theoretical heat needed to heat the reactor is equal to 2464.22 kJ. Applying the correction factor of 4.2, the actual heat needed to heat the reactor using natural gas is estimated at 10349.72 kJ = (4.2 * 2464.22 kJ).

2.2.5 Potassium hydroxide

The theoretical energy consumption for the production of 1 kg of potassium bromide was estimated such as shown in **Table S6**.

Table S6. Input and output streams for the synthesis of potassium hydroxide

Substances	**Empirical formula**	**Inputs**		**Outputs**	
		mols	$\hat{H}$	mols	$\hat{H}$
potassium hydroxide	KOH	10.08	$\hat{H}_1$	-	-
bromine	Br_2	5.04	$\hat{H}_2$	-	-
potassium bromate	$KBrO_3$	-	-	1.68	$\hat{H}_3$
potassium bromide	5KBr	-	-	8.40	$\hat{H}_4$
water	H_2O	-	-	5.04	$\hat{H}_5$

The specific enthalpies $\hat{H}$ for each chemical substance were calculated by **Eq. S3** as follows:

$$\hat{H}_1 = \Delta Hf^{o}_{(KOH)} + \int_{25}^{25} CpdT = \text{-412.71 kJ mol}^{-1} + 0 = \text{-412.71 kJ mol}^{-1}$$

$$\hat{H}_2 = \Delta Hf^{o}_{(Br_2)} + \int_{25}^{25} CpdT = 30.91 \text{ kJ mol}^{-1} + 0 = 30.91 \text{ kJ mol}^{-1}$$

$$\hat{H}_3 = \Delta Hf^{o}_{(KBrO_3)} + \int_{25}^{25} CpdT = \text{-361.00 kJ mol}^{-1} + 0 = \text{-361.00 kJ mol}^{-1}$$

$$\hat{H}_4 = \Delta Hf^{o}_{(KBr)} + \int_{25}^{25} CpdT = \text{-180.08 kJ mol}^{-1} + 0 = \text{-180.08 kJ mol}^{-1}$$

$$\hat{H}_5 = \Delta Hf^{o}_{(H2O4)} + \int_{25}^{25} CpdT = \text{-292.74 kJ mol}^{-1} + 0 = \text{-292.74 kJ mol}^{-1}$$

The enthalpy of reaction was calculated by **Eq. S4**, as follows.

$$\Delta H_r = (1.68 \text{ mol x} - 361.00 \text{ kJ mol}^{-1} + 8.40 \text{ mol x} - 180.08 \text{ kJ mol}^{-1} + 5.04 \text{ mol x} - 292.74 \text{ kJ mol}^{-1}) - (10.08 \text{ mol x} - 412.71 \text{ kJ mol}^{-1} + 5.04 \text{ mol x} - 30.91 \text{ kJ mol}^{-1}) = 409.09 \text{ kJ}$$

So, the total theoretical heat needed to heat the reactor is equal to 409.09 kJ. Applying the correction factor of 4.2, the actual heat needed to heat the reactor using natural gas is estimated at 1718.17 kJ = (4.2 * 409.09 kJ).

2.2.6 3-butyl-1-vinylimidazolium bis(trifluoromethane)sulfonimide

The theoretical energy consumption for the production of 103.41 g of 3-butyl-1-vinylimidazolium bis(trifluoromethane)sulfonimide was estimated such as shown in **Table S7**.

Table S7. Input and output streams for the synthesis of 3-butyl-1-vinylimidazolium bromide

Substances	**Empirical formula**	**Inputs**		**Outputs**	
		mol	$\hat{H}$	**mol**	$\hat{H}$
3-butyl-1-vinylimidazolium bromide	$C_9H_{15}BrN_2$	0.26	$\hat{H}_1$	0.02	$\hat{H}_3$
$LiNTf_2$	$C_2F_6LiO_4S_2N$	0.39	$\hat{H}_2$	0.16	$\hat{H}_4$
3-butyl-1-vinylimidazolium bis(trifluoromethane)sulfonamide	$C_{11}H_{15}F_6N_3O_4S_2$	-	-	0.24	$\hat{H}_5$
lithium bromide	LiBr			0.23	$\hat{H}_6$

$LiNTf_2$: Lithium bis(trifluoromethane)sulfonimide

The specific enthalpies $\hat{H}$ for each chemical substance were calculated by **Eq. S3** as follows:

$$\hat{H}_1 = \Delta Hf^o{}_{(C_9H_{15}BrN_2)} + \int_{25}^{25} CpdT = -205.52 \text{ kJ mol}^{-1} + 0 = -205.52 \text{ kJ mol}^{-1}$$

$$\hat{H}_2 = \Delta Hf^o{}_{(C_2F_6LiO_4S_2N)} + \int_{25}^{25} CpdT = -1147.39 \text{ kJ mol}^{-1} + 0 = -1147.39 \text{ kJ mol}^{-1}$$

$$\hat{H}_3 = \Delta Hf^o{}_{(C_9H_{15}BrN_2)} + \int_{25}^{40} CpdT = -205.52 \text{ kJ mol}^{-1} + (0.27 \text{ kJ mol}^{-1} \text{ K}^{-1} \text{ x } 15 \text{ K})$$

$$= -201.48 \text{ kJ mol}^{-1}$$

$$\hat{H}_4 = \Delta Hf^o{}_{(C_2F_6LiO_4S_2N)} + \int_{25}^{40} CpdT = -1147.39 \text{ kJ mol}^{-1} + (0.27 \text{ kJ mol}^{-1} \text{ K}^{-1} \text{ x } 15 \text{ K})$$

$$= -1142.80 \text{ kJ mol}^{-1}$$

$$\hat{H}_5 = \Delta Hf^o{}_{(C_{11}H_{15}F_6N_3O_4S_2)} + \int_{25}^{40} CpdT = -953.41 \text{ kJ mol}^{-1} + \left(0.54 \text{ kJ mol}^{-1} \text{ K}^{-1} \text{ x } 15\text{K}\right)$$

$$= -350.06 \text{ kJ mol}^{-1}$$

$$\widehat{H}_6 = \Delta Hf^{o}_{(LiBr)} + \int_{25}^{40} CpdT = -350.91 + (0.57\ \text{kJ mol}^{-1}\ \text{K}^{-1}\ \text{x}\ 15\text{K})$$

$$= -350.06\ \text{kJ mol}^{-1}$$

The enthalpy of reaction was calculated by **Eq. S4**, as follows.

$$\Delta H_r = (0.02\ \text{mol x} - 201.48\ \text{kJ mol}^{-1} + 0.16\ \text{mol x} - 1142.8\ \text{kJ mol}^{-1} + 0.24\ \text{mol} - 945.28\ \text{kJ mol}^{-1} + 0.24\ \text{mol x} - 350.06\ \text{kJ mol}^{-1}) - (0.26\ \text{mol x} - 205.52\ \text{kJ mol}^{-1} + 0.39\ \text{mol x} - 1147.39\ \text{kJ mol}^{-1}) = 14.62\ \text{kJ}$$

Therefore, the energy needed to heat the reactor (assuming combustion of natural gas) is estimated at 61.39 kJ = (4.2 * 14.62 kJ).

3 Life cycle inventory results of PIL made from [BVim][NTf_2]

The **Table S8** shows the life cycle inventory results for the 3D part (imidazolium PIL printed part), [BVim][NTf_2] and [BVim][Br], when considering production of 1.2 g of the PIL (1 x FU) and partial recovery (~ 74 %). In **Table S9** are shown the inventories of intermediate substances used in the synthesis of 3-butyl-1vinylimidazolium bromide that were not available in the Ecoinvent database.

Table S10 shows the life cycle inventory results for production of $LiNTf_2$ and the intermediate chemicals that were not available in the Ecoinvent database.

Table S8. Life cycle inventory results for the imidazolium PIL, [BVim][NTf_2] and [BVim][Br] for 1 x FU

3D printing process, production of imidazolium PIL				
	Process Flow	**Amount**	**Unit**	**Source**
Inputs	[BVim][NTf_2]	3.04	g	Primary data
	1,4-butanediol diacrylate	0.35	g	Primary data
	diphenyl(2,4,6-trimethylbenzoyl)phosphine oxide	3.10×10^{-2}	g	Primary data
	isopropanol	0.66	g	Primary data
	mixing (raw materials) – recovered	6.26	g	Primary data
	electricity energy (3D printer)	1.07×10^{-2}	kWh	Primary data
	energy - electricity (mixing- raw materials)	1.04×10^{-2}	kWh	Primary data
	energy – electricity (solvent recovery)	22.40	kJ	Primary data
Outputs	3D part, imidazolium poly(ionic liquid) (PIL)	1.20	g	Primary data
	isopropanol	0.06	g	Primary data
	isopropanol recovered	6.53	g	Primary data
	mixing (raw materials) – recycle	6.26	g	Primary data
	mixing (raw materials) – waste	2.22	g	Primary data
3-butyl-1-vinylimidazolium bis(trifluoromethane)sulfonimide - [BVim][NTf_2]				
Inputs	3-butyl-1-vinylimidazolium bromide	1.79	g	Primary data
	lithium bis(trifluoromethane)sulfonimide	3.34	g	Primary data
	water	5.88	g	Primary data
	dichloromethane	0.79	g	Assumption (**Section 7**)
	magnesium sulfate	2.94	g	Primary data
	electricity energy (synthesis)	3.97	kJ	Calculated (**Section 2.2.6**)
	heat, (natural gas combustion) (solvent recovery)	1.80	kJ	Calculated (**Section 7**)
Outputs	3-butyl-1-vinylimidazolium bis(trifluoromethane)sulfonimide	3.04	g	Calculated (**Section 2.1.6**)
	water	5.88	g	Calculated (**Section 2.1.6**)
	dichloromethane	0.79	g	Assumption (**Section 7**)
	magnesium sulfate	2.94	g	Primary data
	3-butyl-1-vinylimidazolium bromide	1.65	g	Calculated (**Section 2.1.6**)
	lithium bis(trifluoromethane)sulfonimide	1.32	g	Calculated (**Section 2.1.6**)
	lithium bromide	0.61	g	Calculated (**Section 2.1.6**)
3-butyl-1-vinylimidazolium bromide [BVim][Br]				
Inputs	1-vinylimidazole	1.11	g	Primary data
	1-bromobutane	1.26	g	Primary data
	diethyl ether	14.7	g	Primary data
	dichloromethane	3.89	g	Primary data
	electricity energy	1.95	kJ	Calculated (**Section 2.2.1**)
	heat, (natural gas combustion) (solvent recovery)	6.98	kJ	Calculated (**Section 7**)
Outputs	3-butyl-1-vinylimidazolium bromide	1.79	g	Primary data
	diethyl ether	14.7	g	Primary data
	dichloromethane	3.89	g	Primary data
	1-vinylimidazole	0.38	g	Calculated (**Section 2.1.1**)
	1-bromobutane	0.55	g	Calculated (**Section 2.1.1**)

Primary data = Primary data at laboratorial scale. Mixing (raw materials): [BVim][NTf2] + 1,4-butanediol diacrylate + diphenyl(2,4,6-trimethylbenzoyl)phosphine oxide.

Table S9. Life cycle inventory results for the intermediate substances of the ILs that were not available in Ecoinvent database (all scaled to the production of 1 x FU).

1-vinylimidazole				
	Process Flow	Amount	Unit	Source
Inputs	imidazole	0.81	g	Calculated (see **section 2.1.2**)
	dichloroethane	1.18	g	Calculated (see **section 2.1.2**)
	energy - electricity	1.35	kJ	Calculated (see **section 2.2.2**)
Outputs	1-vinylimidazole	1.11	g	Calculated (see **section 2.1.2**)
	imidazole	8.08×10^{-3}	g	Calculated (see **section 2.1.2**)
	dichloroethane	1.18×10^{-2}	g	Calculated (see **section 2.1.2**)
1-bromobutane				
Inputs	hydrobromic acid	0.83	g	Calculated (see **section 2.1.3**)
	butanol	0.76	g	Calculated (see **section 1.1.2**)
	electricity energy	0.74	kJ	Calculated (see **section 2.2.3**)
Outputs	1-bromobutane	1.26	g	Calculated (see **section 2.1.3**)
	hydrobromic acid	8.28×10^{-2}	g	Calculated (see **section 2.1.3**)
	butanol	7.59×10^{-2}	g	Calculated (see **section 2.1.3**)
	water	0.17	g	Calculated (see **section 2.1.3**)
hydrobromic acid				
Inputs	sulfuric acid	1.18	g	Calculated (see **section 2.1.4**)
	potassium bromide	1.43	g	Calculated (see **section 2.1.4**)
	energy – (provided by combustion of natural gas)	8.45	kJ	Calculated (see **section 2.2.4**)
Outputs	sulfuric acid	1.77	g	Calculated (see **section 2.1.4**)
	potassium bromide	0.22	g	Calculated (see **section 2.1.4**)
	potassium bisulfate	1.39	g	Calculated (see **section 2.1.4**)
	hydrobromic acid	0.83	g	Calculated (see **section 2.1.4**)
potassium bromide				
Inputs	potassium hydroxide	0.81	g	Calculated (see **section 2.1.5**)
	bromine	1.15	g	Calculated (see **section 2.1.5**)
	energy – (provided by combustion of natural gas)	2.46	kJ	Calculated (see **section 2.2.5**)
Outputs	potassium bromate	0.40	g	Calculated (see **section 2.1.5**)
	potassium bromide	1.43	g	Calculated (see **section 2.1.5**)
	water	0.13	g	Calculated (see **section 2.1.5**)

Table S10. Life cycle inventory results for $LiNTf_2$ and the intermediate chemicals that were not available in the Ecoinvent database at the scale of production of 1 xFU. All data in the table below is secondary data from the work of Peterson (Peterson, 2013)

	Process Flow	**Amount**	**Unit**
Inputs	trifluoromethanesulfonyl fluoride	3.54	kg h^{-1}
	lithium nitride	0.41	kg h^{-1}
	water – reaction	1.05	kg h^{-1}
	electricity energy	9.21×10^{-2}	kWh
	water – cooling	9.85×10^{-2}	m^3
Outputs	lithium bis(trifluoromethane)sulfonimide	3.34	kg h^{-1}
	lithium (Li^+)	4.04×10^{-4}	kg h^{-1}
	fluoride (F^-)	1.11×10^{-3}	kg h^{-1}
	lithium fluoride	0.60	kg h^{-1}
Inputs	lithium	0.24	kg h^{-1}
	nitrogen	0.16	kg h^{-1}
	electricity energy	5.19	kWh
	water - cooling	1.08×10^{-3}	m^3
Outputs	lithium nitride	0.41	kg h^{-1}
Inputs	electricity energy	10.00	kWh
	water - cooling	2.42×10^{-4}	m^3
	methanesulfonyl fluoride	2.30	kg h^{-1}
	hydrogen fluoride	1.40	kg h^{-1}
Outputs	trifluoromethanesulfonyl fluoride	3.54	kg h^{-1}
	hydrogen	0.14	kg h^{-1}
Inputs	electricity energy	8.20	kWh
	water - cooling	9.74×10^{-3}	m^3
	methanesulfonyl chloride	4.49	kg h^{-1}
	potassium fluoride	5.64	kg h^{-1}
Outputs	methanesulfonyl fluoride	2.30	kg h^{-1}
	potassium (K^+)	1.37	kg h^{-1}
	water waste	5.66	kg h^{-1}
	methanesulfonyl chloride	1.79	kg h^{-1}
	potassium chloride	0.31	kg h^{-1}
	fluoride (F^-)	0.29	kg h^{-1}
	chloride (Cl^-)	0.68	kg h^{-1}
Inputs	electricity energy	0.12	kWh
	water - cooling	0.50	m^3
	methane	0.63	kg h^{-1}
	sulfuryl chloride	5.29	kg h^{-1}
Outputs	methanesulfonyl chloride	4.49	kg h^{-1}
	hydrogen chloride	1.43	kg h^{-1}

4 Method used to estimate the heat of formation

Values of heat of formation that were not available in the literature were calculated using the multivariate linear regression method by Mehrpooya *et al.*(2007) (**Eq. S6**). The descriptors that were found to be of importance were the number of non-hydrogen atoms (nSK), the sum of conventional bond orders (CBO) (not including hydrogen bonds), the number of oxygen atoms (nO), the number of fluorine atoms (nF), and the number of heavy atoms (nHM).

$$\Delta H_f = 50.17 - 80.52nSK + 53.65CBO - 169.22nO - 174.75nF - 266.58nHM \quad \textbf{(Eq. S6)}$$

In this work, this method was used to estimate the heat of formation of the ionic liquids [BVim][NTf_2], [BVim][Br], [Bmim][NTf_2] and [Bmim][Cl]. The heat of formation for ionic liquids can be estimated from sum of the heats of formation of the cation and the anion, minus the lattice energy of the ionic liquid (Dong *et al.*, 2013). However, in this work the lattice energy was neglected and the heats of formation for ionic liquids were estimated from sum of heats of formation of the cation (*e.g.* $BVim^+$) and the anion (*e.g.* NTf_2^-). The effects of these assumptions were evaluated in the sensitivity analysis.

5 Method used to estimate heat capacity values

Ionic liquid heat capacity values that were not available in the literature were calculated according to the Joback group contribution method reported by Stouffer *et al.* (2008). The Joback group contribution method, widely used to predict the ideal gas heat capacities of molecular compounds, was chosen for investigation as a potential predictive tool for ionic liquids. Ideal gas heat capacities are calculated as a function of temperature, based on the summation of contribution parameters for the functional groups present in the molecular structure of the component, using the following equation below:

$$C_p^o(T) = \left[\sum_k n_k A_{Cpk} - 37.93\right] + \left[\sum_k n_k B_{Cpk} + 0.210\right]T + \left[\sum_k n_k C_{Cpk} - 3.91\times10^{-4}\right]T^2 \left[\sum_k n_k D_{Cpk} + 2.06\times10^{-7}\right]T^3 \quad \textbf{(Eq. S7)}$$

Where ACpk, BCpk, CCpk, and DCpk are group contribution parameters; nk is the number of groups of type k in the molecule; and T is the temperature in K. While ideal gas heat

capacities are important thermodynamic properties in their own right, for ionic liquids, it is much more useful to consider liquid heat capacities at typical processing temperatures. By applying the principle of corresponding states, it is possible to use the ideal gas heat capacity, along with other thermodynamic properties of the component, to estimate the liquid heat capacity, using the following equation bellow:

$$\frac{C_p^r}{R} = \frac{C_p - C_p^0}{R} = 1.586 + \frac{0.49}{1-T_r} + \omega \left[4.2775 + \frac{6.3(1-T_r)^{\frac{1}{8}}}{T_r} + \frac{0.4355}{1-T_r} \right]$$

(**Eq. S8**)

6 Sensitivity Analysis: Effect of reagent recovery in the 3D printing step

The **Table S11** shows the amount of flows changed for this analysis. The flows were estimated by material balance. In **Table S12** is shown the value of electricity energy for mixing and preparation of reagents for each scenario evaluated. The electricity energy flows were estimated considering the proportion of energy consumed for mixing and preparation of 3.42 g of mixed reagent.

Table S11. Flows for each reagent recovery rate (in grams)

	73.8 %	**80%**	**90%**	**100%**
Inputs				
[BVim][NTf_2]	3.039	2.573	1.820	1.067
1,4-butanediol diacrylate	0.349	0.296	0.209	0.123
diphenyl(2,4,6-trimethylbenzoyl)phosphine oxide	0.031	0.026	0.018	0.011
reagent recovered	6.257	6.780	7.628	8.476
Outputs				
3D part (PIL)	1.200	1.200	1.200	1.200
waste (mixing reagents)	2.219	1.691	0.848	0.000
reagent recovery	6.257	6.780	7.628	8.476

Table S12. Electricity energy assumed for mixing and preparation of reagents for each scenario

Reagent recovery rate	**Unit**	**Amount**
73.8 %	kWh	1.04E-02
80 %	kWh	8.78E-03
90 %	kWh	6.21E-03
100 %	kWh	3.64E-03

7 Sensitivity Analysis: Effect of solvent recovery

The **Table S13** show the results of solvent recovery and theoretical energy assumed in the second scenario, S2.

Table S13. Solvent recycled and theoretical energy calculate by heat transport for S1 and S2

Solvents	Scenario	Reference flow (g)	Amount recovered (g)	Input and chemical waste (g)	Q (kJ)	Qcal (kJ)
isopropanol[a]	S1	6.59	6.53	0.07	5.33	22.40
	S2	6.59	0.0	6.59	0.00	0.00
dichloromethane[b]	S1	265.00	262.35	2.65	32.70	137.23
	S2	265.00	0.00	265.00	0.00	0.00
diethyl eter[c]	S1	49.91	44.91	0.49	28.30	118.00
	S2	49.91	0.00	49.91	0.00	0.00
dichloromethane[c]	S1	13.30	13.17	0.13	28.20	118.00
	S2	13.30	0.00	1.33	0.00	0.00

[a] cleaning the 3D part; [b] synthesis of 3-butyl-1-vinylimidazolium bis(trifluoromethane)sulphonimide; [c] synthesis of 3-butyl-1-vinylimidazolium bromide.

Table S14. Additional impacts on the S1

		Additional impact on the S1			
	Unit	ILs syntheses[a]		Cleaning the 3D part	
Abiotic depletion	kg Sb eq.	$+ 2.15 \times 10^{-4}$	+ 27.28%	$+ 1.62 \times 10^{-4}$	+ 20.54%
Acidification	kg SO_2 eq.	$+ 2.34 \times 10^{-4}$	+ 7.47%	$+ 4.01 \times 10^{-5}$	+ 1.28%
Cumulative Energy Demand	MJ	$+ 5.19 \times 10^{-1}$	+ 29.75%	$+ 3.61 \times 10^{-1}$	+ 20.70%
Eutrophication	kg PO_4--- eq.	$+ 2.20 \times 10^{-5}$	+ 41.29%	$+ 2.33 \times 10^{-5}$	+ 43.65%
Freshwater aquatic ecotoxicity	kg 1,4-DB eq.	$+ 7.74 \times 10^{-5}$	+ 6.41%	$+ 3.13 \times 10^{-5}$	+ 2.59%
Global warming 100a	kg CO_2 eq.	$+ 1.25 \times 10^{-1}$	+135.64%	$+ 9.27 \times 10^{-3}$	+ 10.09%
Human toxicity 100a	kg 1,4-DB eq.	$+ 1.90 \times 10^{-2}$	+ 29.39%	$+ 3.98 \times 10^{-4}$	+ 0.62%
Marine aquatic ecotoxicity	kg 1,4-DB eq.	$+ 7.23 \times 10^{-4}$	+ 9.64%	$+ 3.59 \times 10^{-4}$	+ 4.79%
Ozone layer depletion 40a	kg CFC-11 eq.	$+ 2.36 \times 10^{-9}$	+ 12.75%	$+ 1.46 \times 10^{-10}$	+ 0.79%

[a] [BVim][NTf_2] and [BVim][Br]

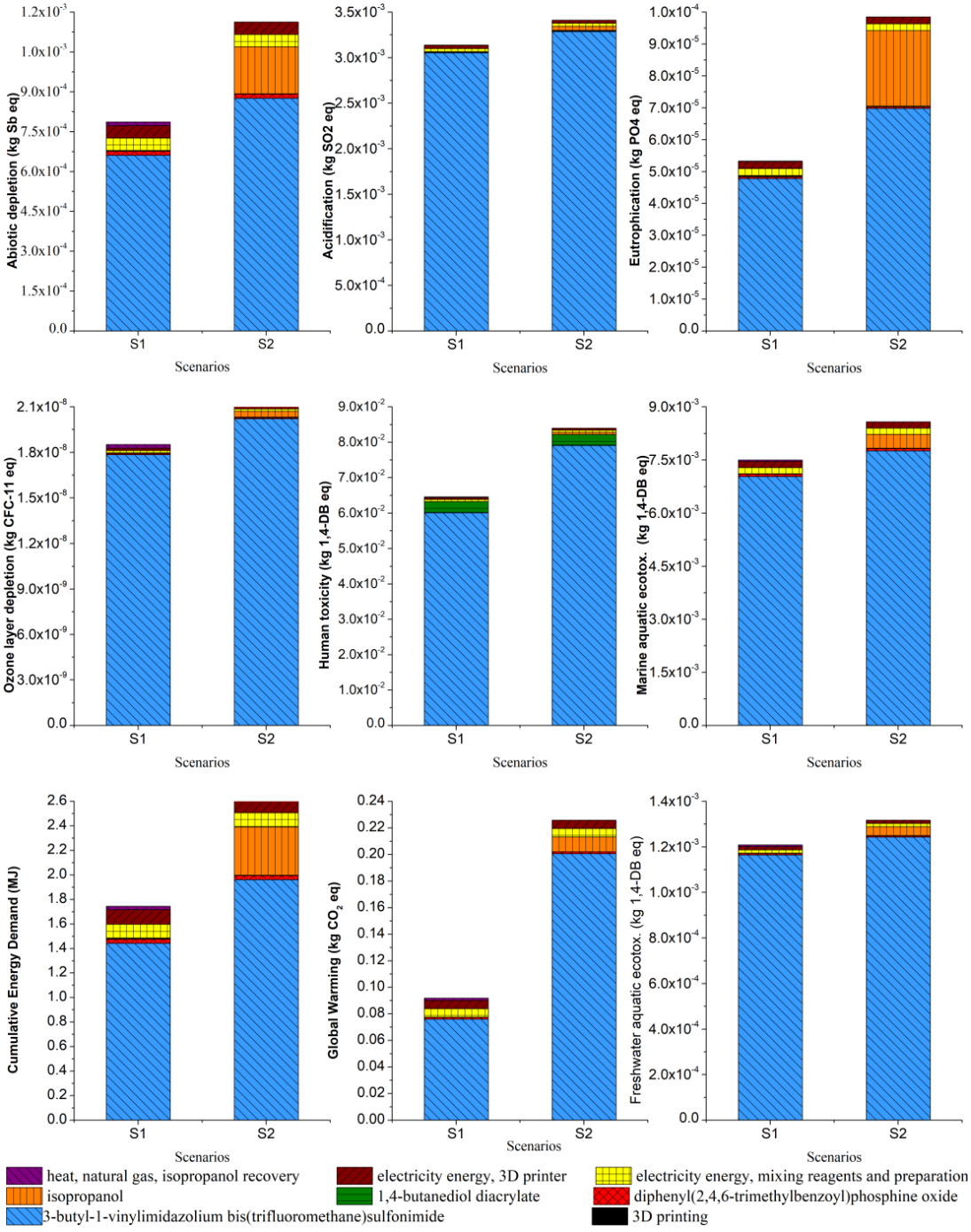

Figure S1. Sensitivity analysis results of scenarios and contribution of inputs; S1: scenario with solvent recovery and S2: scenario without solvent recovery.

8 Comparison between the effect of PIL anion on LCA impact

The effect of changing the anion was estimated using laboratorial scale data and the same parameters used for making PIL printed from [BVim][NTf_2] were considered. Two scenarios have been done to compare the production of PIL with full reagent recovery and partial

recovery (~ 74 %). The inputs and outputs considered for each scenario are show in **Table S15**. However, some chemical substances related to the synthesisof [BVim][$N(CN)_2$] were not available in the Ecoinvent v 3.2 database. Thus, energy and material balances estimation for production of 3-butyl-1-vinylimidazolium dicyanamide, as well as its intermediate substances, were made. The synthesis route of 3-butyl-1-vinylimidazolium dicyanamide is shown in **Figure S2**. The influence of heat of formation and heat capacity parameters, as well as total energy of process calculated for substances for which this data was not readily available, was studied through a sensitivity analysis. The effect of using these data has been considered by varying the impacts of these parameters (arbitrarily) by ± 50%. As it is possible to observe in **Table S23**, the results indicate that the LCA results demonstrated low sensitivity to the degree of variation in the thermodynamic parameters that were evaluated in this work.

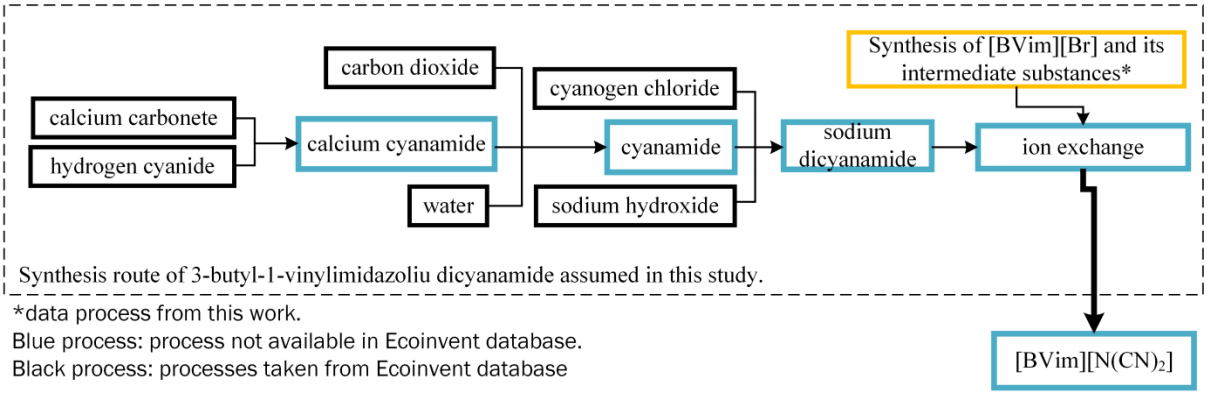

Figure S2. Synthesis route of 3-butyl-1-vinylimidazolium dicyanamide assumed in this study

Table S15. Flows of scenarios for 3D printing of PIL by 3-butyl-1-vinylimidazoliu dicyanamide

	Unit	Scenario 1- (partial recovery)	Scenario 2 - (full recovery)
Inputs			
3-butyl-1-vinylimidazolium dicyanamide	g	1.84	0.96
1,4-butanediol diacrylate	g	0.42	0.21
diphenyl(2,4,6-trimethylbenzoyl)phosphine oxide	g	0.04	0.02
mixing reagent recovered	g	3.11	4.21
solvent (isopropanol)	g	0.66	0.66
electricity energy for mixing reagent	kWh	1.25×10^{-2}	6.51×10^{-3}
electricity energy for printing	kWh	1.07×10^{-2}	1.07×10^{-2}
Outputs			
3D part	g	1.20	1.20
mixing reagent recovery	g	3.11	4.21
waste (raw materials)	g	1.09	0.00
solvent emissions	g	0.66	0.66
solvent recovery	g	5.93	5.93

8.1 Energy and materials balances of 3-butyl-1-vinylimidazolium dicyanamide and its intermediates

This section details the estimation of the energy and material balances for the chemical substances that were not available in either Ecoinvent v 3.2 database, or in previous life cycle studies for production of 3-butyl-1-vinylimidazolium dicyanamide, as well as its intermediate substances.

8.1.1 3-butyl-1-vinylimidazolium dicyanamide

The material balance to production of 217.27 g of sodium 3-butyl-1-vinylimidazolium dicyanamide (217.27 g mol^{-1}, 1 mol) was based on reaction stoichiometry reported by Pedra and Katalin (2011). In this case as the yield is 100 % there was no need to calculate the extent of reaction. Thus, the material balance was calculated from the global stoichiometry of reaction, as follows:

Global stoichiometry of reaction (William, 2010b):

$$NaN(CN)_2 + [BVim][Br] \rightarrow [BVim][N(CN)_2] + NaBr$$

$$NaN(CN)_2 = \frac{1 \text{ mols } NaN(CN)_2}{1 \text{ mols } [BVim][N(CN)_2]} \text{ x } 1 \text{ mol } [BVim][N(CN)_2] = 1 \text{ mol x } 89.03 \text{ g mol}^{-1}$$

$$= 89.03 \text{ g}$$

$$[BVim][Br] = \frac{1 \text{ mols } [BVim][Br]}{1 \text{ mols } [BVim][N(CN)2]} \text{ x } 1 \text{ mol } [BVim][N(CN)2]$$

$$= 1 \text{ mol x } 231.13 \text{ g mol}^{-1} = 231.13 \text{ g}$$

$$[BVmim][N(CN)_2] = \frac{1 \text{ mols}[BVim][N(CN)_2]}{1 \text{ mols } [BVim][N(CN)_2]} \text{ x } 1 \text{ mol } [BVim][N(CN)_2]$$

$$= 1 \text{ mol x } 217.27 \text{ g mol}^{-1} = 217.27 \text{ g}$$

$$NaBr = \frac{1 \text{ mols NaBr}}{1 \text{ mols } [BVim][N(CN)_2]} \text{ x } 1 \text{ mol } [BVim][N(CN)_2] = 1 \text{ mol x } 102.89 \text{ g mol}^{-1}$$

$$= 102.89 \text{ g}$$

The theoretical energy consumption for the synthesis of 217.27 g of 3-butyl-1-vinylimidazolium dicyanamide ($[BVim][N(CN)_2]$) has been estimated based on the heat

requirements of the reactor using **Eqs. S3-S5**. The **Table S16** shows the input and output streams involved in the synthesis of [BVim][$N(CN)_2$].

Table S16. Input and output streams for the production of 3-butyl-1-vinylimidazolium dicyanamide

Substances	**Empirical formula**	**Inputs**		**Outputs**	
		mol	$\hat{H}$	**mol**	$\hat{H}$
sodium dicyanamide	$NaN(CN)_2$	1.00	$\hat{H}_1$	-	-
3-butyl-1-vinylimidazolium bromide	[BVim][Br]	1.00	$\hat{H}_2$	-	-
sodium bromide	NaBr	-	-	1.00	$\hat{H}_3$
3-butyl-1-vinylimidazolium dicyanamide	[BVim][$N(CN)_2$]	-	-	1.00	$\hat{H}_4$

The specific enthalpies $\hat{H}$ for each chemical substance were calculated by Equation S3 as follows:

$$\hat{H}_1 = \Delta Hf^o{}_{(NaN(CN)_2)} + \int_{25}^{25} CpdT = 58.79 \text{ kJ mol}^{-1} + 0 = 58.79 \text{ kJ mol}^{-1}$$

$$\hat{H}_2 = \Delta Hf^o{}_{([BVmim][Br])} + \int_{25}^{25} CpdT = -205.52 \text{ kJ mol}^{-1} + 0 = -205.52 \text{ kJ mol}^{-1}$$

$$\hat{H}_3 = \Delta Hf^o{}_{(NaBr)} + \int_{25}^{25} CpdT = -143.93 \text{ kJ mol}^{-1} + 0 = -143.93 \text{ kJ mol}^{-1}$$

$$\hat{H}_4 = \Delta Hf^o{}_{([BVim][Na(CN)_2])} + \int_{25}^{25} CpdT = 206 \text{ kJ mol}^{-1} + 0 = 206 \text{ kJ mol}^{-1}$$

The enthalpy of reaction was calculated by Equation S4, as follows.

$$\Delta H_r = \left(1 \text{ mol x} - 143.93 \text{ kJ mol}^{-1} + 1 \text{ mol x } 206 \text{ kJ mol}^{-1}\right) - \left(1 \text{ mol x } 58.03 \text{ kJ mol}^{-1} + 1 \text{ mol x} - 205.516 \text{ kJ mol}^{-1}\right) = 208.79 \text{ kJ}$$

Thus, the heat needed to heat the reactor using natural gas is estimated at 876.94 kJ = (4.2 * 208.79 kJ).

8.1.2 Sodium dicyanamide

The material balance to production of 89.03 g of sodium dicyanamide (89.03. g mol^{-1}, 1 mol) was based on the reaction stoichiometry reported by William (2010). In this case as the yield

is 100 % there was no need to calculate the extent of reaction. Thus, the material balance was calculated from the global stoichiometry of reaction, as follows:

Global stoichiometry of reaction (William, 2010b):

$$NH_2CN + 2NaOH + CNCl \rightarrow NaN(CN)_2 + NaCl + 2H_2O$$

$$NH_2CN = \frac{1 \text{ mols } NH_2CN}{1 \text{ mols } NaN(CN)_2} \text{ x } 1 \text{ mol } NaN(CN)_2 = 1 \text{ mol x } 42.04 \text{ g mol}^{-1} = 42.04 \text{ g}$$

$$NaOH = \frac{2 \text{ mols NaOH}}{1 \text{ mols } NaN(CN)_2} \text{ x } 1 \text{ mol } NaN(CN)_2 = 2 \text{ mol x } 39.99 \text{ g mol}^{-1} = 79.99 \text{ g}$$

$$CNCl = \frac{1 \text{ mols CNCl}}{1 \text{ mols } NaN(CN)_2} \text{ x } 1 \text{ mol } NaN(CN)_2 = 1 \text{ mol x } 61.47 \text{ g mol}^{-1} = 61.47 \text{ g}$$

$$NaN(CN)_2 = \frac{1 \text{ mols } NaN(CN)_2}{1 \text{ mols } NaN(CN)_2} \text{ x } 1 \text{ mol } NaN(CN)_2 = 1 \text{ mol x } 89.03 \text{ g mol}^{-1} = 89.03 \text{ g}$$

$$NaCl = \frac{1 \text{ mols NaCl}}{1 \text{ mols } NaN(CN)_2} \text{ x } 1 \text{ mol } NaN(CN)_2 = 1 \text{ mol x } 58.44 \text{ g mol}^{-1} = 58.44 \text{ g}$$

$$H_2O = \frac{2 \text{ mols } H_2O}{1 \text{ mols } NaN(CN)_2} \text{ x } 1 \text{ mol } NaN(CN)_2 = 2 \text{ mol x } 18.01 \text{ g mol}^{-1} = 36.02 \text{ g}$$

The theoretical energy consumption for the synthesis of 89.03 g of sodium dicyanamide has been estimated based on the heat requirements of the reactor using **Eqs. S3-S5**. The **Table S17** shows the input and output streams involved in the synthesis of $NaN(CN)_2$.

Table S17. Input and output streams for the production of sodium dicyanamide

Substances	**Empirical formula**	**Inputs**		**Outputs**	
		mol	$\hat{H}$	**mol**	$\hat{H}$
cyanamide	NH_2CN	1.00	$\hat{H}_1$	-	-
sodium hydroxide	NaOH	2.00	$\hat{H}_2$	-	-
cyanogen chloride	CNCl	1.00	$\hat{H}_3$	-	-
water	H_2O	-	-	2.00	$\hat{H}_4$
sodium chloride	NaCl	-	-	1.00	$\hat{H}_5$
sodium dicyanamide	$NaN(CN)_2$	-	-	1.00	$\hat{H}_6$

The specific enthalpies $\hat{H}$ for each chemical substance were calculated by Equation S3 as follows:

$$\hat{H}_1 = \Delta Hf^{o}_{(NH_2CN)} + \int_{25}^{25} CpdT = 58.79 \text{ kJ mol}^{-1} + 0 = 58.79 \text{ kJ mol}^{-1}$$

$$\widehat{H}_2 = \Delta Hf^{o}{}_{(NaOH)} + \int_{25}^{25} CpdT = -427\ \text{kJ mol}^{-1} + 0 = -427\ \text{kJ mol}^{-1}$$

$$\widehat{H}_3 = \Delta Hf^{o}{}_{(CNCl)} + \int_{25}^{25} CpdT = 137.95\ \text{kJ mol}^{-1} + 0 = 137.95\ \text{kJ mol}^{-1}$$

$$\widehat{H}_4 = \Delta Hf^{o}{}_{([H_2O])} + \int_{25}^{25} CpdT = -292.74\ \text{kJ mol}^{-1} + 0 = -292.74\ \text{kJ mol}^{-1}$$

$$\widehat{H}_5 = \Delta Hf^{o}{}_{(NaCl)} + \int_{25}^{25} CpdT = -411.12\ \text{kJ mol}^{-1} + 0 = -411.12\ \text{kJ mol}^{-1}$$

$$\widehat{H}_6 = \Delta Hf^{o}{}_{(Na(CN)_2)} + \int_{25}^{25} CpdT = 58.79\ \text{kJ mol}^{-1} + 0 = 58.79\ \text{kJ mol}^{-1}$$

The enthalpy of reaction was calculated by Equation S4, as follows.

$$\Delta H_r = \left(1\ \text{mol x} - 292.74\ \text{kJ mol}^{-1} + 1\ \text{mol x} - 411.12\ \text{kJ mol}^{-1} + 1\ \text{mol x } 58.79\ \text{kJ mol}^{-1}\right) - \left(1\ \text{mol x } 58.79\ \text{kJ mol}^{-1} + 1\ \text{mol x} - 427\ \text{kJ mol}^{-1} + 1\ \text{mol x } 137.95\ \text{kJ mol}^{-1}\right) = -280.55\ \text{kJ}$$

Thus, the energy needed to cool the reactor using electricity energy is estimated at 897.76 kJ = (3.2 * |−280.55 kJ|).

8.1.3 Cyanamide

The material balance to production of 42.04 g of cyanamide (42.04. g mol^{-1}, 1 mol) was based on the reaction stoichiometry reported by William (2010). In this case as the yield is 100 % there was no need to calculate the extent of reaction. Thus, the material balance was calculated from the global stoichiometry of reaction, as follows:

Global stoichiometry of reaction (William, 2010b):

$$CaCN_2 + H_2O + CO_2 \rightarrow CaCO_3 + NH_2CN$$

$$CaCN_2 = \frac{1\ \text{mols } CaCN_2}{1\ \text{mols } NH_2CN}\ \text{x } 1\ \text{mol } NH_2CN = 1\ \text{mol x } 80.10\ \text{g mol}^{-1} = 80.10\ \text{g}$$

$$H_2O = \frac{1\ \text{mols } H_2O}{1\ \text{mols } NH_2CN}\ \text{x } 1\ \text{mol } NH_2CN = 1\ \text{mol x } 18.01\ \text{g mol}^{-1} = 18.01\ \text{g}$$

$$CO_2 = \frac{1 \text{ mols } CO_2}{1 \text{ mols } NH_2CN} \text{ x } 1 \text{ mol } NH_2CN = 1 \text{ mol x } 44 \text{ g mol}^{-1} = 44 \text{ g}$$

$$CaCO_3 = \frac{1 \text{ mols } CaCO_3}{1 \text{ mols } NH_2CN} \text{ x } 1 \text{ mol } NH_2CN = 1 \text{ mol x } 100.08 \text{ g mol}^{-1} = 100.08 \text{ g}$$

$$NH_2CN = \frac{1 \text{ mols } NH_2CN}{1 \text{ mols } NH_2CN} \text{ x } 1 \text{ mol } NH_2CN = 1 \text{ mol x } 42.04 \text{ g mol}^{-1} = 42.04 \text{ g}$$

The theoretical energy consumption for the synthesis of 42.04 g of cyanamide has been estimated based on the heat requirements of the reactor using **Eqs. S3-S5**. The **Table S18** shows the input and output streams involved in the synthesis of NH_2CN.

Table S18. Input and output streams for the production of cyanamide

Substances	**Empirical formula**	**Inputs**		**Outputs**	
		mol	$\hat{H}$	**mol**	$\hat{H}$
calcium cyanamide	$CaCN_2$	1.00	$\hat{H}_1$	-	-
water	H_2O	1.00	$\hat{H}_2$	-	-
carbon dioxide	CO_2	1.00	$\hat{H}_3$	-	-
calcium carbonete	$CaCO_3$	-	-	1.00	$\hat{H}_4$
cyanamide	NH_2CN	-	-	1.00	$\hat{H}_5$

The specific enthalpies $\hat{H}$ for each chemical substance were calculated by **Equation S3** as follows:

$$\hat{H}_1 = \Delta Hf^o{}_{(CaCN_2)} + \int_{25}^{25} CpdT = 58.79 \text{ kJ mol}^{-1} + 0 = 58.79 \text{ kJ mol}^{-1}$$

$$\hat{H}_2 = \Delta Hf^o{}_{(H_2O)} + \int_{25}^{25} CpdT = -292.74 \text{ kJ mol}^{-1} + 0 = -292.74 \text{ kJ mol}^{-1}$$

$$\hat{H}_3 = \Delta Hf^o{}_{(CO_2)} + \int_{25}^{25} CpdT = -393.51 \text{ kJ mol}^{-1} + 0 = -393.51 \text{ kJ mol}^{-1}$$

$$\hat{H}_4 = \Delta Hf^o{}_{(CaCO_3)} + \int_{25}^{25} CpdT = -1206.9 \text{ kJ mol}^{-1} + 0 = -1206.9 \text{ kJ mol}^{-1}$$

$$\hat{H}_5 = \Delta Hf^o{}_{(NH_2CN)} + \int_{25}^{25} CpdT = 42.04 \text{ kJ mol}^{-1} + 0 = 58.79 \text{ kJ mol}^{-1}$$

The enthalpy of reaction was calculated by Equation S4, as follows.

$$\Delta H_r = \left(1 \text{ mol x } 58.79 \text{ kJ mol}^{-1} + 1 \text{ mol x} - 1206.9 \text{ kJ mol}^{-1}\right) -$$
$$\left(1 \text{ mol x } 58.79 \text{ kJ mol}^{-1} + 1 \text{ mol x} - 292.74 \text{ kJ mol}^{-1} + 1 \text{ mol x} - 393.509 \text{ kJ mol}^{-1}\right) =$$
$$-520.65 \text{ kJ}$$

Thus, the energy needed to cool the reactor using electrical energy is estimated at 1666.08 kJ = (3.2 * 520.65 kJ).

8.1.4 Calcium cyanamide

The material balance to production of 79.62 g (80.10 g mol^{-1}, 0.99 mol) of calcium cyanamide was based on reaction stoichiometry reported by Bra (Bra, 1963) and the yield is 99.4 %.

Global stoichiometry of reaction: $CaCO_3 + 2HCN \rightarrow CaCN_2 + CO + H_2 + CO_2$

Yield: 79.62 g (99.4 %) (secondary data)

$n_{0\ (CaCO_3)} = 1 \text{ mol} \rightarrow 100.09 \text{ g (secondary data)}$

$n_{0\ (HCN)} = 2 \text{ mol} \rightarrow 54.05 \text{g (secondary data)}$

Limiting reactant/s: calcium carbonate ($CaCO_3$)

First the limiting reagent was determined, as follows:

$$CaCO_3: \ 0.994 \ = \frac{\text{mols reacted}}{1 \text{ mol}}$$

so rearranged for $'\text{mols reacted}' = 0.994 \text{ x } 1 = 0.994 \text{ mol}$

$$HCN: \ 0.994 = \frac{\text{mols reacted}}{2 \text{ mol}}$$

rearranged for $'\text{mols reacted}' = 0.994 \text{ x } 2 \text{ mol} = 1.988 \text{ mol}$

Thus, the limiting reagent is $CaCO_3$ as it is in the smaller molar proportion (Felder and Rousseau, 2005). The extent of reaction was calculated, as follows:

$$\xi_r = 1 \text{ mol} - \frac{(1 \text{ mol} - 0.994 \text{ mol})}{1} = 0.994 \text{ mol}$$

Calculate reaction balance by **Eq. 1** and extent of reaction calculated above:

$n_{(CaCO_3)}$=1 mol + (0.994 mol x -1)=0.006 mol → 0.60 g

$n_{(HCN)}$=2 mol +(0.994 mol x -1)=0. mol → 54.05 g

$n_{(CaCN_2)}$=0 mol + (0.994 mol x 1)=0.994 mol → 79.62 g

$n_{(CO)}$=0 mol + (0.994 mol x 1)=0.994 mol → 27.83 g

$n_{(CO_2)}$=0 mol + (0.994 mol x 1)=0.994 mol → 43.73 g

$n_{(H_2)}$=0 mol + (0.994 mol x 1)=0.994 mol → 1.98 g

The theoretical energy consumption for the synthesis of 42.04 g of calcium cyanamide has been estimated based on the heat requirements of the reactor using **Eqs. S3-S5**. The **Table S19** shows the input and output streams involved in the synthesis of $CaCN_2$.

Table S19. Input and output streams for the production of calcium cyanamide

Substances	**Empirical formula**	**Inputs**		**Outputs**	
		mol	$\hat{H}$	**mol**	$\hat{H}$
calcium carbonete	$CaCO_3$	1.000	$\hat{H}_1$	0.006	$\hat{H}_3$
hydrogen cyanide	HCN	2.000	$\hat{H}_2$	0.012	$\hat{H}_4$
hydrogen	H_2	-	-	0.994	$\hat{H}_5$
carbon dioxide	CO_2	-	-	0.994	$\hat{H}_6$
carbon monoxide	CO	-	-	0.994	$\hat{H}_7$
calcium cyanamide	$CaCN_2$	-	-	0.994	$\hat{H}_8$

The specific enthalpies $\hat{H}$ for each chemical substance were calculated by Equation S3 as follows:

$$\hat{H}_1 = \Delta Hf^o{}_{(CaCO_3)} + \int_{25}^{25} CpdT = -1206.9\ \text{kJ mol}^{-1} + 0 \ = -1206.9\ \text{kJ mol}^{-1}$$

$$\hat{H}_2 = \Delta Hf^o{}_{(HCN)} + \int_{25}^{25} CpdT = 130.50\ \text{kJ mol}^{-1} + 0 = 130.50\ \text{kJ mol}^{-1}$$

$$\hat{H}_3 = \Delta Hf^o{}_{(CaCO_3)} + \int_{25}^{850} CpdT = -1206.9\ \text{kJ mol}^{-1} + (0.08\ \text{kJ mol}^{-1}\ \text{K}^{-1}\ \text{x}\ 825\ \text{K})$$
$$= -1138.01\ \text{kJ mol}^{-1}$$

$$\hat{H}_4 = \Delta Hf^o{}_{(HCN)} + \int_{25}^{850} CpdT = -130.05\ \text{kJ mol}^{-1} + (0.04\ \text{kJ mol}^{-1}\ \text{K}^{-1}\ \text{x}\ 825\ \text{K})$$
$$= 160.11\ \text{kJ mol}^{-1}$$

$$\widehat{H}_5 = \Delta Hf^{o}{}_{(H_2)} + \int_{25}^{850} CpdT = \text{ kJ mol}^{-1} + (0.03 \text{ kJ mol}^{-1} \text{ K}^{-1} \text{ x } 825 \text{ K})$$

$$= 23.79 \text{ kJ mol}^{-1}$$

$$\widehat{H}_6 = \Delta Hf^{o}{}_{(CO_2)} + \int_{25}^{850} CpdT = -393.51 \text{ kJ mol}^{-1} + (0.04 \text{ kJ mol}^{-1} \text{ K}^{-1} \text{ x } 825 \text{ K})$$

$$= -362.87 \text{ kJ mol}^{-1}$$

$$\widehat{H}_7 = \Delta Hf^{o}{}_{(CO)} + \int_{25}^{850} CpdT = -110.53 \text{ kJ mol}^{-1} + (0.03 \text{ kJ mol}^{-1} \text{ K}^{-1} \text{ x } 825 \text{ K})$$

$$= -86.52 \text{ kJ mol}^{-1}$$

$$\widehat{H}_8 = \Delta Hf^{o}{}_{(CaCN_2)} + \int_{25}^{850} CpdT = 58.79 \text{ kJ mol}^{-1} + (0.08 \text{ kJ mol}^{-1} \text{ K}^{-1} \text{ x } 825 \text{ K})$$

$$= 123.31 \text{ kJ mol}^{-1}$$

The enthalpy of reaction was calculated by Equation S4, as follows.

$$\Delta H_r = \left(0.006 \text{ mol x} - 1138.01 \text{ kJ mol}^{-1} + 0.012 \text{ mol x } 160.11 \text{ kJ mol}^{-1} + 0.994 \text{ mol x } 23.79 \text{ kJ mol}^{-1} + 0.994 \text{ mol x } 123.31 \text{ kJ mol}^{-1} + 0.994 \text{ mol x} - 362.87 \text{ kJ mol}^{-1} + 0.994 \text{ mol x} - 86.52 \text{ kJ mol}^{-1}\right) - \left(1 \text{ mol x} - 1206.9 \text{ kJ mol}^{-1} + 2 \text{ mol x} 130.5 \text{ kJ mol}^{-1}\right) = 640.51 \text{ kJ}$$

Thus, the heat needed to heat the reactor using natural gas is estimated at 2690.14 kJ = (4.2 * 640.51 kJ).

9 Comparison between monomer IL and conventional IL

The system boundaries considered for this LCA comparison between [BVim][NTf_2] and [Bmim][NTf_2] are shown in **Figure S3**. The data related to the synthesis of [Bmim][NTf_2] was considered by Dunn *et al.* (2012). According to that author, for the production of 28.0 mmol of [Bmim][NTf_2], 38.8 mmol of [Bmim][Cl] and 41.0 mmol of $LiNTf_2$ were needed and the yield is 72 %. The inventory data of [Bmim][Cl] was determined by Righi *et al.* (2011) and its intermediate substances, which were not available in the Ecoinvent database, were determined by Mehrkesh and Karunanithi (2016) (see **Table S20**).

Table S20. LCI of [Bmim][Cl] and intermediate substances that were not available in the Ecoinvent database

	Flows	**Amount**	**Unit**	**Source**
synthesis of [bmim][Cl]				Righi *et al*.(2011)
Input	n-methylimidazole	0.49	kg	
	1-chlorobutane	0.61	kg	
	heat	1.50	MJ	
	electric energy	0.21	MJ	
Output	[bmim]Cl	1.00	kg	
synthesis of n-methylimidazole				Mehrkesh *et al*.(2016)
Input	glyoxal	0.93	kg	
	methylamine	0.20	kg	
	formaldehyde	0.52	kg	
	ammonia	0.11	kg	
	heat	0.59	MJ	
	electrical energy	0.11	kWh	
Output	n-methylimidazole	0.39	kg	
synthesis of 1-chlorobutane				Righi *et al*.(2011)
Input	butanol	0.50	kg	
	hydrochloric acid	0.25	kg	
	heat	0.27	MJ	
	electric energy	0.08	MJ	
Output	1-chlorobutane	0.61	kg	

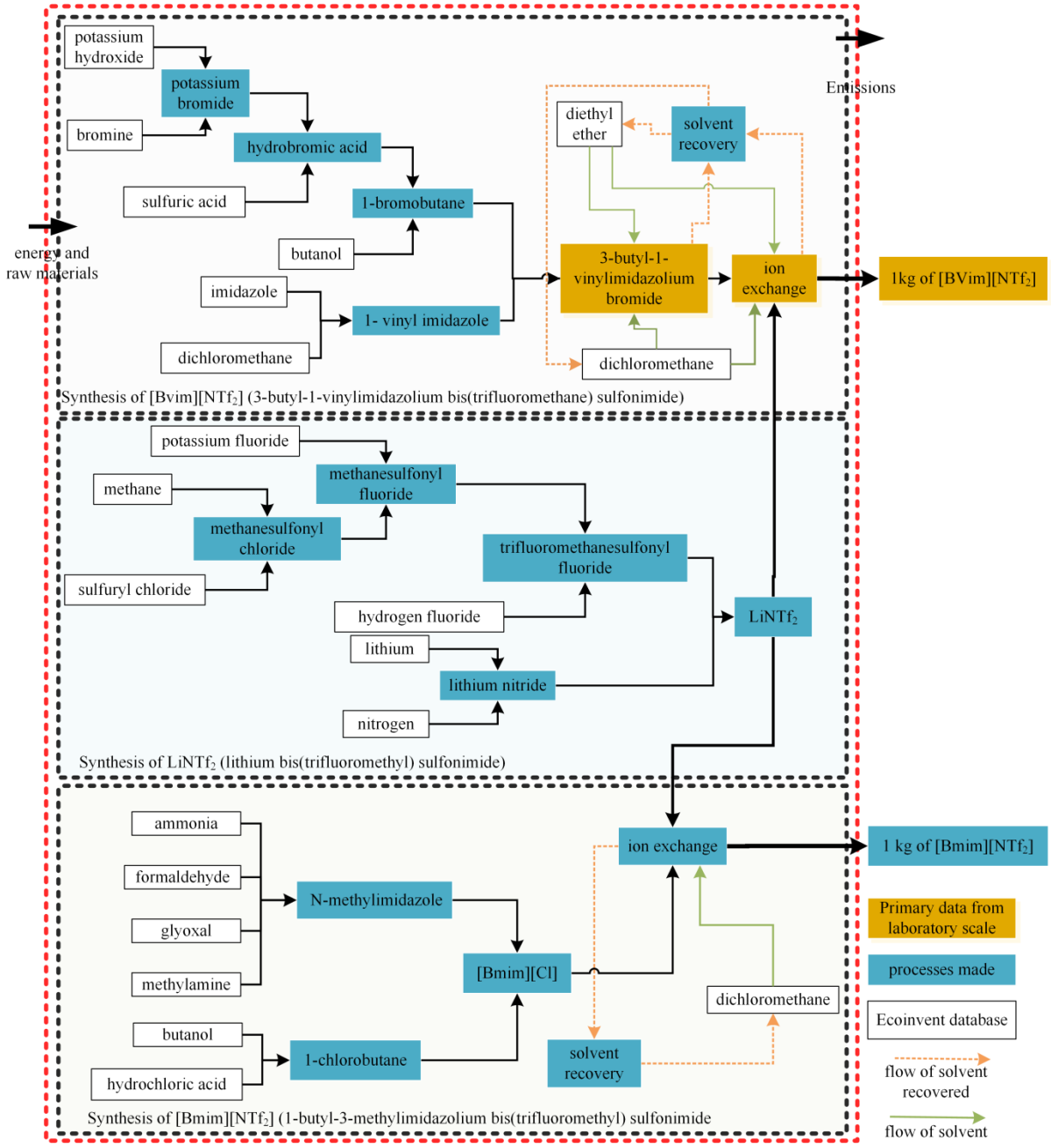

Figure S3. Comparison between the system boundaries for production of the [Bmim][NTf_2] and [BVim][NTf_2]

9.1 1-butyl-3-methylimidazolium bis(trifluoromethane)sulfonimide

This section details the estimation of the quantities of the material and energy balances for 1-butyl-3-methylimidazolium bis(trifluoromethane)sulfonimide ([Bmim][NTf_2]). The data used for these calculations have been listed in **Table S1**.

Reaction initial data by Dunn *et al*. (2012).

Global stoichiometry of reaction: [Bmim][Cl] + $LiNTf_2$ → [Bmim][NTf_2] + LiCl

Yield: 72 %

$n_{0\ ([Bmim][Cl])} = 38.8$ mmol → 6.79 g

$n_{0\ (LiNTf_2)} = 41.0$ mmol → 11.79 g

$n_{([Bmim][NTf_2])} = 28.0$ mmol → 11.77 g

First the limiting reagent was determined, as following:

$$[Bmim][Cl]:\ 0.72 = \frac{\text{mols reacted}}{38.8\ \text{mmol}} = 27.94\ \text{mmol}$$

$$LiNTf_2:\ 0.72 = \frac{\text{mols reacted}}{41.0\ \text{mmol}}$$

$$\text{rearranged for 'mols reacted'} = 0.72 \text{ x } 41.0\ \text{mmol} = 29.5\ \text{mmol}$$

Thus, the limiting reagent is [Bmim][Cl] due it showed less molar proportion (Felder and Rousseau, 2005). Next it the extent of reaction was calculated, as following:

$$\xi_r = 38.8 - \frac{(38.8 - 27.94)}{+1} = 27.94$$

Calculate reaction balance by equation 1 and extent of reaction calculated above:

$n_{([bmim][Cl])} = 38.8 + (27.94 \text{ x } -1) = 10.83$ mmol → 1.89 g

$n_{(LiNTf_2)} = 41.0 + (27.94 \text{ x } -1) = 13.03$ mmol → 3.73 g

$n_{LiCl} = 0 + (27.94 \text{ x } +1) = 27.94$ mmol → 1.19 g

The theoretical energy consumption for the synthesis of 11.74 g of 1-butyl-3-methylimidazolium bis(trifluoromethane)sulfonimide ([Bmim][NTf_2]) has been estimated based on the heat requirements of the reactor using **Eqs. S3-S5**. The **Table S21** shows the input and output streams involved in the synthesis of [Bmim][NTf_2].

Table S21. Input and output streams for the production of 1-butyl-3-methylimidazolium bis(trifluoromethanesulfonyl)imide

Substances	Empirical formula	Inputs		Outputs	
		mol	$\hat{H}$	mol	$\hat{H}$
1-butyl-3-methylimidazolium bis(trifluoromethane)sulfonimide	[Bmim][NTf_2]	-	-	0.03	$\hat{H}_3$
1-butyl-3-methylimidazolium chloride	[Bmim][Cl]	0.04	$\hat{H}_1$	0.01	$\hat{H}_4$
lithium bis(trifluoromethane)sulfonimide	$LiNTf_2$	0.04	$\hat{H}_2$	0.01	$\hat{H}_5$
lithium chloride	LiCl	-	-	0.03	$\hat{H}_6$

The specific enthalpies $\hat{H}$ for each chemical substance were calculated by Equation S3 as follows:

$$\hat{H}_1 = \Delta Hf^o{}_{([bmim][Cl])} + \int_{25}^{25} CpdT = -111.29 \text{ kJ mol}^{-1} + 0 = -111.29 \text{ kJ mol}^{-1}$$

$$\hat{H}_2 = \Delta Hf^o{}_{(LiNTf_2)} + \int_{25}^{25} CpdT = -1147.39 \text{ kJ mol}^{-1} + 0 = -1147.39 \text{ kJ mol}^{-1}$$

$$\hat{H}_3 = \Delta Hf^o{}_{([bmim][Cl])} + \int_{25}^{25} CpdT = -980.18 \text{ kJ mol}^{-1} + 0 = -980.18 \text{ kJ mol}^{-1}$$

$$\hat{H}_4 = \Delta Hf^o{}_{([bmim][Cl])} + \int_{25}^{25} CpdT = -278.49 \text{ kJ mol}^{-1} + 0 = -278.49 \text{ kJ mol}^{-1}$$

$$\hat{H}_5 = \Delta Hf^o{}_{(LiNTf_2)} + \int_{25}^{25} CpdT = -1147.39 \text{ kJ mol}^{-1} + 0 = -1147.39 \text{ kJ mol}^{-1}$$

$$\hat{H}_6 = \Delta Hf^o{}_{(LiCl)} + \int_{25}^{25} CpdT = -408.27 \text{ kJ mol}^{-1} + 0 = -408.27 \text{ kJ mol}^{-1}$$

The enthalpy of reaction was calculated by Equation S4, as follows.

$$\Delta H_r = \left(0.03 \text{ mol x} - 980.18 \text{ kJ mol}^{-1} + 0.011 \text{ mol x} - 278.49 \text{ kJ mol}^{-1} + 0.01 \text{ mol} - 1147.39 \text{ kJ mol}^{-1} + 0.03 \text{ mol x} - 408.27 \text{ kJ mol}^{-1}\right) - \left(0.04 \text{ mol x} - 1147.39 \text{ kJ mol}^{-1} + 0.04 \text{ mol x} - 278.49 \text{ kJ mol}^{-1}\right) = 1.05 \text{ kJ}$$

Thus, the heat needed to heat the reactor using natural gas is estimated at 4.41 kJ = (4.2 * 1.05 kJ).

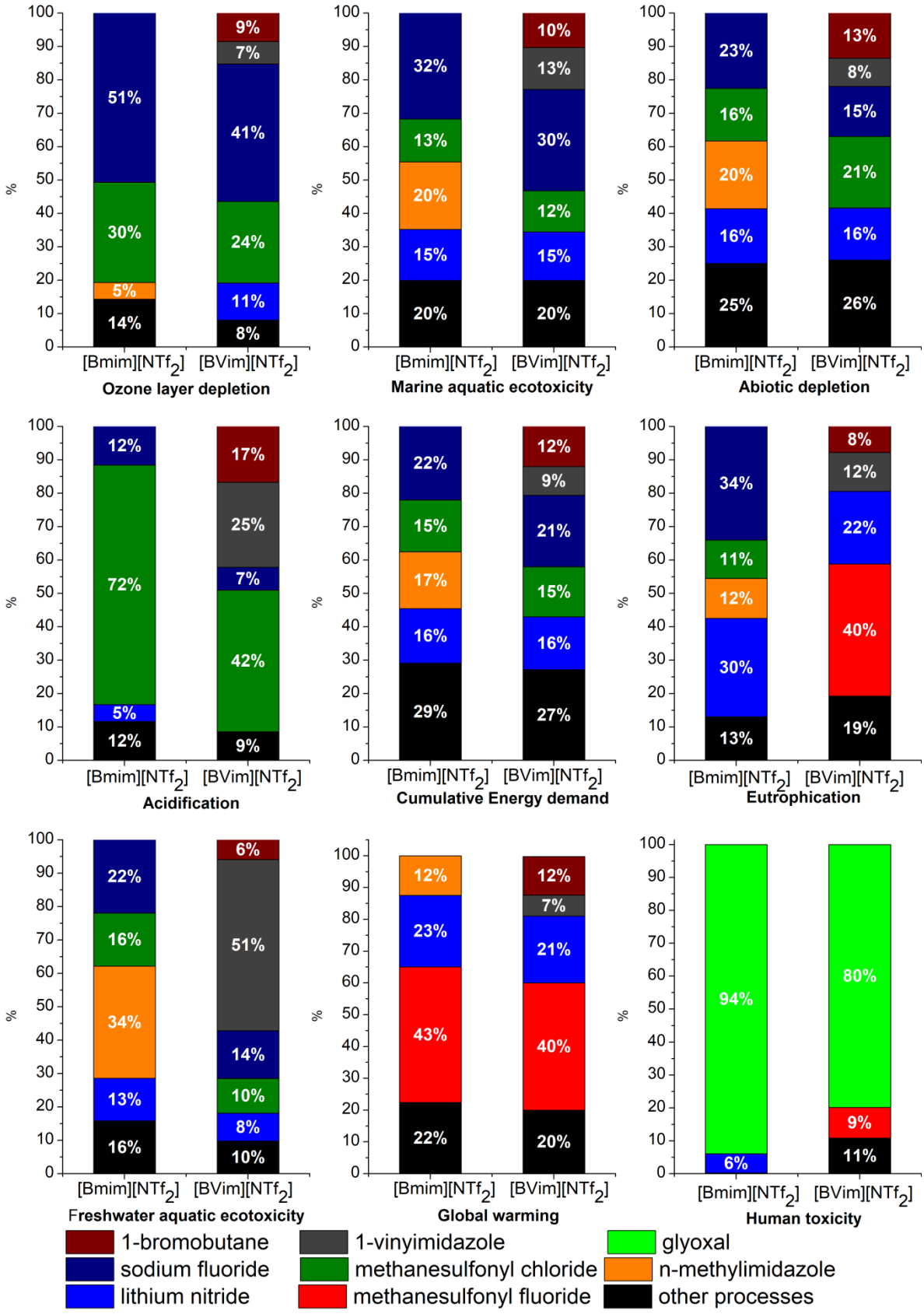

Figure S4.Comparison results of monomer IL versus conventional by contribution analysis

10 Sensitivity Analysis: Effect of thermodynamic parameters calculated results

Table S22 shows the results sensitivity analysis by varying the impacts of thermodynamic parameters calculated (arbitrarily) by ± 50% for PILs made from [BVim][NTf_2].

Table S22. Sensitivity analysis results of the heat formation and heat capacity parameters estimated.

Impact categories	ΔHf				Cp	
	[BVim][NTf_2]	$LiNTf_2$	[BVim][Br]	$C_5H_6N_2$	$C_9H_{15}BrN_2$	$C_5H_6N_2$
Abiotic depletion	1.59 %	0.30 %	0.03 %	0.14 %	0.03 %	0.02 %
Acidification	0.31 %	0.12 %	0.01 %	0.03 %	0.01 %	0.00 %
Eutrophication	1.08 %	0.46 %	0.02 %	0.10 %	0.02 %	0.01 %
Global warming	1.85 %	0.40 %	0.03 %	0.17 %	0.03 %	0.02 %
Ozone layer depletion	0.24 %	0.25 %	0.00 %	0.02 %	0.00 %	0.00 %
Human toxicity	0.25 %	0.04 %	0.00 %	0.02 %	0.00 %	0.00 %
Freshwater aquatic ecotoxicity	1.37 %	0.00 %	0.01 %	0.03 %	0.01 %	0.00 %
Marine aquatic ecotoxicity	0.66 %	0.20 %	0.01 %	0.06 %	0.01 %	0.01 %
Cumulative Energy Demand	1.79 %	0.37 %	0.19 %	0.36 %	0.19 %	0.00 %

ΔHf: heat of formation; Cp: Enthalpy of capacity; [BVim][NTf_2]: 3-butyl-1-vinylimidazolium bis(trifluoromethane)sulfonimide; $LiNTf_2$: lithium bis(trifluoromethane)sulfonimide; [BVim][Br]: 3-butyl-1-vinylimidazolium bromide; $C_5H_6N_2$: 1-vinyl imidazole. Note: the Cp sensibility analysis results of [BVim][NTf_2] and $LiNTf_2$ showed values of 0.00 % being removed from table.

Table S23 shows the results sensitivity analysis by varying the impacts of thermodynamic parameters calculated (arbitrarily) by ± 50% for PILs made from [BVim][$N(CN)_2$].

Table S23. Sensitivity analysis results of the heat formation, heat capacity parameters and total energy of process estimated.

Impact categories	ΔHf + Cp		Total energy of process			
	IL[a]	$NaN(CN)_2$	IL[a]	$NaN(CN)_2$	NH_2CN	$CaCN_2$
Abiotic depletion	0.15 %	1.03 %	0.53 %	1.07 %	1.00 %	2.37 %
Acidification	0.01 %	0.21 %	0.03 %	0.22 %	0.06 %	0.14 %
Eutrophication	0.03 %	0.86 %	0.10 %	0.89 %	0.18 %	0.44 %
Global warming	0.16 %	1.16 %	0.55 %	1.21 %	1.04 %	2.45 %
Ozone layer depletion	0.15 %	0.21 %	0.54 %	0.21 %	1.02 %	2.42 %
Human toxicity	0.01 %	0.09 %	0.05 %	0.09 %	0.09 %	0.21 %
Freshwater aquatic ecotoxicity	0.04 %	0.16%	0.13 %	0.17 %	0.25 %	0.60 %
Marine aquatic ecotoxicity	0.05 %	0.53 %	0.16 %	0.55 %	0.31 %	0.96 %
Cumulative Energy Demand	0.13 %	1.25 %	0.50 %	1.25 %	1.00 %	2.23 %

[a]IL: 3-butyl-1-vinylimidazolium dicyanamide ([BVim][$N(CN)_2$]); $NaN(CN)_2$: sodium dicyanamide; NaH_2CN: cyanamide; $CaCN_2$: calcium cyanamide.

11 References

ATcT (Active Thermochemical Tables), n.d. Thermochemical Tables [WWW Document]. URL https://atct.anl.gov/

Blanchard, A.A., Phelan, J.W., Davis, A.R., 1936. Synthetic Inorganic Chemistry, 5th ed. John Wiley & Sons, Inc., London.

Booth, H.S., 1939. Inorganic Syntheses, Volume I., in: Booth, H.S. (Ed.), Inorganic Syntheses, Volume I Edited. McGraw-Hill Book Company, Inc., New York, pp. 151–157. https://doi.org/10.1002/9780470132326

Bra, G., 1963. Handbook of Inorganic Chemistry. Ferdinard Enke Verlag, London.

Cuéllar-Franca, R.M., García-Gutiérrez, P., Taylor, S.F.R., Hardacre, C., Azapagic, A., 2016. A novel methodology for assessing the environmental sustainability of ionic liquids used for CO2 capture. Faraday Discuss. 192, 283–301. https://doi.org/10.1039/C6FD00054A

Cui, J., Gao, N., Li, J., Wang, C., Wang, H., Zhou, M., Zhang, M., Li, G., 2015. Poly(ionic liquid)-based monodisperse microgels as a unique platform for producing functional materials. J. Mater. Chem. C 3, 623–631. https://doi.org/10.1039/C4TC02487G

DETHERM (Society for Chemical Engineering and Biotechnology), 2018. Thermophysical Property Data [WWW Document]. URL http://detherm.cds.rsc.org/detherm/index.php (accessed 5.11.18).

Ding, J., Shen, J., 2012. Method for preparation of N-vinylimidazole. Chinese Patent CN102382059 (A).

Dong, L.L., He, L., Tao, G.H., Huang, M., Hu, C., 2013. Theoretical enthalpies of formation of [AA]X and [AAE]X type amino acid ionic liquids. J. Chem. Eng. Data 58, 1176–1185. https://doi.org/10.1021/je301285c

Dunn, M.H., Cole, M.L., Harper, J.B., 2012. Effects of an ionic liquid solvent on the synthesis of γ-butyrolactones by conjugate addition using NHC organocatalysts. RSC Adv. 2, 10160. https://doi.org/10.1039/c2ra21889e

Emel'yanenko, V.N., Verevkin, S.P., Heintz, A., 2007. The Gaseous Enthalpy of Formation of the Ionic Liquid 1-Butyl-3-methylimidazolium Dicyanamide from Combustion Calorimetry, Vapor Pressure Measurements, and Ab Initio Calculations. J. Am. Chem. Soc. 129, 3930–3937. https://doi.org/10.1021/ja0679174

Felder, R.M., Rousseau, R.W., 2005. Elementary Principes of Chemical Processes, 3rd ed. John Wiley & Sons, Inc., USA.

Green, D.W., Perry, R.H., 1999. Physical and Chemical Data, in: Green, D.W. (Ed.), Perry's

Chemical Engineer's Handbook. Montreal, pp. 173–174.

Kamm, O., Marvel, C.S., 1921. Alkyl and Alkylene Bromides. Org. Synth. 1, 3. https://doi.org/10.15227/orgsyn.001.0003

Lee, J., Emon, M.O.F., Vatani, M., Choi, J.-W., 2017. Effect of degree of crosslinking and polymerization of 3D printable polymer/ionic liquid composites on performance of stretchable piezoresistive sensors. Smart Mater. Struct. 26, 035–043. https://doi.org/10.1088/1361-665X/aa5c70

Mehrkesh, A., Karunanithi, A.T., 2016. Life-Cycle Perspectives on Aquatic Ecotoxicity of Common Ionic Liquids. Environ. Sci. Technol. 50, 6814–6821. https://doi.org/10.1021/acs.est.5b04721

Mehrkesh, A., Karunanithi, A.T., 2013. Energetic ionic materials: How green are they? A comparative life cycle assessment study. ACS Sustain. Chem. Eng. 1, 448–455. https://doi.org/10.1021/sc3001383

NIST (National Institute of Standards and Technology), 2018. NIST Chemistry WebBook [WWW Document]. NIST Chem. Webb. URL https://webbook.nist.gov/chemistry/ (accessed 5.11.18).

Peterson, J.E., 2013. Ionic Liquid/CO2 Co-Fluid Refrigeration: CO2 Solubility Modeling and Life Cycle Analysis. PhD Thesis, University of Notre Dame.

Petra, C., Katalin, B., 2011. Application of Ionic Liquids in Membrane Separation Processes, in: Kokorin, A. (Ed.), Ionic Liquids: Applications and Perspectives. InTech Europe, Croatia, p. 674. https://doi.org/10.16085/j.issn.1000-6613.2010.11.032

Righi, S., Morfino, A., Galletti, P., Samorì, C., Tugnoli, A., Stramigioli, C., 2011. Comparative cradle-to-gate life cycle assessments of cellulose dissolution with 1-butyl-3-methylimidazolium chloride and N-methyl-morpholine-N-oxide. Green Chem. 13, 367. https://doi.org/10.1039/c0gc00647e

Stouffer, S., Guttman, L., Suchman, E., Lazarsfeld, P.F., Star, S., Clausen, J., 2008. Heat Capacities of Ionic Liquids as a Function of Temperature at 0.1 MPa. Measurement and prediction. J. Chem. Eng. Data 53, 2148–2153. https://doi.org/10.1021/je800335v

Vatani, A., Mehrpooya, M., Gharagheizi, F., 2007. Prediction of standard enthalpy of formation by a QSPR model. Int. J. Mol. Sci. 8, 407–432. https://doi.org/10.3390/i8050407

William, C., 2010a. Cyanamides, in: Kirk-Othmer Encyclopedia of Chemical Technology. American Cancer Society, pp. 1–15. https://doi.org/10.1002/0471238961.0325011416012005.a01.pub3

William, C., 2010b. Cyanamides, in: Kirk-Othmer Encyclopedia of Chemical Technology. Wiley, pp. 1–15. https://doi.org/10.1002/0471238961.0325011416012005.a01.pub3

Wojnarowska, Z., Knapik, J., Jacquemin, J., Berdzinski, S., Strehmel, V., Sangoro, J.R., Paluch, M., 2015. Effect of Pressure on Decoupling of Ionic Conductivity from Segmental Dynamics in Polymerized Ionic Liquids. Macromolecules 48, 8660–8666. https://doi.org/10.1021/acs.macromol.5b02130

Yang, M., Zhao, J.-N., Liu, Q.-S., Sun, L.-X., Yan, P.-F., Tan, Z.-C., Welz-Biermann, U., 2011. Low-temperature heat capacities of 1-alkyl-3-methylimidazolium bis(oxalato)borate ionic liquids and the influence of anion structural characteristics on thermodynamic properties. Phys. Chem. Chem. Phys. 13, 199–206. https://doi.org/10.1039/C0CP01744B

6. CONCLUSÕES

Nesta secção, as conclusões serão divididas em dois blocos, sendo eles: revisão do estado da arte do uso da ACV para avaliar os LIs e Avaliação do Ciclo de Vida dos PILs sintetizados por impressão 3D.

6.1. Capítulo I

Neste trabalho uma revisão sobre o uso da ACV para avaliar o desempenho ambiental de LIs foi realizada com objetivo de fornecer uma visão geral atualizada sobre o tema. O estudo foi conduzido considerando alguns critérios relacionados à metodologia da ACV e buscou nortear a revisão sobre as quatro etapas da metodologia.

Apesar das dificuldades relatadas para condução dos estudos, especialmente devido à lacuna de dados de inventários de ciclo de vida dos LI e seus intermediários, a partir de uma série de suposições e abordagens, a metodologia da avaliação do ciclo de vida vem sendo empregada e apresenta fundamental importância para a compreensão dos reais impactos ambientais dessas substâncias emergentes.

Por outro lado, o uso da ACV não acompanhou o rápido desenvolvimento dessas novas substâncias e apenas uma pequena parcela dos LIs desenvolvidos foram analisados até o momento. A maioria dos estudos de ACV de LI cobriram principalmente o cátion $[Bmim]^+$.

Estudos prévios demostraram que dependendo das questões específicas a serem respondidas pela análise, diferentes abordagens de ciclo de vida (variando de portão-ao-portão, do berço-ao-portão e do berço-ao-túmulo) e métodos de avaliação

de impacto foram aplicados. Todavia, a abordagem do berço-ao-portão foi a mais empregada e o método de avaliação de impacto CML 2001 foi o preferencial. Constatou-se também que algumas práticas são recomendadas na ACV de LI como por exemplo: utilizar uma abordagem que não negligencie as fases do ciclo de vida como a abordagem *life-cycle tree*, considerar a reutilização e reciclagem dos LI e o rendimento das reações que envolvem as sínteses dos LIs e suas substâncias intermediárias.

De forma geral, há uma lista de questões que precisam de mais precisão para a aplicação da ACV para avaliar os processos de LI. Essas questões são; acesso a dados abrangentes e adequados do inventário de ciclo de vida na fase de análise de inventário, e o desenvolvimento e inclusão de fatores de caracterização de impactos de LI na fase subsequente de avaliação de impacto. Além disso, na fase de interpretação recomenda-se, especialmente devido às características emergentes destas substâncias, o uso de métodos para avaliação da qualidade de dados.

Uma limitação comum em todos os estudos avaliados é que os possíveis impactos associados à liberação direta de LIs no meio ambiente não foram considerados. Cabe salientar que as limitações relacionadas aos fatores de impactos não podem justificar a negligência de emissões de LI. Neste sentido, práticas como o uso do rendimento reacional menor que 100 % são recomendadas.

Por fim, esta revisão apresenta uma série de recomendações com objetivo de nortear a condução de futuros estudos de ACV relacionados aos líquidos iônicos.

6.2. Capítulo II

Neste trabalho um estudo de ACV para o processo de impressão 3D de poli (líquidos iônicos) à base de imidazólio por processo baseado em estereolitografia foi conduzido. A construção do ICV foi majoritariamente realizada considerando a abordagem *life-cycle tree*. Além disso, foram considerados dados primários e um rendimento de reação menor que 100 %.

Este estudo demonstra que o processo de fabricação aditiva é tecnicamente viável e não exacerba os impactos ambientais a partir de monômeros de líquidos iônicos. No entanto, excelentes oportunidades para mitigar os impactos do CV dos PILs estão associadas a esta etapa. A recuperação total dos reagentes é crucial, tanto quanto a escolha do ânion para o desempenho ambiental da impressão 3D do PIL. A mudança do ânion NTf_2^- pelo $N(CN)_2^-$, do precursor do PIL, apresentou redução significativa dos impactos em todas as categorias avaliadas no CV do PIL. Neste caso, o ânion $N(CN)_2^-$ apresentou menor impacto que o ânion NTf_2^- para os PILs imidazólicos.

Os resultados da análise de contribuição sugerem que o ânion NTf_2^- teve a maior contribuição para os impactos ambientais no ciclo de vida do PIL estudado principalmente devido a substâncias intermediárias (fluoreto de metanossulfonila e nitreto de lítio) usadas para a síntese de $LiNTf_2$.

Para entender como esses impactos se comparam a um líquido iônico homogêneo análogo, foi feita uma comparação entre o monômero [BVim][NTf_2] e o análogo [Bmim][NTf_2]. Os resultados indicam que a natureza do monômero teve impacto comparável ao LI convencional ([Bmim][NTf_2]). Este resultado sugere que os monômeros de LI são viáveis em termos de impactos ambientais com vantagem adicional, como a sua versatilidade devido às possíveis mudanças na estrutura de dupla ligação.

A análise comparativa do uso de precursores de PIL com um ânion diferente indicou que a mudança de ânion tem influência sobre o desempenho ambiental de PILs.

Este trabalho representa a primeira fase em direção ao estudo quantitativo de dados, que será de grande apoio para a tomada de decisões para os processos de impressão de PILs. Além disso, os resultados deste estudo ajudam a identificar os principais aspectos e impactos ambientais que envolvem a produção dos monômeros de IL, PILs e manufatura aditiva.

7. REFERÊNCIAS BIBLIOGRÁFICAS

ABNT. **NBR ISO 14040: Gestão Ambiental - Avaliação do ciclo de vida - Princípios e estrutura**. Rio de Janeiro: [s.n.].

ABNT. **NBR ISO 14044. Gestão Ambiental – Avaliação do ciclo de vida – Requisitos e orientações**. Rio de Janeiro, Brazil: [s.n.].

ALVIZ, P. L. A.; ALVAREZ, A. J. Comparative life cycle assessment of the use of an ionic liquid ([Bmim]Br) versus a volatile organic solvent in the production of acetylsalicylic acid. **Journal of Cleaner Production**, v. 168, p. 1614–1624, 2017.

ANDRZEJEWSKA, E. Photoinitiated polymerization in ionic liquids and its application. **Polymer International**, v. 66, n. 3, p. 366–381, 2017.

AYALNEH TIRUYE, G. et al. All-solid state supercapacitors operating at 3.5 V by using ionic liquid based polymer electrolytes. **Journal of Power Sources**, v. 279, p. 472–480, 1 abr. 2015.

BARROS, S.; ZWOLINSKI, P.; MANSUR, A. I. **Where do the environmental impacts of Additive Manufacturing come from? Case study of the use of 3d-printing to print orthotic insoles**. 12ème Congrès International de Génie Industriel (CIGI 2017). **Anais**...Compiegne: 2017Disponível em: <http://cigi2017.utc.fr>

BAUMERS, M. et al. Charting the Environmental Dimensions of Additive Manufacturing and 3D Printing. **Journal of Industrial Ecology**, v. 21, p. 9–14, 2017.

BIKAS, H.; STAVROPOULOS, P.; CHRYSSOLOURIS, G. Additive manufacturing methods and modeling approaches: A critical review. **International Journal of Advanced Manufacturing Technology**, v. 83, n. 1–4, p. 389–405, 2016.

BURGUETE, M. I. et al. Pd catalysts immobilized onto gel-supported ionic liquid-like phases (g-SILLPs): A remarkable effect of the nature of the support. **Journal of Catalysis**, v. 269, n. 1, p. 150–160, 1 jan. 2010.

CERDAS, F. et al. Life Cycle Assessment of 3D Printed Products in a Distributed Manufacturing System. **Journal of Industrial Ecology**, v. 21, n. S1, p. S80–S93, 2017.

CUÉLLAR-FRANCA, R. M. et al. A novel methodology for assessing the environmental sustainability of ionic liquids used for CO2 capture. **Faraday Discussions**, v. 192, p. 283–301, 2016.

CVJETKO BUBALO, M. et al. A brief overview of the potential environmental hazards of ionic liquids. **Ecotoxicology and Environmental Safety**, v. 99, n. November, p. 1–12, 2014.

DE BRUIJN, H.; DUIN, R. VAN; HUIJBREGTS, M. A. J. **Handbook on Life Cycle Assessment**. USA: Kluwer Academic Publishers, 2002. v. 7

DISASA IRGE, D. Ionic Liquids: A Review on Greener Chemistry Applications, Quality Ionic

Liquid Synthesis and Economical Viability in a Chemical Processes. **American Journal of Physical Chemistry**, v. 5, n. 3, p. 74, 2016.

DUFLOU, J. R. et al. Towards energy and resource efficient manufacturing: A processes and systems approach. **CIRP Annals - Manufacturing Technology**, v. 61, n. 2, p. 587–609, 2012.

DUPONT, J. et al. Transition-metal nanoparticles in imidazolium ionic liquids: recyclable catalysts for biphasic hydrogenation reactions. **Journal of the American Chemical Society**, v. 124, n. 16, p. 4228–4229, 2002.

DUPONT, J. From Molten Salts to Ionic Liquids: A " Nano " Journey. **Accounts of chemical research**, v. 44, p. 1223–1231, 2011.

EMEL'YANENKO, V. N.; VEREVKIN, S. P.; HEINTZ, A. The Gaseous Enthalpy of Formation of the Ionic Liquid 1-Butyl-3-methylimidazolium Dicyanamide from Combustion Calorimetry, Vapor Pressure Measurements, and Ab Initio Calculations. **J. Am. Chem. Soc.**, v. 129, n. 8, p. 3930–3937, 2007.

FARAHIPOUR, R.; KARUNANITHI, A. Life Cycle Environmental Implications of CO2 Capture and Sequestration with Ionic Liquid 1-butyl-3-methylimidazolium acetate. **ACS Sustainable Chemistry & Engineering**, v. 2, p. 2495–2500, 2014.

FORD, S.; DESPEISSE, M. Additive manufacturing and sustainability: an exploratory study of the advantages and challenges. **Journal of Cleaner Production**, v. 137, p. 1573–1587, 2016.

GEBLER, M.; SCHOOT UITERKAMP, A. J. M.; VISSER, C. A global sustainability perspective on 3D printing technologies. **Energy Policy**, v. 74, n. C, p. 158–167, 2014.

GHANDI, K. A Review of Ionic Liquids , Their Limits and Applications. **Green and Sustainable Chemistry**, v. 4, n. February, p. 44–53, 2014.

HAGIWARA, R.; LEE, J. S. Ionic Liquids for Electrochemical Devices. **Electrochemistry**, v. 75, n. 1, p. 23–34, 5 jan. 2007.

HECKENBACH, M. E. et al. Meta-analysis of ionic liquid literature and toxicology. **Chemosphere**, v. 150, p. 266–274, 2016.

HISCHIER, R.; WALSER, T. Life cycle assessment of engineered nanomaterials: State of the art and strategies to overcome existing gaps. **Science of the Total Environment**, v. 425, p. 271–282, 2012.

HUANG, R. et al. Environmental and Economic Implications of Distributed Additive Manufacturing The Case of Injection Mold Tooling. v. 00, n. 0, 2017.

HUANG, S. H. et al. Additive manufacturing and its societal impact: A literature review. **International Journal of Advanced Manufacturing Technology**, v. 67, n. 5–8, p. 1191–1203, 2013.

JACQUEMIN, L.; PONTALIER, P.-Y.; SABLAYROLLES, C. Life cycle assessment (LCA) applied to the process industry: a review. **International Journal of Life Cycle Assessment**, v. 17, p. 1028–1041, 2012.

KARJALAINEN, E. et al. Tunable Ionic Control of Polymeric Films for Inkjet Based 3D Printing. **ACS Sustainable Chemistry & Engineering**, v. 6, n. 3, p. 3984–3991, 9 fev. 2018.

KELLENS, K. et al. Environmental Impact of Additive Manufacturing Processes: Does AM Contribute to a More Sustainable Way of Part Manufacturing? **Procedia CIRP**, v. 61, n. Section 3, p.

582–587, 2017.

KIM, T. et al. Synthesis of Phase Transferable Graphene Sheets Using Ionic Liquid Polymers. **ACS Nano**, v. 4, n. 3, p. 1612–1648, 2010.

KRALISCH, D. et al. Energetic, environmental and economic balances: Spice up your ionic liquid research efficiency. **Green Chemistry**, v. 7, n. 5, p. 301–309, 2005.

KREIGER, M.; PEARCE, J. M. Environmental life cycle analysis of distributed three-dimensional printing and conventional manufacturing of polymer products. **ACS Sustainable Chemistry and Engineering**, v. 1, n. 12, p. 1511–1519, 2013.

LEI, Z. et al. Introduction: Ionic Liquids. **Chemical Reviews**, v. 117, n. 10, p. 6633–6635, 2017.

LU, J.; YAN, F.; TEXTER, J. Advanced applications of ionic liquids in polymer science. **Progress in Polymer Science**, v. 34, n. 5, p. 431–448, 2009.

MA, J. et al. An Exploratory Investigation of Additively Manufactured Product Life Cycle Sustainability Assessment. **Journal of Cleaner Production**, v. 192, p. 55–70, 2018.

MAMI, F. et al. Evaluating Eco-Efficiency of 3D Printing in the Aeronautic Industry. **Journal of Industrial Ecology**, v. 21, 2017.

MAO, H. et al. Preparation of poly(ionic liquids)-functionalized polypyrrole nanotubes and their electrocatalytic application to simultaneously determine dopamine and ascorbic acid. **Journal of Materials Chemistry B**, v. 3, p. 5310–5317, 2015.

MECERREYES, D. Polymeric ionic liquids: Broadening the properties and applications of polyelectrolytes. **Progress in Polymer Science (Oxford)**, v. 36, n. 12, p. 1629–1648, 2011.

MEHRKESH, A.; KARUNANITHI, A. T. Life-Cycle Perspectives on Aquatic Ecotoxicity of Common Ionic Liquids. **Environmental Science and Technology**, v. 50, n. 13, p. 6814–6821, 2016a.

MEHRKESH, A.; KARUNANITHI, A. T. Life-Cycle Perspectives on Aquatic Ecotoxicity of Common Ionic Liquids. p. 1–12, 2016b.

MEHRKESH, A.; KARUNANITHI, A. T. Life Cycle Perspectives on Human Health Impacts of Ionic Liquids. **bioRxiv**, p. 091454–091466, 2016c.

MONTOLIO, S. et al. AuNP − Polymeric Ionic Liquid Composite Multicatalytic Nanoreactors for One-Pot Cascade Reactions. 2016.

NGO, T. D. et al. Additive manufacturing (3D printing): A review of materials, methods, applications and challenges. **Composites Part B: Engineering**, v. 143, n. December 2017, p. 172–196, 2018.

ODIAN, G. **Principles of Polymerization**. 4th. ed. Hoboken, NJ, USA: John Wiley & Sons, Inc., 2004.

PETERSON, J. E. **Ionic Liquid/CO2 Co-Fluid Refrigeration: CO2 Solubility Modeling and Life Cycle Analysis**. [s.l.] PhD Thesis, University of Notre Dame, 2013.

PHAM, T. P. T.; CHO, C.-W.; YUN, Y.-S. Environmental fate and toxicity of ionic liquids: A review. **Water Research**, v. 44, n. 2, p. 352–372, 2010.

PLECHKOVA, N. V; SEDDON, K. R. Applications of ionic liquids in the chemical industry. **Chemical Society reviews**, v. 37, p. 123–150, 2008.

QIAN, W.; TEXTER, J.; YAN, F. Frontiers in poly(ionic liquid)s: syntheses and applications. **Chem. Soc. Rev.**, v. 46, n. 4, p. 1124–1159, 2017.

RADOŠEVIĆ, K. et al. In vitro cytotoxicity assessment of imidazolium ionic liquids: Biological effects in fish Channel Catfish Ovary (CCO) cell line. **Ecotoxicology and Environmental Safety**, v. 92, p. 112–118, 2013.

RIDUAN, S. N.; ZHANG, Y. Imidazolium salts and their polymeric materials for biological applications. **Chemical Society Reviews**, v. 42, n. 23, p. 9055, 4 nov. 2013.

RIGHI, S. et al. Comparative cradle-to-gate life cycle assessments of cellulose dissolution with 1-butyl-3-methylimidazolium chloride and N-methyl-morpholine-N-oxide. **Green Chemistry**, v. 13, n. 2, p. 367–375, 2011.

SADEGHPOUR, M.; YUSOFF, R.; AROUA, M. K. Polymeric ionic liquids (PILs) for CO2 capture. **Reviews in Chemical Engineering**, v. 33, n. 2, p. 183–200, 2017.

SANS, V. et al. Polymer-supported ionic-liquid-like phases (SILLPs): Transferring ionic liquid properties to polymeric matrices. **Chemistry - A European Journal**, v. 17, n. 6, p. 1894–1906, 7 fev. 2011.

SCHULTZ, A. R. et al. 3D Printing Phosphonium Ionic Liquid Networks with Mask Projection Microstereolithography. **ACS Macro Letters**, v. 3, n. 11, p. 1205–1209, 2014a.

SCHULTZ, A. R. et al. 3D Printing Phosphonium Ionic Liquid Networks with Mask Projection Microstereolithography. **ACS Macro Letters**, v. 3, n. 11, p. 1205–1209, 18 nov. 2014b.

SHAPLOV, A. S.; PONKRATOV, D. O.; VYGODSKII, Y. S. Poly(ionic liquid)s: Synthesis, properties, and application. **Polymer Science Series B**, v. 58, n. 2, p. 73–142, 2016.

SINGH, S.; RAMAKRISHNA, S.; SINGH, R. Material issues in additive manufacturing: A review. **Journal of Manufacturing Processes**, v. 25, p. 185–200, 2017.

SREENIVASAN, R.; GOEL, A.; BOURELL, D. L. Sustainability issues in laser-based additive manufacturing. **Physics Procedia**, v. 5, n. PART 1, p. 81–90, 2010.

TOKUDA, M. et al. Preparation of Polymer Particles Containing Reduced Graphene Oxide Nanosheets Using Ionic Liquid Monomer. 2016.

TORRALBA-CALLEJA, E.; SKINNER, J.; GUTIÉRREZ-TAUSTE, D. CO2 Capture in Ionic Liquids: A Review of Solubilities and Experimental Methods. **Journal of Chemistry**, v. 473584, n. 16, p. 1–15, 2013.

UNEP/SETAC. **Towards a Life Cycle Sustainability Assessment:Making informed choices on products**. [s.l: s.n.].

WALES, D. J. et al. 3D-Printable Photochromic Molecular Materials for Reversible Information Storage. **Advanced Materials**, v. 30, n. 26, p. 1800159, abr. 2018.

WANG, X. et al. 3D printing of polymer matrix composites: A review and prospective. **Composites Part B: Engineering**, v. 110, p. 442–458, 2017.

WASSERSCHEID, P.; WELTON, T. **Ionic liquids in Synthesis**. 1. ed. London: Wiley-VCH, 2008. v. 2

WELLS, A. S.; COOMBE, V. T. On the freshwater ecotoxicity and biodegradation properties of some common ionic liquids. **Organic Process Research and Development**, v. 10, n. 4, p. 794–798,

2006.

WELTON, T. Room-Temperature Ionic Liquids. Solvents for Synthesis and Catalysis - Chemical Reviews (ACS Publications). **Chemical Reviews**, v. 99, n. 1, p. 2071–2083, 1999.

WITTBRODT, B. T. et al. Life-cycle economic analysis of distributed manufacturing with open-source 3-D printers. **Mechatronics**, v. 23, n. 6, p. 713–726, 2013.

YAN, F. et al. Enhanced Proton Conduction in Polymer Electrolyte Membranes as Synthesized by Polymerization of Protic Ionic Liquid-Based Microemulsions. **Chemistry of Materials**, v. 21, n. 8, p. 1480–1484, 28 abr. 2009.

YANG, Y. et al. Energy Consumption Modeling of Stereolithography-Based Additive Manufacturing Toward Environmental Sustainability. **Journal of Industrial Ecology**, v. 21, p. S168–S178, 2017.

YUAN, J.; MECERREYES, D.; ANTONIETTI, M. Poly(ionic liquid)s: An update. **Progress in Polymer Science**, v. 38, n. 7, p. 1009–1036, 2013.

ZHANG, Y.; BAKSHI, B. R.; DEMESSIE, E. S. Life cycle assessment of an ionic liquid versus molecular solvents and their applications. **Environmental Science and Technology**, v. 42, n. 5, p. 1724–1730, 2008.

ZHAO, J. et al. Solvent-free ionic liquid/poly(ionic liquid) electrolytes for quasi-solid-state dye-sensitized solar cells. **Journal of Materials Chemistry**, v. 21, n. 20, p. 7326, 3 maio 2011.

ZHAO, Y. et al. Toxicity of ionic liquids: Database and prediction via quantitative structure-activity relationship method. **Journal of Hazardous Materials**, v. 278, 2014.

ZHENG, D. et al. **A review of imidazolium ionic liquids research and development towards working pair of absorption cycleRenewable and Sustainable Energy Reviews**, 2014.

ZHU, S. et al. A Mini-Review on Greenness of Ionic Liquids. **Chemical and Biochemical Engineering Quarterly**, v. 23, n. 2, p. 207–211, 2009.

APÊNDICE A – DADOS DA MODELAGEM

Na Tabela 1 são apresentados os dados relacionados à modelagem utilizada no software SimaPro®. Na Tabela 2 a 13 são apresentados os processos modelados, as fontes das bases de dados utilizadas e uma breve descrição.

Tabela 1. Dados da modelagem realizada no software SimaPro®

Dados	**Informações**
Software	SimaPro versão *faculty* 8.4.0.0
Projeto	Ionic Liquids V2
Category type	Material
Process identifier	FacPUCRS000039814400094
Database	ecoinvent v 3.2
Data e Hora:	24/03/2018, 19:13

Tabela 2. Base de dados utilizada para modelagem do Poli(líquido iônico) impresso (continua)

Produtos	**Fonte da base de dados**	**Descrição**
3D part - reagent recovery ~74 percent and 99 % of solvent recovery	Este trabalho	Poli(líquido iônico) impresso
Mix (Raw materials, recycle)	Este trabalho	Reagentes em refluxo
Materiais/combustíveis	**Fonte da base de dados**	**Descrição**
3-butyl-1-vinylimidazolium bis(trifluoromethane)sulfonimide - 99 % of solvent recovery	Este trabalho	líquido iônico
1,4-Butanediol diacrylate	ecoinvent database	reagente
diphenyl(2,4,6-trimethylbenzoyl)phosphine oxide	ecoinvent database	reagente
Isopropanol {GLO}| market for | Alloc Def, U	ecoinvent database	solvente
Mix (Raw materials, recycle)	Este trabalho	refluxo de reagente
Eletricidade/calor	**Fonte da base de dados**	**Descrição**
Electricity, medium voltage {GB}| market for | Alloc Def, U LAB – mix	Adaptado de ecoinvent database	Energia consumida em kWh para mistura dos reagentes
Electricity, medium voltage {GB}| market for | Alloc Def, U LAB - 3D printing	Adaptado de ecoinvent database	Energia consumida em kWh pela impressora 3D
Heat, central or small-scale, natural gas {GLO}| market group for | Alloc Def, U	Adaptado de ecoinvent database	Energia consumida em kWh para recuperação do solvente Isopropanol
Emissões para o ar	**Fonte da base de dados**	**Descrição**
2-Propanol	n.a.	Emissão indoor

Tabela 2. Base de dados utilizada para modelagem do Poli(líquido iônico) impresso (conclusão)

Fluxos finais de resíduos	**Fonte da base de dados**	**Descrição**
Chemical waste, regulated	n.a.	substâncias química (reagentes e produtos) descartados durante o processo

n.a.: não aplicável.

Tabela 3. Base de dados utilizada para modelagem do 3-butyl-1-vinylimidazolium bis(trifluoromethane)sulfonimide

Produtos	**Fonte da base de dados**	**Descrição**
3-butyl-1-vinylimidazolium bis(trifluoromethane)sulfonimide - 99 % of solvent recovery	Este trabalho	líquido iônico
Materiais/combustíveis	**Fonte da base de dados**	**Descrição**
3-butyl-1-vinylimidazolium bromide - 99% solvent recovery	Este trabalho	líquido iônico
bis(trifluoromethane)sulfonimide lithium salt	Este trabalho	líquido iônico
Dichloromethane {GLO}| market for | Alloc Def, U	ecoinvent database	Solvente
Magnesium sulfate {GLO}| market for | Alloc Def, U	ecoinvent database	Sal utilizado como secante
Eletricidade/calor	**Fonte da base de dados**	**Descrição**
Heat, central or small-scale, natural gas {GLO}| market group for | Alloc Def, U	Adaptado de ecoinvent database	Energia consumida em kWh para recuperação do solvente
Heat, central or small-scale, natural gas {GLO}| market group for | Alloc Def, U	Adaptado de ecoinvent database	Energia consumida em kWh para sínteses
Emissions para o ar	**Fonte da base de dados**	**Descrição**
Methane, dichloro-, HCC-30	n.a.	Emissão indoor
Emissions para água	**Fonte da base de dados**	**Descrição**
Organic compounds (unspecified)	n.a.	emissões de organicos que não reagiram
Bromide	n.a.	Emissões relacionadas aos saís de bromo decorrentes da reação
Lithium	n.a.	Emissões relacionadas aos saís de lítio decorrentes da reação
Magnesium compounds, unspecified	n.a.	Emissões relacionadas ao sal secante

n.a.: não aplicável.

Tabela 4. Base de dados utilizada para modelagem do 3-butyl-1-vinylimidazolium bromide

Produtos	Fonte da base de dados	Descrição
3-butyl-1-vinylimidazolium bromide - 99% solvent recovery	Este trabalho	líquido iônico
Materiais/combustíveis	Fonte da base de dados	Descrição
n-vinyimidazole	Este trabalho	reagente

Tabela 4. Base de dados utilizada para modelagem do 3-butyl-1-vinylimidazolium bromide (conclusão)

1-bromobutane	Este trabalho	reagente
Diethyl ether, without water, in 99.95% solution state {GLO}| market for | Alloc Def, U	ecoinvent database	Solvente
Dichloromethane {GLO}| market for | Alloc Def, U	ecoinvent database	Solvente
Eletricidade/calor	Fonte da base de dados	Descrição
Electricity, medium voltage {GB}| market for | Alloc Def, U LAB	Adaptado de ecoinvent database	Energia consumida em kWh para síntese
Heat, central or small-scale, natural gas {GLO}| market group for | Alloc Def, U	Adaptado de ecoinvent database	Energia consumida em kWh para recuperação do solvente
Emissions para o ar	Fonte da base de dados	Descrição
Diethyl ether	n.a.	Emissão indoor
Methane, dichloro-, HCC-30	n.a.	Emissão indoor
Fluxo finais de resíduos	Fonte da base de dados	
Chemical waste, regulated	n.a.	substâncias química descartadas

Tabela 5. Base de dados utilizada para modelagem do n-vinyimidazole

Produtos	**Fonte da base de dados**	**Descrição**
n-vinyimidazole	Este trabalho	reagente
Materiais/combustíveis	**Fonte da base de dados**	**Descrição**
Imidazole {GLO}| market for | Alloc Def, U	ecoinvent database	reagente
Ethylene dichloride {GLO}| market for | Alloc Def, U	ecoinvent database	reagente
Eletricidade/calor	**Fonte da base de dados**	**Descrição**
Electricity, medium voltage {GB}| market for | Alloc Def, U LAB	Adaptado de ecoinvent database	Energia consumida em kWh para síntese
Emissions para o ar	Fonte da base de dados	Descrição
Ethane, 1,2-dichloro-	n.a.	Emissão indoor
Imidazole	n.a.	Emissão indoor
Emissions para a água	**Fonte da base de dados**	**Descrição**
Hydrogen chloride	n.a.	substâncias química (reagentes e produtos) descartados

n.a.: não aplicável.

Tabela 6. Base de dados utilizada para modelagem do 1-bromobutane

Produtos	**Fonte da base de dados**	**Descrição**
1-bromobutane	Este trabalho	reagente
Materiais/combustíveis	**Fonte da base de dados**	**Descrição**
1-butanol {GLO}| market for | Alloc Def, U	ecoinvent database	reagente
hydrobromic acid	Este trabalho	reagente
Eletricidade/calor	**Fonte da base de dados**	**Descrição**
Electricity, medium voltage {GB}| market for | Alloc Def, U LAB	ecoinvent database	Energia consumida em kWh para síntese
Emissões para o ar	**Fonte da base de dados**	**Descrição**
1-Butanol	n.a.	Emissão indoor
Hydrogen bromide	n.a.	Emissão indoor
Emissões para água	**Fonte da base de dados**	**Descrição**
Waste water	n.a.	Resíduo

n.a.: não aplicável.

Tabela 7. Base de dados utilizada para modelagem do hydrobromic acid

Produtos	**Fonte da base de dados**	**Descrição**
hydrobromic acid	Este trabalho	Descrição
Materiais/combustíveis	**Fonte da base de dados**	**Descrição**
Potassium Bromide	ecoinvent database	Descrição
Sulfuric acid {GLO}| market for | Alloc Def, U	ecoinvent database	Descrição
Eletricidade/calor	**Fonte da base de dados**	**Descrição**
Electricity, medium voltage {GB}| market for | Alloc Def, U LAB	Adaptado de ecoinvent database	Energia consumida em kWh para síntese
Emissões para o ar	**Fonte da base de dados**	**Descrição**
Sulfuric acid	n.a.	Emissão indoor
Potassium bromate	n.a.	Emissão indoor
Fluxo finais de resíduos	Fonte da base de dados	
Chemical waste, regulated	n.a.	substâncias química (reagentes e produtos) descartados durante o processo

n.a.: não aplicável.

Tabela 8. Base de dados utilizada para modelagem do hydrobromic acid

Produtos	**Fonte da base de dados**	**Descrição**
Potassium Bromide	Este trabalho	reagente
Materiais/ combustíveis	**Fonte da base de dados**	**Descrição**
Potassium hydroxide {GLO}| market for | Alloc Def, U	ecoinvent database	reagente
Bromine {GLO}| market for | Alloc Def, U	ecoinvent database	reagente
Eletricidade/ calor	**Fonte da base de dados**	**Descrição**
Electricity, medium voltage {GB}| market for | Alloc Def, U LAB	Adaptado de ecoinvent database	Energia consumida em kWh para síntese
Emissiões para o ar	**Fonte da base de dados**	**Descrição**
Potassium bromate	n.a.	Emissão indoor
Waste water	n.a.	Emissão indoor

n.a.: não aplicável.

Tabela 9. Base de dados utilizada para modelagem do bis(trifluoromethane)sulfonimide lithium salt

(continua)

Produtos	**Fonte da base de dados**	**Descrição**
bis(trifluoromethane)sulfonimide lithium salt	Este trabalho	reagente
Entradas conhecidas da natureza (recursos)	**Fonte da base de dados**	**Descrição**
Water, cooling, unspecified natural origin, GLO	ecoinvent database	Água utilizada para resfriamento
Materiais/ combustíveis	**Fonte da base de dados**	**Descrição**
Trifluoromethanesulfonyl fluoride	Este trabalho	reagente
Lithium Nitride	Este trabalho	reagente
Water, deionised, from tap water, at user {GLO}| market for | Alloc Def, U	ecoinvent database	solvente
Eletricidade/calor	**Fonte da base de dados**	**Descrição**
Electricity, medium voltage {GB}| market for | Alloc Def, U LAB	Adaptado de ecoinvent database	Energia consumida em kWh para síntese

Tabela 9. Base de dados utilizada para modelagem do bis(trifluoromethane)sulfonimide lithium salt

(conclusão)

Emissões para água	**Fonte da base de dados**	**Descrição**
Lithium	n.a.	Emissão indoor
Fluorine	n.a.	Emissão indoor

n.a.: não aplicável.

Tabela 10. Base de dados utilizada para modelagem do lithium nitride

Produtos	**Fonte da base de dados**	**Descrição**
lithium nitride	Este trabalho	reagente
Entradas conhecidas da natureza (recursos)	**Fonte da base de dados**	**Descrição**
Water, cooling, unspecified natural origin, GLO	ecoinvent database	Água utilizada para resfriamento
Materiais/ combustíveis	**Fonte da base de dados**	**Descrição**
Lithium {GLO}| market for | Alloc Def, U	ecoinvent database	reagete
Nitrogen, liquid {GLO}| market for | Alloc Def, U	ecoinvent database	reagete
Eletricidade/calor	**Fonte da base de dados**	**Descrição**
Electricity, medium voltage {GB}| market for | Alloc Def, U LAB	Adaptado de ecoinvent database	Energia consumida em kWh para síntese

Tabela 11. Base de dados utilizada para modelagem do trifluoromethanesulfonyl fluoride

Produtos	**Fonte da base de dados**	**Descrição**
trifluoromethanesulfonyl fluoride	Este trabalho	reagente
Entradas conhecidas da natureza (recursos)	**Fonte da base de dados**	**Descrição**
Water, cooling, unspecified natural origin, GLO	ecoinvent database	Água utilizada para resfriamento
Materiais/ combustíveis	**Fonte da base de dados**	**Descrição**
Methane sulfony fluoride	Este trabalho	reagente
Hydrogen fluoride {GLO}| market for | Alloc Def, U	ecoinvent database	reagente
Eletricidade/calor	**Fonte da base de dados**	**Descrição**
Electricity, medium voltage {GB}| market for | Alloc Def, U LAB	Adaptado de ecoinvent database	Energia consumida em kWh para síntese
Emissões para o ar	**Fonte da base de dados**	**Descrição**
Hydrogen	n.a.	Emissão indoor

n.a.: não aplicável.

Tabela 12. Base de dados utilizada para modelagem do methane sulfony fluoride (continua)

Produtos	**Fonte da base de dados**	**Descrição**
Methane sulfony fluoride	Este trabalho	Reagente
Entradas conhecidas da natureza (recursos)	**Fonte da base de dados**	**Descrição**
Water, cooling, unspecified natural origin, GLO	ecoinvent database	água utilizada para refrigeração

Tabela 12. Base de dados utilizada para modelagem do methane sulfony fluoride (conclusão)

Materiais/ combustíveis	**Fonte da base de dados**	**Descrição**
Methanesufonyl_Chloride	Este trabalho	reagente
Sodium fluoride {GLO}| market for | Alloc Def, U	ecoinvent database	reagente
Eletricidade/calor	**Fonte da base de dados**	**Descrição**
Electricity, medium voltage {GB}| market for | Alloc Def, U LAB	Adaptado de ecoinvent database	Energia consumida em kWh para síntese
Emissões para água	**Fonte da base de dados**	**Descrição**
Potassium	n.a.	Emissão indoor
Chloride	n.a.	Emissão indoor
Fluoride	n.a.	Emissão indoor
Waste water	n.a.	Emissão indoor

n.a.: não aplicável.

Tabela 13. Base de dados utilizada para modelagem do methanesufonyl chloride

Produtos	**Fonte da base de dados**	**Descrição**
Methanesufonyl_Chloride	Este trabalho	reagente
Entradas conhecidas da natureza (recursos)	**Fonte da base de dados**	**Descrição**
Water, cooling, unspecified natural origin, GLO	ecoinvent database	água utilizada para refrigeração
Materiais/ combustíveis	**Fonte da base de dados**	**Descrição**
Natural gas, high pressure {GLO}| market group for | Alloc Rec, U	ecoinvent database	reagente
Sulfuryl chloride {GLO}| market for | Alloc Def, U	ecoinvent database	reagente
Materiais/ combustíveis	**Fonte da base de dados**	**Descrição**
Electricity, medium voltage {GB}| market for | Alloc Def, U LAB	Adaptado de ecoinvent database	Energia consumida em kWh para síntese
Emissões para o ar	**Fonte da base de dados**	**Descrição**
Sulfuric acid	n.a.	Emissão indoor

n.a.: não aplicável.

Pontifícia Universidade Católica do Rio Grande do Sul
Pró-Reitoria de Graduação
Av. Ipiranga, 6681 - Prédio 1 - 3º. andar
Porto Alegre - RS - Brasil
Fone: (51) 3320-3500 - Fax: (51) 3339-1564
E-mail: prograd@pucrs.br
Site: www.pucrs.br